“Structure and functional analysis of the African Swine Fever virus encoded CD2v/EP402R protein and investigation of its role in virus persistence in pigs”

by

Mr. Muneeb Islam (6427206)

Submitted for the Degree of Doctor of Philosophy

Department of Infectious pathology and zoonotic diseases
School of Veterinary Medicine
Faculty of Health and Medical Sciences
University of Surrey

Supervisors:
Dr. Daniel Horton (Principle Supervisor) & Dr. Arnoud Van Vliet (Co-supervisor),
School of Veterinary Medicine, University of Surrey.

In collaboration with

Dr. Linda Dixon (Principle Investigator) & Dr. Ana Reis (Co-Supervisor),
African Swine Fever Virus Group (ASFV), The Pirbright Institute (IAH).

Table of Contents

ABSTRACT

1.0 INTRODUCTION

1.1 AFRICAN SWINE FEVER 1

1.2 AFRICAN SWINE FEVER VIRUS 2

1.3 ASFV HOSTS AND TRANSMISSION 6

1.4 VIRUS DISTRIBUTION 7

1.5 ASFV ENTRY AND ASSEMBLY IN CELLS 8

- **CLATHRIN MEDIATED ENDOCYTOSIS 10**
- **MACROPINOCYTOSIS 11**

1.6 ASFV PATHOGENESIS 13

1.7 PATHOLOGY OF ASFV INFECTION 14

1.8 VACCINE APPROACHES 16

1.9 ASFV REPLICATION & TRANSCRIPTION 20

1.10 ASFV GENOME AND PROTEINS INVOLVED IN IMMUNE EVASION 25

1.11 TRANSLATION.....32

1.12 CELLULAR SECRETORY PATHWAY..... 34

1.13 TRANSMEMBRANE PROTEINS 36

1.13.1 CLASSIFICATION OF MEMBRANE PROTEINS ON BASIS OF STRUCTURE 36

1.13.2 CLASSIFICATION OF TRANSMEMBRANE PROTEIN BASED ON TOPOLOGY.....40

1.14 PROTEIN TRANSLOCATION INTO ER 41

1.15 PROCESS OF GLYCOSYLATION..... 45

1.16 ROLE OF EP153R IN ASFV INFECTION 46

1.17 ROLE OF CD2V IN ASFV INFECTION 49

OBJECTIVES 53

2.0 STRUCTURAL, FUNCTIONAL AND EXPRESSION ANALYSIS OF MUTATIONS IN CD2V PROTEIN TO DETERMINE CRITICAL AMINO ACID RESIDUES INVOLVED IN HAD

2.1 INTRODUCTION 54

2.2 ALIGNMENT OF ASFV BENIN 97/1 ENCODED CD2V PROTEIN WITH HUMAN AND PIG CD2 55

2.3 DESIGN OF MUTATIONS IN CD2V PROTEIN TO REDUCE BINDING OF ERYTHROCYTES (BATCH-1) 59

2.4 OPTIMIZATION OF CD2V PROTEIN EXPRESSION BY IMMUNOFLUORESCENCE 63

2.5 EXPRESSION ANALYSIS OF WT-CD2V BY WESTERN BLOT AND IMMUNOFLUORESCENCE 65

2.6 EXPRESSION ANALYSIS OF CD2V MUTANTS BY WESTERN BLOT AND IMMUNOFLUORESCENCE 69

2.6.1 EXPRESSION ANALYSIS OF 1ST BATCH CD2V MUTANTS BY IMMUNOFLUORESCENCE AND WESTERN BLOT 69

2.6.2 HAD ANALYSIS OF 1ST BATCH OF CD2V MUTANTS 75

2.7 DESIGN OF MUTATIONS IN CD2V PROTEIN TO REDUCE BINDING OF RED BLOOD CELLS (BATCH-2) 77

2.7.1 EXPRESSION ANALYSIS OF 2ND BATCH CD2V MUTANTS BY WESTERN BLOT AND IMMUNOFLUORESCENCE 81

2.7.2 HAD ANALYSIS OF 2ND BATCH CD2V MUTANTS 86

2.8 DESIGN OF MUTATIONS IN CD2V PROTEIN TO REDUCE BINDING OF RED BLOOD CELLS (BATCH-3) 88

2.8.1 MUTANTS CD2V DESIGNED BY FOLLOWING A PREDICTED MODEL GENERATED BY PYMOL (BATCH-3) 89

2.8.2 EXPRESSION ANALYSIS OF 3RD BATCH CD2V MUTANTS BY WESTERN BLOT AND IMMUNOFLUORESCENCE 93

2.8.3 FUNCTIONAL ANALYSIS OF 3RD BATCH MUTANTS BY HAD ASSAY 98

2.9 DETECTION OF WT-CD2VHA ON THE CELL SURFACE USING SERUM 104

2.10 DETECTION OF CD2V MUTANTS ON THE CELL SURFACE USING SERUM 107

2.11 DISCUSSION 115

3.0 EXPRESSION AND FUNCTIONAL ANALYSIS OF WILD TYPE CD2V AND REDUCED HAD MUTANTS IN ASFV INFECTED CELLS.

3.1 INTRODUCTION 119

3.2 Expression analysis of VP-WT-CD2vHA, VP-CD2vE99RHA and VP-CD2vY102DHA in ASFV infected WSL cells by Western blot 120

3.3 Expression analysis of pVP-WT-CD2vHA, pVP-CD2vE99RHA and pVP-CD2vY102DHA in ASFV infected WSL cells by Immunofluorescence 122

3.4 Analysis of HAD induced by pVP-WT-CD2vHA, pVP-CD2vE99RHA and pVP-CD2vY102DHA in ASFV infected WSL cells 125

3.5 Expression of analysis of WT-EP153RV5 in MVA-T7 infected Vero cells by immunofluorescence 129

3.6 Co-localisation analysis of WT-CD2vHA and WT-EP153RV5 in MVA-T7 infected Vero cells 133

3.7 Expression of analysis of VP-WT-EP153RV5 in ASFV infected WSL cells by immunofluorescence 135

3.8 Detection of ASFV expressed proteins on the cell surface in non-permeable WSL cells by immunofluorescence 138

3.9 Design of the plasmid construct for making BeninΔDP148RΔEP153R- CD2vE99R (Rec A) 142

3.10 Design of the plasmid construct for making BeninΔDP148RΔEP153RΔCD2v (Rec B) .. 146

3.11 Expression analysis of the plasmid construct (pUC57-VP30mNeon+VP-CD2vE99R) for BeninΔEP153RΔDP148R-CD2vE99R in ASFV infected WSL cells 148

3.12 Confirmation of a non-HAD phenotype induced by transfection of a plasmid construct for BeninΔDP148RΔEP153R-CD2vE99R (Rec A) in ASFV Benin CD2v infected cells 150

3.13 Analysis of expression of mNeongreen and CD2vE99R in cells infected with recombinant ASFV BeninΔDP148RΔEP153R-CD2vE99R (Rec A) by immunofluorescence 152

3.14 Confirmation that HAD is not-induced in cells infected with Recombinant virus BeninΔDP148RΔEP153R- CD2vE99R (Rec A)..... 153

3.15 Discussion 155

4.0 Determine the role of CD2v, EP153R in viremia, and persistence in pigs.

4.1 Introduction..... 158

4.2 Design of animal immunisation and challenge experiment with recombinant BeninΔDP148RΔCD2v Virus (experiment 1)..... 159

4.3 Clinical signs post-immunization and challenge (experiment 1) 160

4.4 Pathological and macroscopic evaluation at Necropsies (experiment 1) 163

4.5 Detection of genome copies in whole blood by qPCR in pigs immunised with BeninΔDP148RΔCD2v (Group C) post-immunization (experiment- 1)..... 164

4.6 Detection of genome copies in different blood fractions by qPCR in pigs immunised with BeninΔDP148RΔCD2v (Group C) post-immunization (experiment- 1)..... 166

4.7 Detection of antibody responses by ELISA in pigs immunised with BeninΔDP148RΔCD2v (Group C) in experiment 1 169

4.8 Detection of IFN responses by ELIspot in pigs immunised with BeninΔDP148RΔCD2v (Group C) in experiment 1..... 170

4.9 Design of animal immunisation and challenge experiment with attenuated BeninΔDP148RΔEP153RΔCD2v, and BeninΔDP148RΔEP153R-CD2vE99R Virus (experiment 2)..... 172

4.10 Clinical signs post-immunization and challenge (experiment 2)..... 173

4.11 Pathological and macroscopic evaluation at Necropsies (experiment 2) 176

4.12 Virus genome detected in blood from pigs immunised with BeninΔDP148RΔEP153RΔCD2v (Group A) or BeninΔDP148RΔEP153RCD2vE99R (Group B) Experiment 2..... 178

4.12.1 BeninΔDP148RΔEP153RΔCD2v (Group A): 178

4.12.2 BeninΔDP148RΔEP153RCD2vE99R (Group B)..... 180

4.13 Detection of infectious virus in pigs immunised with BeninΔDP148RΔEP153R-CD2vE99R (Group B) recombinant virus 181

4.14 Detection of genome copies in different blood fractions by qPCR in pigs immunised with BeninΔDP148RΔEP153RΔCD2v (Group A) or BeninΔDP148RΔEP153R-CD2vE99R (Group B) (experiment- 2): 183

4.15 Detection of antibody responses by ELISA in pigs immunised with BeninΔDP148RΔEP153RΔCD2v (Group A) or BeninΔDP148RΔEP153RCD2vE99R (Group B) in experiment 2. 186

4.16 Detection of IFN responses by ELIspot in pigs immunised with BeninΔDP148RΔEP153RΔCD2v (Group A) or BeninΔDP148RΔEP153RCD2vE99R (Group B) in experiment 2. 188

4.17 Comparative analysis of genome copies numbers in blood from pigs in experiment 1 & 2..... 190

4.17.1 Genome copies number comparison post-immunisation: 190

4.17.2 Genome copies number comparison post- challenge: 192

4.18 Comparative analysis of recombinant viruses based on genome copy number in different blood fractions 193

4.19 Comparative analysis of antibody responses by ELISA in pigs immunised with BeninΔDP148RΔCD2v (Group C) in experiment 1 or BeninΔDP148RΔEP153RΔCD2v (Group A) or BeninΔDP148RΔEP153RCD2vE99R (Group B) in experiment 2. 197

4.20 Comparative analysis of IFN responses by ELIspot in pigs immunised with BeninΔDP148RΔCD2v (Group C) in experiment 1 or with BeninΔDP148RΔEP153RΔCD2v (Group A) or BeninΔDP148RΔEP153RCD2vE99R (Group B) in experiment 2. 198

4.21 Discussion..... 201

5.0 Materials and Methods.....

5.1 Bioinformatics Methods 207

5.1.1 Primer designing 207

5.1.2 Multiple sequence alignments 207

5.1.3 Maps for CD2v mutants in pcDNA3..... 208

5.1.4 Protein modelling tool 208

5.2 DNA Methods 209

5.2.1 Polymerase chain reaction 209

5.2.2 Gel Electrophoresis 209

5.2.3 Cloning 209

5.2.4 Strategy for constructing mutant versions of the CD2v gene..... 210

5.2.5 Sequencing PCR 213
5.2.6 Plasmid DNA isolation 214
5.2.7 Ligation 214
5.2.8 Cloning 214
5.2.9 Transformation of E. coli 215
5.2.10 Chemically competent cells 216
5.2.11 Site directed mutagenesis 217
5.3 Cell culture and protein methods 217
5.3.1 Primary and secondary cells 217
5.3.2 Transfection of adherent cell cultures using TransIT-LT1 219
5.3.3 Infection of adherent cell cultures with MVA-T7 219
5.3.4 Immunofluorescence labelling of cells grown on coverslips 219
5.3.5 Haemadsorption Assay 221
5.3.6 Viruses stocks (Growth and harvest) 221
5.3.7 Titrations (HAD50/ml and TCID50/ml) 222
5.3.8 Western blot 223
5.4 Animal experiments methods 225
5.4.1 Plasma collection from blood samples 225
5.4.2 Buffy coat and RBC collection from blood samples 226
5.4.3 Genome extraction 227
5.4.4 Real time qPCR 227
List of buffers 228
appendix 1 229
appendix 2 230
appendix 3 234
6.0 Summary 236

- What other residues are present in the ligand binding domain? 239
- What is the ligand for CD2v? And is the ligand expressed on other cells? 240
- Is CD2v also involved in virus entry? 240
- What other possible roles does C-type lectin may have? And how is it involve in HAD? 241
- Investigation of safety issues relating to vaccine development 242
- Is the cost effective production of the vaccine candidate possible? 243
- What would be the ideal vaccine against ASF? 244

- **WHAT ARE THE MAJOR CHALLENGES IN THE DEVELOPMENT OF VIABLE AND EFFECTIVE VACCINE AGAINST ASF?.....245**

REFERENCES: 246

Declaration

***I** hereby declare that this thesis and the work to which it refers are the results of my own efforts. Any ideas, data, images or text resulting from the work of others (whether published or unpublished) are fully identified as such within the work and attributed to their originator in the text, bibliography or in footnotes. This thesis has not been submitted in whole or in part for any other academic degree or professional qualification. I agree that the University has the right to submit my work to the plagiarism detection service Turnitin (UK) for originality checks. Whether or not drafts have been so assessed, the University reserves the right to require an electronic version of the final document (as submitted) for assessment as above.*

Mr. Muneeb Islam

Signed; Muneeb Islam

27th September, 2020.

Permission to copy

UNIVERSITY OF SURREY

Access to and reproduction of thesis title

STRUCTURE AND FUNCTIONAL ANALYSIS OF THE AFRICAN SWINE FEVER VIRUS ENCODED CD2V/EP402R PROTEIN AND INVESTIGATION OF ITS ROLE IN VIRUS PERSISTENCE IN PIGS

Mr. Muneeb Islam

PhD veterinary medicine **September 2020**
(Department of infectious pathology and zoonotic diseases)

Access to any of the contents of this thesis should not be made available to anyone without written prior permission of the representative of post graduate student, supervisors or their representative at placement organisation and degree awarding institution.

OR

The contents of this thesis may under the auspices of the Department of infectious pathology and zoonotic diseases, School of veterinary medicine, Faculty of Health and medical sciences, University of Surrey, be accessed for the purposes of research but may not be copied without written consent of representative of University of Surrey.

OR

The contents of this thesis may be made available for the purposes of research but may not be accessed or copied without the written consent of representative of The Pirbright Institute.

OR

I agree that a copy may be made available of the whole or any part of the above-mentioned thesis title without further reference to the undersigned.

Signature; Muneeb Islam

Date; 27th September, 2020.

Abbreviations:

Ab	**Antibody**
Amp	**Ampicillin**
AP-1	**Adaptor protein**
ASF	**African swine fever**
ASFV	**African swine fever virus**
Bcl-2	**B-cell lymphoma 2**
BH domain	**Bcl-2 Homology domain**
BIR1	**BAK1-interacting receptor-like kinase 1**
BIR2	**BAK1-interacting receptor-like kinase 2**
bp	**Base pair**
CAGE	**Cap analysis gene expression**
DNA	**Deoxyribonucleic acid**
dNTPs	**Deoxy nucleoside triphosphate**
EB	**Elution buffer**
EDTA	**Ethylene diamine tetra acetic acid**
ELISA	**Enzyme linked immunosorbent assay**
ELIspot	**Enzyme linked immunoabsorbent spot**
EM	**Electron microscopy**
ER	**Endoplasmic reticulum**
ERAD	**Endoplasmic reticulum associated degredation**
GalNac	**N-acetylgaltoseamine**
GlcNac	**N-acetylglucoseamine**
HAD	**Haemadsorption**
IAP	**Inhibitors of apoptosis proteins**
IFN	**Interferon**
IRF3	**Interferon regulatory factor 3**
IRF7	**Interferon regulatory factor 3**
ISG	**Interferon-stimulated gene**
JAKs	**Janus kinases**

Kan	**Kanamycin**
Kbp	**Kilo basepair**
kDa	**KiloDalton**
LB	**Lysogeny broth, Luria broth**
Man	**Mannose**
Mg	**Milligram**
Min	**Minutes**
mM	**Milli molar**
MOI	**Multiplicity of infection**
MTOC	**Microtubule-organizing center**
MVA	**Modified vaccinia Ankara**
NF-κB	**Nuclear factor kappa-light-chain-enhancer of activated B cells**
ng	**Nano gram**
NK	**Natural killer**
ORF	**Open reading frame**
p	**Plasmid**
P53	**Tumour protein p53**
PBM	**Porcine bone marrow cells**
PBMC	**Peripheral blood mononuclear cells**
PCNA	**Proliferating cell nuclear antigen**
PCR	**polymerase chain reaction**
Pfu	**Plaque forming unit**
pmol	**Pico moles**
RBC	**Red blood cells**
RBP	**RNA-binding proteins**
RPM	**Revolution per minute**
Sec	**Second**
SH3	**SRC Homology 3 Domain**
siRNA	**Small interfering ribonucleic acid**
SOC	**Super optimal broth**

STATs	**Signal transducer and activator of transcription proteins**
TBE	**Tris borate EDTA**
TGN	**Trans-Golgi network**
TLR3	**Toll-like receptor 3**
TNF	**Tumour necrosis factor**
TNF	**Tumour necrosis factor**
TNFR2	**Tumour necrosis factor receptor 2**
TRAF	**TNF receptor associated factors**
TRAF1	**Tumour necrosis factor receptor associated factor 1**
TRAF2	**Tumour necrosis factor receptor associated factor 2**
TRIF	**TIR-domain-containing adapter-inducing interferon-β**
UPR	**Unfolded protein response**
V	**Volts**
VP	**Viral promoter**
WBC	**White blood cells**
WSL	**Wild boar lung cells**
WT	**Wild type**
Δ	**Delta (refers to the deletion)**
°C	**Degree Celsius**
µg	**Microgram**
µl	**Microliter**

ABSTRACT:

ABSTRACT:

African swine fever is a viral haemorrhagic disease of domestic pigs and wild boar and is a serious threat to the economy of many countries. No vaccines are available to induce protection in pigs against this lethal disease. The most promising approach for vaccine development is the use of modified live attenuated vaccines (MLAV) and these can confer high levels of protection. One MLAV candidate is a gene-deleted genotype I Benin 97/1 strain (BeninΔDP148R), which lacks the DP148R gene. The BeninΔDP148R confers 100% protection in immunized pigs following challenge with parental pathogenic Benin 97/1, but adverse clinical signs associated with viremia and extended persistence of virus were observed. In this thesis, the mechanism by which the ASFV CD2v transmembrane protein, coded for by the EP402R gene, binds to red blood cells was investigated. Functional amino acid residues in CD2v that are involved in binding red blood cells (HAD) were identified by introducing single or multiple amino acid substitutions into the predicted ligand-binding domain on the CD2v protein. Mutations of the residues glutamic acid at position 99 or tyrosine at position 102 were shown to reduce HAD to the expressed CD2v protein. However, the expression of the ASFV membrane protein EP153R was shown to rescue the reduced HAD capacity of mutant CD2v proteins. This indicated that EP153R protein can augment this function of CD2v. To examine the effect of reducing the capacity of ASFV to cause HAD on virulence, levels and persistence of the virus in blood, two recombinant viruses were tested by immunisation of pigs. In the first virus deletion of the EP402R gene from the BeninΔDP148R virus genome was shown to dramatically reduce the period of virus persistence in blood, although moderate levels of virus and clinical signs were observed. In the second virus, the EP153R gene was deleted and the EP402R gene was

replaced with a gene expressing a non-HAD CD2v with the amino acid residue glutamic acid at position 99 substituted with arginine in the genome of ASFV BeninΔDP148R. Immunisation of pigs showed the virus persistence in blood was reduced to 2 days, the onset and duration of clinical signs were decreased (1 day) and the viremia was also reduced by approximately 3 thousand-fold. This demonstrated that deletion of EP153R and the insertion of mutant CD2vE99R balanced the level of virus attenuation, and hence resulted in a reduced virus persistence, mild clinical signs for a reduced duration, a decrease in viremia and provided overall protection of 83.3%. This recombinant virus has an increased safety profile compared to the parental virus (BeninΔDP148R) and is a promising vaccine candidate.

Acknowledgments:

"A goal is a dream with a deadline" – Napoleon Hill

I would like to express my special appreciation, gratitude and thanks to my supervisor Dr. Linda Dixon, you have been a tremendous mentor for me. I would like to thank you for encouraging me and to for allowing me to grow, thank you for the opportunity to study in the United Kingdom. I am also thankful to Dr. Ana Reis my co-supervisor for guiding me through every step in this long and exciting journey, and for teaching me to plan and design experiments. I would like to thank Dr. Anusyah Rathakrishnan for generating the recombinant viruses, and my previous co-supervisor Lynnette Goatley for her care and motivation in my first year. I am grateful to my university supervisors Dr. Simon Graham (ex-supervisor) and Dr. Daniel Horton for their valuable suggestions. A special thanks to Dr. Lynda Moore for her support and care throughout my stay at Pirbright. Finally, I would like to thank all member of ASFV group for the nice conversations.

What about those dreams and goals?

My PhD degree has nearly ended; my own dream has almost become real with the realization of this degree.

My thoughts and appreciation go to my beloved wife Mrs. Faiza Muneeb for her supportive role, tender care, and motivation which contributed a lot in achieving my goal. My special gratitude goes to my beloved parents Mr. & Mrs Islam for their prayers, financial support and for believing in me. Last but the most important, my gratitude is expressed to my creator.

"Structure and functional analysis of the African Swine Fever virus encoded CD2v/EP402R protein and investigation of its role in virus persistence in pigs"

Mr. Muneeb Islam (PhD Student) – Department of Infectious pathology and zoonotic diseases, FHMS, University of Surrey (6427206)

Dr. Daniel Horton (Principle Supervisor) & Dr. Arnoud Van Vliet (Co-supervisor)

School of Veterinary Medicine, University of Surrey

In collaboration with

Dr. Linda Dixon (Principle Investigator) & Dr. Ana Reis (Co-Supervisor)

African Swine Fever Virus Group (ASFV), the Pirbright Institute (IAH)

1.0 Introduction:

1.1 African Swine Fever (ASF):

African swine fever (ASF) is a highly contagious viral haemorrhagic disease of domestic pigs (Costard et al., 2009). It was first described in Kenya by Montgomery as a pathological disease of domestic pigs (Montgomery, 1921). ASF has a high case fatality rate up to 100% and the highly virulent strains (for example; Benin 97/1, Georgia 2007) can kill a domestic pig within 7-10 days post-infection (Takamatsu et al., 1999). Based on severity of disease, ASF is classified in three forms: acute, sub-acute and chronic. Acute forms of disease typically result in death in almost all animals. Extensive haemorrhages in spleen, lymph nodes, kidneys, gastrointestinal and respiratory tracts are observed. Haemorrhages on the skin can also be observed, especially in peripheral regions such as on the ears, tail, and trotters as well as vomiting and diarrhoea. In sub-acute forms of disease similar post-mortem and clinical signs are observed as in acute forms but these may take longer to develop and fatality is lower. A proportion of infected animals, varying between 30 and 50%. survive, . . Typical signs of the chronic form of disease include loss of condition, swelling of the joints,

necrotic skin lesions, respiratory distress and cardiac signs (Murcia et al., 2009)(King et al., 2011). ASF is considered the most important and challenging disease of pigs. The ASF virus can be spread into disease free areas via different routes, including trade in livestock and animal products, movement of wild suids, contaminated vehicles and vectors (Sanchez-Cordon et al., 2018). Animals can become infected when ingestion or direct contact with contaminated products or animals. ASFV can infect animals via oral, nasal, ocular penetration and subcutaneous routes (Chenais et al., 2019). The infected animals shed the virus in excretions and secretion including urine and faeces. High levels of virus are present in blood and after death the contaminated carcasses are sources of virus dissemination in the environment. It has been reported that the virus can persist in blood, tissues and pork products for extended periods of months or years (Davies et al., 2017; McKercher et al., 1978).

1.2 African swine fever virus:

African swine fever virus (ASFV) is the causative agent of ASF. It is the sole member of the virus family *Asfarviridae* of the *Asfivirus* genus and is the only known DNA arbovirus. The genome structure and replication mechanism of ASFV is similar to poxviruses however they are placed in distinct families because of structural and sequence differences (ICTV ninth report. 2009). Both virus families are included in the "Phylum "Nucleocytoviricota" (ICTV Master Species List 2019.v1) which are proposed to have a common ancestor. The Nucleocytoviricota contains eight taxonomic families of the most complex large DNA viruses (Iyer et al., 2001). Currently, 24 genotypes of ASFV have been identified based on the partial sequencing of the ASFV B646L gene that encodes the viral capsid protein p72, (Achenbach et al., 2016; Quembo et al., 2018) and 8 serotypes based on the viral CD2v (EP402R) and C-type lectin (EP153R) protein sequences (Malogolovkin, Burmakina, Titov, et al., 2015;

Malogolovkin, Burmakina, Tulman, et al., 2015). The extracellular ASFV appears icosahedral in shape with an average diameter of 200nm and has a complex structure with an icosahedral representation containing five concentric layers: the central nucleoid, the core shell, the inner envelope, the icosahedral capsid and the outer envelope (see figure 1.1) (Carrascosa et al., 1984; Salas & Andres, 2013). The nucleoid contains the double-stranded DNA molecule with cross-linked genome termini and other factors including the transcription machinery. This includes genes for six subunits of RNA polymerase encoded by EP1242L (RPB2), C147L (RPB6), NP1450L (RPB1), H359L(RPB3-11), D205R (RPB5) , CP80R (RPB10), a putative poly A polymerase encoded by C475L, capping enzymes encoded by (NP868R) and transcription factors i.e. TFIIB (C315R), transcription elongation factor S-II (I243L), four putative factors encoded by G1340L, I243L, B175L and B385R (Alejo et al., 2018). The nucleoid also contains DNA binding protein p10 encoded by K78R and P11.6 encoded by A104R (See figure 1.2) (Alejo et al., 2018).

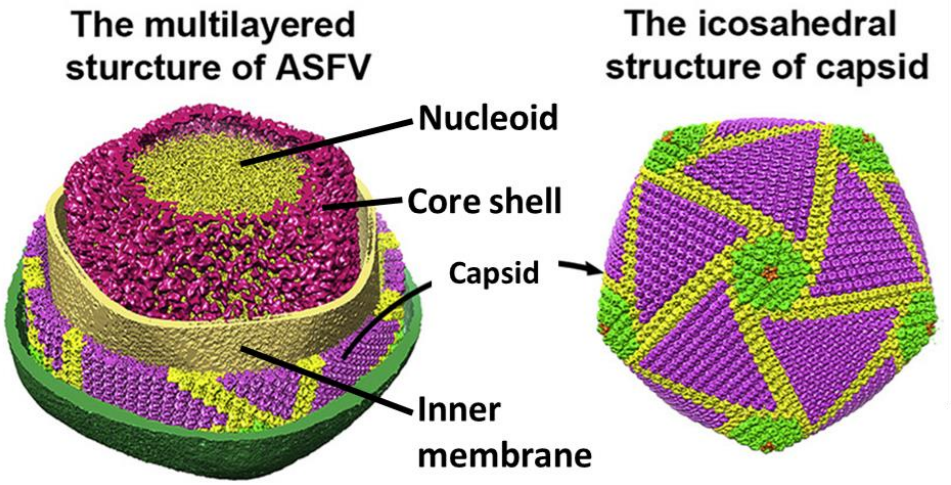

Figure 1.1: ASFV Structure: a graphical representation of the typical African swine fever virus and the cryo-EM reconstruction of capsid, adapted from; (Liu et al., 2019)

The nucleoid is wrapped by a core shell which is a highly organised thick protein layer of 30nm. The core shell is assembled from the processing products of two important polyproteins pp220, encoded by CP2475L, is cleaved to produce the mature virion proteins (P150, P37, P14, P34). Polyprotein pp60, encoded by CP530R, is cleaved to P35 and P15. Both polyproteins are cleaved by a virus encoded SUMO-like protease (S273R) (Alejo et al., 2003). The inner envelope surrounding the core shell was suggested to be derived from the endoplasmic reticulum (ER) membrane of the host cell (Cobbold & Wileman, 1998). However, later investigation using electron microscopy of ultrathin Epon sections of viral intermediates suggested that the inner envelope is derived from a collapsed two membrane cisternae present in the maturation site of the virus within the precursor viral membranous structures (Andres et al., 1998; Salas & Andres, 2013). The viral proteins p54 encoded by E183L, p17 encoded by D117L, pE248R encoded by E248R and p12 encoded by O61R are present in the inner envelope formed as shown in figure 1.2 (Alejo et al., 2018; Salas & Andres, 2013).

Electron microscopy revealed that approximately 2000 capsomers in a hexagonal prism pattern to form the ASFV capsid. The p72 protein, encoded by B646L gene, is the major structural component of the capsid (Garcia-Escudero et al., 1998) and its incorporation into the virion requires a virus encoded chaperone B602L (Cobbold & Wileman, 1998). Recently published cryo-EM structural studies showed that the capsid consists of 8,280 copies of the double jelly-roll major capsid protein p72 (B646L) arranged in trimers displaying a pseudo-hexameric morphology, 60 copies of the penton protein p49 (B438L), and at least 8,340 copies of minor capsid proteins (Andres et al., 2020; Liu et al., 2019). The minor capsid proteins (P2, P3, P4, P5, P6, P7, P8, P9, P10, P11, P12, P13, and P14) form a network immediately below the outer capsid shell. Most minor capsid proteins are at the interface between neighbouring capsomers and are most likely

to function to stabilize the entire capsid (Liu et al., 2019). The penton proteins, p49 (B438L), are required for icosahedral structural stability by plugging each of the 12 icosahedral vertices (Andres et al., 2020; Epifano et al., 2006). The outer envelope is only present on the extracellular virus particle and is acquired during the virus budding process from infected cells. The outer membrane contains protein CD2v coded for by EP402R gene and is required for the extracellular virions and infected cells to attach to the red blood cells (RBC). Analysis of the ASFV particle proteome showed that CD2v is to date the only viral protein identified on the outer membrane of the virus (see figure 1.2) (Alejo et al., 2018).

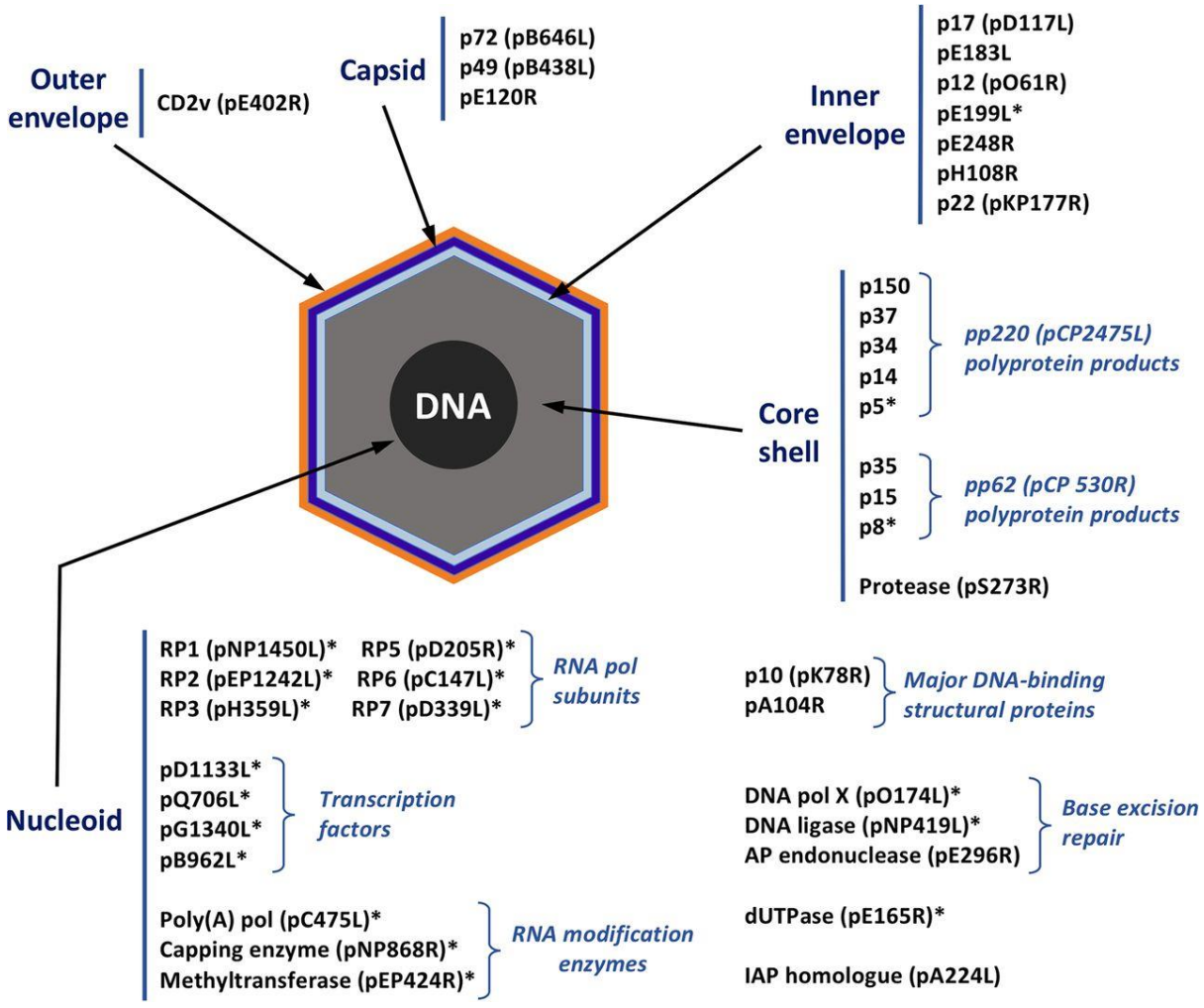

Figure 1.2: Structural proteins of ASFV; A schematic presentation of 40 important viral proteins present in the 5 structural domains (the outer envelope, capsid, inner envelope, core shell and nucleoid) of ASFV particle. Source:(Alejo et al., 2018).

1.3 ASFV hosts and transmission:

ASFV transmission mainly depends on the type of host and the transmission cycle involved among hosts (Costard et al., 2013). ASFV has various susceptible species and natural reservoir hosts. Susceptible species domestic pigs and wild boar can be infected and develop varying disease signs depending on the virus isolate. However, the natural reservoir hosts can tolerate the virus and develop an asymptomatic infection. The virus can persist in the reservoir hosts for a longer period. Soft ticks of the genus *Ornithodoros*, mainly argasid ticks of the *Ornithodoros moubata* species, serve as vectors and a reservoir host. Warthogs (*Phacochoerus africanus*) and bush pigs (*Potamchoerus porcus*) are also reservoir hosts involved in maintaining a reservoir and spread of ASFV in Africa (Gogin et al., 2013). ASFV is generally spread by contact with infectious animals or fomites, ingestion of contaminated pig products and tick bites (Plowright at al. 1994). Three different epidemiologic transmission cycles (sylvatic, tick-pig and domestic) have been described in different hosts (see figure 1.3).The sylvatic cycle in Africa involves virus replication in warthogs (*Phacochoerus africanus aethiopicus*), bush pigs (*Potamchoerus porcus*) and soft ticks (*Ornithodoros species*) without causing disease. This sylvatic cycle is believed to be the origin of the tick-pig cycle and the domestic cycle and hence considered as the origin of the disease (Chenais & Fischer, 2018). The second cycle involves ticks and domestic pigs (*Sus scrofa*

domesticus), in which a sporadic emergence of disease may occur in pigs (Plowright at al. 1994) and has only been described in Sub-Saharan Africa, Spain and Portugal (Chenais & Fischer, 2018). The third transmission cycle involves direct transmission among domestic pigs or from contaminated pig products to the pigs without involvement of ticks (Costard et al., 2013). Recently another transmission cycle was reported, the wild boar habitat cycle which involves transmission from wild boar and contaminated products, including carcasses to pigs or other wild boar (see figure 1.3) (Chenais et al., 2018).

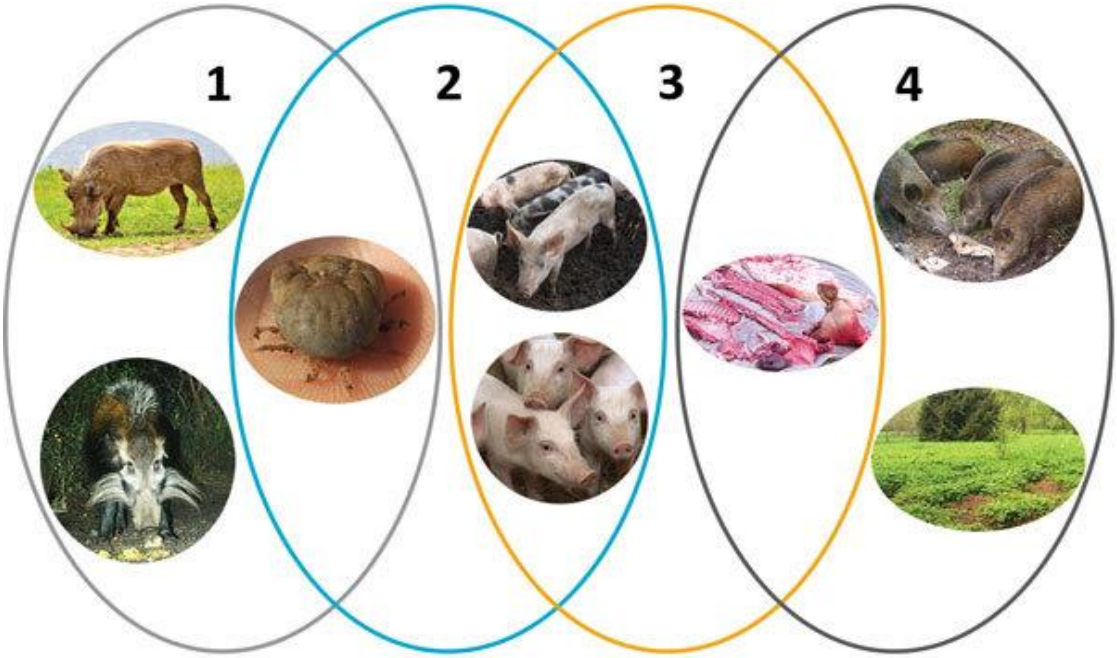

Figure 1.3: ASFV transmission: The epidemiological transmission cycle of ASFV (1) shows the sylvatic cycle, (2) shows the tick-pig cycle (3) shows the domestic pig cycle and (4) shows the wild boar habitat cycle. (Chenais et al., 2018).

1.4 Virus Distribution:

ASFV was first reported in east Africa in the early 1900s and was identified as an acute haemorrhagic fever with high mortality rate. The disease spread to most Sub-Saharan African countries but was confined to the African continent until it was introduced to Europe in 1957. This transcontinental spread of ASFV first occurred in Portugal in 1957

and 1960, the disease was then spread to other countries in Europe and became endemic in Spain; sporadic outbreaks also occurred in other countries including France, Italy, Belgium, Netherlands, Malta (Sanchez-Vizcaino et al., 2013). The disease was eradicated from Spain and Portugal in the mid-1990s but remains endemic in Sardinia following its introduction there in 1978. In 2007, the next spread of ASFV outside of Africa occurred to Georgia in the Caucasus region. ASFV is thought to have been introduced to the Black Sea harbour Port of Poti via infected pork from ships being fed to pigs as swill (Rowlands et al., 2008). From Georgia, the disease spread to the Russian Federation. In 2012 ASFV was introduced to Ukraine and to Belarus in 2013. In 2014, the infection reached the European Union and has spread extensively through Lithuania (2014), Poland (2014), Latvia (2014) and Estonia (2014) where the disease became endemic in the wild boar population. In the European Union the disease is still expanding its territory and outbreaks were reported in Belgium, Bulgaria, Hungary, Romania, Moldova and the Czech Republic from 2017-2018 (Guinat et al., 2016). The situation worsened with the introduction of ASFV into China in 2018. China is the world's largest pig producer, consumer and contains half of the world pig population (Ge et al., 2018). The introduction to China dramatically expanded the spread of ASFV and was followed by detection in countries neighbouring China, including; Mongolia, North Korea, Philippines, Myanmar, Laos, South Korea, Indonesia, Vietnam and Cambodia. The continued spread of ASFV in Southeast Asia, Africa and Europe has a high socioeconomic impact including loss of trade, loss of businesses, decrease in pork production impact on farmers and reduction in the number of pig herds at the national level (reviewed by (Dixon et al., 2020). The UK authorities (DEFRA) estimate the risk of ASFV introduction as "moderate" although risks of an outbreak of disease are "low".

1.5 ASFV Entry and assembly in cells:

The entry mechanism of ASFV into cells is regulated by various signalling pathways, factors and interaction with cell surface receptors. ASFV exploits the cellular endocytic pathways to enter the host cell (Andres, 2017). In early studies, it was reported that ASFV enters host cells via receptor mediated endocytosis and several macrophage surface receptors have been proposed to have a role in entry including CD163 and CD45. CD163 is a scavenger receptor and is expressed on mature macrophages. Incubation of alveolar macrophages with anti-CD163 monoclonal antibodies reduced virusinfection suggesting a role for CD163 in virus entry(Sanchez-Torres et al., 2003). However, recent studies have shown that CD163 may be involved but may not be essential, as in porcine bone marrow cells (PBM) the infection rate showed good correlation with CD45 but intermediate correlation with CD163 (Lithgow et al., 2014). The ASFV strain NHV/P68 was also shown to be efficiently produced in wild boar cells although only 6% of the cells were positive for CD163 (Sanchez et al., 2017). Moreover, when genetically edited CD163 knock -out pigs were infected with Georgia 2007/1 strain no differences were observed in the progression of the disease compared to the wild type pigs (Popescu et al., 2017). This data indicated that CD163 is not essential for infection but may be involved in entry in some way.

Earlier studies reported an ASFV encoded p12 protein was involved in virus attachment to the host cells, as this protein bound to ASFV susceptible-Vero cells but not to the resistant IBRS-2 cells (Carrascosa et al., 1991). Other proteins have also been suggested to have a role in virus entry including, the p54 (E183L) protein which has shown to interact with dynein minus-end microtubule associated motor protein. Also antibodies against p54 (E183L) inhibited the first step of the viral infection cycle related to viral attachment (Alonso et al., 2001; Gomez-Puertas, Rodriguez, et al., 1998). Similarly, antibodies against the p30 (CP204L) protein inhibited attachment and internalization of

ASFV, indicating a role for p30 (CP204L) in this process (Gomez-Puertas, Rodriguez, et al., 1998). An additional model for entry of ASFV into macrophages was proposed which involves the Fc-receptor mediated entry of antibodies bound to virus particles. This entry route may explain an accelerated progression of the disease observed in vaccinated pigs compared to naïve pigs (Argilaguet et al., 2011). This model was further supported by a study in which an increase in infection rate was observed in cells treated with serum from immunised pigs (Perez-Nunez et al., 2019). In contrast, another study showed that convalescent serum from pigs infected with ASFV E75 strain neutralized viral infection of cells by some virulent ASFV strains but not by tissue-culture adapted strains (Zsak et al., 1993). The contradictory data suggests that further investigation is required to elucidate the facilitation of ASFV entry by the Fc receptor. Recent studies have shown that the entry pathway for ASFV into its primary target cells (macrophages/monocytes) occurs via two pathways which significantly contribute to the viral entry and replication in macrophages. These entry mechanisms include; (i) clathrin- and dynamin-mediated endocytosis, (ii) actin mediated macropinocytosis (Andres, 2017).

(i) Clathrin- and dynamin-mediated endocytosis;

Clathrin mediated endocytosis (CME) involves the receptor-dependent internalization of virus particles through the formation of a clathrin coat underneath the plasma membrane (McMahon & Boucrot, 2011). Clathrin-coated pits bud into the cytoplasm after a scission event assisted by the GTPase dynamin. The resulting coated vesicles, with an internal diameter of 60–200 nm, deliver the viral cargo into peripheral early endosomes. These vesicles eventually mature into perinuclear late endosomes and then into lysosomes (Smith & Helenius, 2004). Viral decapsidation occurs at the acidic intraluminal

pH in mature endosomal compartments between 30- and 45-min post-infection. ASFV core particles bud from the late endosomes following a fusion event between the virus internal membrane and the endosome membrane. The viral protein pE248R is also involved in the fusion event (Alonso et al., 2013), reviewed by (Galindo & Alonso, 2017)(see figure 1.5a).

(ii) Actin mediated macropinocytosis:

Macropinocytosis involves a non-selective uptake of extracellular fluid and particles driven by actin-dependent evaginations of the plasma membrane (Kerr & Teasdale, 2009). Macropinocytosis is constitutively active in macrophages and dendritic cells but it is also triggered by some growth factors as well as by a number of viruses. Macropinocytosis is mediated by actin and is also assisted by dynamin to induce the formation of typical macropinocytic structures such as lamellipodia circular ruffles, or blebs. ASFV binding to cells doesn't induce macropinocytosis but exploits the cellular mechanism of fluid uptake for its entry into host cell. Macropinosomes undergo a maturation program reminiscent of that of classical endosomes as shown in figure 1.5a (Hernaez et al., 2016).

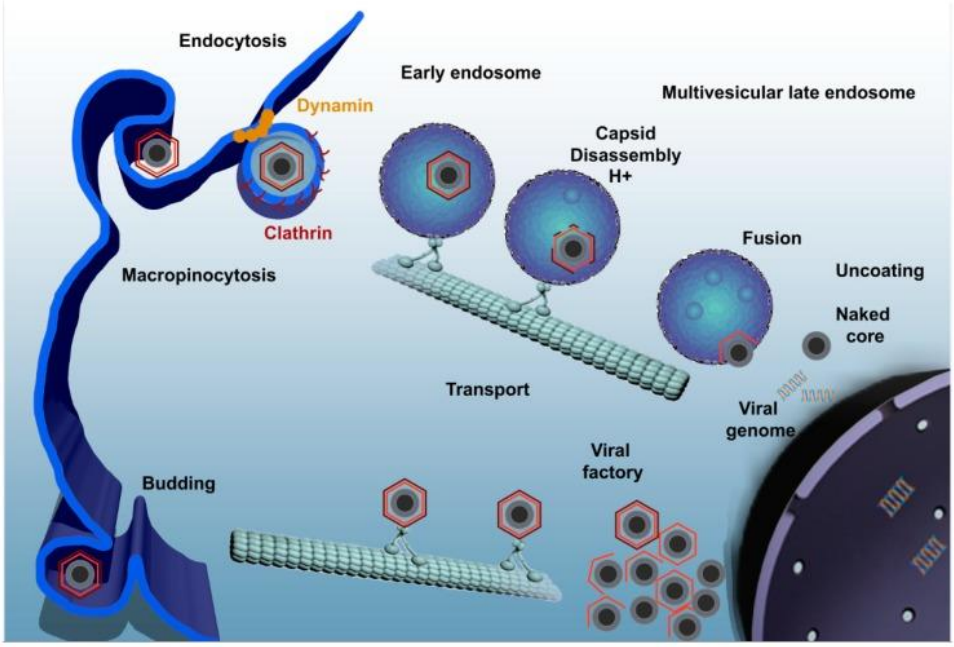

Figure 1.5a; ASFV entry pathways: A schematic representation of ASFV entry mechanisms into swine macrophages, showing two pathways; clathrin-mediated endocytosis and actin-mediated macropinocytosis. Source (Galindo & Alonso, 2017)

Once the virus core is delivered in the cytoplasm, the transcriptional machinery within the nucleoid is activated to synthesise and modify early RNAs, and establish specialized assembly areas in the cytoplasm called viral factories (Salas & Andres, 2013). The viral factory is localized close to the nucleus as a single and large perinuclear area at the microtubule organizing centre MTOC. The viral factories are surrounded by host endoplasmic reticulum (ER) membranes. Viral proteins, DNA, immature and mature virions, and abundant virus-induced membranes are accumulated in the viral factories. When newly synthesized virions are assembled,viral DNA and other components of the nucleoid are encapsidated to form intracellular mature virions (Galindo & Alonso, 2017). The mature virus particles are transported from the viral factories to the cell surface by kinesin motors and this requires the capsid protein pE120R. The mature particles egress from the host cell by budding at the plasma membrane acquiring an

outer envelope in the process (see figure 1.5b) (Andres et al., 2001; Jouvenet et al., 2004).

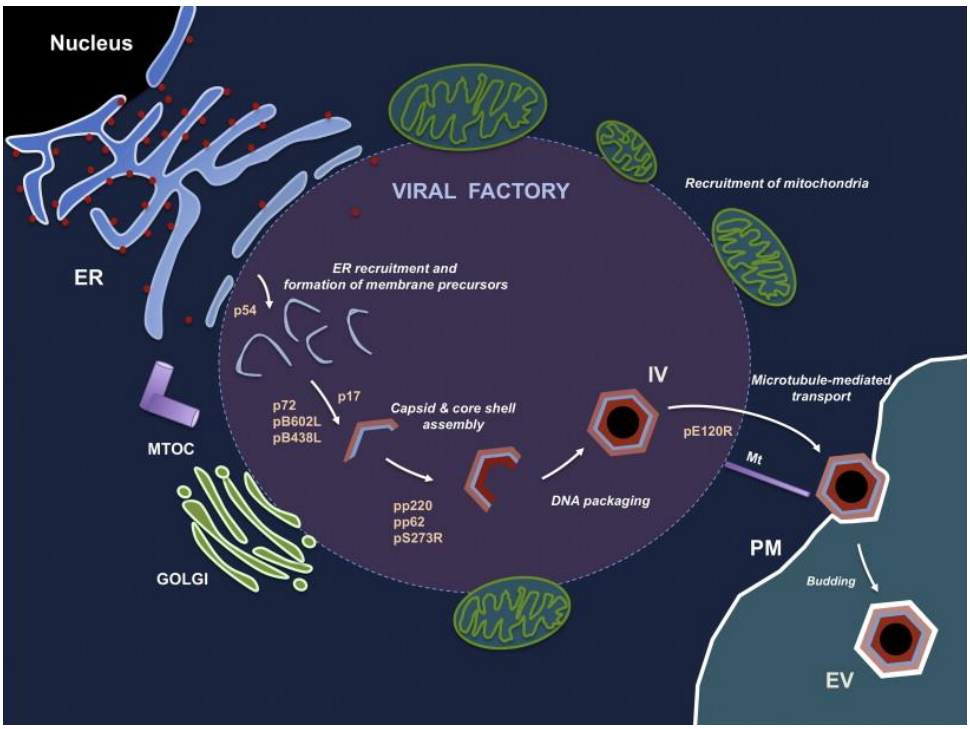

Figure 1.5b: ASFV assembly and exit: A schematic diagram showing the different steps involve in virus assembly with in the viral factories) and exit mechanism of the virus from host cell, source (Salas & Andres, 2013).

1.6 ASFV Pathogenesis:

ASFV infection is initiated after the virus particles enter cells via the oral-nasal route of the pig or subcutaneously following the bite of an infected tick or through scratches. It has been proposed that the virus preferentially invades the host via nasal, bronchial, or the gastric mucosae. It was reported that the virus initially infects the pharyngeal tonsil and from there the infection progress to the lymph nodes where it replicates extensively and spreads to the secondary organs (Greig, 1972). The virus then migrates to other organs and replicates in different cells including macrophages and dendritic cells of the mononuclear phagocytic system (Javier et al., 1993). In late phases of the

disease infection is also detected in endothelial cells, platelets, neutrophils, hepatocytes, lymphocytes and megakaryocytes. Infection may result in release of various inflammatory mediators that cause severe injury to endothelial cells (Gomez-Villamandos et al., 2013). ASFV mainly damages the lymphoid organs (spleen, lymph nodes, thymus, and tonsils) and this may be due to the massive destruction by apoptosis of B and T lymphocytes and macrophages in the acute form of disease (Salguero et al., 2005). The mechanism by which apoptosis of bystander apoptosis in lymphocytes is induced is unknown. One suggestion is that it may be mediated by release of factors including TNF-alpha from infected cells. ASFV was shown to induce an increased secretion of pro-inflammatory cytokines including IL-1, TNF-α, and IL-6 in infected cells at early stage of the disease (del Moral et al., 1999). Recent studies based on transcriptome analysis suggested that cytokines of the TNF family may have a major role in ASF pathogenesis by inducing apoptosis in bystander lymphocytes. The up-regulation of pro-inflammatory cytokines and the down-regulation of anti-inflammatory cytokines may significantly contribute to pathogenesis (Zhu et al., 2019).

1.7 Pathology of ASFV infection:

As discussed in section 1.3, African wild suids tolerate infection and are resistant to disease although the mechanisms for disease resistance aren't known. ASFV isolates are classified based on their virulence from high to low virulence and e the disease is classified based on the clinical observation as peracute (or hyperacute), acute, subacute, or chronic (reviewed by (Salguero, 2020). The highly virulent isolates of ASFV including recent genotype II isolates (e.g Georgia 2007/1) can cause peracute or acute disease and have a case fatality rate that approaches 100% in domestic pigs (Leitao et al., 2001). The clinical signs associated with peracute infection include high fever (above 42°C), respiratory distress, lethargy, anorexia and sometimes sudden death

without developing any clinical signs or gross lesions that are often observed at post mortem (Sanchez-Cordon et al., 2018). Infection with moderately virulent isolates can cause signs similar to the acute form of the disease in naïve pigs however mortality is reduced by 30-50%. The clinical signs associated with acute infection include high temperatures (40°C-42°C), anorexia, lethargy, centripetal cyanosis (may be found on ears, limbs, snout, abdomen, tail, and perianal area), respiratory distress, pulmonary oedema, skin lesions, petechial haemorrhages or ecchymosis. Other clinical signs may include nasal discharges (often with blood), vomiting, diarrhoea (may be stained with blood) and abortion in pregnant sows (Sanchez-Vizcaino et al., 2015). The pathological observations at post-mortem are characterized by splenomegaly, multifocal haemorrhagic lymphadenitis (mostly affecting gastro-hepatic, renal and abdominal lymph nodes), and petechial haemorrhages on kidneys. Haemorrhages may also be observed on submandibular, retropharyngeal, inguinal lymph nodes, in the mucosa or the serosa of different organs, the epicardium in the heart or the urinary bladder, (reviewed by (Salguero, 2020). Animals infected with moderately virulent isolates can develop subacute infection with a mortality rate reduced by between 30-50%. The clinical signs associated with subacute infections include haemorrhages and oedema, this form of the disease often causes more severe lesions than the acute form of ASF. The pigs usually die between 7-20 days post infection and the death may either occur during an initial thrombocytopenia and leukopenia or during a “recovery” phase, with erythrodiapedesis induced by vasodilation (reviewed by (Sanchez-Cordon et al., 2018; Sanchez-Vizcaino et al., 2015). The pathological lesions observed at post-mortem include hydro pericardium, ascites, oedema, splenomegaly (complete or partial), haemorrhagic lymphadenitis, petechial haemorrhages and multifocal pneumonia (Gomez-Villamandos et al., 2003). The low virulence isolates may result in chronic

lesions with low viremia and fever post-infection, or an asymptomatic infection (Leitao et al., 2001).

In advanced stages of the disease, virus persistence may occur in the infected host as virus particles have been observed in lymphocytes and platelets despite apparent recovery of the animals (Gomez-Villamandos et al., 2013). One previous study showed that the viral DNA persisted in PBMC for more than 500 days post-infection in pigs that recovered from acute ASF, although infectious virus was not detected (Carrillo et al., 1994). The authors suggest that monocytes and macrophages may remain persistently infected. An early study on virus distribution in whole blood, plasma, RBC and WBC subpopulation has shown that during infection in pigs, 90% of the virus in whole blood is associated with RBC and in the WBC's subpopulation the virus was associated mainly with lymphocytes and neutrophils (Wardley & Wilkinson, 1977). Another study showed that the virus can persist up to 48 days post-infection in lymph nodes and tonsils and for up to 32 days post infection in lymphocytes within the recovered animals. The virus also persisted in blood and spleen, but was slowly cleared and became undetectable at day 48 post-infection, This indicates that ASFV was able to persist preferentially in cells in lymph nodes and the tonsil (Oura et al., 1998). A recent study has shown that experimental infection of pigs with a virus attenuated by gene deletion BeninΔDP148R induced good protection following challenge, however, the virus genome persisted in blood for an extended period (up to 60 days p.i) whereas infectious virus was not detected beyond day 30 p.i (Reis et al., 2017). This suggest that a proportion of virus may not be replicating and may remain attached to cells in blood and losing infectivity over time.. Other than domestic pigs, ASFV can persistently infect ticks and virus can be isolated from infected ticks for several years

post-infection. Persistent infections are also thought to occur in adult warthogs (Jori et al., 2013).

1.8 Vaccine approaches:

The pursuit of developing an effective vaccine for ASFV has been hindered due to the genetic complexity of the virus and our limited understanding of ASFV infection and immunity including virulence factors, the correlates of protection and reasons for the failure to develop neutralizing antibodies (Barasona et al., 2019; Gaudreault & Richt, 2019). Multiple vaccine development strategies have been employed which provide varying levels of protection. Inactivated virus particles do not provide protection while the modified live attenuated vaccine (MLAV) and subunit vaccine approaches have shown promising but inconsistent results (Gaudreault & Richt, 2019).

i. Antigen based subunit vaccines:

The development of subunit vaccines depends on the identification of immunogenic and protective ASFV antigens. Different ASFV proteins have been identified which can provide partial protection against lethal infection with virulent ASFV. The main targets for development of subunit vaccines have included ASFV structural protein (p30/CP204L, p54/E183L, p72/B646L, pp62/ CP530R) and membrane proteins for example CD2v/EP402R. These immunogenic proteins have been evaluated and tested either individually or as cocktails for their ability to induce protection against lethal challenge with ASFV (Gaudreault & Richt, 2019; Perez-Nunez et al., 2019). Initial studies were focused on delivery of recombinant proteins. and the first reported immunisation which induced protection against ASFV challenge was a baculovirus expressed CD2v protein. Two pigs immunised with recombinant CD2v protein were protected and survived challenge with virulent Eurasian genotype 1 isolate (E75) (Ruiz-

Gonzalvo et al., 1996). The structural proteins p54 (E183L) and p30 (CP204L) were evaluated individually in immunization and challenge experiment but did not induce protection. However, when pigs were immunised with a cocktail of both proteins and challenged with the E75 strain 50% of the pigs survived and a delay in the onset of clinical signs and reduced viremia were observed (Gomez-Puertas, RODRI´GUEZ, et al., 1998). In contrast, immunization of pigs with a cocktail of p30 (CP204L), p54 (E183L), p72 (B646L), p22 expressed in recombinant baculoviruses did not induced protection against the homologous challenge with ASFV Pr4 isolate. Although neutralizing antibodies against these proteins were induced these were insufficient to induce protection. This contrasted with previous observations using recombinant CD2v, since in these experiments protection of 2 pigs was observed in the absence of neutralizing antibodies (Neilan et al., 2004). Recently, it was shown that immunization of pigs with a pool of replication deficient recombinant adenoviruses expressing 8 antigens (B602L, B646L, CP204L, E183L, E199L, EP153R, F317L, MGF505-5R) conferred 100% protection to the pigs following a lethal challenge with OURT88/1(Goatley et al., 2020).

ii. DNA based sub-unit vaccines:

In pursuit of effective vaccines against ASFV, strategies for developing a DNA based subunit vaccine weretested. Similar molecular targets that were used in the antigen-based subunit vaccine were also evaluated in DNA based vaccines. A plasmid containing the P30/CP204Lgene fused with P54/E183L did not induce protection in pigs following an immunization and challenge experiment. However, pigs immunized with a DNA vaccine containing a swine leukocyte antigen SLA-II gene fused with

P30/CP204L and P54/E183L genes induced both cellular and antibody responses but didn't induce protection following challenge (Argilaguet et al., 2011), reviewed by (Gaudreault & Richt, 2019; Jia et al., 2017). In another experiment, instead of SLA-II the N-terminal extracellular domain of CD2v was fused to P30/CP204L and P54/E183L. Immunization of pigs with this construct induced both B and T-cell responses however no protection was observed (Argilaguet et al., 2012). Further investigation was performed by fusing the ubiquitin gene to the chimeric ASFV gene fusion construct to target proteins to the proteasome for presentation with SLA-I. Immunisation with this construct provided protection in a small percentage of pigs following challenge (Argilaguet et al., 2012). This indicated that cellular responses against ASFV correlated with protection, as no neutralizing antibodies were detected in the pigs that survived.

iii. Modified live attenuated vaccines:

The continued spread of ASFV in Southeast Asia, Africa and Europe has increased the demand of an effective vaccine to protect the pigs and to address the food security concerns in different regions. The most extensively studied and promising approach is the use of modified live attenuated vaccines (MLAV) which confer protection against the homologous strain. Some examples of heterologous protection have also been published (Gaudreault & Richt, 2019). Several MLAV candidates have been tested which induced good protection (up to 100%) in pigs when challenged with the lethal parental strain. However, in some cases adverse clinical signs were observed in vaccinated pigs including signs of a chronic form of disease and hence these could not be used as viable vaccines (Abrams et al., 2013; Leitao et al., 2001). Previous studies have shown that immunisation of pigs with naturally attenuated ASFV strain OURT88/3 followed by closely related OURT88/1 induced protection in pigs when

challenged with the either Benin97/1 (genotype 1) or Uganda (genotype X) isolates (King et al., 2011). The deletion of CD2v/EP402R from the ASFV strain BA71 highly attenuated the virus. Immunization of pigs with BA71ΔCD2v conferred protection when challenged with the parental strain (BA71), and with two heterologous ASFV virulent strains E75 and Georgia2007/1. The cross protection was correlated with the induction of $CD8^+$T cells which had ability for recall with both BA71 and E75 strains (Monteagudo et al., 2017). Another experiment confirmed that CD8+T cells are required for protection. In this experiment 4 pigs were immunised with the naturally attenuated ASFV OURT88/3 strain and CD8+ lymphocytes were depleted by treatment with anti-CD8+ antibodies. The pigs were challenged with the virulent OURT88/1 and 3 pigs developed acute ASF and were euthanized, the only pig that survived was not fully depleted of $CD8^+$ lymphocytes. This provided evidence for the importance of $CD8^+$ lymphocytes in protection against or survival from ASFV challenge (Oura et al., 2005). The naturally attenuated non-haemadsorbing ASFV strain NH/P68 confers protection in pigs against the virulent ASFV L60 and the protection was shown to be correlated with increased NK cell activity (Leitao et al., 2001). Several studies have been carried out using MLAV with virulence gene/genes deleted. A complete list of the MLAV tested with the protection outcome are shown on table 1.2 (see below).

Table 1.2; Modified and naturally live attenuated vaccine candidates that showed promising results for development of MLAV, adopted from (Arias et al., 2017) .

ASFV MLAV	**Challenge**	**Protection against**
NHV/P68	L60, ARM07	Heterologous strains

OURT88/3	OURT88/1, UG65	Homologous and Heterologous strains
Georgia07Δ9GL &DP96R/UK	Georgia07	Homologous strain
Ba71ΔCD2/EP402R	Ba71, E75, Georgia07	Homologous and Heterologous strains
BeninΔMGF	Benin 97/1	Homologous strain
NH/P68ΔA238L	NH/P68, ARM07	Homologous and Heterologous strains
BeninΔDP148R	Benin 97/1	Homologous strain

One of the MLAV candidate includes BeninΔDP148R, the DP148R gene is non-essential for virus replication in macrophages however its deletion significantly reduced the virulence of the virus *in vivo*. The BeninΔDP148R confers 100% protection in immunized pigs following challenge with parental pathogenic Benin 97/1 but adverse clinical signs associated with viremia and extended persistence of virus was observed (Reis et al., 2017).

1.9 ASFV Replication & Transcription:

ASFV contains a linear double-stranded DNA genome which varies from 170 to 193 kbp and contains 150-167 open reading frames depending on the isolate The variation in the genome size of different ASFV isolates is due to loss or gain of members of multigene families (MGFs 100, 110, 300, 360, 505/530 and family p22) (Dixon et al., 2013). However, small variations in the genome size among isolates are also associated with the variation in the number of short tandem repeats. The functions of encoded

proteins include enzymes and factors required for genome replication and transcription as well as a DNA repair system. In addition, virus structural proteins and other proteins required for assembly are encoded. Many virus proteins are not essential for replication in cells but have roles in inhibiting host defence mechanisms. Those identified include inhibitors of; apoptosis, type I interferon responses and stress responses (Dixon et al., 2019). In addition, two adhesion proteins, CD2v/EP402R and EP153R, that are the subject of this thesis, have roles in modulating the host response and are described in more detail later in this chapter (see section 1.18 & 1.19).

The virus mostly replicates in perinuclear area of the cytoplasm and does not require the host RNA polymerase (Salas et al., 1986) . An early stage of DNA replication occurs in the nucleus however the biological significance of such replication is still unclear (Rodriguez & Salas, 2013). Recently it was shown that QP509L, which encodes for a RNA helicase and is essential for viral replication, was detected in the nucleus. An siRNA targeting QP509L showed 99.4% reduction in viral progeny, indicating a possible role of the nucleus in viral replication (Freitas et al., 2019). The RNA transcription initiates immediately after the virus entry into the cell from partially uncoated core particles using the virus genome as template and the virus encoded transcription machinery packaged in the core (Galindo & Alonso, 2017). Early transcripts code for enzymes required for DNA replication as well as proteins involved in immune evasion. DNA replication initiates from about 6 hours post-infection in cytoplasmic factory areas. The early genes are transcribed by the virus encoded RNA polymerase in partially uncoated viral cores using enzymes packaged in the virus particle. The transcripts of ASFV are modified by addition of a 5′ cap and 3′ polyA tail (Rodriguez & Salas, 2013; Salas et al., 1981). Previous studies suggest that an NTPase enzyme encoded by C962R as well as F1055L protein are most likely to be involved

in initiating the viral DNA replication. The NTPase shows similarity to vaccinia virus D5 protein, which has an N-terminal primase domain and C-terminal helicase domain. The F1055L protein shows some similarity to UL-9 origin-binding protein of herpesvirus, UL-9 functions as a helicase and is essential for replication (De Silva et al., 2007; Iyer et al., 2001; Weller & Coen, 2012).

The proteins that are involved in ASFV replication also include; p11.6 histone like protein encoded by A104R, DNA topoisomerase type II encoded by P1192R, and DNA ligase (Coelho et al., 2016; Frouco et al., 2017; Hammond-Kosack et al., 1992). The viral proteins that are involved in replication of the virus genome include a DNA polymerase encoded by G1211R (Hubner et al., 2018) and a proliferating cell nuclear antigen PCNA-like protein, encoded by E301R. E301R may facilitate the attachment of DNA polymerase to the viral DNA (Granja et al., 2004; Oliveros et al., 1997),

Once the DNA replication initiates in the cytoplasm a shift in pattern of virus gene transcription occurs. Late transcripts include those coding for virus structural proteins and those involved in assembly as well as enzymes and factors packaged in the virus core for use early in the next round of infection. DNA replication involves formation of head to head concatemers (Salas et al., 1986). These concatemeric genomes are processed into single units containing terminal crosslinks and are packaged into virus particles within the viral factories (Gonzalez et al., 1986). The proteins involved in processing of concatemeric genomes into unit length include an ERCC4- like nuclease encoded by EP364R, and the lambda type exonuclease encoded by D345L may also be involved in this process (Iyer et al., 2006). The mature virus particle contains the RNA transcription machinery and early transcription factors which are also encoded in the virus genome, hence virus transcription is independent of the host transcription machinery (Tulman et al., 2009). Previous studies have shown that inhibition of the

cellular RNA polymerase II had no effect on the viral transcription and therefore this cellular activity is not essential. This indicates that all temporal classes of ASFV genes are transcribed by the virus-encoded RNA polymerase (Salas et al., 1988). It was also shown that the extracts obtained from mature virus particles were transcription competent. The virus encodes proteins for transcription and modification of viral mRNA which includes; RNA polymerase, a poly (A) polymerase, and mRNA capping enzyme (Salas et al., 1981). The ASFV genes do not contain introns and splicing of transcripts is not known to occur, as expected from the cytoplasmic replication of ASFV. Gene expression is regulated by cis-DNA elements (promoters) that are recognised by temporally expressed sequence specific transcription factors. The genes contain a short promoter sequence that is recognised by viral transcriptional factors specific for viral gene expression at different stages (Sanchez et al., 2013). Recent studies on the ASFV proteome and transcriptome have shown 21 genes (19% of the genome) are involved in the transcription and modification of mRNAs (see table 1.1, see figure 1.4) (Alejo et al., 2018; Cackett et al., 2020). The virus genes are defined based on the differential expression patterns obtained using RNA-seq and CAGE-seq into different classes; early (up-regulated), early (down-regulated), late (up-regulated) and late (down-regulated) genes. Some genes were expressed at a more constant level at both early and late times (Cackett et al., 2020).

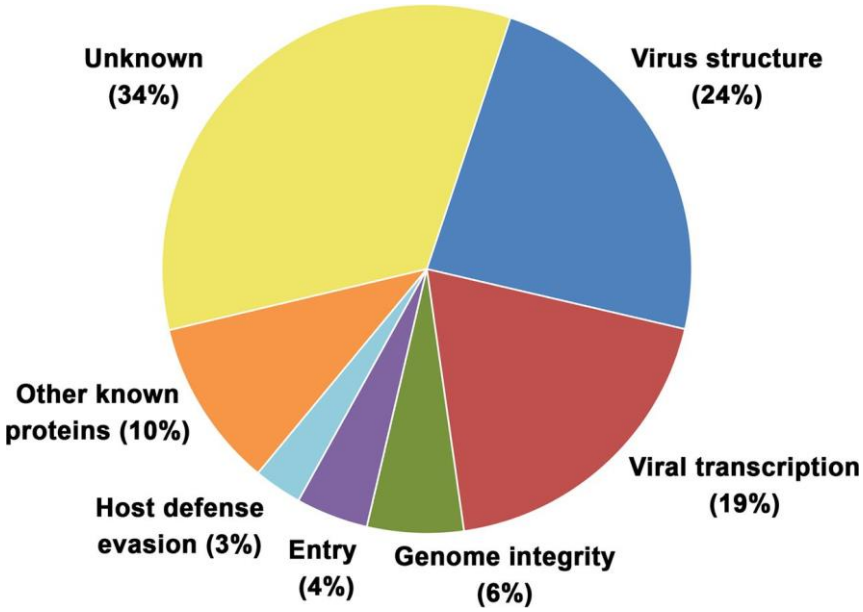

Figure 1.4: Classification of ASFV proteins: the proteins identified in ASFV proteome are shown based on their functional characteristics, source; (Alejo et al., 2018).

Table 1.1: **ASFV genes involved in RNA transcription and modification** (Alejo et al., 2018; Freitas et al., 2019; Rodriguez & Salas, 2013).

S.No	ASFV encoded genes	Role in transcription and modification
1.	P1192R	DNA topoisomerase ll
2.	D250R	mRNA decapping enzyme
3.	NP868R	Capping enzyme
4.	C475L	Poly(A) polymerase
5.	C315R	TFllB
6.	I243L	TFllS
7.	G1340L	VACV A7-like
8.	B962L	VACV I8-like
9.	B175L	VACV A1-like

10.	B385R	VACV A2-like
11.	A859L	VACV A18-like
12.	NP140L, EP1242L, H359L, D205R, C147L, D339L, CP80R.	RNA polymerase subunits (RPB1, RPB2, RPB3, RPB5, RPB6, RPB7, RPB10)
13.	Q706L, QP509L	RNA helicase

1.10 ASFV genome and proteins involved in immune evasion:

The ASFV genome is a linear double-stranded DNA molecule that ranges in length between isolates from about 170 to 193 kbp and contains 151-167 ORFs (described in section 1.9). The genes encoded are closely spaced and encoded on both DNA strands, the genes do not contain introns and splicing of transcripts does not occur. The gene transcription is regulated by a short promoter sequence present upstream of each gene and these are recognised by the viral RNA polymerase (see section 1.9, transcription) (Dixon et al., 2013). The functions of encoded proteins include enzymes and factors required for genome replication and transcription as well as a DNA repair system. In addition, virus structural proteins and other proteins required for assembly are encoded. Many virus proteins are not essential for replication in cells but have roles in inhibiting host defence mechanisms (see figure 1.6). Those identified include inhibitors of; apoptosis, type I interferon responses and stress responses (Dixon et al., 2019).

Figure 1.6 ASFV genome organisation: A graphical abstract of ASFV Georgia genome showing different genes. Each arrow represents a gene, the colour of the arrow indicates the function and the direction of the arrow represent the direction of the reading frame, source; (Dixon et al., 2013).

a) Interferon inhibitory proteins:

The ASFV genome contains multiple genes that inhibit type I interferon responses in infected macrophages. These genes include multigene families 360 (MGF360) and MGF530/505 which are reported to suppress type I interferon response as deletion of genes that belong to these families showed an increased induction of type 1 IFN and the genes stimulated by type I IFN in infected macrophages (Dixon et al., 2019). Deletion of the members of MGFs did not reduce virus replication in macrophages and these genes are not essential for replication (Reis et al., 2016). The A276R gene (also

named MGF360-15R) inhibits the induction of type I IFN via both TLR3 and the cytosolic sensing pathways by inhibiting IRF3 through a mechanism independent of IRF7 and NF-κB transcription factors. Another gene A528R (also named MGF505-7R) inhibits the type I IFN induction through the inhibition of both IRF3 and NF-κB transcription factors (Correia et al., 2013). The ASFV pI329 L protein is similar to cellular TLR3; it is a highly glycosylated protein expressed in the cell membranes and inhibits TLR3-mediated induction of IFN- β and activation of both NF-κB and IRF3. The pI329 L protein was indicated to target TRIF, an adaptor protein in this pathway (de Oliveira et al., 2011). The ASFV A528R gene encodes a protein that can inhibit both the type I and type II IFN signalling pathways, hence limiting the impact of IFN I and IFN II on induction of the JAK-STAT pathway and expression of interferon stimulated genes (ISGs), however, the mechanism by which A528R suppresses the induction of IFNs is not well described (Dixon et al., 2019). An attenuated recombinant virus which induces good levels of protection, BeninΔMGF (with deletion of MGF360-10L, 11L, 12L, 13L, 14L- MGF530/505-1R, 2R and 3R and interruption of MGF360-9L and MGF530/505-4R), induced expression of moderate levels of IFN-β mRNA in macrophages *in vitro* while in virulent Benin 97/1 the levels of IFN-β mRNA expressed were barely detectable (Reis et al., 2016). These results confirm the importance of the type I IFN system in controlling ASFV replication and activating a protective immune response in infected pigs. An increased induction of type I IFN in infected macrophages would lead to amplification of this signal in neighbouring cells and induction of ISGs to activate innate responses and reduce virus replication (Dixon et al., 2019).

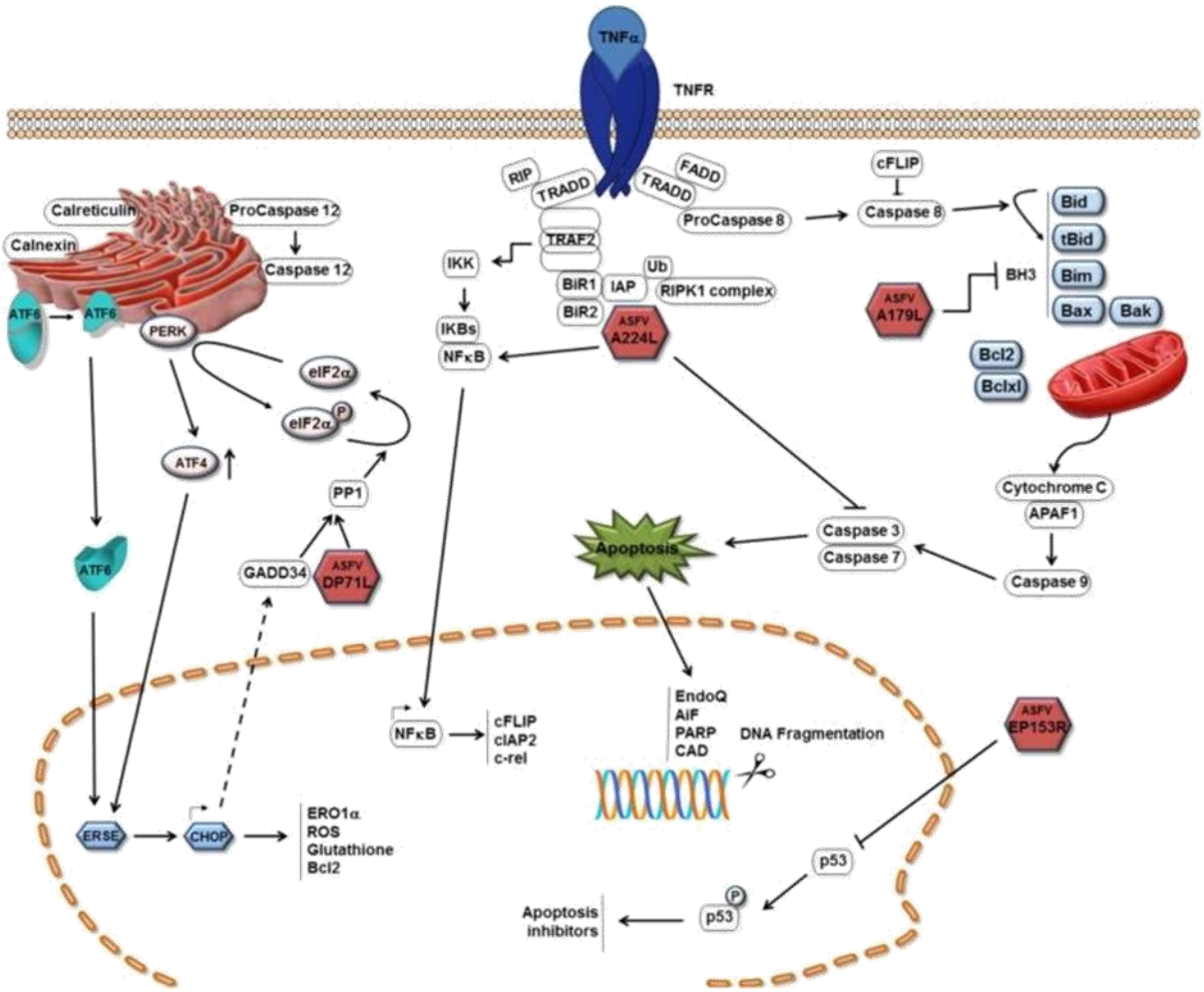

<u>Figure 1.7: Mechanisms of apoptosis inhibition by ASFV;</u> the graphical abstract of the pathways by which ASFV inhibits induction of apoptosis in infected cells, source; (Dixon et al., 2019).

b) Apoptosis inhibitory proteins:

The induction of apoptosis in cells has the effect of limiting replication and spread of viral progeny. The ASFV genome encodes for different proteins that inhibit apoptosis, to prolong cell survival such that progeny virions are produced. These proteins are described below.

- **Inhibitor of apoptosis family member (IAP):** The inhibitor of apoptosis protein family (IAP) were first identified in baculovirus and shown to inhibit cell death in insect cells by binding and stabilising an insect cellular IAP (Clem, 2015). In mammalian cells, the cellular IAPs (cIAP) were reported as proteins that bound indirectly to TNFR2 through TRAF1 and TRAF2 via BIR domains. A single cellular IAP molecule binds to a TRAF2 trimer and inhibits caspase 3 and caspase-mediated apoptosis, the cIAP bind to TRAF1 via the BIR1 domain (Varfolomeev et al., 2007) while the BIR2 domain bind to the processed caspase 3 and the inhibitory domain. The BIR2 domain can inhibit both caspase 3 and 7 (see figure 1.7) (Takahashi et al., 1998)

The ASFV genome contains an ORF, A224L, which codes for an IAP-like protein. The A224L protein is 224 amino acids long and well conserved in different ASFV isolates (Dixon et al., 2017). The A224L protein also contains a BIR domain which is a hallmark of the IAP family. Expression of the A224L IAP-like protein in cells substantially inhibited caspase 3 activity and cell death when cells were treated with TNF-α. Multiple studies have investigated the role of A224L, the transient expression of A224L inhibited cell death induced by cycloheximide or staurosporine. A deletion mutant lacking A224L was shown to have an increase in proteolytic cleavage of caspase 3 compared to the cells infected with wild type virus, suggesting that A224L may directly interact with the processed fragment of caspase 3 (Nogal et al., 2001). The transient expression of A224L has been shown to activate an NF-kB-dependent reporter, the activation of NF-kB, mediated by TNFR2, can inhibit apoptotic cell death by activating transcription of several anti-apoptotic genes including IAP and Bcl-2 family members (Rodriguez et al., 2002). Deletion of the A224L from the virulent Malawi isolate did not affect levels

of virus replication *in vitro* and did not reduce virulence in infected pigs. The published data has confirmed that A224L IAP-like protein can inhibit cell death in mammalian cells, however, no effect was observed on ASFV replication *in vitro* or virulence *in vivo* following the deletion of the gene from a virulent isolate (Neilan et al., 1997).

- **Bcl-2 family member:**

The ASFV genome encodes for an A179L protein which is a member of the B-cell lymphoma-2 (Bcl-2) family. Members of this family can be either pro-apoptotic or anti-apoptotic depending on the number of Bcl-2 homology regions and their interaction with proteins from the Bcl-2 family (Dixon et al., 2019). The A179 L protein contains domains similar to all BH domains and interacts with several pro-apoptotic BH3 only domain proteins. It has been shown that A179 L binds with the highest affinity to the BH3 domain of truncated Bid, Bim, Puma and also with the downstream Bak and Bax proteins (see figure 1.7) (Banjara et al., 2017). It was also shown that A179 L protein has a potential role in inhibiting autophagy mediated by binding to the BH3 domain of Beclin-1 (Hernaez et al., 2013).

- **C-type lectin family;**

The ASFV genome contains an ORF, EP153R, which encodes for a protein containing a C-type lectin-like domain (CTLD) which is a hallmark of the C-type lectin family. The EP153R is non-essential for virus replication but has been reported to inhibit apoptosis, acting through the p53 pathway and caspase 3 activation (see figure 1.7) (Hurtado et al., 2004). The role of EP153R in ASFV infection and immune evasion is described in detail in (section 1.16).

This section provides an overview of the cell biology of the secretory pathway and an introduction to the proteins investigated in this study, since part of the work described in this thesis is linked with the processing and expression of membrane proteins CD2v and EP153R.

1.11 Translation:

Since viruses do not encode the cell protein translation machinery they must use the host cell protein translation machinery. The multi-subunit eukaryotic translation initiation factor, eIF4F, is comprised of three proteins; a cap-binding protein (eIF4E) that binds with the 5' cap structure of the cellular mRNAs, an ATP-dependent RNA helicase (eIF4A) that unwinds the secondary structure of the mRNA at the initiation codon. These proteins are assembled on a large scaffolding protein elf4G which facilitates ribosome recruitment and processing of capped host mRNAs (Walsh, 2010). The cap-binding protein and the poly-A binding protein interact primarily with the N-terminal domain of the large scaffolding protein elf4G, this interaction allows the recruitment of mRNA (Imataka et al., 1998). The RNA helicase, eIF4A, mitogen-activated kinase 1 (Mnk-1) and the multi-subunit eIF3 interact with the C-terminal domain of elf4G and form a complex (eIF) that binds to the 40S ribosomal subunit (Prevot et al., 2003). In eukaryotic cells, the functions of eIF4F are regulated by intracellular and extracellular signals through the process of phosphorylation. After the factors are assembled on the cap, the helicase activity of the eIF4F complex unwinds the secondary structure in the 5'- untranslated region to facilitate the scanning by the ribosome (Ling et al., 2005). The pre-initiation complex present on the small subunit of the ribosome moves along the 5- untranslated region until it encounters a start codon. The large ribosomal subunit binds to the pre-initiation complex and the translation of mRNA is initiated (Walsh, 2010). Moreover, there are several eIF4E-binding proteins

(4E-BPs) that can sequester the eIF4E, in the hypo-phosphorylated state. The 4E-BPs bind to the same site on eIF4E as eIF4G and this inhibits the formation of the eIF4F complex (Richter & Sonenberg, 2005). The hyperphosphorylation of 4E-BPs results in the release of these proteins from eIF4E, and their subsequent binding with eIF4G, thereby assembling an active eIF4F complex (Gingras et al., 2001). Viruses have adopted multiple mechanisms to target the eIF4F complex, for example; several RNA viruses encode proteases that can cleave eIF4G and inhibit host protein synthesis by inactivating the eIF4F complex and upregulating the translation of the viral mRNA by cap-dependent process (Lloyd, 2006). Several DNA viruses have also been reported to influence the eIF4F complex, for instance, the Adenovirus induce dephosphorylation of eIF4E and 4E-BPs at later stages of infection and thus inhibit the cap-dependent translation of host mRNA (Castello et al., 2009). Other DNA viruses such as herpes simplex virus type-1 and vaccinia virus mRNAs are translated in a cap-dependent manner. These viruses can induce the formation of the eIF4F complex to enhance viral protein synthesis (Walsh et al., 2008). The mRNA transcripts of ASFV are capped and polyadenylated, although it encodes for several enzymatic activities, ASFV relies on the cellular translation machinery for protein synthesis (Kuznar et al., 1980). ASFV also promotes the formation of the eIF4F complex by phosphorylating the eIF4E and eIF4G at Ser209 and Ser1108, respectively, the phosphorylation of these residues correlates with the upregulation of viral protein synthesis. It was shown that the inhibition of phosphorylation of either eIF4GI or eIF4E partially affects viral protein synthesis (Castello et al., 2009). ASFV infection also results in the distribution of translation initiation and elongation factors within and around the viral factories. ASFV infections also induce phosphorylation of eIF4E and increased levels of eIF4F (Walsh, 2010).

1.12 Cellular secretory pathway:

The term ‘secretory pathway’ refers to the dynamic movement of proteins and lipids between sub-cellular compartments. Several processes in the biogenesis of proteins are regulated by the movement and progression through this pathway including; post-translation modification, packaging and transport of the proteins within and outside the cells (Wiedemann & Cockcroft., 1998). More than 30% of all proteins expressed by a eukaryotic cell are exported from the ER and transported to the *cis*-Golgi and the *trans*-Golgi network (TGN), where specific folding, glycosylation and export reactions take place (De Matteis & Luini., 2008). The transport of the nascent protein begins after they are translocated into the ER. The folding and the addition of core N-glycans occur in the ER. The proteins are then exported in the COPII vesicles to the ER-Golgi intermediate compartment (ERGIC) and eventually transported to the Golgi complex. The cargo is first delivered to the *cis*-Golgi and then gradually progresses to the TGN, the glycosylation of the cargo proteins occur during progress from the cis- Golgi to the TGN within the maturing cisternae (Stanley et al., 2009). The resident Golgi and ER proteins are recycled in the COPI vesicles (Arakel & Schwappach., 2018). The cargo proteins are sorted in the TGN into different vesicles and exported to their final destination; the plasma membrane or lysosomes (De Matteis & Luini., 2008). The TGN serves as the sorting station for the proteins delivered via the secretory pathway and the vesicles that deliver the protein to its site of action are derived from the membranes of TGN (Clermont et al., 1995). The movement of the proteins through the secretory pathway utilizes energy and is an ATP-dependent process. However, to maintain the

protein quality the cells utilize 2 main quality control pathways; the unfolded protein response (UPR) pathway and the ER-associated degradation (ERAD) pathway (Hwang & Qi, 2018). The UPR pathway is activated in response to the cellular stress generated by the accumulation of unfolded proteins in the ER, this pathway is also triggered in response to physical conditions and maintains homeostatic control (Ellgaard & Helenius, 2003). When the proteins are unfolded, they accumulate in the ER in excess and this is detected by the UPR system via different sensors (IRE1, PERK, ATF6) that trigger multiple responses. For instance, the responses include increase in the level of chaperones to facilitate protein folding, reduced levels of protein synthesis and increased delivery of proteins to the ER degradation system (Ron & Walter, 2007). The ERAD degrades the unfolded proteins by incorporation of a poly-ubiquitin signal thus directing them to the proteasome for degradation (Meusser et al., 2005).

Viruses exploit the cellular secretory pathway during the infection to control the transport of host proteins (McCrossan *et al*.., 2020). ASFV also modulates the cellular secretory pathway. Reorganisation of membrane transport mechanisms may enable ASFV to disrupt the expression of host membrane proteins (Netherton *et al*.,2006). ASFV has been reported to redistribute the TGN, this was detected by staining the TGN distal secretory pathway marker protein TGN46 and the TGN Adaptor protein complex AP1 by immunofluorescence. The TGN46 signal disappeared at 16 hours post-infection *in vitro* suggesting the redistribution of the TGN46 to other membrane compartments. The loss of the TGN46 signals was not due to the degradation of TGN46, as the level of TGN46 remained the same in infected and uninfected cells. The site of redistribution is unclear, the plasma membrane and the ER are the proposed sites for TGN redistribution (McCrossan *et al*.., 2020). Another study was carried out to confirm the effects of ASFV infection on trafficking of Cathepsin D and the function of the TGN.

This indicated that ASFV slows down the transport of Cathepsin D to the lysosome, suggesting that ASFV blocks the transport of Cathepsin D to the lysosomal compartments (McCrossan *et al*.., 2020). A recent study, using a temperature-sensitive G protein of vesicular stomatitis virus, reported that the disruption of the TGN components is microtubule-dependent and that ASFV significantly slows down the rate at which proteins are transported to the cell surface (Netherton *et al*.,2020).

1.13 Transmembrane Proteins:

Transmembrane proteins are a type of integral membrane protein that passes through the lipid bilayer of the cell membrane such that the polypeptide chain is exposed on both sides of the membrane. The orientation and insertion of the transmembrane proteins within the ER lipid bilayer is determined by the sequence and function of the cytosolic and non-cytosolic domains of the transmembrane proteins (Mothes et al., 1997). The extracellular and cytosolic domains of transmembrane proteins contain hydrophilic amino acids residues whereas the transmembrane domain is embedded within the lipid bilayer and is composed of hydrophobic amino acids residues. The α-helix of a transmembrane domain contains 18-21 amino acid residues and is sufficient to span the usual length of a lipid bilayer. Since transmembrane proteins penetrate through the cell membrane; they are in contact with the cytoplasm at one side of the membrane and with the extracellular matrix or membrane organelle contents on the other (Albers W.,2012, Albert B. 2002).

1.13.1 Classification of membrane proteins on basis of structure:

The endoplasmic reticulum (ER) is the main assembly site for all membrane proteins. The topology of the membrane proteins is determined at the ER as the majority of these proteins contains a hydrophobic stretch of amino acids which is integrated into the ER

membrane (Alder & Johnson., 2004). Depending on the correct folding and orientation in the ER, these proteins are then transported to their localization sites (Pryer et al., 1992). The structure of transmembrane proteins has been resolved by X-ray crystallography, electron microscopy and Nuclear magnetic resonance spectrometry and are classified into two basic types; (i) alpha-helical, (ii) beta-barrels (Ubarretxena-Belandia & Stokes., 2010).

(i) Alpha-helical proteins; In eukaryotic cells, the α-helical transmembrane proteins are present on the plasma membrane and constitute a major proportion of transmembrane proteins. These membrane proteins are involved in several major cellular processes including signalling and ion exchange (Almen et al., 2009). In this class of proteins, the α-helical conformation is due to the presence of a highly hydrophobic domain embedded in the lipid bilayer and a hydrophilic domain (present inside the penetrating portion of the transmembrane protein). These domains are linked by polar peptide bonds and can form hydrogen bonds which give rise to the α-helical structure. The number of TM domains may vary in helical membrane proteins and the helices embedded in the membrane determine the folds of a helical membrane protein. The folding mechanism of these proteins into their native structure is poorly understood. (Bocharov et al., 2010, McKay et al., 2018). Based on the number of TM helices, alpha-helical transmembrane proteins are classified into two types; (a) Single-span transmembrane α-helix protein, (b) Multi-span transmembrane α-helix protein (McKay et al., 2018).

a) **Single-span transmembrane α-helix proteins** are also known as bitopic proteins as they contain one transmembrane domain. These proteins fully span the cell membrane and contain an extracellular domain on one side and a cytoplasmic domain on the other side (Albert B. 2002). These transmembrane proteins comprise 50% of all transmembrane proteins. The TM domain contains a hydrophobic patch of 20 amino acids that functions as an anchor connecting the two extra-membranous parts of the protein (Zviling et al., 2007). However, the function of single-pass transmembrane proteins is not limited to anchoring, it was shown that human glycophorin A dimerization is driven by the interactions between its transmembrane domains (Bormann et al., 1989). When two single-pass proteins penetrate the plasma membrane, they interact may with one other by a non-covalent bond and form a dimer. Two types of dimer can be formed, a homodimer that contain two of the same single-pass proteins and a heterodimer that contains two different single-pass proteins. Earlier studies suggest that the homo- and hetero-dimerization involves the extracellular and cytoplasmic domains, however, recent studies have shown that the TM domain is critical for the modulation and dimerization of bitopic proteins (Singh & Jois, 2018).

b) **Multi-span transmembrane α-helix protein:** Multi-span proteins are also called polytopic protein as they contain two or more transmembrane domains and the polypeptide chain passes the cell membrane many times (Albert B., 2002). The active site of polytopic proteins is located within the transmembrane helical bundle which interact and form a complex three-dimensional TM structure (Zviling et al., 2007). Initially, when multiple

membrane spanning proteins are inserted in the membrane, the transmembrane domains are apart from one another (Cymer et al., 2012). As they pass through the lipid bilayer, these proteins interact with lipid molecules through non-covalent bonds and eventually, the helix-helix interaction also begins as the protein segments approach each other. An example of a multiple span protein is GPRC (G protein-coupled receptor) (Neumann et al., 2014).

(i) **Transmembrane β-barrels;** In eukaryotic cells, one of the two main classes of integral membrane proteins are β-barrel membrane proteins and they are exclusively present on the outer membrane. The topology of the transmembrane protein containing the beta-barrel have the simplest up and down orientation reflecting their common ancestral origin in Eukaryotes (Walther et al., 2009). The β-barrel membrane proteins are involved in signalling, membrane biogenesis and have a significant role in other key cellular processes including acting as transporters, porins, enzymes, virulence factors and receptors (Fairman et al., 2011). Beta barrel structure is made up of β-sheets. These β-sheets are arranged in an anti-parallel organisation to form a cylindrical structure called a beta-barrel. As these structures are hollow inside, they form porins through which polar substances can enter or leave the cell (Hohr et al., 2018; Sun et al., 2004). The amino acids present on the exterior surface of the beta-barrel structure are hydrophobic, as they as in continuous contact with lipid molecules of the membrane while the amino acids on the inner surface of the beta-barrel structure are hydrophilic amino acids (Zhang & Han, 2016).

1.13.2 Classification of transmembrane protein based on topology:

Membrane topology provides two-dimensional structural information about a membrane protein, indicating the number of transmembrane (TM) segments and the orientation of soluble domains relative to the plane of the membrane. TM segments are oriented correctly during biosynthesis of the membrane protein, as membrane proteins are co-translationally translocated and inserted across the membrane (Lee & Kim., 2014). Although each membrane protein must contain some phase-generating signal (topogenic signals), the membrane topology of proteins is also influenced by translocation components and the membrane environment (Lee & Kim., 2014).

Transmembrane proteins are also classified based on the position of the amino and carboxyl-termini on the different sides of the lipid bilayer (Albert B., 2002). The determination of the orientation of the transmembrane proteins is linked with the charged amino acids and follow the “in” and “out” rule. The positively charged amino acids within the transmembrane domain are preponderantly found within the cytoplasmic facet of the membrane, and this phenomenon is known as the “positive inside rule” (Lee & Kim., 2014).

Several mutation studies have shown that the addition or removal of charged residues flanking the TM domain influences the orientation of the TM domain according to a positive inside rule. This demonstrates that the positively charged amino acids residues in the flanking region of the TM domain are prominent "inside" topogenic signals

(Almen et al., 2009; Lerch-Bader et al., 2008; Sakaguchi et al., 1992). Based on topology, transmembrane proteins are classified into four major types; Types I, II, III and IV.

Type I transmembrane proteins are anchored to the lipid membrane by stop-transfer anchor sequences and their N-terminal domains are targeted to the lumen of the endoplasmic reticulum (ER) during synthesis. However, types II and III transmembrane proteins are anchored with a signal anchor sequence, type II has a C-terminal domain that targets the ER lumen, whereas type III has an N-terminal domain that targets the ER lumen. Type IV is subdivided into IVA with an N-terminal cytoplasmic targeting domain and IVB with an N-terminal luminal targeting domain (Lodish et al., 2007). The implications for the division in the four types are especially manifest at the time of ER bound translation and translocation when the protein has to be passed through the ER membrane in a direction dependent on the sequence and type of membrane protein.

1.14 Protein translocation into ER:

In eukaryotic cells, the endoplasmic reticulum is where the secretory pathway begins; All proteins enter the ER or are translocated either after or simultaneously as they are synthesized on cytoplasmic ribosomes, except the cytoplasmic resident proteins (Avendano-Monsalve et al., 2020). These include, proteins that are secreted from the cells, embedded in the plasma membrane, transmembrane proteins, integral cell surface proteins and proteins on intracellular compartments that are assembled in the ER (Sabatini et al., 1982). Before reaching their final destinations, these proteins are folded, assembled, and modified in the ER, a third of the eukaryotic proteome is processed in the ER (Wang & Ye, 2020). Protein translocation is a process by which proteins move between cellular compartments. It is a critical process in protein biogenesis and involves partial or complete translocation of proteins across the eukaryotic endoplasmic reticulum membrane or the prokaryotic plasma membrane (Rapoport, 2007). In protein biogenesis, translocation plays a central role and is linked to the protein quality control process, errors in protein folding, post-translational modifications and localization

(Wang & Ye, 2021). The proteins synthesized in the cytoplasm often need to traverse across the lipid bilayers of cellular compartments via a proteinaceous channel to reach their destination (Wang & Ye, 2021). The transport occurs through the hydrophilic protein conducting channel known as the Sec translocon which is central to this task (Niesen et al., 2020). This channel is involved in both the translocation of nascent proteins across cell membranes and the integration of proteins into the lipid bilayer (Matlack et al., 1998). The Sec translocon channels are formed by a conserved heterotrimeric membrane protein complex the Sec61 (eukaryotes) or SecY complex (prokaryotes) (Wu et al., 2019). Translocation of proteins can occur via two highly conserved pathways; (i) co-translational translocation pathway, during which insertion into the ER lumen or membrane occurs simultaneously with protein synthesis, (ii) post-translational translocation pathway; in which translocation occurs after a polypeptide has been completely synthesized (Kellogg et al., 2021).

(i) Co-translational translocation pathway; This translocation pathway is utilized by proteins bearing a signal peptide at the amino-terminus (N-terminal) or containing a hydrophobic transmembrane domain (TMD). The proteins synthesized by this mechanism are translated by ER bound ribosomes, the insertion of nascent proteins into the ER lumen or membrane occurs concurrently with translation (Zimmermann et al., 2011). The N terminus of the nascent protein bearing the signal sequence emerges from the larger subunit of the ribosome. The signal sequence contains a hydrophobic chain of 6-12 amino acids that interacts with signal recognition protein (SRP) present in the cytosol. The SRP contains three binding domains; the first domain binds the signal peptide immediately after it emerges from the larger subunit of the ribosome. The second domain binds to the larger subunit of the ribosome and ceases further translation of the protein. The third domain binds to the SRP receptor located in the ER

membrane near the Sec61 translocon (Akopian et al., 2013). This interaction of SRP (3rd domain) with its receptor mediates the formation of a complex on the ER membrane, the signal peptide is transferred to the Sec61 translocon causing the disassociation of SRP from the ribosome (Nyathi et al., 2013). The translation of the polypeptide resumes after the disengagement of the SRP from the ribosome. The Sec61 translocon receives nascent chains and utilizes the energy from translating ribosomes to transport polypeptides across the ER membrane into the lumen (Zimmermann et al., 2011). The signal sequence at the N-terminus is cleaved from all secreted proteins and many transmembrane proteins by proteins called signal peptidases, which are present in the ER (Hegde & Bernstein., 2006). Besides importing protein into the ER lumen Sec61 has other functions, it contains a hinge that opens laterally during the translocation and allows the proteins to insert into the ER membrane. This occurs when a peptide containing the TMD passes through the Sec61 translocon (Mandon et al., 2009). The translocation of membrane proteins is linked to the membrane integration of hydrophobic TMDs via a translocon lateral gate (Zimmermann et al., 2011). In co-translational translocation the proteins directed to the ER contain at least one transmembrane domain, these are hydrophobic regions that primarily consist of nonpolar amino acid residues and can pass through the bilayer once or several times (Sharpe et al., 2010). When inserted in the ER membrane these proteins maintain their orientation in the ER and the Golgi, hence, the regions facing the cytosol in the ER will face the cytosol when it reaches its ultimate destination (Lamond., 2002). Therefore, it’s essential that these domains are inserted in the ER membrane with a specific orientation and this is determined by the charge of the amino acids on either side of the signal sequence. The ER lumen contains Ca+ ions and giving the ER a net positive charge while the cytosol maintains a net negative charge. The positively charged amino

acids will preferentially orient towards the cytosol while negatively charged amino acids will orient towards the ER lumen. The orientation of the first hydrophobic TMD of a protein determines the orientation of the subsequent TMDs (Dowhan & Bogdanov., 2009). Finally, the protein is folded in the ER lumen and the correctly folded proteins are then transported to the Golgi apparatus, where they are further modified and transported to the lysosomes or the plasma membrane (Swanton & Bulleid, 2003). (ii) Post-translational translocation; is similar to the protein import that occurs in other organelles. This pathway is utilized by proteins bearing a suboptimal signal sequence or the tail-anchored membrane proteins carrying a single membrane targeting TMD at the C-terminus (Wang & Ye, 2020). The translocation occurs after the nascent polypeptide is completely synthesized or after the protein translation is completed in the cytosol before ER targeting. The nascent polypeptides are retained in an unfolded and translocation competent state by cytosolic chaperones (HSP70 or the Bag6-SGTA holdase system) (Ngosuwan et al., 2003). These proteins contain an ER signal sequence that is recognized and bound by the Sec61 translocon with the aid of accessory proteins Sec62 and Sec63 which facilitate the translocation (Gemmer & Forster., 2020). The interaction of the Sec62-Sec63 sub-complex to the Sec61 translocon triggers the opening of the lateral gate and induces the insertion of low hydrophobic signal sequences into the channel (Itskanov & Park., 2019; Wu et al., 2019). This signal sequence can be located anywhere on the peptide and is composed of a region of hydrophobic amino acid flanked by two hydrophilic regions. The attached chaperones separate from the remaining polypeptide as the signal sequence is pushed into the lateral gate (Matlack et al., 1998). When the protein binds the Sec61 translocon a small part of the protein is extended into the ER lumen and is immediately bound by BiP which prevents the protein from slipping back out of the channel. Particles in a fluid are subject

to random movement called Brownian motion, and this causes new regions to emerge in the ER lumen. The BiP binds to the newly imported regions and prevents slipping back of the peptide and the Brownian motion assists the pulling of the polypeptide into the ER (Rapoport, 2007). The transport of the peptide into the ER doesn't require energy, however, releasing the BiP from the protein utilizes energy from ATP hydrolysis. In tail-anchored proteins, Bag6 and SGTA form a chaperone complex that interacts with an ATPase (TRC40) for membrane integration (Chio et al., 2017).

1.15 Process of glycosylation:

Glycosylation is a very common modification of protein and lipid, and most glycosylation reactions occur in the Golgi (Stanley, 2011). During the co-translational translocation of proteins with glycosylation signals into the ER, N-glycans are added to a proportion of the Asn-X-Ser/Thr consensus motif for N-linked glycosylation (Kelleher & Gilmore, 2006). The presence of this consensus motif doesn't always reflect the degree of glycosylation. Following translocation of glycoproteins into the *cis*-Golgi they are loaded with mannose residues that are attached to GlcNAc2. Typically 8-9 mannose residues are loaded on each glycosylation site (Stanley et al., 2015). In the case of glycoproteins that are expressed on the cell surface or secreted from cells, these mannose residues may remain unchanged when they progress through the Golgi, although N-glycans are routinely processed in the Golgi. The *cis*-Golgi contains α-mannosidases that trim the linear chain of 8-9 mannose residues to produce Man5GlcNAc2Asn; a substrate of the medial Golgi GT GlcNAcT-I (Stanley et al., 2009). The modification by GlcNAcT-I and the addition of GlcNAc to Man5GlcNAc2Asn induces the synthesis of complex and hybrid N-linked glycans. The latter keeps 5 mannose residues and adds Gal, sialic acid and other sugars to the arm that received GlcNAc. However, the complex N-linked glycan removes 2 from the 5

mannose residues and replaces it with another GlcNAc to produce complex N-glycans. In some cases, the complex N-glycans branched further (up to 6 times) and several more sugars may be added such as Gal, GlcNAc, GalNAc, Fuc, Sia, and disaccharide units (Stanley et al., 2015). The process of glycosylation is controlled by a variety of Glucosyltransferases, sugar synthases and transporters present in the Golgi. Other factors also influence this process such as the luminal environment (e.g; PH) or the structure and organisation of Golgi membranes. The variation of the PH can interfere with the process of glycosylation, the Golgi regulates the PH through an anion channel (Maeda & Kinoshita, 2010). A delay in the progression of glycoproteins within the secretory pathway has been observed in cells that are deficient or lacking the anion channels, and the glycoproteins that progress through the pathway are often truncated in these cells. In another study, the CMP-Sia or GDP-fucose transporter were knocked-down using RNAi and a delay in progression of the glycoproteins was observed. A reduced amount of the nucleotide sugar transporter in cells can produce glycoproteins with truncated glycans which eventually accumulate in the Golgi and do not proceed further through the secretory pathway. This triggers the ER stress pathways in the cells (Xu et al., 2010). The addition of N-glycans by the glycosyltransferase and the further processing by glycosidase occurs in the Golgi in a stepwise manner, the glycans gradually build up during progression and exit through the Golgi membrane. hence, the level and type of glycans can be used as a marker for glycoproteins that pass through the Golgi. The high mannose N-glycans present in glycoproteins in the cis Golgi are susceptible to the cleavage by Endo H or N-glycansae. However, complex N-glycans are resistant to Endo H and remain sensitive to N-glycanase (Stanley, 2011).

1.16 Role of EP153R in ASFV infection:

Lectins are generally considered as non-enzymatic proteins acting as receptors for carbohydrate ligands (Kaltner & Gabius, 2001). C-type lectins are Ca2+ -dependent glycan-binding proteins. The property of binding to glycans is due to the amino acid residues that cooperate with Ca2+ to bind the hydroxyl groups of sugars. C-type lectins usually oligomerize and form homodimers or homotrimers which enable them to interact with multivalent ligands (Cummings & McEver., 2017). C-type animal lectins are proteins found in serum, the extracellular matrix, and cellular membranes. They exhibit Ca2+ -dependent carbohydrate-binding activity to enable their recognition of both endogenous and exogenous specific glycol-conjugates in animals. Several cells of the immune system (macrophages, B, T, and natural killer cells) display receptors with sequence similarity to C-type lectins, thus involving these mammalian lectins both in cell-to-cell interactions and in pathogen recognition by their ability to mediate discrimination between self and foreign (Weis et al., 1998). C-type lectin proteins function as adhesion and signalling receptors in many immune functions, such as inflammation and immunity to virus infected cells. C-type lectin-like domains (CTLD) are found on viral envelope proteins and in the outer-membrane adhesion proteins (e.g. in the envelope protein of Epstein–Barr virus). The gp42 protein of Epstein–Barr virus (EBV) has a CTLD that is like that of NK cell receptors. The ectodomain of the poxvirus protein A33 has two CTLDs in dimeric form, which resemble the CTLDs of the NK cell receptor lectins. However, neither of these domains in these viral proteins bind either Ca2+ or glycans (Cummings & McEver., 2017). These proteins have proven or putative roles in virus infectivity, cell to cell spreading, inhibition of cell-mediated cytotoxicity, or hemadsorption. However, the actual function of many of the viral C-type lectin homologues in immune evasion or the virus infective cycle remains to be determined. ASFV EP153R encodes for a C-type lectin-like protein, it is a type II

transmembrane protein containing an N-terminal cytoplasmic domain (1-30 residues) a predicted transmembrane domain (positions 30 to 49), a stretch of 20 amino acids followed by a C- terminal extracellular domain (64-153 residues) which contains the C-type lectin domain (Hurtado et al., 2011). It is predicted from the sequence that EP153R is glycosylated since it contains eight putative N- linked glycosylation sites as well as three predicted phosphorylation sites and two myristoylation sites (Galindo et al., 2000). The EP153R gene is transcribed during both the early (6 hpi) and the late phases of the infectious cycle. The EP153R contains a cell attachment (RGD) sequence and significant homology with the N-terminal region of CD44 molecules involved in cellular adhesion and T-cell activation (Hurtado et al., 2004). The EP153R also shares sequence similarity to swine CD69 and structural similarity with some CTLD which lack the Ca2+binding site involved in sugar recognition of other proteins that resemble CD69 (such as; human CD94 and murine Ly49A). The predicted structural alignment also shows there are conserved cysteine residue in EP153R that form 2 disulphide bonds. However, other C-type lectin molecules have additional disulphide bonds. Apart from the difference in the number of disulphide bonds, the overall structure of CD69, CD94 and Ly49A are almost identical to that predicted for the EP153R protein (Hurtado et al., 2011). A previous study showed that CD2v is required for binding of red blood cells to ASFV infected cells (HAD). Although the EP153R protein does not induce HAD alone it was indicated to increase binding of red blood cells in the presence of CD2v (Galindo et al., 2000). This was indicated since a recombinant ASFV (BA71VΔEP153R) lacking the EP153R gene showed reduced HAD in infected cells compared to the parental BA71V (Galindo et al., 2000). EP153R is reported to be involved in the down-regulation of MHC 1 by inhibiting the process of exocytosis of these molecules from the ER to the cell surface. When the expression of EP153R was

inhibited by siRNA transfection during ASFV infection, an increased expression of MHC-1 was observed. In addition a recombinant virus lacking EP153R showed a higher level of SLA-1, the porcine equivalent of MHC-1, expression on the cell surface during infection of porcine cells (Hurtado et al., 2011). Another study suggested a role of EP153R in inhibiting caspase3 activation and apoptosis induced both in ASFV infected cells and in EP153R transfected cells treated with different pro-apoptotic stimuli (Hurtado et al., 2004).

1.17 Role of CD2v in ASFV infection:

ASFV genomes contain an ORF, EP402R, which encodes for a protein named CD2v because of its similarity to the T-lymphocyte surface adhesion receptor CD2 (Rodriguez et al., 1993a). CD2v is expressed late during infection as a glycoprotein and the topology of the protein resembles type I transmembrane proteins (Goatley & Dixon, 2011). The N-terminal extracellular domain of CD2v contains a signal peptide, two immunoglobulin domains that resemble those of the human and other mammalian CD2 proteins, a transmembrane region and a C-terminal cytoplasmic domain (Galindo et al., 2000). It has been reported that CD2v encoded by different isolates contains a varying number of predicted N-linked glycosylation sites (15 to 25 sites) (Kay-Jackson et al., 2004; Malogolovkin, Burmakina, Tulman, et al., 2015). A key defined function of CD2v is the attachment of erythrocytes to the ASFV infected cells expressing CD2v protein (haemadsorption, HAD) and in the attachment of extracellular virus particles to the erythrocytes (Borca et al., 1994). However, the function of CD2v is not limited to HAD, it has been reported to be involved in reducing the mitogen dependent proliferation of lymphocytes in PBMC cultures (Borca et al., 1998). Previous studies

have shown the role of CD2v in infecting the *Ornithodoros* tick vector, a 1000-fold increase in virus replication in ticks was observed when the non-functional CD2v and C-type lectin were restored in a non-HAD naturally attenuated strain of ASFV (Rowlands et al., 2009). Recent studies suggest its role in disturbing cellular traffic as the C-terminal domain of CD2v interacts with regulatory trans-Golgi network (TGN) protein AP-1 which is a key element in cellular traffic (Perez-Nunez et al., 2015). Another study has suggested its involvement in vesicle transport and signal transduction based on evidence from direct binding studies and interactions detected using the yeast two-hybrid system. In this study, it was shown that the cytoplasmic tail of CD2v (which contains proline-rich repeats PPPKPC) interacts with cytoplasmic adaptor protein SH3P7, an actin-binding adaptor protein involved in diverse cellular functions (Kay-Jackson et al., 2004). In cells transfected with a plasmid expressing CD2v, localisation late during ASFV infection was observed mainly in the perinuclear membrane compartments and surrounding virus factories (Kay-Jackson et al., 2004). It was also suggested that CD2v has a role in the generation of these viral structures and hence in disturbing cellular traffic as it localises around the viral factories in ASFV infected cells (Perez-Nunez et al., 2015). As mentioned above, the infected cells express CD2v on the cell surface and erythrocytes attach to CD2v on the surface of infected cells. The virus may acquire CD2v protein during the budding process from infected cells. Proteomic analysis of ASFV particles identified CD2v as the only virus protein present on the outer membrane of the virus (Alejo et al., 2018). The extracellular virions (containing CD2v on the outer membrane) are observed in EM images bound to the RBC and in pits on the surface. The mature virus particles can be observed at the plasma membrane in the infected cells with RBC attached tightly at this point (see figure 1.8) The attachment to red blood cells was shown to be mediated by expression of CD2v as

the disruption of the gene that codes for CD2v, EP402R, in ASFV BA71V isolate did not affect the virus growth rate *in vitro* but abrogated the ability of the virus to induce the haemadsorption of red blood cells to the surface of infected cells. This result demonstrates that the CD2v protein encoded by EP402R is directly involved in the haemadsorption phenomenon induced by the infection of susceptible cells with ASFV (Borca et al., 1994; Rodriguez et al., 1993a).

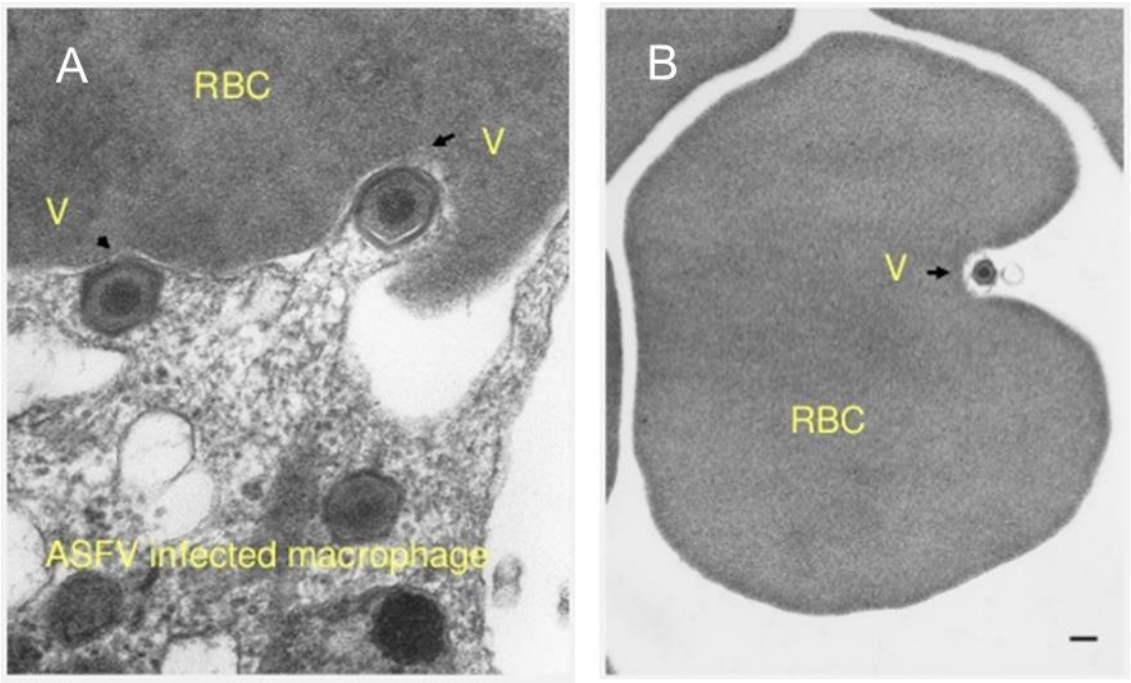

Figure 1.8: Egress and binding of CD2v: (A) the image shows ASFV infected cells with attached RBC and the budding of the virions. (B) The image shows the binding of the extracellular virion to the RBC (PC: Sharon Brookes).

CD2v has been identified in three forms in transfected cells, an N-terminal glycosylated, C-terminal non-glycosylated, and a full-length glycosylated form. One possibility is that these forms are produced by proteolytic cleavage. This could occur either in the ER or Golgi compartments (Goatley & Dixon, 2011). It was also suggested that the N-terminal immunoglobulin-like domain is likely to be responsible for the rosetting of erythrocytes around the infected cells (Borca et al., 1998). Previous studies

have shown that CD2v is immunogenic, the first reported recombinant protein which induced protection against ASFV challenge was a baculovirus expressed CD2v protein. Hence CD2v was suggested to be a candidate for subunit vaccine (see section 1.8 for detail) (Burmakina et al., 2016; Ruiz-Gonzalvo et al., 1996). The CD2v protein is expressed by most ASFV isolates, only a few isolates have been described which do code for CD2v and cause HAD. The sequence is well conserved among Genotype I isolates obtained from a broad range of countries over a wide period (Bastos et al., 2003). Previous studies have shown that deletion of CD2v from virulent ASFV Malawi isolate did not reduce virus virulence in pigs, although a delay in the onset of clinical signs and virus dissemination was observed, suggesting a role for CD2v in virus dissemination and viremia (Borca et al., 1998). Recently, it was shown that deletion of CD2v from the BA71 virulent strain resulted in virus attenuation (Monteagudo et al., 2017). However, deletion of CD2v from ASFV Georgia07 did not reduce virus virulence in pigs, although a delay in onset of clinical signs and virus dissemination was observed, supporting the role of CD2v in virus persistence (Borca, O'Donnell, et al., 2020). In humans, CD2 is present on the surface of T-lymphocytes and mainly binds to the CD58 protein (sometimes with CD59 and in rats the ligand for CD2 is CD48) present on the surface of the antigen-presenting cells. This binding stabilises interactions with T cell receptors during the formation of the immunological synapse (see figure 1.9) (Dustin, 2014; Ikemizu et al., 1999; Milstein et al., 2008). The ligand for the ASFV encoded CD2v is not known.

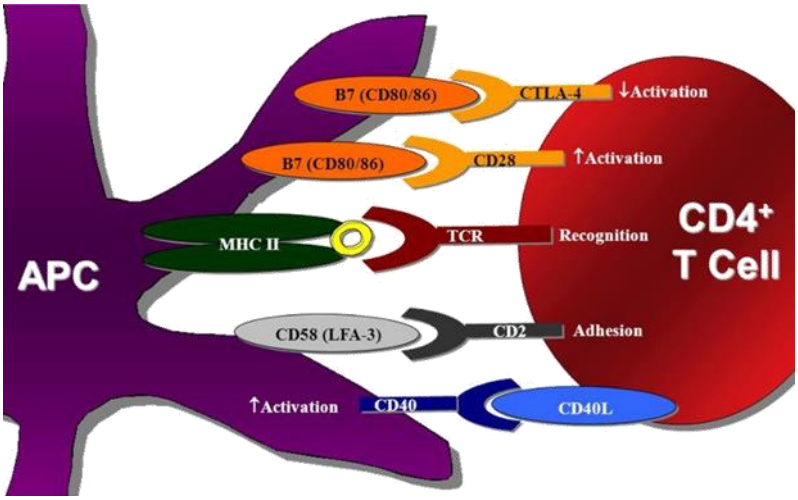

Figure 1.9: Interaction of antigen-presenting cells (APC) with T-lymphocytes: the image shows the human immunological synapse between APC and T-lymphocytes, the adhesion molecule CD2 interacts with CD58 (previously known as LFA-3).

Objectives

The overall aim of the project is to investigate the molecular mechanisms involved in the binding of red blood cells to ASFV infected cells and extracellular virions. This knowledge will be used to determine the role of HAD in ASFV persistence in blood and induction of clinical signs in pigs infected with gene-deleted or gene-modified ASFV. To achieve this, several objectives are planned.

- The amino acid residues involved in binding of the CD2v protein to red blood cells to cause HAD will be identified.
- The role of other proteins that are predicted to be involved in this process will be investigated.
- The effect of deleting or modifying the genes identified from the genome of the moderately attenuated ASFV strain Benin 97/1(ΔDP148R) will be studied in cells and following infection of pigs.

This studies will help to establish the role of HAD in the duration and level of virus persisting in blood of infected pigs.

CHAPTER 2- Structural, functional and expression analysis of mutations in CD2v protein to determine critical amino acid residues involved in HAD.

2.1 Introduction:

The previously attenuated strain of ASFV, BeninΔDP148R, induced 100% protection of pigs immunized with BeninΔDP148R and challenged with the lethal Benin 97/1 strain. However, adverse clinical signs were observed following immunization and high genome copy numbers were detected in blood (up to 10^6 genome copies/ml) which persisted for up to 60 days (Reis et al., 2017). ASFV contains an ORF, EP402R encoding CD2v protein, which has been shown to be required for the attachment of erythrocytes to infected cells and the binding of the extracellular virion to the erythrocytes (Borca et al., 1994; Rodriguez et al., 1993a). CD2v is expressed as a type I transmembrane protein on the surface of ASFV infected cells and also detected in areas around virus factories in infected cells transfected with plasmids expressing the protein (Goatley & Dixon, 2011; Perez-Nunez et al., 2015). The extracellular N-terminal domain has two immunoglobulin-like domains (Ig-domain) which resemble those in host CD2. Based on results, including determination of the structures of CD2 bound to its ligand CD58 (Wang et al., 1999), it is predicted that the first N-terminal Ig domain of CD2v is involved in attachment to the ligand on RBC. The virus particles acquire CD2v upon egress from the infected cells and it is described as the only known protein present on the outer membrane of the virus (Alejo et al., 2018). CD2v also has other function (see chapter 1, section 1.19). The attached red blood cells may mask the ASFV infected cells and virions from the immune system and possibly inhibit the interaction between T-cells and antigen presenting cells which may limit cellular immune responses (see chapter 1, section 1.12). The RBC attached to the infected cells may contribute to the virus dissemination as the virus immediately binds to the RBC

upon egress from the infected cell. The aim of the work described in this chapter was to design mutations in the CD2v Ig domain 1 and to investigate which residues in the CD2v extracellular N-terminal domain were important for binding to red blood cells. The critical amino acid residues were determined by mutational analysis of the first Ig-domain, neutral or drastic charge change substitutions were introduced in the predicted ligand-binding domain of CD2v to reduce or inhibit the binding of CD2v, transiently expressed in cells, with RBC.

In this chapter, I have presented the strategy for designing 21 CD2v mutants, the optimisation; expression, processing and localization of the ASFV (Benin97/1) encoded wild type CD2v protein and the mutants in the absence of other ASFV proteins in transfected cells. The mutants were further tested for their ability to cause HAD in transfected Vero cells, the analysis was performed using immunofluorescence, Western blot and HAD assay.

2.2 Alignment of ASFV Benin 97/1 encoded CD2v protein with human and pig CD2:

Multiple sequence alignments were performed to investigate the similarity between ASFV Benin encoded CD2v and the CD2 molecule present on the surface of T lymphocytes of rat, pig, and human. It was previously reported that the extracellular N-terminal domain of CD2 (rat, human) contains two immunoglobulin (Ig) domains and mutagenesis analysis determined that the ligand-binding domain is present in the Ig domain 1 (Peterson & Seed, 1987). Similarly, the N-terminal domain of CD2v encoded by ASFV contains the two Ig like domains which are also predicted to be involved in the attachment of erythrocyte to the infected cells (see figure 2.1a) (Borca et al., 1998). However, the CD2v protein contains varying number of predicted N-linked

glycosylation sites (15 to 25 sites depending on the isolate) while host CD2 contain 3 predicted N-linked glycosylation sites (see figure 2.1b) (Kay-Jackson et al., 2004; Malogolovkin, Burmakina, Tulman, et al., 2015).

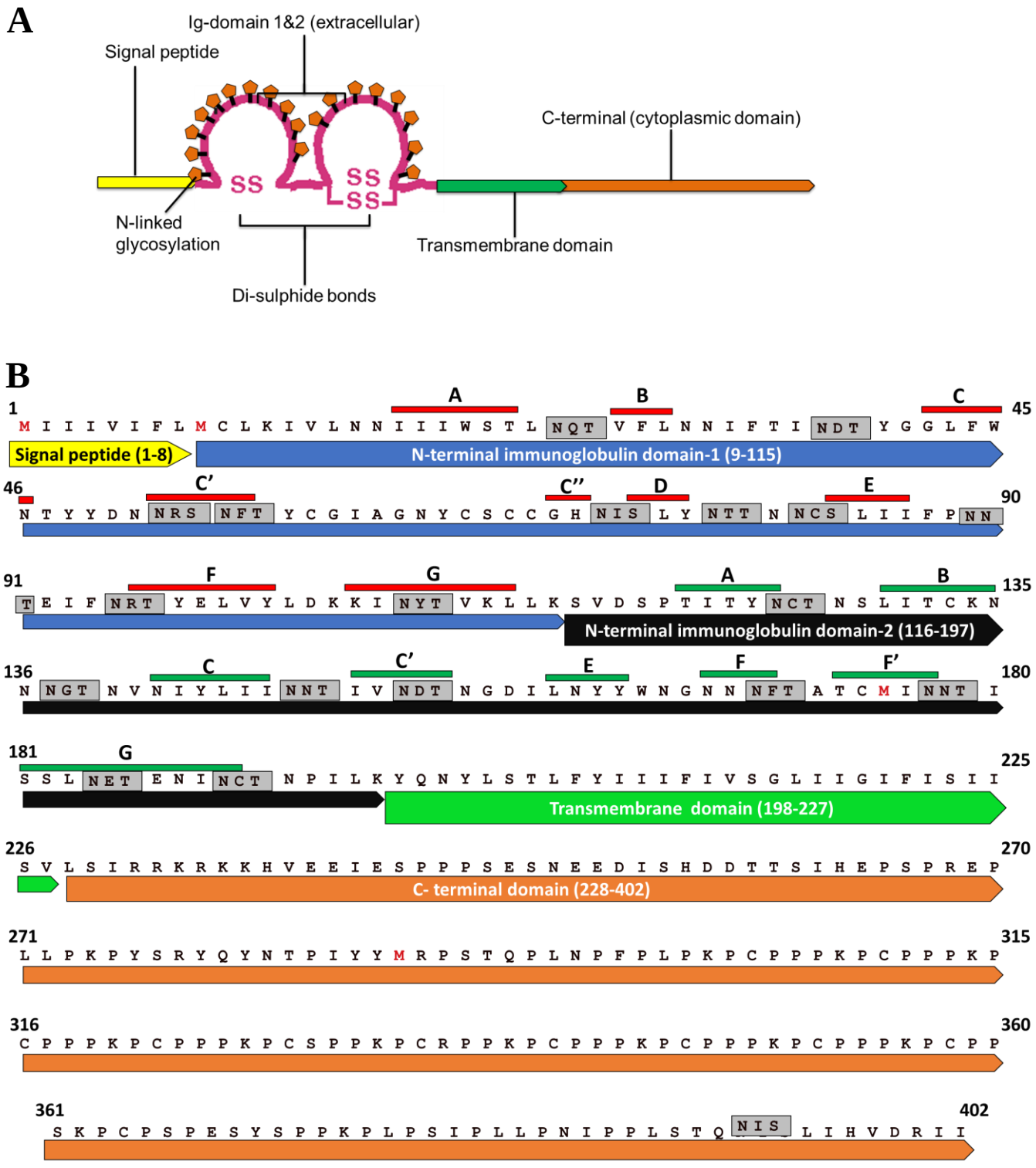

Figure 2.1a; A graphical representation of CD2v; the image shows the sequence from Benin07/1 isolate which is typical of structures of CD2v from other isolates. The signal peptide is followed by 2 immunoglobulin like domains which contain cysteine residues that forms disulphide bonds. The Ig domain 1 contains two cysteine residues that form a single disulphide bond, while Ig domain 2 contains four cysteine residues and forms two predicted disulphide bonds. Both Ig-domains are highly glycosylated (11 predicted sites in domain 1 & 8 sites in domain 2), the membrane proximal Ig domain 2 maintains the ligand binding domain at a distance from the membrane. The extracellular domain is followed by a transmembrane region and the cytoplasmic domain. **Figure 2.1b: ASFV Benin 97/1 encoded CD2v;** Amino acid sequence of CD2v, showing the N-terminal (extracellular) Ig-domain 1 & 2 (blue and black). In Ig-domain 1 the β- sheets containing the β- strands A, B, C, C', C'', D, E, F, G are shown by a red bar and these were named after the respective strands in the mammalian CD2 structure. Similarly, in Ig-domain 2 the β- sheets containing the β- strands A, B, C, C', E, F, F', G are shown by green bars and were named after the respective strands in the mammalian CD2 structure. The predicted N-linked glycosylation sites are shown in the grey shaded box, the residues in the predicted transmembrane domain are labelled green and the residue in the C-terminal cytoplasmic domain are labelled brown.

The first reported model of rat CD2 Ig domain was generated by nuclear magnetic resonance (NMR) and later the structure of the complete extracellular domain of CD2 was determined from the crystal structure (Driscoll et al., 1991; Jones et al., 1992). This allowed the human CD2 domain 1 model to be generated and based on the model the functional amino acid residues of human CD2 involved in binding to its ligand CD58 were determined (Somoza et al., 1993). The aim in studies described in this chapter was to investigate if the critical amino acid residues reported for human and rat CD2

(domain 1) are conserved in the ASFV encoded CD2v (domain 1) or if ligand attachment is mediated by different residues. The interaction of host CD2 with its ligand is transient whereas CD2v appears to bind to its ligand by a stable interaction. The sequences of CD2/CD2v were obtained online from the National Center for Biotechnology Information (NCBI) and the multiple sequence alignment was performed online using the clustalW software. The results showed that CD2v shares low sequence similarity to CD2 from rat or human, however, they share structural and functional domains including the two immunoglobulin domains (see figure 2.2). The disulfide bonds formed between the cysteine residues of the adjacent loops are considered to be the hallmark of the immunoglobulin superfamily (IgSF). The alignment showed that the cysteine residues are conserved in Benin CD2v, human, rat, and pig encoded CD2, indicating structural similarity. The human CD2 sequence was found to be significantly similar to the rat (54%) and pig (60%) CD2 sequences (See figure 2.2). Comparison of these sequences also identified that some of the amino acid residues (for example F56, L103 highlighted in black boxes in figure 2.2), that were shown from previous studies to be important for attachment of erythrocytes to human CD2, were also conserved in CD2v of several ASFV isolates including Benin 97/1 (see figure 2.2 and 2.3). Mutation of these conserved residues resulted in either partial or complete inhibition of binding of erythrocytes to CD2 (Peterson and Seed., 1987).

Figure 2.2: Multiple sequence alignment of CD2 and CD2v; Multiple sequence alignment of Ig domains (1 &2) of ASFV Benin 97/1 encoded CD2v protein with Ig domains (1 &2) of CD2 (rat, human, and pig) showing the conserved residues in immunoglobulin domain 1 & 2 (*). The residues shown in the grey box are the functional residues in human CD2 and have an effect on rosette formation (Peterson & Seed, 1987). The residues shown in light orange box are the functional residues that are critical for interaction between CD2-CD58 (Somoza et al., 1993), the conserved cysteine residues (highlighted yellow) form a disulphide bond and shows the structural similarity between CD2 (rat, human and pig) and CD2v (Benin).

2.3 Design of mutations in CD2v protein to reduce binding of erythrocytes (BATCH-1):

Mutant versions of the ASFV Benin 97/1 EP402R gene were designed based on information from a previous publication (Peterson & Seed, 1987) which investigated

the ligand-binding sites of human CD2 present on the surface of T lymphocytes. This was performed by introducing mutations in human Ig-domain 1 in defined epitopes recognized by monoclonal antibodies. Some of these mutations resulted in partial rosetting of human and sheep erythrocytes around lymphocytes (Peterson & Seed, 1987) (see figure 2.2). In a later study, the amino acid residues in the human CD2 that were required for the interaction between CD2 and its ligand CD58 were determined based on a predicted structure of human CD2 (Ig domain 1) followed by mutagenesis analysis and by the ability of the mutants to induce HAD. It was shown that the ligand binding domain of CD2 for both human and sheep CD58 are present in the β-sheet within β strand C (K44, E46), C' (R58, K59), and the loop connecting β strand F & G (Somoza et al., 1993) (see figure 2.2).

Mutations were designed to determine the amino acid residues in ASFV Benin97/1 encoded CD2v which are involved in the attachment of erythrocytes to the infected cells. A multiple sequence alignment of ASFV encoded CD2v protein sequences available online from NCBI (https://www.ncbi.nlm.nih.gov/nuccore) and Viral Bioinformatics Resource Centre (VBRC) (https://4virology.net/) was performed to identify the conserved residues between ASFV isolates and the potential ligand-binding domain. The expectation was that conserved residues are likely to be involved in the functions of CD2v including HAD. This alignment of CD2v was compared with Human, Pig, and rat CD2 sequences to further investigate the critical residues (see figures 2.2 and 2.3).

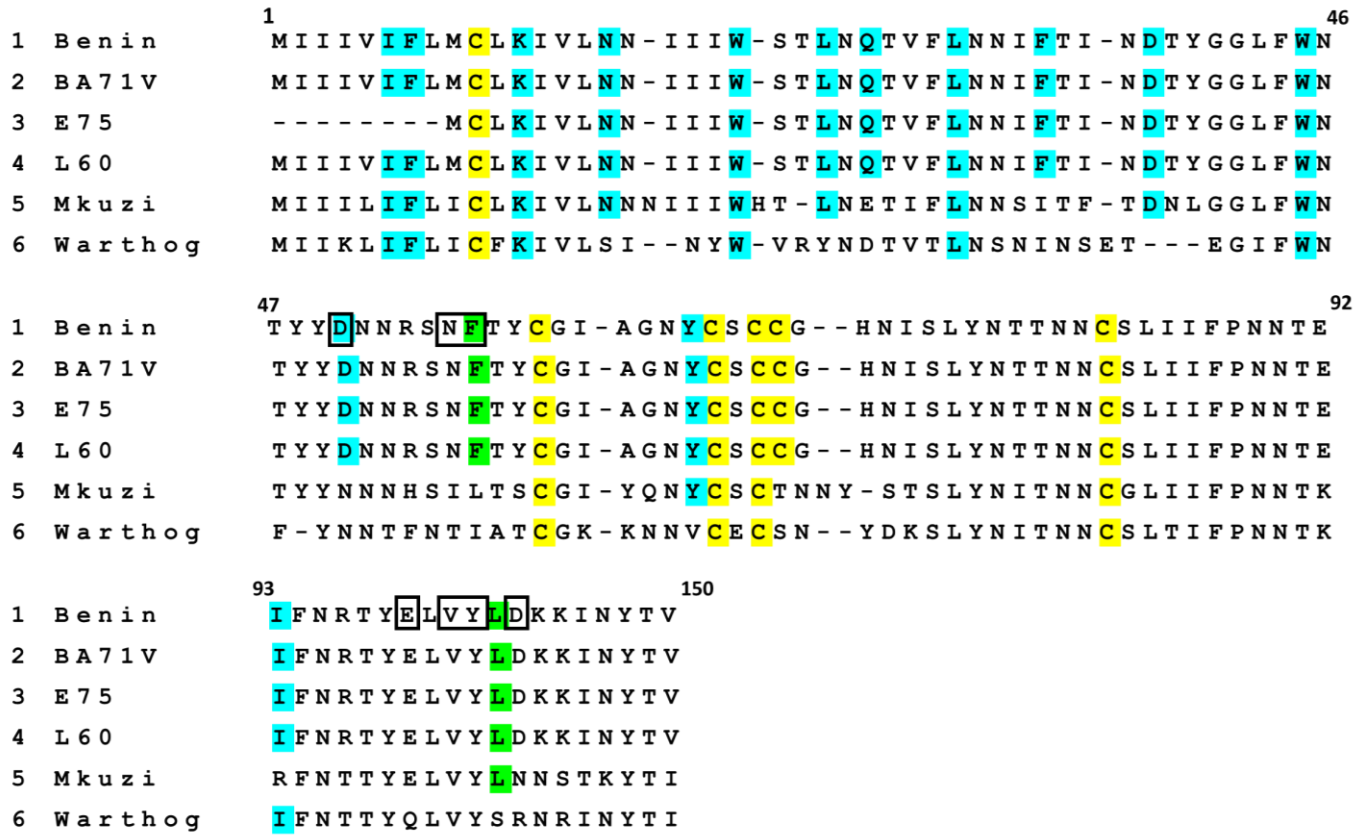

<u>Figure 2.3; Multiple sequence alignment of CD2v (From 1-150 residues)</u>: The alignment of CD2v encoded by different ASFV isolates shows the conserved residues in Ig-domain 1. The functional residues in human CD2 that are conserved in CD2v are highlighted in green, the conserved cysteine residues (highlighted yellow) showing the structural similarity among CD2v proteins. The conserved residues in human CD2 and CD2v are highlighted cyan and the residues selected for mutations are shown in a box.

The data from the alignment showed that Benin encoded CD2v and human CD2 are divergent in sequences however, comparison of these sequences identified that some of the amino acid residues that were shown from previous studies to be important for HAD in human CD2 were conserved in Benin 97/1 encoded CD2v. The substitution strategy of human CD2 mutants that resulted in partial rosetting is shown in Table

2.1. Some of the residues in human encoded CD2 that were shown to be critical for interaction with CD58 are conserved in Benin 97/1 CD2v, these residues along with other residues that were conserved in other ASFV isolates and were predicted to be critical for binding of erythrocytes to CD2v were selected for mutations (see figure 2.4). In mutant 1, two amino acid residues (D50 & F56) that were conserved in human CD2 and Benin encoded CD2v were substituted at position D50 with a G residue and at F56 with V. These substitutions were chosen following the same strategy used for substitution in the human CD2 sequence (see table 2.1). In mutant 2, the conserved amino acid residue (F56) was substituted with arginine (F56R) along with asparagine at position N55, which was conserved in most CD2v proteins encoded by different ASFV isolates (N55S). Similarly, in mutant 3 the N55 and F56 amino acid residues were substituted with arginine (F56R) and leucine (N55L). In mutant 4, the F56 amino acid residue was substituted with positively charged lysine (F56K). Some of the residues in the second monoclonal antibody binding epitope of human CD2 were also conserved in CD2v, in mutant 5 the D104 residue, which was conserved in the rat CD2 and CD2v, was substituted with histidine (D104H). In mutant 6, the tyrosine Y102 was substituted with negatively charged aspartic acid (Y102D) while in mutant 7 two residues, E99 and V101, were substituted with lysine (E99K) and isoleucine (V101I) (see figure 2.4).

Table 2.1: Strategy for substituting the amino acid residues in functional domains of human CD2 that resulted in partial HAD.

Residues in human CD2	**Substitution of residues**	**HAD (erythrocytes rosettes)**
Aromatic Amino Acid	Aliphatic/ Neutral /basic amino acids	Partial rosettes (+/-)

Acidic Amino acids	Basic / Unique Amino Acids	Partial rosettes (+/-)
Neutral	Basic Amino Acids	Partial rosettes (+/-)
Aromatic amino acid	Acidic amino acid	Very low rosettes (+/-)

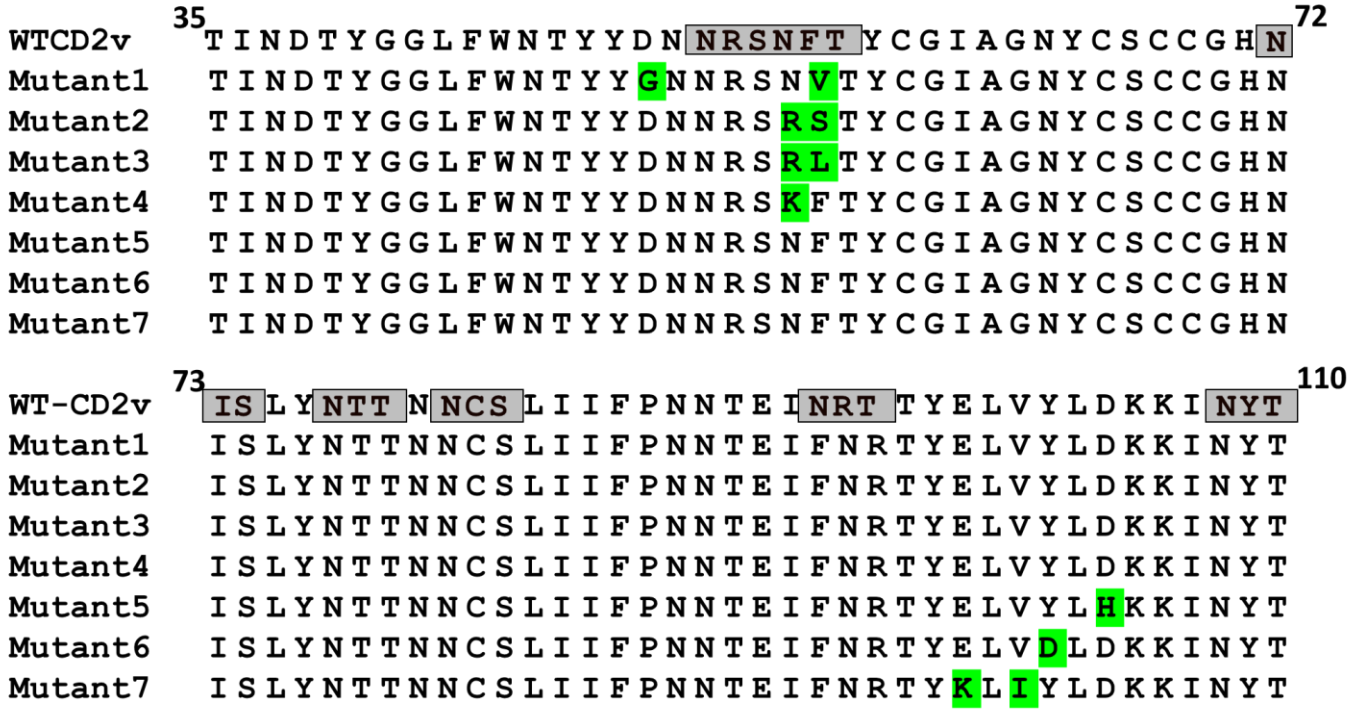

Figure 2.4: **Sequences of batch 1 mutants (from residue 35-110):** The amino acid sequences of the Benin CD2v mutants (Ig-domain 1) are shown, the top sequence corresponds to the wild type CD2v sequence. The substitutions at different positions (D50, F56, E99, V100, Y102 and D104) are highlighted in green. The predicted N-linked glycosylation sites are shown in grey shaded boxes.

2.4 Optimization of CD2v protein expression by immunofluorescence;

The wild type full length CD2v/EP402R without a stop codon was amplified by PCR from Benin 97/1 genomic DNA. The primers used for amplification contained restriction enzyme sites for cloning. The amplified CD2v gene was cloned into pcDNA3 vector backbone containing an HA tag (see appendix 1 for primer sequences). CD2v was cloned under control of the T7 promoter (pWT-CD2vHA) and was

expressed by using two different transient expression systems. It was important to determine which system expresses CD2v efficiently and in sufficient amounts to carry out the functional HAD assay. A similar experiment in which expression of CD2v protein was driven by the CMV promoter in uninfected cells showed reduced HAD phenotype in functional assays compared to the transient T7 RNA polymerase driven expression system (data not shown).

The expression of pWT-CD2vHA was driven by either MVA-T7 or Fowlpox-T7 (Das et al., 2000; Sutter et al., 1995), they are highly attenuated Poxviruses that do not undergo a complete replicative cycle. They express most of their proteins and form cytoplasmic factories, both viruses contain a bacteriophage T7 RNA polymerase gene under the control of a Poxvirus early promoter. The expressed T7 RNA polymerase drives high levels of expression of genes under control of the T7 promoter, these viruses do not cause cytopathic effect in Vero or MDBK cells (Das et al., 2000; Sutter et al., 1995). The cytoplasmic factories are detectable 2 hours post-infection and can be visualized with a fluorescent dye (Moss, 2013).

Vero cells grown on coverslips were infected either with Fowlpox-T7 or MVA-T7 at MOI-1 (see section 5.3.3) and were transfected with plasmid pWT-CD2vHA (see section 5.3.2). The cells were fixed, permeabilized and stained with anti-HA (rat) primary antibody and probed with alexaflour 568 (anti-rat IgG) secondary antibody (see section 5.3.4). The viral factories and the nucleus were stained with 4′,6-diamidino-2-phenylindole (DAPI) florescent dye. The results showed that pWT-CD2vHA is expressed in the cells infected either with MVA-T7 or Fowlpox-T7. However, the cells infected with MVA-T7 expressed CD2v efficiently and in higher amounts compared to cells infected with Fowlpox-T7 . This was sufficient to carry out functional HAD assays (see figure 2.5).

In Fowlpox-T7 infected cells the amount of protein localised close to the viral factories was low compared to the MVA-T7 infected cells. It was also observed that in MVA-T7 infected cells most of the protein was localised close to the MVA-T7 viral factories, as shown before for infections with ASFV strains where CD2v was localised around ASFV viral factories (Goatley & Dixon, 2011; Perez-Nunez et al., 2015).

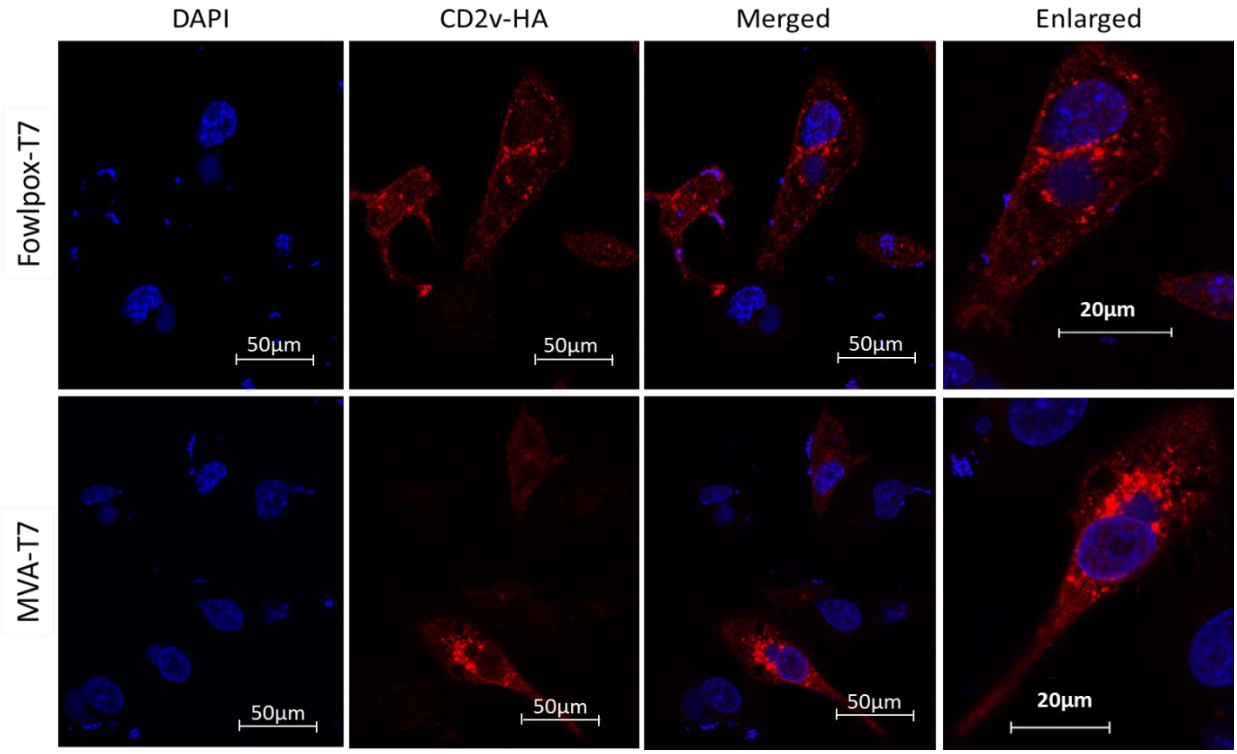

Figure 2.5: Optimization of CD2v expression: Confocal images showing the expression of pWT-CD2vHA (shown in red). Vero cells were infected with either Fowlpox-T7 or MVA-T7 at MOI-1 and transfected with pWT-CD2vHA. The viral factories and the nucleus were stained with DAPI (shown in blue), the images were captured by keeping the gain constant.

2.5 Expression analysis of WT-CD2v by Western blot and immunofluorescence;

The expression, distribution and localisation of ASFV (Benin 97/1) encoded CD2v was observed by Western blot and immunofluorescence. The plasmid construct pWT-

CD2vHA (containing full length EP402R/CD2v tagged with an HA epitope) under the control of the T7 promoter was used in a transient MVA-T7 expression system (described above in this chapter). The pWT-CD2vHA was analysed by Western blot to investigate if the protein is expressed at the correct size and glycosylated. Previously it was shown that CD2v was expressed in three forms; full length glycosylated form, full length non-glycosylated form, truncated N terminal and truncated C-terminal forms (Goatley & Dixon, 2011). Vero cells were infected with MVA-T7 at MOI 1 and transfected with pWT-CD2vHA (see sections 5.3.2 & 5.3.3). A control for glycosylation was included where cells were treated with tunicamycin, which inhibits protein folding and transit through the ER (Wang et al., 2015). The cells were lysed, and a Western blot was performed on the extracts (according to the method described in see section 5.3.8).

The result provided evidence that CD2v is expressed at the correct size (see figure 2.6). The predicted size of full length CD2v from the sequence is 42kDa however, after post-translational modification by extensive glycosylation the size changes to 102kDa (Goatley & Dixon, 2011). The band detected at 102kDa correspond to full length glycosylated form of CD2v, and the band at 42kDa corresponds to the full length non-glycosylated form of CD2v. The C-terminal cytoplasmic domain of CD2v was detected at 26kDa (see figure 2.6), the cytoplasmic domain does not contain glycosylation sites as described previously (Goatley & Dixon, 2011; Perez-Nunez et al., 2015). The truncated N-terminal fragment was not detected in these experiments as expected since the C-terminal HA tag is missing from this fragment. An additional band was detected at 29kDa in both untreated and tunicamycin-treated cells but not in the mock (cells only) and is unclear what it corresponds to, although it does contain the C-terminal HA

tag. The results provided evidence that CD2v was expressed, glycosylated, processed in the correct forms and cleaved to produce the sizes previously observed.

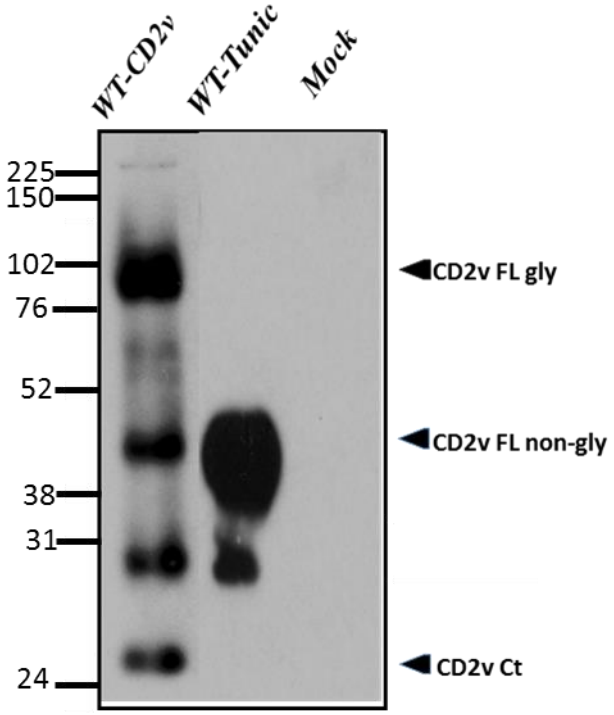

Figure 2.6. Vero cells mock infected or infected with MVA-T7 (MOI 1), transfected with pWT-CD2vHA, treated or untreated with tunicamycin:. Cell lysates were prepared and separated by SDS-PAGE, probed with anti-HA (rat) primary antibody and anti-HA HRP secondary antibody. The image shows full length glycosylated CD2v (102 kDa), full length non-glycosylated CD2v (42 kDa), C terminal domain (26 kDa) and an additional band at 29 kDa.

To further investigate the expression and localisation of pWT-CD2vHA, Vero cells were infected with MVA-T7 at MOI1 and were transfected with pWT-CD2vHA (see section 5.3.2 &5.3.3). The cells were fixed, permeabilised and stained with anti-HA (rat) primary antibody and probed with alexaflour 568 (anti-rat IgG) for immunofluorescence (see section 5.3.4). The expression, distribution and localization of ASFV Malawi CD2v has been previously described, similar results were observed

for ASFV Benin 97/1 wild type CD2v (Goatley & Dixon, 2011). The CD2v was localised as punctate staining close to the MVA-T7 viral factories and was distributed in the cytoplasm in MVA-T7 infected cells (see figure 2.7).

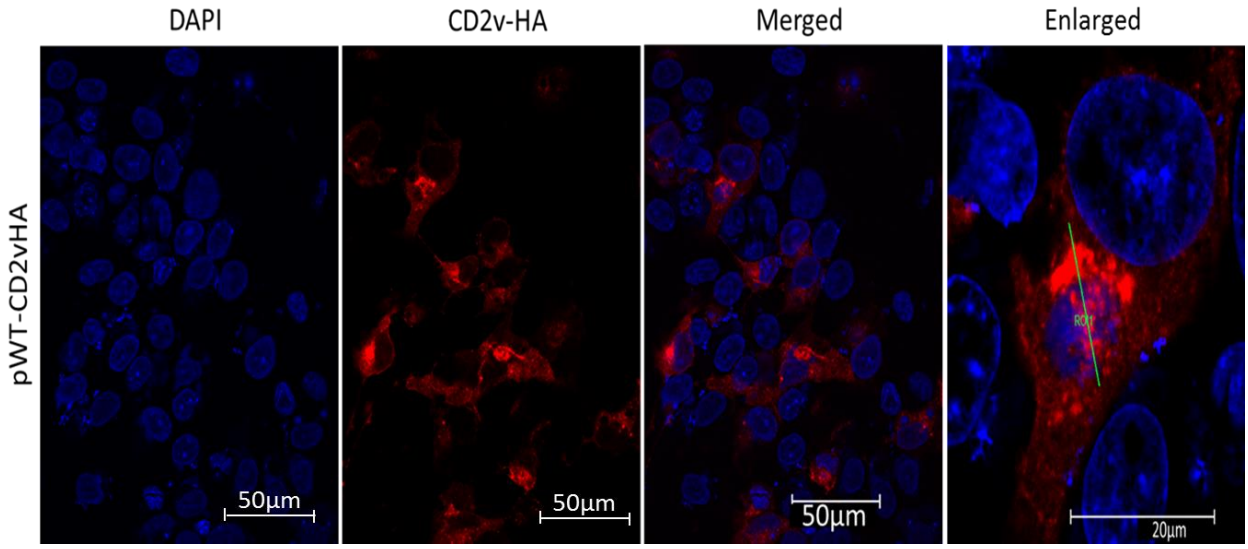

Figure 2.7: Vero cells infected with MVA-T7 at MOI 1 and transfected with pWT-CD2vHA. Cells were fixed, permeabilized and stained with anti-HA rat IgG (primary antibody) and probed with anti-rat IgG Alexaflour 568 (secondary antibody) shown in red. The nucleus and viral factories were stained with DAPI shown in blue (scale bar; 50um), the enlarged image showing the co-localization around MVA-T7 induced virus factories (scale bar; 20um).

It was previously reported that in ASFV (Malawi) infected cells CD2v exists in two forms, a full length glycosylated CD2v (102 kDa) and a non-glycosylated C-terminal domain (26 kDa). Another band of 89kDa was observed using the anti-V5 antibody which detected the N-terminally tagged protein and was suggested that it may be a processed full-length glycosylated N-terminal domain of CD2v (Goatley & Dixon, 2011). Further investigation is required, such as pulse chase labelling from full length to processed form, to confirm the fragments were derived by proteolytic processing to produce the N and C-terminal fragments. Detection of both fragments of the predicted

combined size of the full length protein supports the view that they are generated by proteolytic processing (Goatley & Dixon, 2011). The processing probably occurs within the luminal domain either in the endoplasmic reticulum (ER) or Golgi compartments (Goatley & Dixon, 2011). As the HA tag is cloned at the C-terminal (cytoplasmic domain) it was difficult to conclude that the expressed protein was transported to the cells surface. However, it was observed that some of the protein was localised close to the plasma membrane, suggesting that it is transported to the cell's surface.

2.6 Expression analysis of CD2v mutants by Western blot and immunofluorescence;

As previously described the CD2v mutants were designed and constructed in 3 batches and were also analysed by Western blots, immunofluorescence and HAD assays in batches. It was important to confirm the expression of each of the mutants as the substitutions might interfere with protein folding and may possibly direct the protein to the proteasome for degradation.

2.6.1 Expression analysis of 1ST Batch CD2v mutants by immunofluorescence and Western blot;

The expression analysis of the 1st batch of CD2v mutants was performed by immunofluorescence and Western blot. It was necessary to determine the expression of CD2v mutants and to detect the mutants were expressed at the correct sizes. The mutation introduced into CD2v may interfere with cleavage, transport of the mutant to cell surface, with protein folding and structure which may possibly direct the protein to the proteasome for degradation. This would affect the functional analysis of mutations introduced when performing the HAD assay. I designed six mutants of CD2v protein

by introducing either single or double amino acid substitutions in the immunoglobulin domains -1 following previously published data on defining epitopes in human (Peterson & Seed, 1987). These mutants were cloned into pcDNA3 containing an HA-tag under the control of the T7 promoter and transient expression in Vero cells was driven by MVA-T7 (the mutants design is described in section 2.3 and strategy for cloning is described in section 5.2.6).

To investigate if the proteins were expressed at the correct size, processed by glycosylation and cleaved, Vero cells were infected with MVA-T7 at MOI1 and were transfected with pWT-CD2vHA and plasmid constructs expressing the mutant proteins (see section 5.3.2 & 5.3.3). A control for glycosylation was included by treating the cells with tunicamycin, which inhibits protein folding and transit through the ER (Wang et al., 2015). A Western blot was performed according to the method outlined in section 5.3.8 (chapter 5). The results showed that CD2v mutants were expressed at the correct size, all mutants were expressing the full-length glycosylated form of CD2v detected at 102 kDa. The full length non-glycosylated form of CD2v was detected in all mutants (42 kDa). The non-glycosylated C-terminal domain was also detected in all mutants (26 kDa) (see figure 2.8). This provide evidence that CD2v mutants were expressed, glycosylated and processed in correct sizes similar to the wild type CD2v. The amount of protein varied in cell lysates possibly due to difference in transfection efficiency although differences in protein expression or stability cannot be excluded.

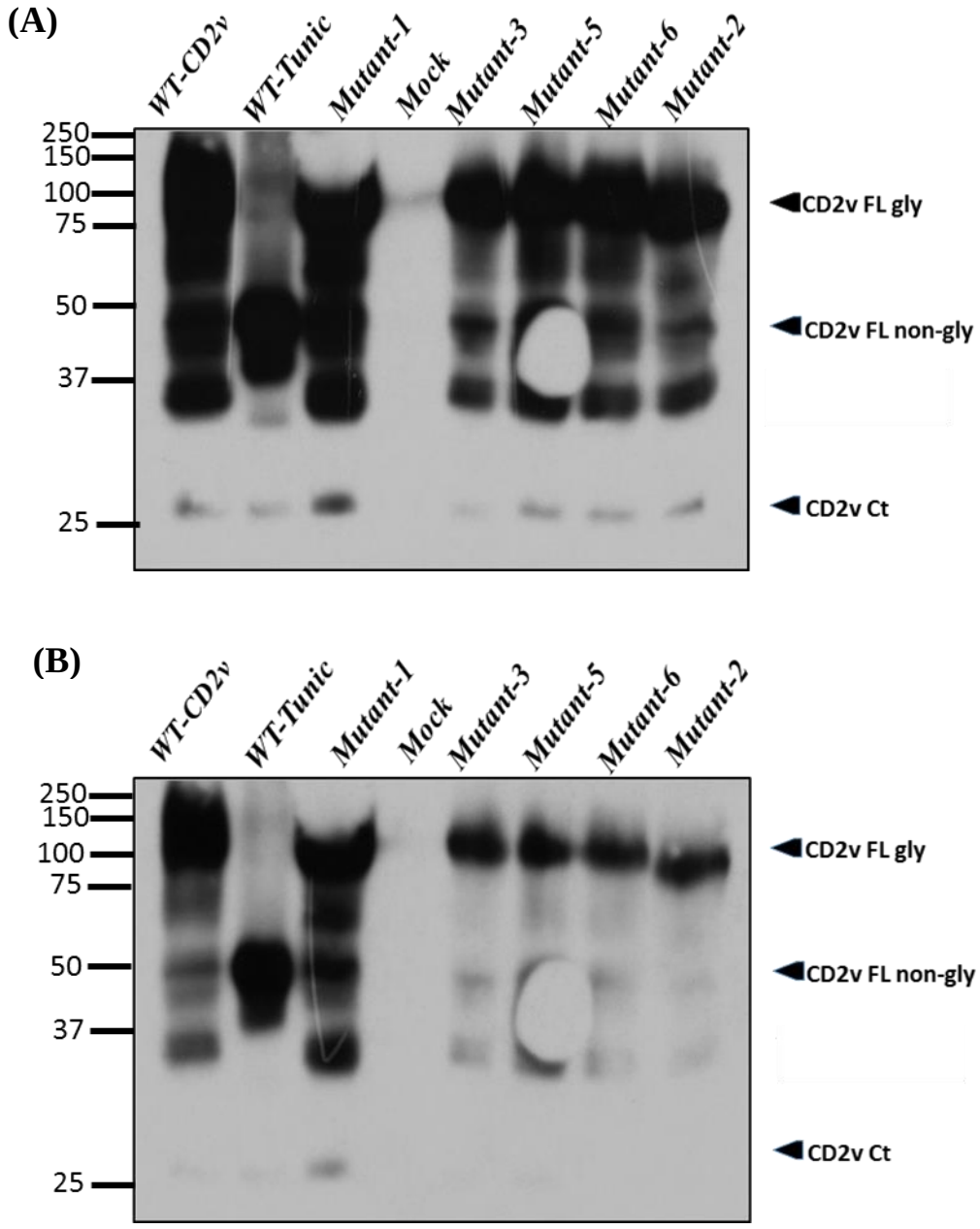

Figure 2.8; Vero cells mock-infected or infected with MVA-T7 (MOI 1), transfected with plasmids expressing pWT-CD2vHA and the mutant CD2v proteins. 1,3, 5, 6, 2. Lysates were prepared from cells expressing wild type or mutant CD2v as indicated, and with pWT-CD2vHA control treated with tunicamycin. The cell lysates were separated by SDS-PAGE, probed with anti-HA primary antibody and anti-HA HRP secondary antibody. The image shows full length glycosylated CD2v (102

kDa), full length non-glycosylated CD2v (42 kDa) and the C terminal domain (26 kDa). Image B shows a less exposed blot.

Immunofluorescence was performed to further investigate if the expressed mutant CD2v proteins have similar distribution and localisation pattern as the pWT-CD2vHA. Vero cells were infected with MVA-T7 at MOI-1 and transfected either with pWT-CD2vHA or plasmids expressing the mutant CD2v proteins (see section 5.3.2 & 5.3.3). The cells were fixed, permeabilized and stained with anti-HA (rat) primary antibody and probed with Alexaflour 568 (goat anti-rat IgG) secondary antibody for immunofluorescence (see section 5.3.4). The results showed that the mutant CD2v proteins were expressed with a similar distribution to the WT-CD2vHA and were localised in punctate regions closed to the MVA-T7 viral factories. The proteins were distributed in the cytoplasm with some of the protein close to the plasma membrane (see figure 2.9). However, it was not clear if the extracellular domain of the protein is expressed on the surface since these constructs are detected using an antibody against an HA epitope fused to the C-terminus. Therefore, the expression and localisation of either a full length CD2v or the cleaved C-terminus of CD2v could be detected. However, the detection of CD2v close to the plasma membrane suggest that the cleaved and/or the full length CD2v may be transported to the cell surface.

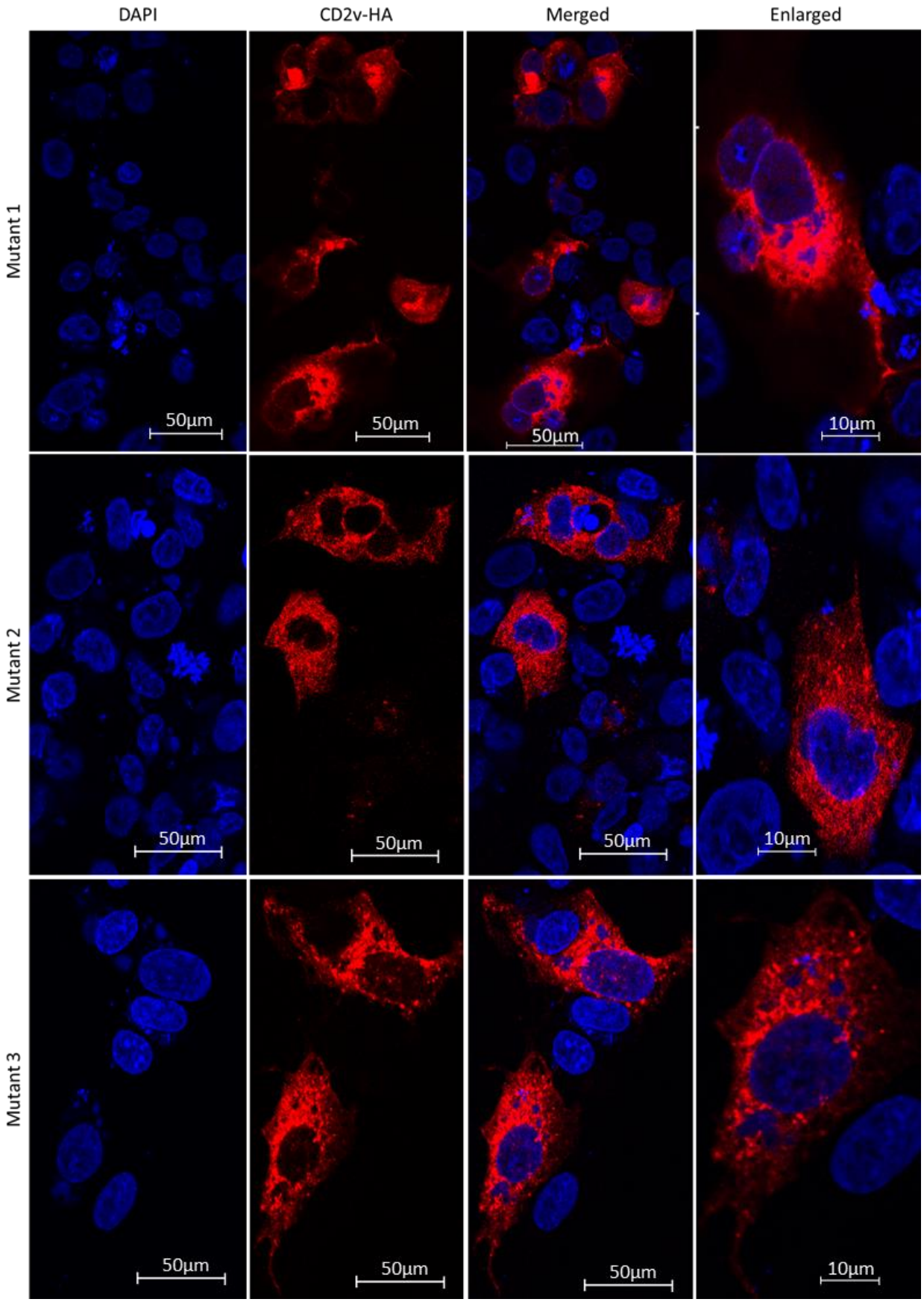
DAPI
CD2v-HA
Merged
Enlarged
Mutant 1
Mutant 2
Mutant 3
50μm
50μm
50μm
10μm
50μm
50μm
50μm
10μm
50μm
50μm
50μm
10μm

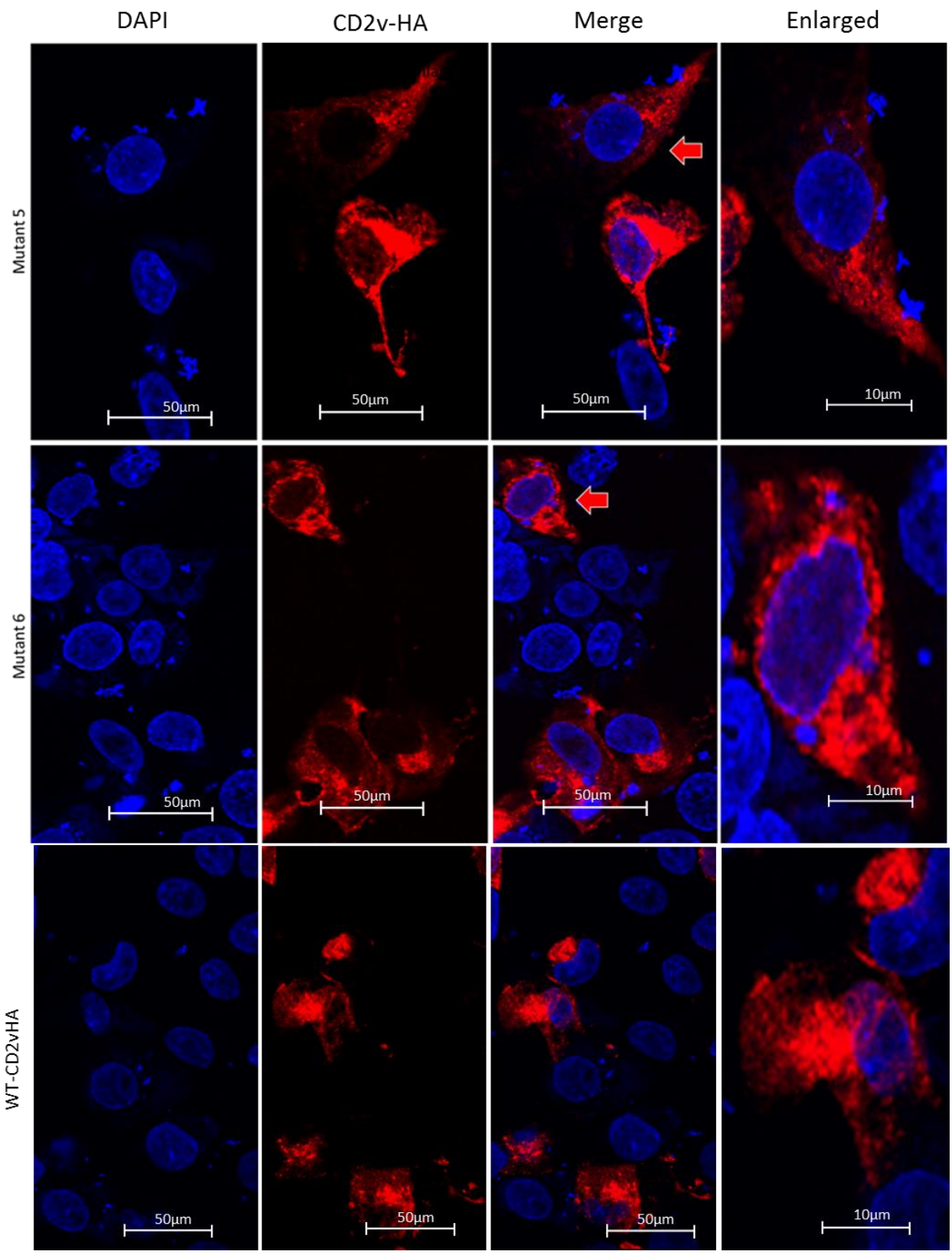

Figure 2.9: <u>Vero cells infected with MVA-T7 and transfected with pWT-CD2vHA and mutants CD2v.</u> The cells were fixed and stain with anti-HA (primary antibody), and probed with anti-rat IgG Alexaflour 568 (secondary antibody) shown in red. The

nucleus and viral factories were stained with DAPI shown in blue, the red arrow indicates the cell shown in the enlarged panel.

2.6.2 HAD analysis of the 1st batch of CD2v mutants;

After confirmation of expression by immunofluorescence and Western blot, CD2v mutants were analysed by functional HAD assay. This experiment was performed to investigate the effect of mutations on attachment of erythrocytes to the cells expressing CD2v. The difference in HAD phenotype was determined by comparing cells expressing the mutants with pWT-CD2vHA. Vero cells were infected with MVA-T7 at MOI-1 and transfected with either pWT-CD2vHA or plasmids expressing mutant CD2v proteins (see section 5.3.2 & 5.3.3). A HAD assay was performed on the cells expressing pWT-CD2v and mutant CD2v proteins, as describes in chapter 5 (section 5.3.5). The levels of erythrocyte binding to each mutant CD2v were determined by comparing with the pWT-CD2vHA. The results showed that cells expressing CD2v mutants had similar HAD compared to the WT-CD2vHA except for mutant 6. Interestingly, the amount of RBC attached to cells expressing mutant 6 was reduced (see figure 2.10). Attempts were made to detect the reduction in binding of RBC based on size using the MACSquant analyser, however no difference was observed between the cells-only control and the pWT-CD2vHA HAD cells. Another attempt was made to detect reduction of RBC binding by confocal microscopy. To optimise the approach Vero cells grown on cover slips were co-transfected with pWT-CD2vHA and a plasmid construct expressing green fluorescence protein (GFP). A HAD assay was performed according to the method outlined in section 5.3.5. The cells were then fixed with 4% PFA and the cover slips were mounted on the glass slides, the slides were observed by confocal microscope using the bright field and the 488 channel to detect GFP and pWT-

CD2vHA expressing HAD cells. However, only non-HAD GFP expressing cells were detected.

A delay in HAD was also observed in cells expressing mutant 6, which has a substitution at position 102 from Y→D. In cells expressing WT-CD2vHA, HAD was observed 30 minutes after the blood was added however, HAD caused by mutant Y102D was delayed up to 18 hours. The HAD assay for mutant 6 was repeated several times (individually and with newly designed mutants) and approximately 40-50 cells showing reduced HAD were observed in 10 fields.

In collaboration with Dr. Simon Davis (University of Oxford, UK) and Dr. Shinji Ikemizu (Kumamoto University, Japan) a predicted model of the structure of CD2v protein was generated. In this model the Y102 is predicted to be buried in the structure and is not exposed but is in involved in polar interactions with K106 and with I108 on the opposite loop. Substituting Y102 with aspartic acid was predicted to impair the polar contact between Y102, K106 and I108. This could result in a shift in charges which impairs other polar contacts of this loop (see figure 2.25).

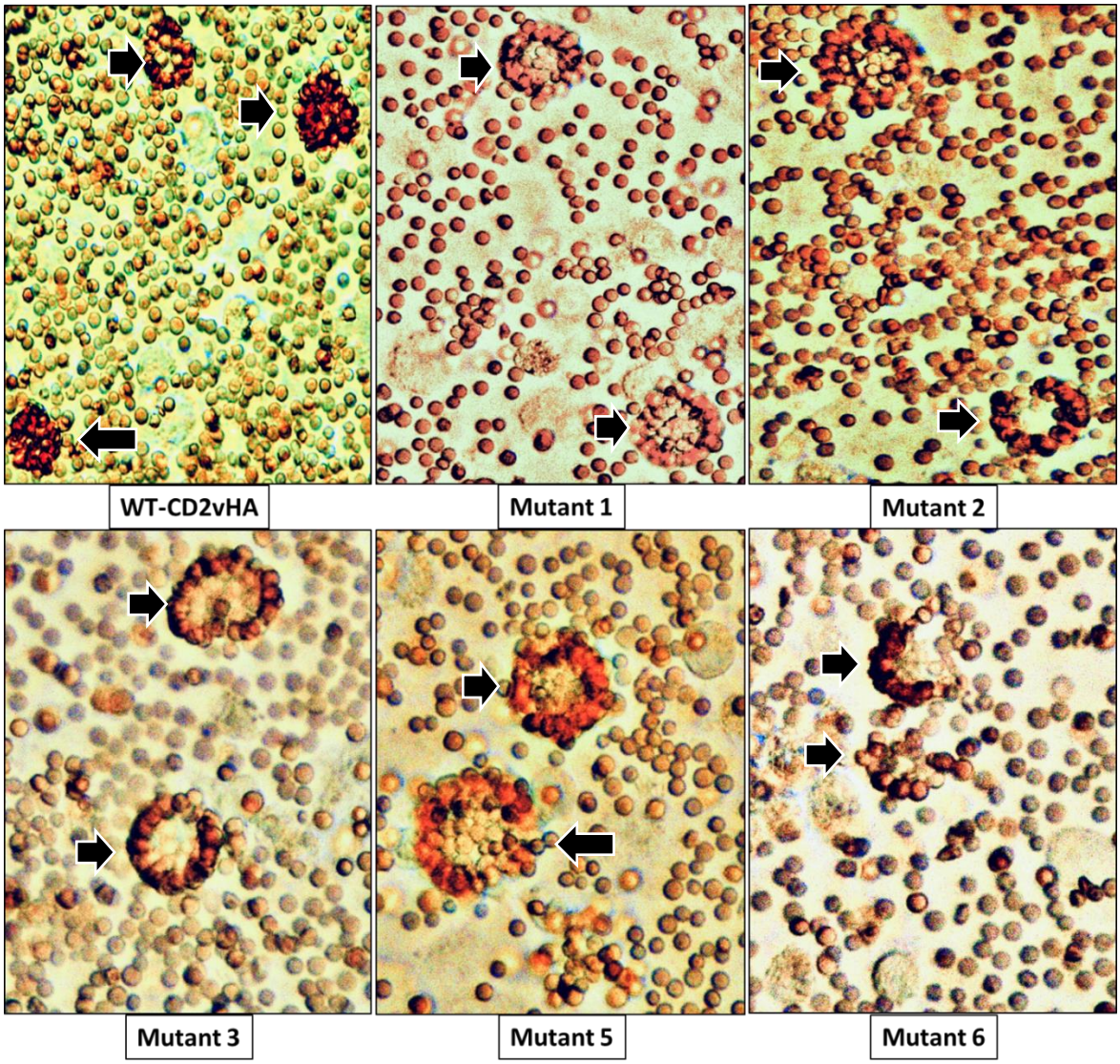

Figure 2.10; <u>Vero cells infected with MVA-T7 and transfected with CD2v mutants (batch 1).</u> Cells were detached and whole pig blood was added 24 hours post infection/transfection. The cells expressing mutant CD2v proteins are HAD apart from mutant 6, which is partially HAD. The images were captured after 42 hours post infection with a Leica microscope attached to a 2.5 Megapixel HD Microscope Camera (Leica MC120 HD)

2.7 Design of mutations in CD2v protein to reduce binding of red blood cells (BATCH-2):

Previous data available for rat and human CD2 suggests that the ligand-binding domain is located in β- strands particularly in the GFCC' region (van der Merwe et al., 1995;

Wang et al., 1999). A model for CD2v (Ig domain 1) was designed by Dr. Ana Reis (The Pirbright Institute) using Raptor X online protein modelling tool (see figure 2.11a). The predicted model showed 8 loops (ABCC'DEFG) in the β- sheets, the charged, exposed, glycosylated and the conserved residues between human and Benin CD2v were substituted with alanine (see figure 2.11b). The aim was to identify mutations that abrogated HAD and then mutate the substituted amino acid residues one by one to narrow it down to a single residue. The new mutants were designed based on the predicted model of the CD2v immunoglobulin domain (see figure 2.11a). The amino acid residues (F44, Y48, R53, Y58, D104, K105 and K106) that were exposed on the surface of the molecule were planned to be mutated including the glycosylation sites (N52, N55, N77, N81 and N108) in the Ig domain 1. The new mutations were introduced in the predicted β-sheets (GFCC') of CD2v immunoglobulin domain, each mutant had a unique group of amino acid residues mutated. In mutant 2.1 the amino acid residues in Ig domain 1, with either positively or negatively charged side chains (R53, E99, D104, K105, K106), were substituted with alanine (see figure 2.11b). In mutant 2.2, the same charged residues (as in mutant 2.1) in Ig-domain 1 were substituted with alanine along with the N residue in the putative glycosylation sites (N52, N55, N77, N108) to investigate the role of glycosylation in HAD. In mutant 2.3, the charged amino acid residues (same residues as in mutant 2.1 & 2.2) along with predicted exposed hydrophobic residues (F44, Y48, Y58, Y102) were mutated to alanine to investigate if these exposed residues may be involved in HAD. In mutant 2.4, the charged and exposed hydrophobic residues (same as in mutant 2.3) along with the N residue of the predicted glycosylation sites (N52, N55, N77, N108) were mutated with alanine. In mutant 2.5, the charged and exposed hydrophobic residues (same as mutant 2.4) along with the N residue of the potential glycosylated residues (N52 &

N55) present in the β-sheets (loop C') were substituted with alanine (see figure 2.11a & 2.11b). The mutant 2.6 also had charged, exposed, hydrophobic and the N residue of the potentially glycosylated site (E99, Y102, D104, K105, K106, N108) were mutated with alanine in the β-sheets (loop G and F) (see figure 2.6a & 2.6b). In mutant 2.7, the N residues of the putative glycosylated sites (N81, N125, N137), that were conserved in human and Benin WT-CD2v, were mutated and substituted with alanine. The mutant CD2v sequences were assembled by using Vector NTI software and were analysed for a premature stop codons. The immunoglobulin domains containing the mutations were ordered from GeneArt as DNA fragments and were delivered pre-cloned in pMK vector which were transformed and amplified in bacterial cells. The pMK vector containing the fragments with mutations in Ig domains were digested by *Scal* and *Mfel* restriction sites and used to replace the Ig domain of pWT-CD2vHA cloned into pcDNA3. An HA-tag was fused in frame at the C-terminus. All mutants were successfully cloned except for mutant 2.5 which didn't work after several attempts. The cloned mutants were transformed into bacterial *E.coli* (DH5α) cells and were grown in midi preps, the mutant plasmid DNA was isolated and was sequenced by Sanger sequencing using T7 forward and reverse primers (see appendix 1 for primer sequences). These mutants were then used for transfection into cells (see section 2.7.1).

A

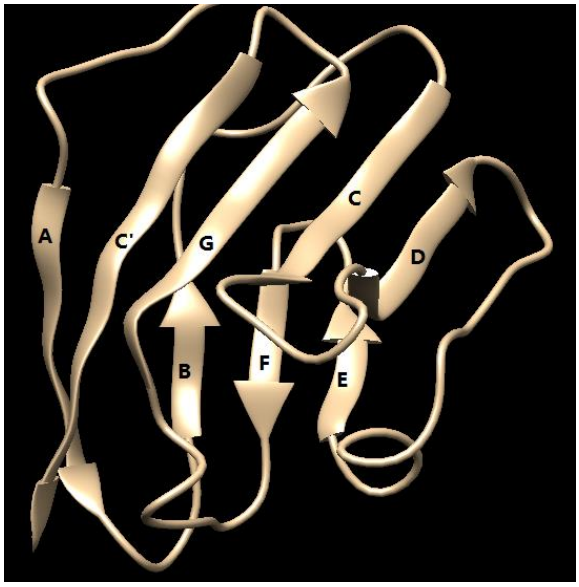

B

```
          41  C          C'                    C''  D        E                  94
WT-CD2v   GGLFWNTYYDNNRSNFTYCGIAGNYCSCCGHNISLYNTTNNCSLIIFPNNTEIF
Mut-2.1   GGLFWNTYYDNNASNFTYCGIAGNYCSCCGHNISLYNTTNNCSLIIFPNNTEIF
Mut-2.2   GGLFWNTYYDNAASAFTYCGIAGNYCSCCGHNISLYATTNNCSLIIFPNNTEIF
Mut-2.3   GGLAWNTAYDNNASNFTACGIAGNYCSCCGHNISLYNTTNNCSLIIFPNNTEIF
Mut-2.4   GGLAWNTAYDNAASAFTACGIAGNYCSCCGHNISLYATTNNCSLIIFPNNTEIF
Mut-2.5   GGLAWNTAYDNAASAFTACGIAGNYCSCCGHNISLYNTTNNCSLIIFPNNTEIF
Mut-2.6   GGLFWNTYYDNNRSNFTYCGIAGNYCSCCGHNISLYNTTNNCSLIIFPNNTEIF
Mut-2.7   GGLFWNTYYDNNRSNFTYCGIAGNYCSCCGHNISLYNTTNACSLIIFPNNTEIF
          95  F          G                    A        B        C          180
WT-CD2v   NRTYELVYLDKKINYTVKLLKSVDSPTITYNCTNSLITCKNNNGTNVNIYLIINNTI
Mut-2.1   NRTYALVYLAAAINYTVKLLKSVDSPTITYNCTNSLITCKNNNGTNVNIYLIINNTI
Mut-2.2   NRTYALVYLAAAIAYTVKLLKSVDSPTITYNCTNSLITCKNNNGTNVNIYLIINNTI
Mut-2.3   NRTYALVALAAAINYTVKLLKSVDSPTITYNCTNSLITCKNNNGTNVNIYLIINNTI
Mut-2.4   NRTYALVALAAAIAYTVKLLKSVDSPTITYNCTNSLITCKNNNGTNVNIYLIINNTI
Mut-2.5   NRTYELVYLDKKINYTVKLLKSVDSPTITYNCTNSLITCKNNNGTNVNIYLIINNTI
Mut-2.6   NRTYALVALAAAIAYTVKLLKSVDSPTITYNCTNSLITCKNNNGTNVNIYLIINNTI
Mut-2.7   NRTYELVYLDKKINYTVKLLKSVDSPTITYACTNSLITCKNNAGTNVNIYLIINNTI
```

Figure 2.11a: Predicted model of CD2v Ig-domain 1; the predicted 3D model of CD2v immunoglobulin domain showing the β-sheets (GFCC' region) that are predicted to be involved in protein-protein interactions (source: RaptorX protein modelling). **Figure 2.11b: Alignment of batch-2 mutants (from residue 41-180);** new mutants with a different combination of amino acid residues (F44, Y48, N52, R53, N55, Y58, N77, N81, E99, Y102, D104, K105, K106, N108, N125, N137) substituted in the predicted β-sheets (loop GFCC') of CD2v immunoglobulin domains were generated to

determine the functional amino acid residues involved in HAD. The substituted alanine residues are highlighted green, the predicted N-linked glycosylation sites are shown in grey shaded boxes, the β-strands in Ig-domain 1 are indicated by the red bar and the β-strands in Ig-domain 2 are indicated by the green bar.

2.7.1 Expression analysis of 2ND Batch CD2v mutants by Western blot and Immunofluorescence:

The expression of these mutant CD2v proteins (batch 2) was analysed by Western blot and immunofluorescence using confocal microscopy. As explained above, it was important to confirm expression, localisation and processing of the mutant CD2v proteins before proceeding with the functional HAD assay.

To investigate if the mutant CD2v proteins are expressed at the correct size and processed (glycosylated), Vero cells were infected with MVA-T7 (MOI 1) and were transfected with plasmid constructs expressing mutant CD2v proteins (Batch-2) (see section 5.3.2 & 5.3.3). A Western blot was performed on the cell extracts according to the method described in chapter 5 (section 5.3.8).

The results showed that all mutant CD2v proteins were expressed (see figure 2.12), the band detected at 102 kDa corresponds to the full length glycosylated CD2v and the band detected at 42kDa corresponds to full length non-glycosylated form of CD2v. The non-glycosylated C-terminal domain was detected at 26kDa in mutant 2.1 & 2.2 and not in n mutant 2.4, 2.6, and 2.7. The data provide evidence that mutants CD2v proteins were expressed, and glycosylated similar to the pWT-CD2vHA. Detection of the C-terminal 26kDa fragment and levels of protein were variable possibly due to transfection efficiency or differences in protein expression or stability.

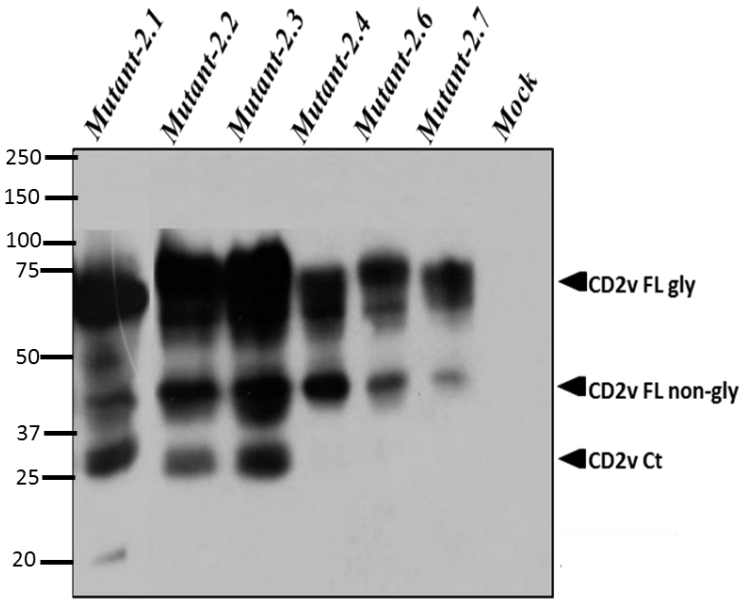

Figure 2.12: Vero cells mock-infected or infected with MVA-T7 (MOI 1), transfected with pWT-CD2vHA and the plasmid expressing mutant CD2v proteins. The cell lysates were prepared and were separated by SDS-PAGE, probed with anti-HA primary antibody and anti-HA HRP secondary antibody. The image is showing full length glycosylated CD2v (102 kDa), full length non-glycosylated CD2v (42 kDa) and C terminal fragments (26 kDa).

To further investigate, immunofluorescence was performed to analyse if the expressed CD2v mutants have similar distribution and localisation patterns as the pWT-CD2vHA. Vero cells were infected with MVA-T7 at MOI-1 and were transfected either with pWT-CD2vHA or the plasmid constructs expressing mutant CD2v proteins (see section 5.3.2 & 5.3.3). The cells were fixed, permeabilised and stained with anti-HA (rat) primary antibody and probed with alexaflour 568 (goat anti-rat IgG) secondary antibody (see section 5.3.4). This experiment was performed several times for mutant 2.1 and 2.2 while for the remaining mutants the experiment was performed once (mutant 2.3, 2.4, 2.6 and 2.7) and more than 50 cells were observed expressing mutant CD2v protein. The results showed that the mutant CD2v proteins were expressed and

were distributed in the cytoplasm and some of the protein was localised close to the plasma membrane (see figure 2.13). However, it was not clear if the protein was expressed on the cell surface as the HA tag was fused to the cytoplasmic domain. Expression of the proteins was concentrated around the MVA-T7 viral factories. It appeared that mutant 2.1, 2.2 and 2.3 proteins were localised in punctate areas close to the MVA-T7 viral factories, however, in cells expressing mutant 2.4 and 2.6 the protein appeared more dispersed while in cells expressing mutant 2.7 the protein localised in punctate areas close to the nucleus.

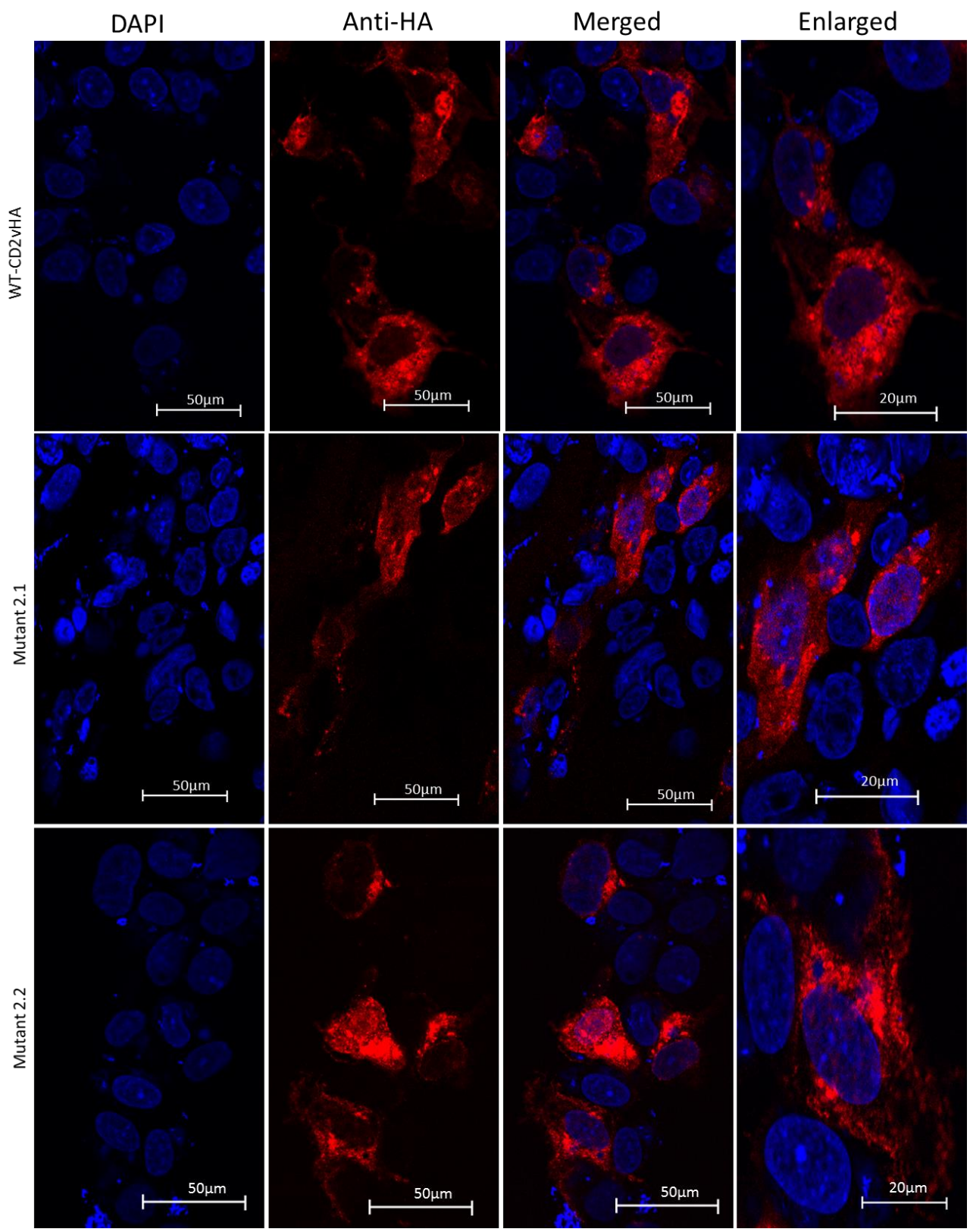
DAPI
Anti-HA
Merged
Enlarged
WT-CD2vHA
Mutant 2.1
Mutant 2.2
50µm
50µm
50µm
20µm
50µm
50µm
50µm
20µm
50µm
50µm
50µm
20µm

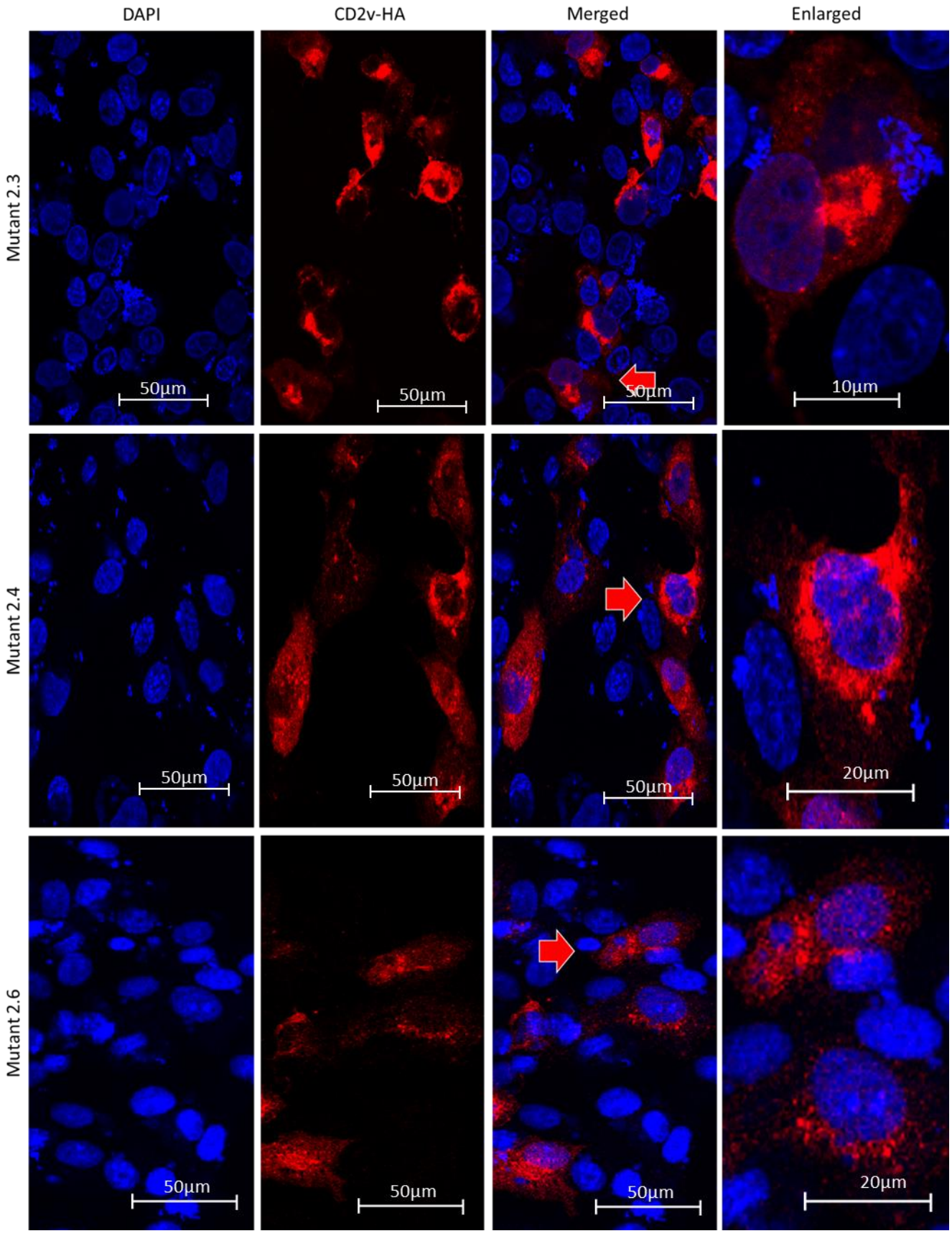
DAPI
CD2v-HA
Merged
Enlarged
Mutant 2.3
Mutant 2.4
Mutant 2.6
50μm
50μm
50μm
10μm
50μm
50μm
50μm
20μm
50μm
50μm
50μm
20μm

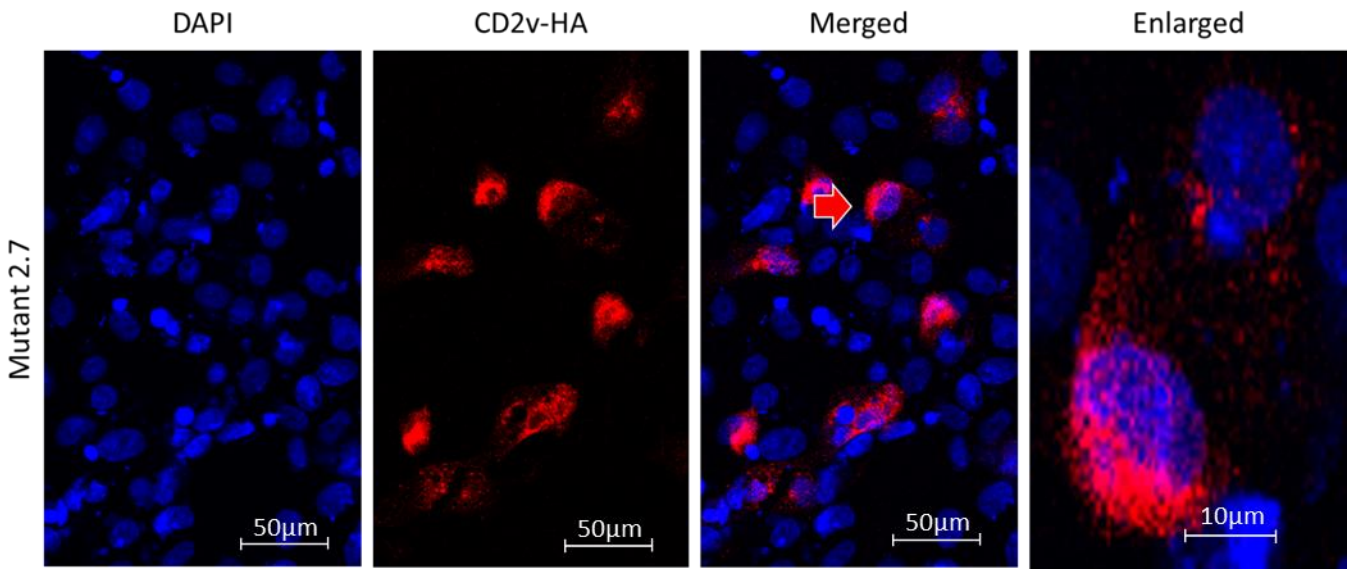

Figure 2.13; <u>Vero cells infected with MVA-T7 and transfected either with pWT-CD2vHA or mutants CD2v (batch 2).</u> The cells were fixed and stain with anti-HA (rat) primary antibody, and were probed with anti-rat IgG Alexaflour 568 (secondary antibody) shown in red. The nucleus and viral factories were stained with DAPI shown in blue.

2.7.2 HAD analysis of 2nd batch CD2v mutants:

The expression of the mutant CD2v was confirmed by immunofluorescence and Western blot (see section 2.7.1). This experiment was performed to investigate the effect of mutations on the attachment of erythrocytes to the cells expressing CD2v mutants. The difference in HAD phenotype was determined by comparing the mutants with pWT-CD2vHA. Vero cells were infected with MVA-T7 at MOI-1 and transfected either with pWT-CD2vHA or plasmid constructs expressing mutant CD2v proteins (batch 2). A HAD assay was performed as described in chapter 5 (section 5.3.5) on the cells expressing pWT-CD2vHA and mutant CD2v proteins. The levels of erythrocyte binding to each mutant CD2v were determined by comparing with the pWT-CD2vHA. The experiment was repeated three times and 1-2 HAD cells were observed in each

field for the HAD mutant (2.2), while in control (pWT-CD2vHA) more than 15 HAD cells were observed in each field. The results showed all mutants in batch 2 showed a negative HAD phenotype except for mutant 2.2 which induced the formation of extremely low rosettes (see figure 2.14). Furthermore, mutant 2.1 (non-HAD) and mutant 2.2 (partial HAD) have similar charged amino acid residues substituted apart from the removal of 4 putative glycosylation sites in mutant 2.2 (N52A, N55A, N77A, N108A). This supports the hypothesis that more glycosylation of CD2v protein may shield amino acids involved in binding to RBC and result in reduced HAD. Therefore, mutation of glycosylation sites, which shield residues important for attachment to RBC, may conversely increase HAD as observed for mutant 2.2.

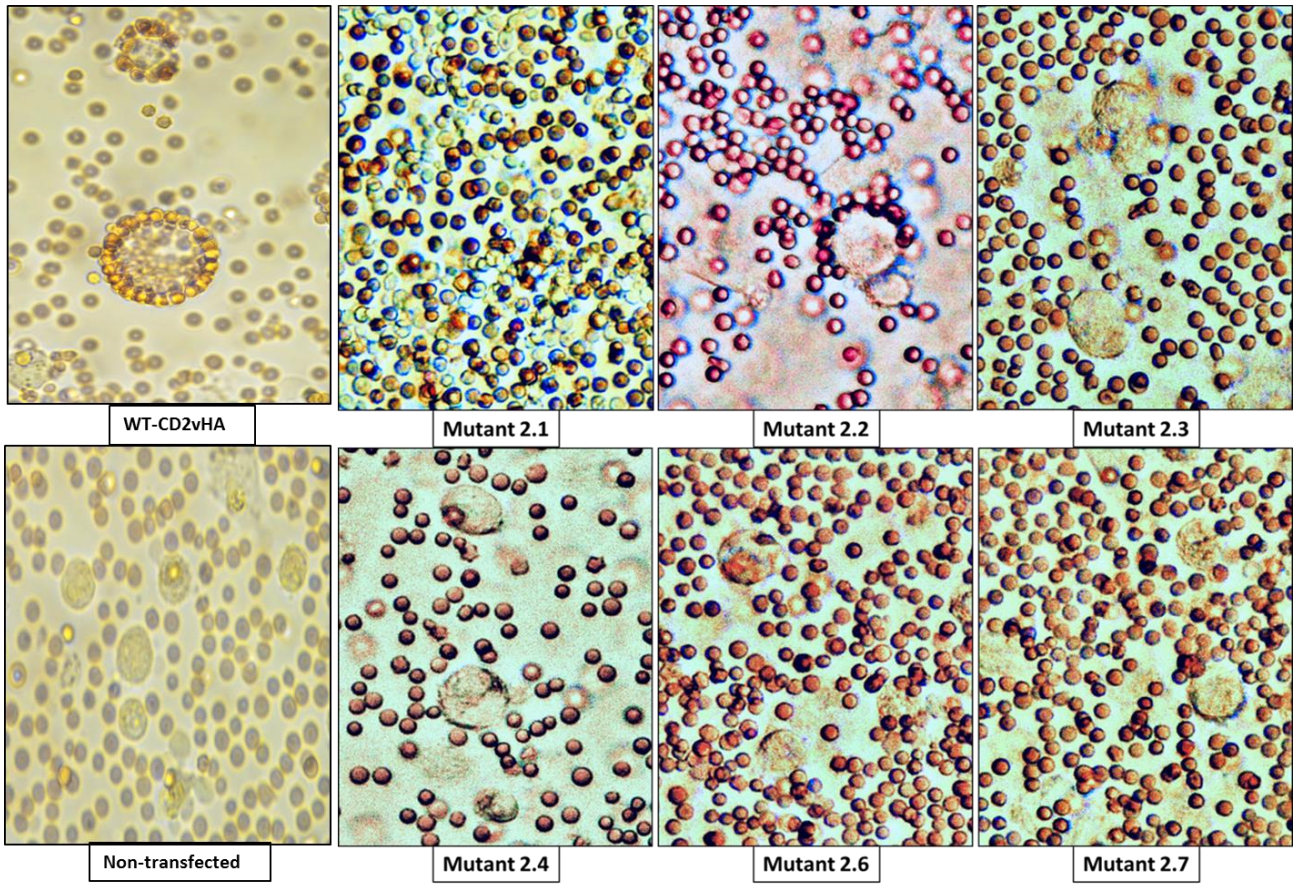

Figure 2.14: <u>Vero cells infected with MVA-T7 at MOI-1 and transfected with CD2v mutants (batch 2).</u> Cells were detached and whole pig blood washed and diluted in PBS (1:4) was added. The cells were incubated for 18 hours to induce HAD, the cells expressing CD2v mutants were non-HAD except for mutant 2.2 (1-2 HAD cells/field), which was partial HAD. The experiment was repeated three times to confirm that the results are consistent.

2.8 Design of mutations in CD2v protein to reduce binding of red blood cells (BATCH-3):

To design more CD2v mutants a predicted model for CD2v was generated in collaboration with Dr. Shinji Ikemizu (Kumamoto University, Japan) and Dr. Simon Davis (Oxford University, UK) following the alignment of the Ig domain of human, rat, and ASFV encoded CD2v from different isolates (see figure 2.2). The idea was to identify functional amino acid residues and to construct mutants with single amino acid substitutions, as the multiple substitutions might interfere with protein folding. This may also affect the structure of the molecule and direct the protein for degradation or may inhibit the interaction with the ligand due to changes to the structure. The new substitutions were designed to make drastic changes in charge to selected residues and thus disrupt the ligand binding and force it apart from CD2v. In a previous study, it was reported that charged residues contribute little binding energy to the interaction between CD2 and CD48 (rat CD2 ligand). However, the loss of charged residues significantly reduce ligand binding specificity (Davis et al., 1998). The aim was to identify the critical residues involved in the interaction between CD2v and its ligand without disrupting the structure of the protein. These mutants will eventually be used to construct a recombinant non-HAD virus expressing CD2v (chapter 3). The data from the CD2v model and alignments (see figure 2.2 & 2.10a) indicated that drastic charge alteration mutations may be required in the GFCC' region of β-sheets in the

immunoglobulin domains to reduce HAD, similar to mutational analysis performed for rat and human encoded CD2 (van der Merwe et al., 1995; Wang et al., 1999). The previously tested mutant 6 (Y102D) that resulted in very low rosetting has a drastic substitution in the G region of β-sheets (described in section 2.8.1). The tyrosine residue (Y102) was substituted with a negatively charged aspartic acid (D102) residue and may thus have had a more dramatic effect. It was also suggested that a charged residue should be substituted with the oppositely charged residue to reduce the binding affinity in the ligand-binding domain. Subsequently all the mutants were expressed in Vero cells grown on coverslips and expression was analysed by confocal microscopy to confirm localization, Western blotting was performed to determine any difference in the molecular weight or glycosylation of mutant and WT-CD2vHA proteins. Finally, the mutants were tested by HAD assay to analyse difference or reduction in HAD (see section 2.8.2).

2.8.1 Mutants CD2v designed by following a predicted model generated by Pymol (Batch-3):

The predicted model of Benin WT-CD2v was designed by Dr. Simon Davis (Oxford University) and Dr. Shinji Ikemizu (Kumamoto University, Japan) using Pymol protein modelling software. The aim was to compare the predicted Benin model with the human CD2 model (Wang et al., 1999) and substitute the residues in the region that was reported to involve in human CD2-CD58 interaction. Previously published data on mutational analysis of human and rat have suggested that the receptor-ligand interaction involves the major β-sheet faces of the adhesion domains of both CD2 and its counter receptor (Arulanandam et al., 1994; Ikemizu et al., 1999). The data from mutational analysis correlates with the nuclear magnetic resonance (NMR) solution structure of CD2 and the crystal structure of CD2 and CD58, confirming that the interaction domain

is in the β- sheets (Sun et al., 1999; Wang et al., 1999). Although the sequences of human CD2 and Benin CD2v are divergent, they share a structural similarity in the extracellular N-terminal immunoglobulin domain, especially in the β- sheets. The cysteine residues in the β-sheets that are considered as the hallmark of the immunoglobulin superfamily (IgSF) are conserved between human CD2 and CD2v, these residues form a disulphide bond. The predicted Benin CD2v model suggests that the Ig-domain 1 contain a single disulphide bond form between cysteine 59 and cysteine 82 on the adjacent loop (see figure 2.2 & 2.15). The alignment of human and ASFV encoded CD2 protein showed that the Ig-domain 2 contain double disulphide bonds, one is formed between C127 and C192 while the second bond is formed between C134 and C174 (see figure 2.2). As described previously the ligand-binding domain of human CD2 is located at the top region of the β- sheets, the amino acid residues with either charged or hydrophobic side chains were predicted to have an effect on the binding of CD2v with its ligand (see figure 2.15).

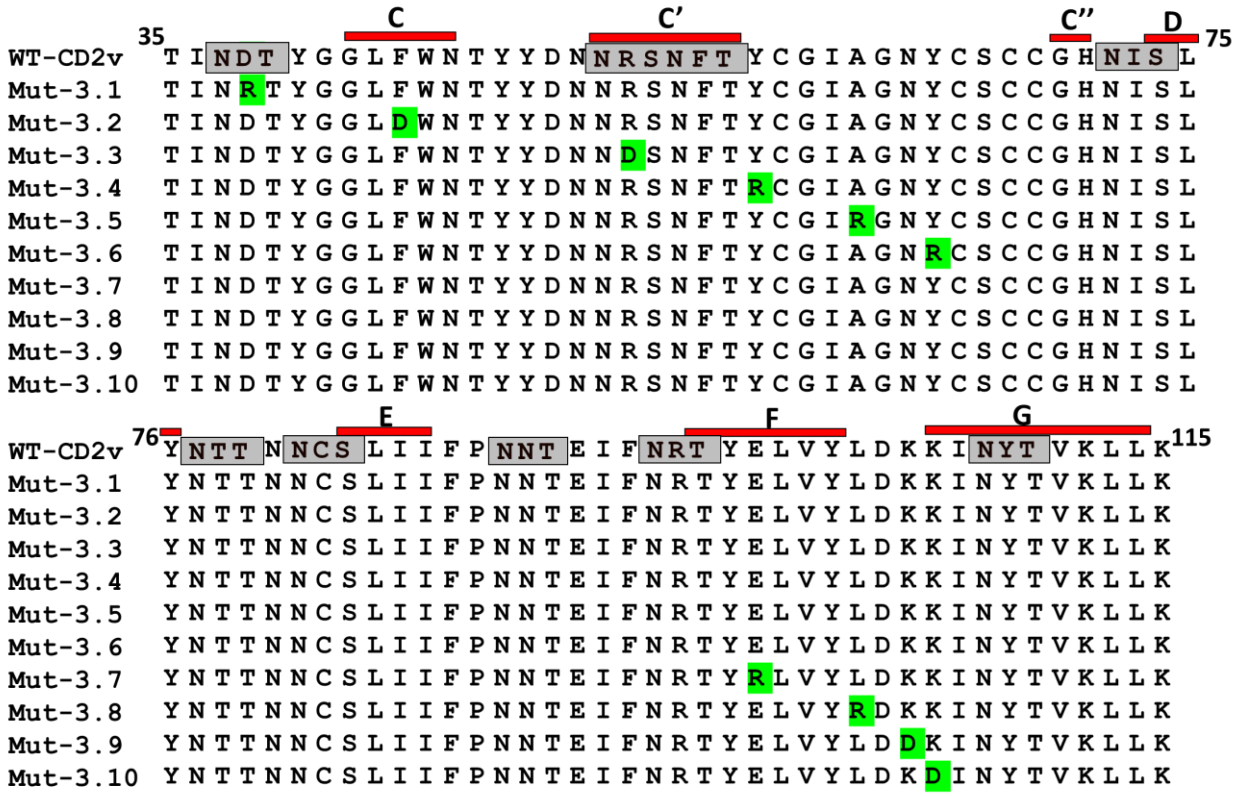

Figure 2.15: Alignment of batch-3 mutants (from residue 35-115). Mutants with a single amino acid residues Y58R, A62R, E99R, K105D, K106D, R53D, L103R, Y65R, D38R, F44D substituted in the CD2v immunoglobulin domain-1 were generated to determine the functional amino acid residues involved in HAD. The substituted residues are highlighted green, the predicted N-linked glycosylation sites are shown in grey shaded boxes, and the predicted β-sheets are indicated by the red bar.

It was proposed to introduce drastic mutation in the ligand-binding domain of CD2v to inhibit binding to its ligand and to substitute the negatively charged residues with positively charged residue, and *vice versa*. Similarly, the hydrophobic amino acid residues were substituted with negatively charged residues. To identify functional amino acid residues in Benin encoded CD2v, 10 mutants were designed based on the information from the predicted Benin CD2v model (see figure 2.15 and 2.16). The predicted functional amino acid residues were substituted with oppositely charged

residues, the mutant sequences were analysed by Dr Ana Reis (The Pirbright Institute) using Vector NTI software and were constructed using site-directed mutagenesis (SDM). The primers for site-directed mutagenesis were designed by Dr Ana Reis (the Pirbright institute) using Agilent technologies Quickchange primer design online tool (see chapter 5, section 5.2.11). I analysed the CD2v mutant plasmid constructs and validated their expression by Western blot and confocal, the functional analysis of the CD2v mutants were performed by setting up haemadsorption assays (see section 2.8.2).

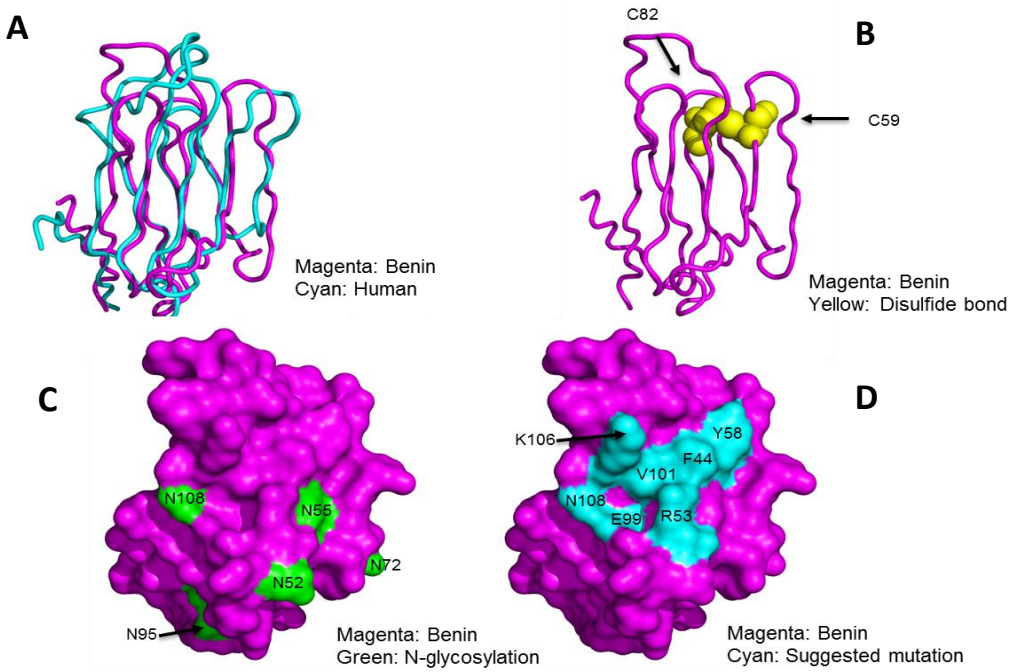

Figure 2.16: The predicted model CD2v IG-domain: (A) A predicted ribbon structure of Benin CD2v Ig compared with human CD2 showing the conserved structural region (B) Predicted model of Benin CD2v showing the cysteine residues with disulphide bonds. (C) Predicted surface model of CD2v Ig-domain showing the potential N-linked glycosylation residue. (D) Predicted CD2v model showing the residues predicted to involve in the binding of CD2v to its ligand.

2.8.2 Expression analysis of 3rd Batch CD2v mutants by Western blot and Immunofluorescence:

As described above, the batch 3 mutants were designed and constructed by Dr Ana Reis (The Pirbright Insitute), I analysed the expression of these mutant CD2v proteins by confocal microscopy and Western blot to confirm their expression, localisation and processing. Western blots were performed to analyse if the mutants were expressed and processed to the correct sizes, observed for pWT-CD2vHA.

Vero cells were infected with MVA-T7 (MOI 1) and transfected with plasmid constructs expressing either pWT-CD2vHA or mutant CD2v proteins (batch 3). The cells were lysed, and a Western blot was performed on the extracts according to the method described in section 5.3.8. The results showed that all batch 3 mutant CD2v proteins were expressed at the correct size, the full-length glycosylated form of CD2v was detected in all mutants at 102 kDa. The full length non-glycosylated form of CD2v was detected at 42kDa in mutants pCD2vD38R, pCD2vR53D, pCD2vA62R, pCD2vK105D, pCD2vK106D and pCD2vE99R. The non-glycosylated C-terminal 26 kDa band was detected in mutants pCD2vY65D, pCD2vK105D, pCD2vK106D and pCD2vE99R. An additional band of 29 kDa was detected in cells expressing pCD2vY65D, pCD2vK105D, pCD2vK106D, pCD2vR53D, pCD2vA62R and pCD2vE99R mutant CD2v proteins. This provides evidence that batch 3 CD2v mutants were expressed, glycosylated and processed in correct sizes similar to the wild type CD2v (pWT-CD2vHA) As mentioned previously these mutants were constructed using site-directed mutagenesis and were not all analysed at the same time, therefore the Western blot data for these mutants are on separate blots and are shown in Appendix 3.

To further investigate, immunofluorescence was performed to analyse if the expressed mutants have similar distribution and localisation pattern as the pWT-CD2vHA. Vero cells were infected with MVA-T7 at MOI-1 and transfected with either pWT-CD2vHA or plasmid constructs expressing mutant CD2v proteins (see section 5.3.2 & 5.3.3). The cells were fixed, permeabilised and stained with anti-HA (rat) primary antibody, probed with alexaflour 568 (goat anti-rat IgG) secondary antibody and were observed by immunofluorescence (see section 5.3.4). The results showed that the mutant CD2v proteins were expressed and localised similar to the WT-CD2vHA, in a punctate pattern concentrated close to the MVA-T7 viral factories. The mutant CD2v proteins were distributed in the cytoplasm and some of the protein was localised close to the plasma membrane (see figure 2.17). The detection of CD2v close to the plasma membrane suggests that the C-terminal processed and/or the full length CD2v may be transported to the cell surface. However, it was not clear if the extracellular domain of the protein was expressed on the surface.

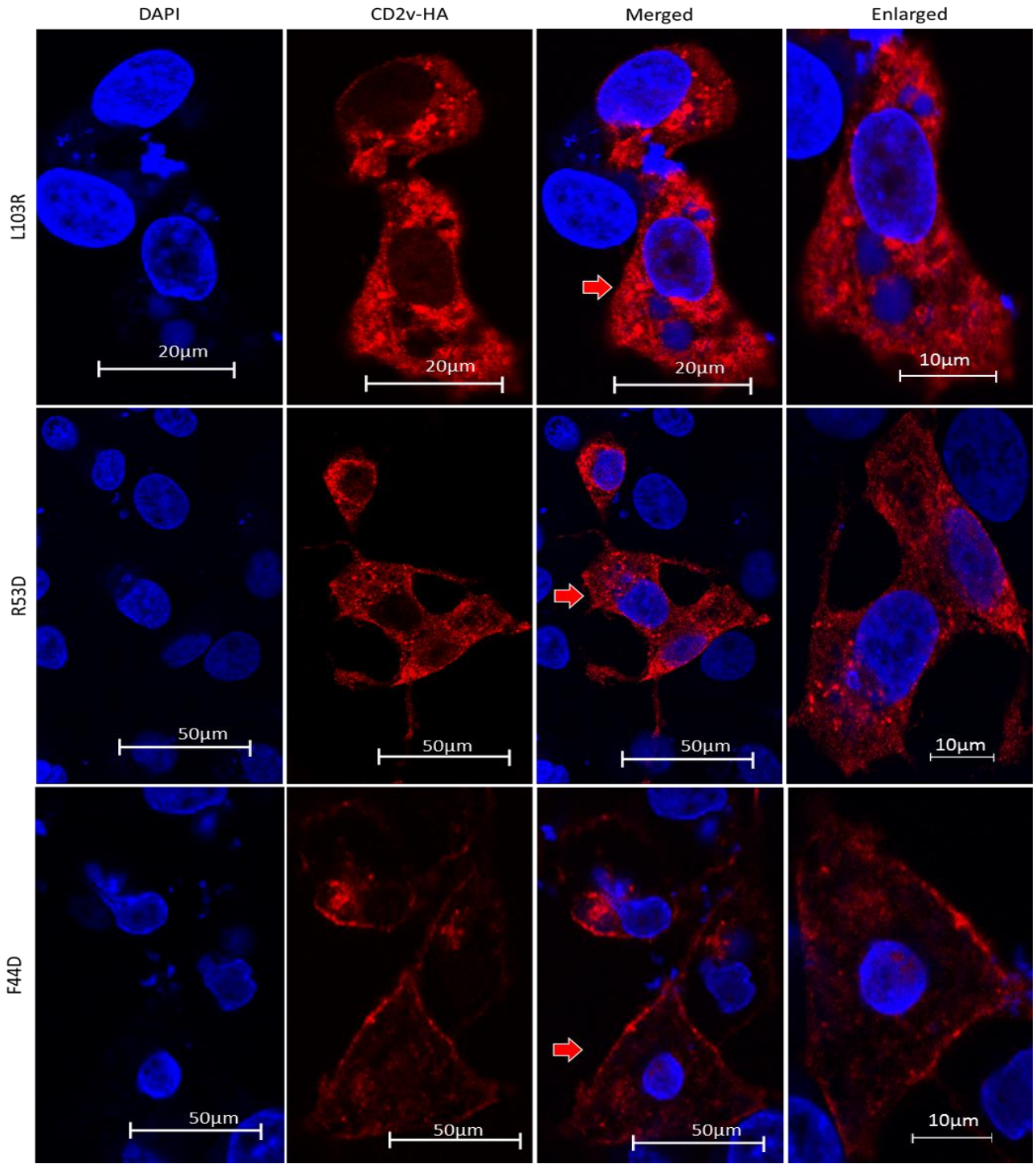
DAPI
CD2v-HA
Merged
Enlarged
L103R
R53D
F44D
20μm
20μm
20μm
10μm
50μm
50μm
50μm
10μm
50μm
50μm
50μm
10μm

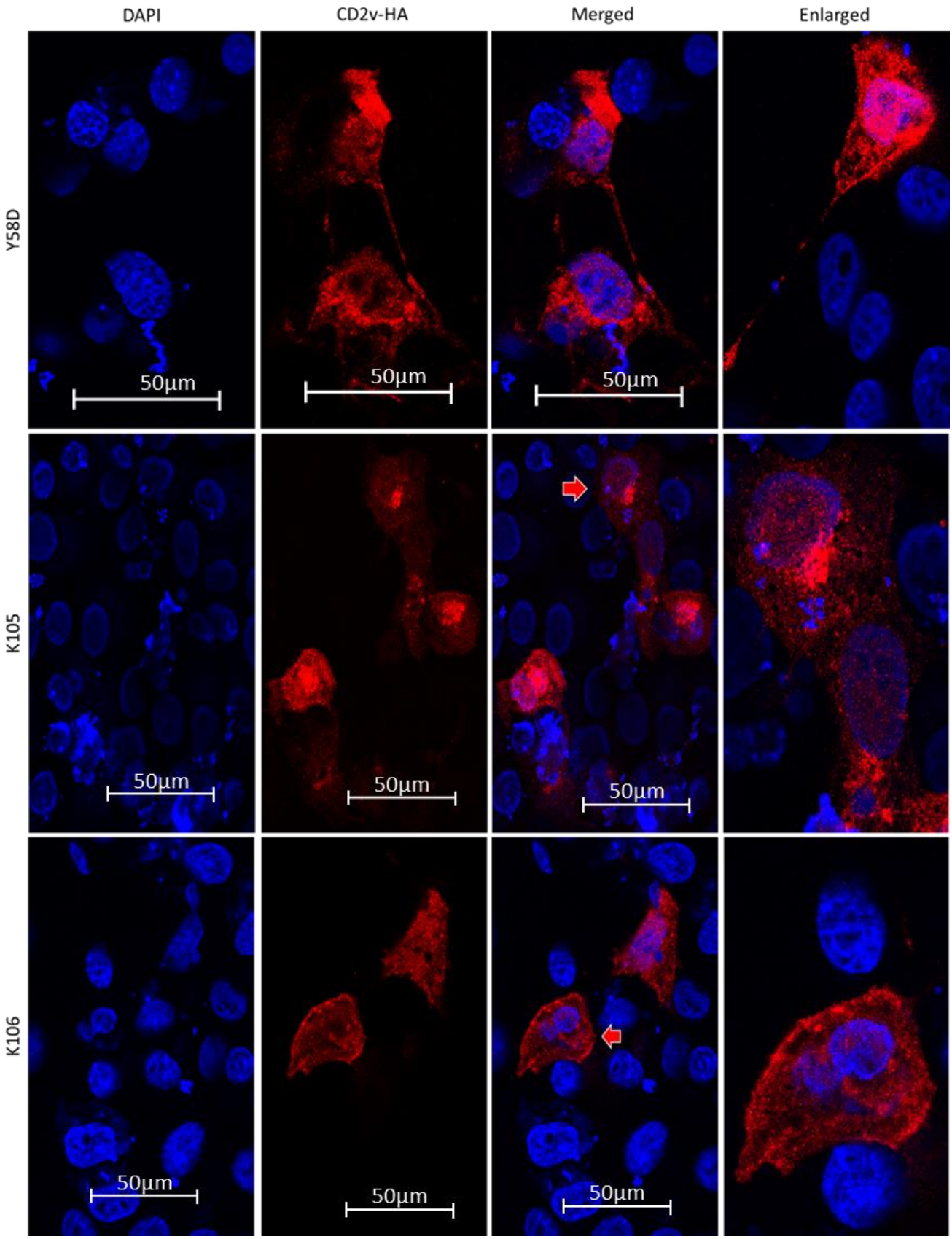
DAPI
CD2v-HA
Merged
Enlarged
Y58D
K105
K106
50μm

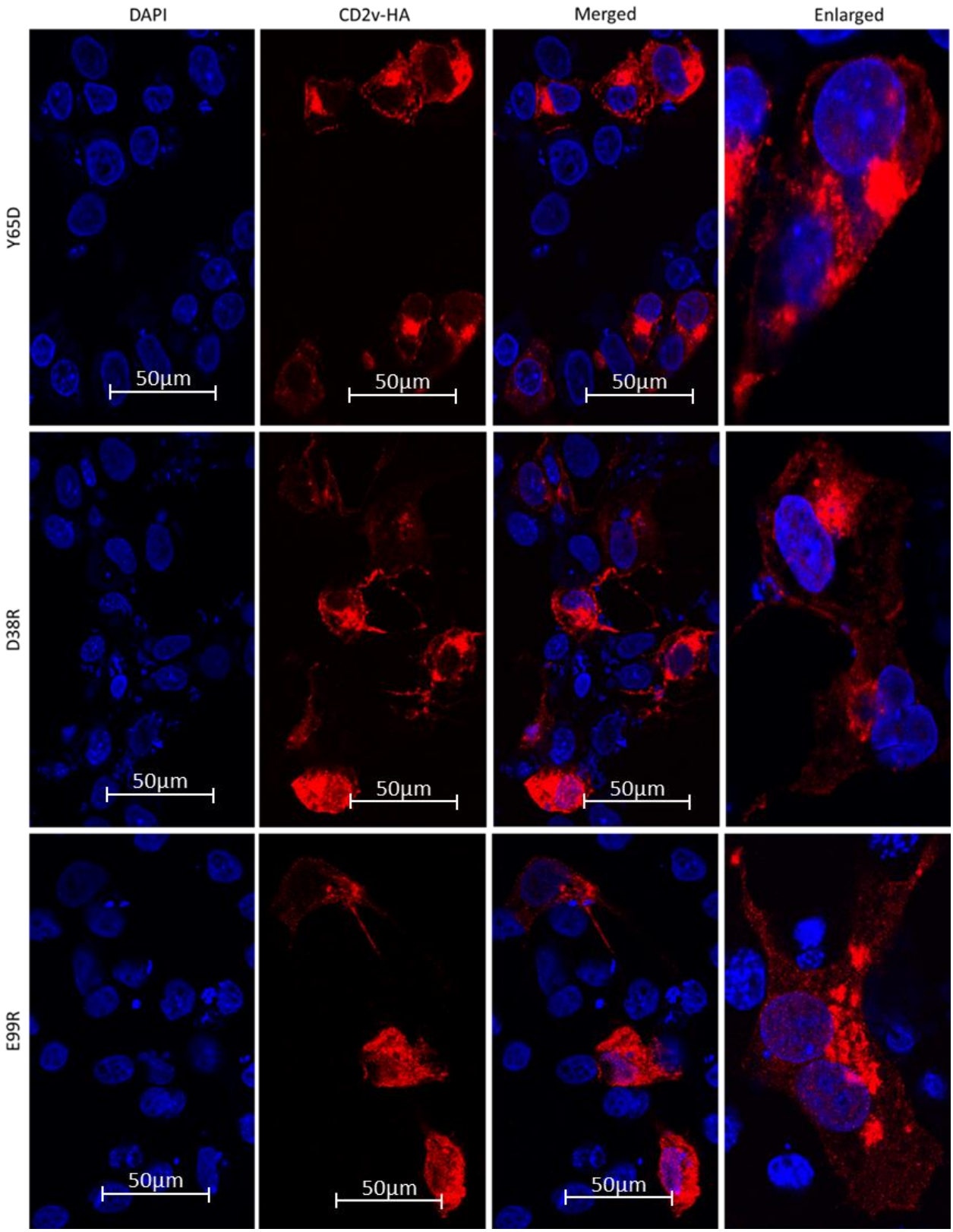
DAPI
CD2v-HA
Merged
Enlarged
Y65D
D38R
E99R
50µm

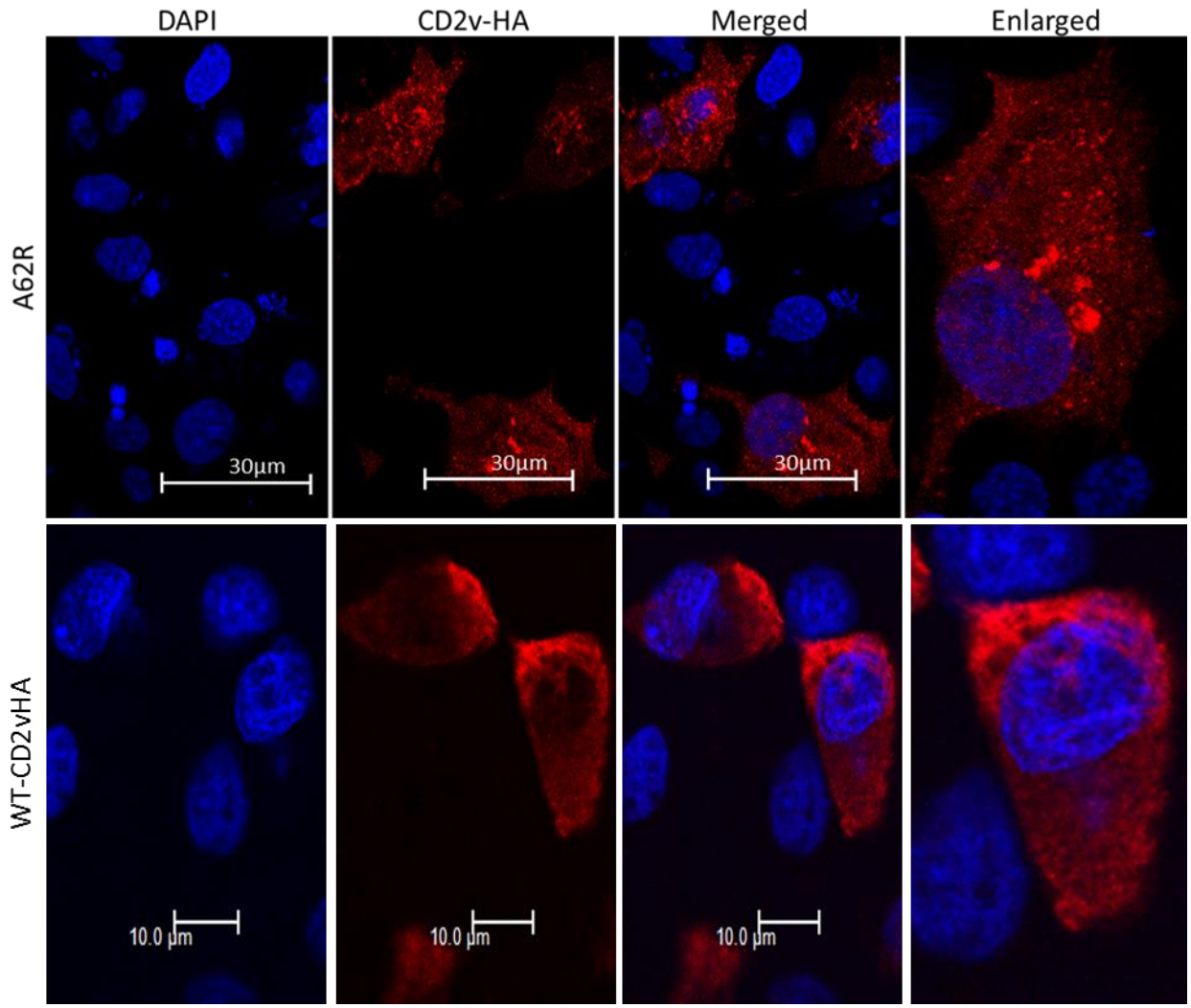

Figure 2.17: <u>Vero cells infected with MVA-T7 and transfected with plasmid constructs expressing mutant CD2v proteins (batch 3).</u> The cells were fixed and stained with anti-HA (primary antibody) and probed with anti-rat IgG Alexaflour 568 (secondary antibody) shown in red. The nucleus and viral factories were stained with DAPI shown in blue.

2.8.3 Functional analysis of 3rd batch mutants by HAD assay:

The expression of mutant CD2v proteins (batch 3) was confirmed by confocal microscopy and Western blot in MVA-T7 infected and transfected Vero cells. A HAD assay was performed to observe the effect of these mutations on binding of RBC to the cells expressing the mutant proteins. The difference in HAD phenotype was determined

by comparing cells expressing the mutant CD2v proteins with the cells expressing pWT-CD2vHA (see section 5.3.5). The results provided evidence that all mutant CD2v in batch 3 were HAD except for pCD2vE99R which showed no HAD. The drastic mutation (from E99 to R) and switching of a negatively charged residue to positively charged residue completely abrogated the binding of RBC to the expressed CD2vE99R (see figure 2.18). The evidence indicates that E99 is a critical amino acid residue involved in HAD and that alteration of the charged residues from negative to a positive residue had an impact on the ligand binding. In human CD2, the residue L103 was shown to be critical however in ASFV Benin encoded CD2v no difference in CD2v function was observed when the same residue was (L103) mutated.

This experiment was repeated twice and more than 50 HAD cells were observed in those expressing all mutants except for mutant CD2vE99R.

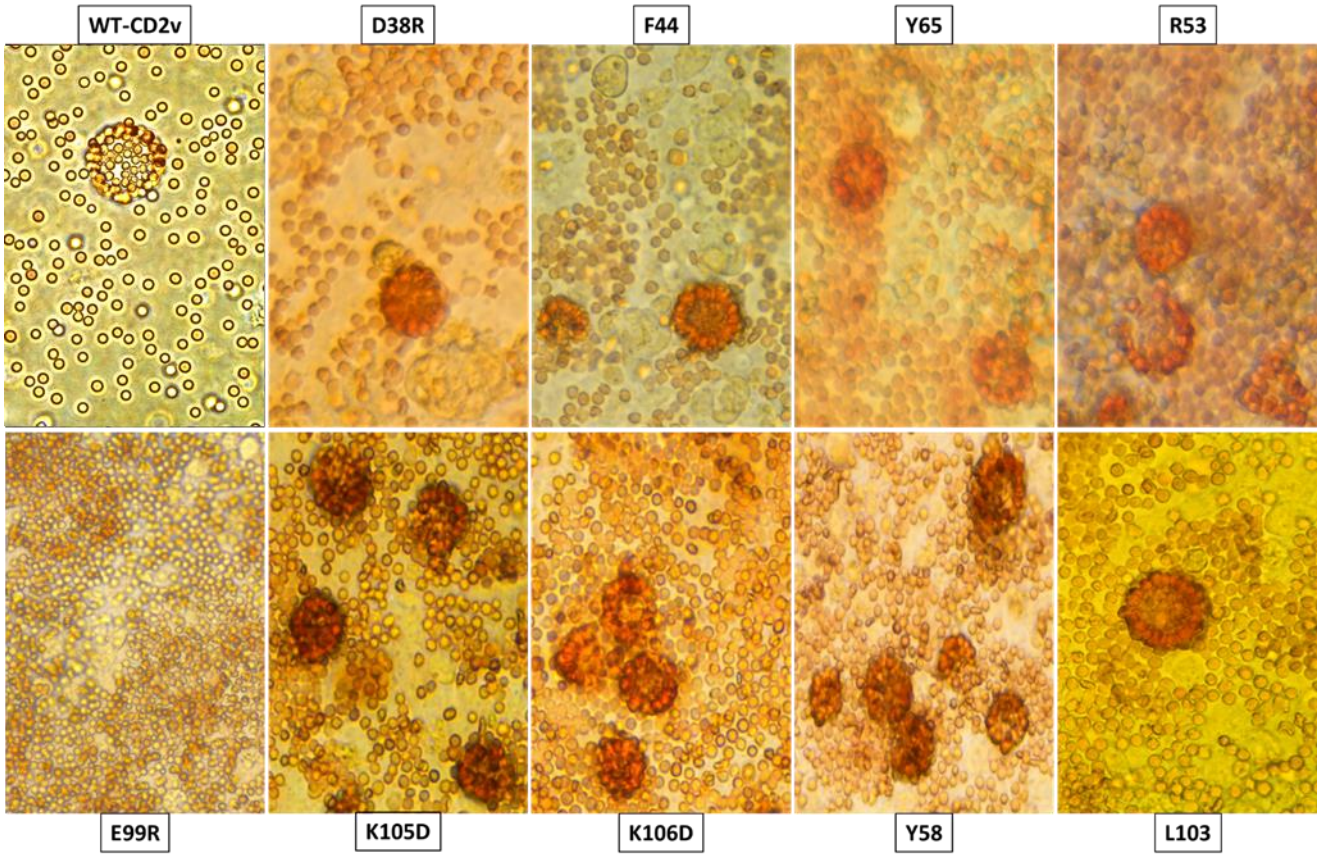

Figure 2.18: <u>Vero cells infected with MVA-T7 and transfected with plasmid expressing mutant CD2v (batch 3).</u> The cells were detached and whole pig blood RBCs was added 24 hours post infection/transfection. The image shows the HAD cells expressing either WT-CD2v or CD2v mutant, apart from CD2vE99R which had no detectable HAD.

After analysis of all batch 3 mutants by confocal and HAD assay following Western blot, only one mutant pCD2vE99R completely abrogated the attachment of RBC to cells expressing E99R. A Western blot was performed (using the same conditions as described in chapter 5, section 5.3.3) to confirm that CD2v mutant pCD2vE99R (non-HAD), pCD2vY102D and pCD2v2.2 (reduced HAD) were expressed, glycosylated and processed in correct sizes similar to the pWT-CD2vHA. A control for glycosylation was included to identify the non-glycosylated form of CD2v. The cells were treated with tunicamycin, which inhibits protein folding and transit through ER. This

experiment was performed to investigate the degree of glycosylation of the WT-CD2vHA and mutant CD2v proteins. This would indicate how much of the proteins enters the secretory pathway and the progression through the secretory pathway since the glycosyl groups added undergo maturation during this process. The results showed that full length glycosylated pWT-CD2vHA and the mutant CD2v proteins pCD2vE99R, pCD2vY102D and pCD2v2.2 were detected at 102kDa. The non-glycosylated full-length WT-CD2vHA and the mutant CD2v protein pCD2vE99R and pCD2v2.2 were detected at 42kDa. The non-glycosylated full length mutant pCD2vY102D was not detected, also the pCD2vY102D protein was detected at a lower level than WT-CD2v and other mutant CD2v proteins. The full length non - glycosylated pCD2v2.2 (42kDa) was detected at high levels, possibly the CD2v2.2 protein expression at high levels in individual transfected cells may result in a delay in progression through the secretory pathway and hence higher levels of the 42kDa non-glycosylated protein. This may also be due to the disruption of 4 putative glycosylation sites that might affect folding of the expressed protein and possibly results in a delay in progression through the secretory pathway. The C-terminal domain was detected at 26kDa in pWT-CD2vHA, pCD2vE99R, pCD2vY102D and pCD2v2.2 (see figure 2.19). The additional band at 29kDa was detected in pWT-CD2vHA (tunicamycin-treated and untreated), pCD2vE99R and pCD2v2.2 but not in pCD2vY102D. These results confirm that both reduced HAD and non-HAD CD2v mutants were expressed and processed into full length glycosylated and non-glycosylated forms.

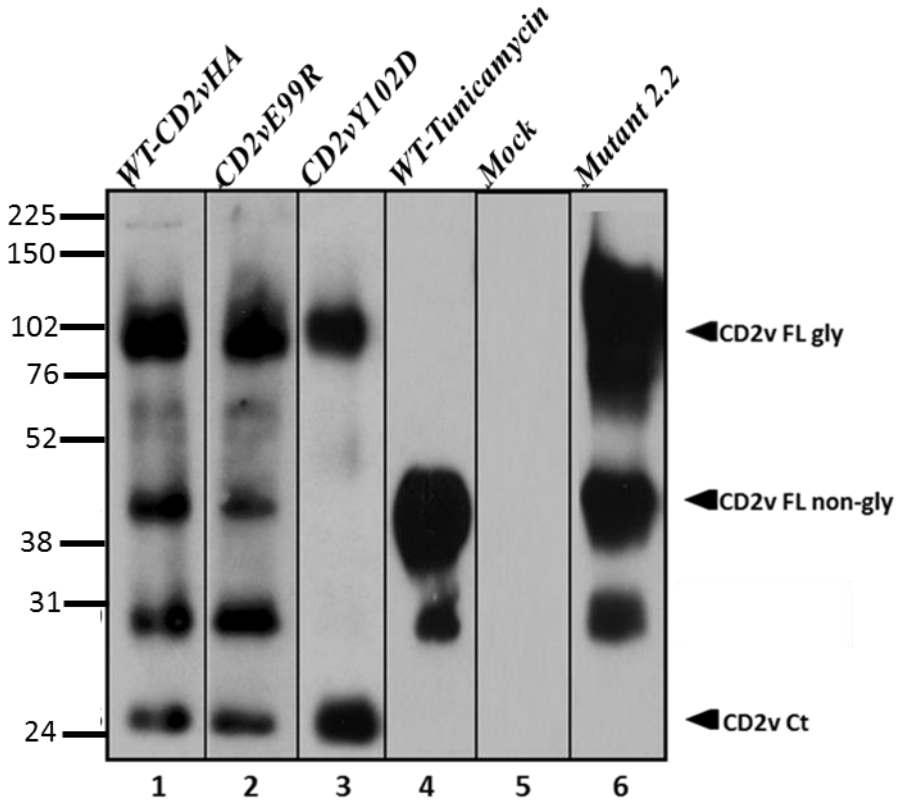

Figure 2.19: Western blot showing expression of wild type and mutant CD2v. Extracts from cells transfected with plasmids expressing WT-CD2vHA (Lane 1) and pCD2vE99R (Lane 2), pCD2vY012D (lane 3) and pCD2v2.2 (lane 6). Lane 4 shows WT-CD2v from tunicamycin treated cells. Plasmids were transfected into Vero cells and lysates collected at 24 h post-transfection. In the image the 102kDa band corresponds to full length glycosylated CD2v, the band at 42kDa corresponds to full length non-glycosylated CD2v, the bands detected at 26 and 29 kDa corresponds to C-terminal CD2v fragments.

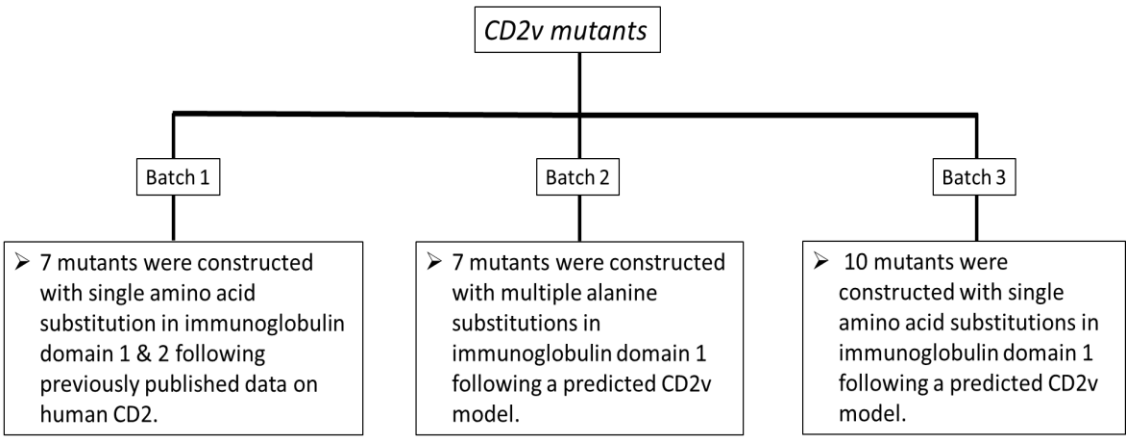

Figure 2.20: Summary of the constructed CD2v mutants: A schematic diagram shows the 24 CD2v mutants constructed in different batches following various strategies.

Table 2.2; List of CD2v mutants, showing the position of the substitution and its effect on protein expression (Western blot and confocal) and HAD assay.

Plasmid constructs	Substitutions/Mutations	Western blot	IF	HAD
Batch-1				
Mutant 1	***D50G, F56V***	++++	++++	++++
Mutant 2	***F56S, N55R***	+++	+++	++++
Mutant 3	***N55R, F56L***	+++	+++	++++
Mutant 5	***D104H***	+++	+++	++++
Mutant 6	***Y102D***	+++	+++	+
Batch-2				
Mutant 2.1	***R53A, E99A, D104A, K105A, K106A***	+++	+++	-
Mutant 2.2	***N52A, R53A, N55A, N77A, E99A, D104A, K105A, K106A, N108A***	+++	+++	+
Mutant 2.3	***F44A, Y48A, R53A, Y58A, E99A, Y102A, D104A, K105A, K106A***	++++	+++	-
Mutant 2.4	***N52A, R53A, N55A, Y58A, N77A, E99A, Y102A, D104A, K105A, K106A, N108A***	++	+	-
Mutant 2.6	***E99A, Y102A, D104A, K105A, K106A, N108A***	++	+	-

Mutant 2.7	***N81A, N125A, N137A***	**+**	**+**	**-**
Batch-3				
Mutant 3.1	***D38R***	++++	+++	+++
Mutant3.2	***F44D***	++++	+++	++++
Mutant 3.3	***R53D***	+++	++	+++
Mutant 3.4	***Y58R***	++++	++++	++++
Mutant 3.5	***A62R***	++++	++++	++++
Mutant 3.6	***Y65D***	++++	+++	+++
Mutant 3.7	***E99R***	++++	++++	-
Mutant 3.8	***L103R***	++++	++++	++++
Mutant 3.9	***K105D***	++	++	++++
Mutant 3.10	***K106D***	+	++	+++

The columns show from left the Plasmid used in the experiment, Substitution/Mutations (the mutation introduced), Western blot (Amount of protein detected by western blot), IF (amount of protein detected by immunofluorescence), columns shown in green are mutants resulted in reduced HAD phenotype. The + sign correspond to the level of similarity with WT-CD2vHA (++++)

2.9 Detection of WT-CD2vHA on the cell surface using serum:

The expression analysis of mutant CD2v proteins (CD2vY102D, CD2vE99R and CD2v2.2), which resulted in reduced or non-HAD phenotypes did not confirm the cell surface expression of the proteins as the HA- tag was located at the C-terminal (cytoplasmic domain) of CD2v. It was important to analyse the surface expression of these mutants to confirm that the reduced HAD phenotype is not due to the reduced expression of the mutants on the cell surface. To investigate this, immunofluorescence was performed using pig serum collected at different time point's post-immunisation with attenuated ASFV (Reis et al., 2016; Reis et al., 2017) . To perform this, 16 different

pig sera samples were screened to detect WT-CD2vHA on the cell surface in both permeable and non-permeable cells.

Vero cells were infected with MVA-T7 at MOI-1 and transfected with pWT-CD2vHA (see section 5.3.2 & 5.3.3). The coverslips were split into two groups; (i) Permeabilised (to detect CD2v within the cell using serum), (ii) Non-permeabilised (to detect CD2v on the cell surface using serum). The cells were permeabilized using 0.2% triton X-100 (only permeable group), the cells were then stained with pig serum (primary antibody) and probed with goat anti-pig 488 secondary antibody (see section 5.3.4). The results showed that out of 16 serum samples only 3 samples detected pWT-CD2vHA in permeable and non-permeable cells (see table 2.3). The serum samples that detected CD2v were from termination day of the animal experiment BeninΔDP148R and BeninΔMGF (Reis et al., 2016; Reis et al., 2017). All sera were positive in commercial ELISA assays based on detection of antibodies to the major capsid protein p72/B646L (Reis et al., 2016; Reis et al., 2017). The detection of few positive sera may be due to CD2v being hidden from the immune system in infected pigs either by binding of virus particles to RBC or by the extensive glycosylation. The positive sera samples detected pWT-CD2vHA in permeable cells in the cytoplasm close to the MVAT7 viral factories and close to the plasma membrane, similar to what was observed before in cells stained with anti-HA. In non-permeable cells pWT-CD2vHA was clearly detected on the cell surface (see figure 2.21), these CD2v seropositive samples were then used to detect the mutants CD2v protein on cell surface.

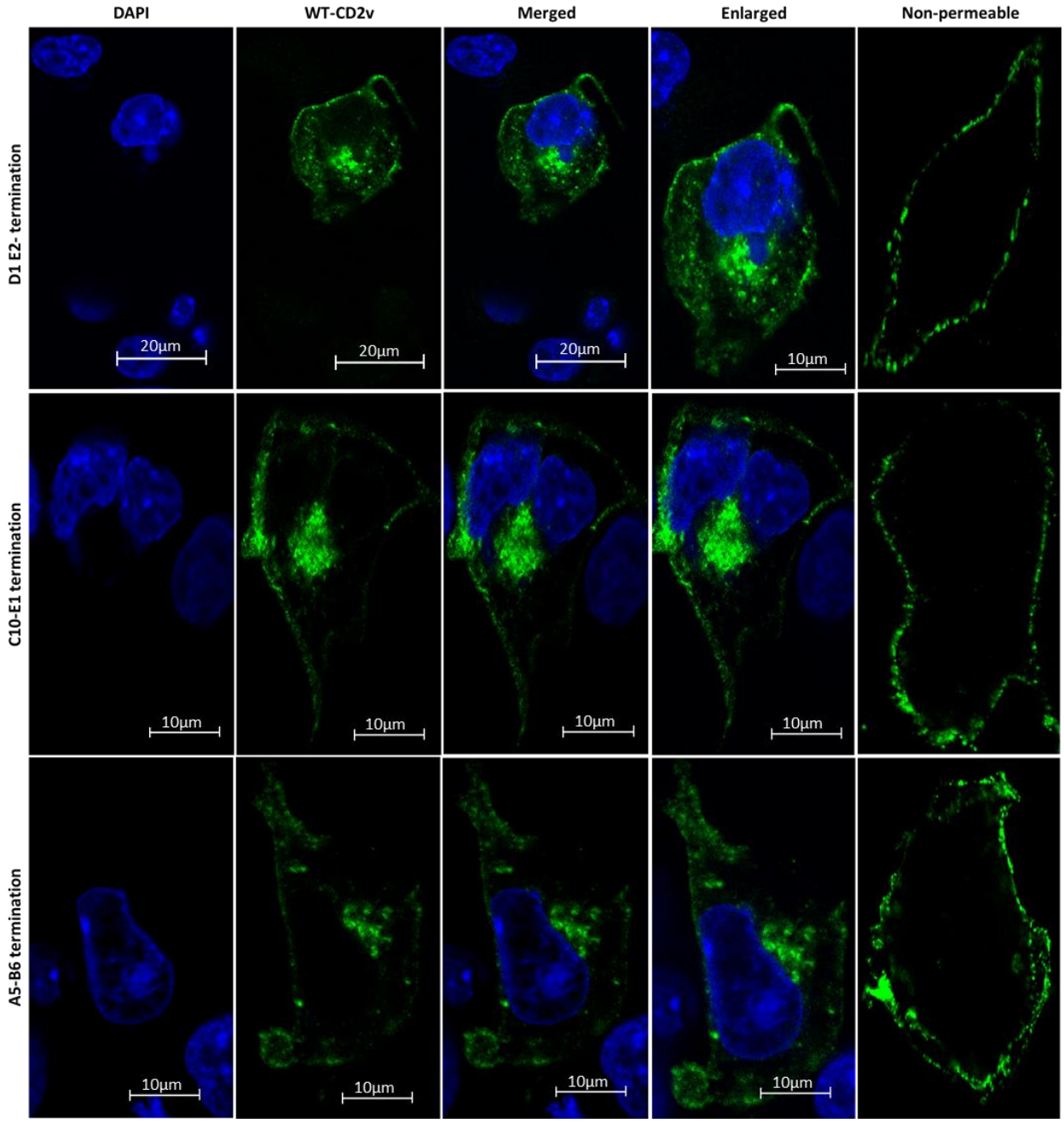

Figure 2.21: Vero cells infected with MVA-T7 and transfected with pWT-CD2v in two groups permeabilized and non-permeabilized. The permeable cells were treated with 0.2% triton X-100. The cells were then stained with different serum from immunized pigs and probed with anti-pig 488 secondary antibody (shown in green). In permeable cells the nucleus was stained with DAPI (in blue).

Table 2.3: List of serum samples screened for detection of WT-CD2v on the cell surface.

Sample	Isolate	Date	IF perm	IF NP
D10-B5	MGF	Day 45	-VE	-VE
A3-B2	MGF	Termination	-VE	-VE
F4-E1	DP148R	Day 45	-VE	-VE
C10-E1	DP148R	Termination	+VE	+VE
E5-B5	MGF	Termination	-VE (detected something in nucleus)	-VE
D6-B1	MGF	Termination	-VE	-VE
E1-B6	MGF	Day 45	-VE	-VE
D9-B4	MGF	Day 45	Background	-/+VE
F5-E2	DP148R	Day 45	-VE	-VE
E1-B3	MGF	Termination	Too much background	Too much background
E4-B4	MGF	Termination	-VE	-VE
D8-B3	MGF	Day 45	-VE	-VE
D7-B2	MGF	Day 45	-/+ Poor detection	-/+ Poor detection
D1-E2	DP148R	Termination	+VE	+VE
D10-B1	MGF	Termination	Background	+VE
A5-B6	MGF	Termination)	+VE	+VE

Columns show Sample; Sample location, Isolate; Attenuated ASFV *strain used for Immunisation, Date; sample collection date, Perm IF; Permeabilized immunofluorescence data, IF NP; non-permeabilized immunofluorescence data, column highlighted in green shows CD2v seropositive samples.*

2.10 Detection of CD2v mutants on the cell surface using serum:

The pig serum samples which were identified (see section 2.9) to detect pWT-CD2vHA (in permeable & non permeable cells) were then used to evaluate the expression of mutant CD2v protein CD2vE99R and CD2vY102D on the cell surface. This was very critical to detect the expression of CD2v mutants on the cell surface as there was a

possibility that the reduced HAD or non-HAD phenotype might be due to the reduced or no expression of mutant CD2v proteins on the cell surface. Vero cells infected with MVA-T7 at MOI-1 were transfected with pWT-CD2vHA, pCD2vE99R and pCD2vY102D. The cells grown on coverslips were divided into two groups (permeable and non-permeable) and were treated according to the method described in section 2.9.

The results showed the detection of CD2v mutants on the cell surface in non-permeable cells and in the cytoplasm and close the MVA-T7 viral factories in the permeable cells. In cells transfected with a plasmid expressing pCD2vE99R, the level of expression on the cell surface (non-permeable), and in the cytoplasm and close to the viral factories (permeabilized) seems to be similar to the pWT-CD2vHA (see figure 2.22). These data exclude the possibility that the non-HAD phenotype of pCD2vE99R was due to the lack of expression on the cell surface and provided evidence that E99 is indeed a functional amino acid residue involved in binding of CD2v to RBC.

In non-permeable cells transfected with a plasmid expressing pCD2vY102D, the level of expression on the cell surface was reduced when compared with the pWT-CD2vHA. The protein was detected on one side of the cell surface, this may indicate that the reduction in HAD observed in pCD2vY102D was due at least partly to the reduced amounts of CD2v expressed at the cell surface. This experiment was performed once, more than 20 cells were observed expressing WT-CD2vHA and CD2vE99R (in both groups), however 5-7 cells were observed expressing mutant CDvY102D. In the context of the predicted CD2v model (see figure 2.16), it was proposed that the substitution from Y102D might disrupt the folding of the protein. No staining was detected in the cells only control or in the MVA-T7 infected cells confirming that the CD2v protein was specifically detected.

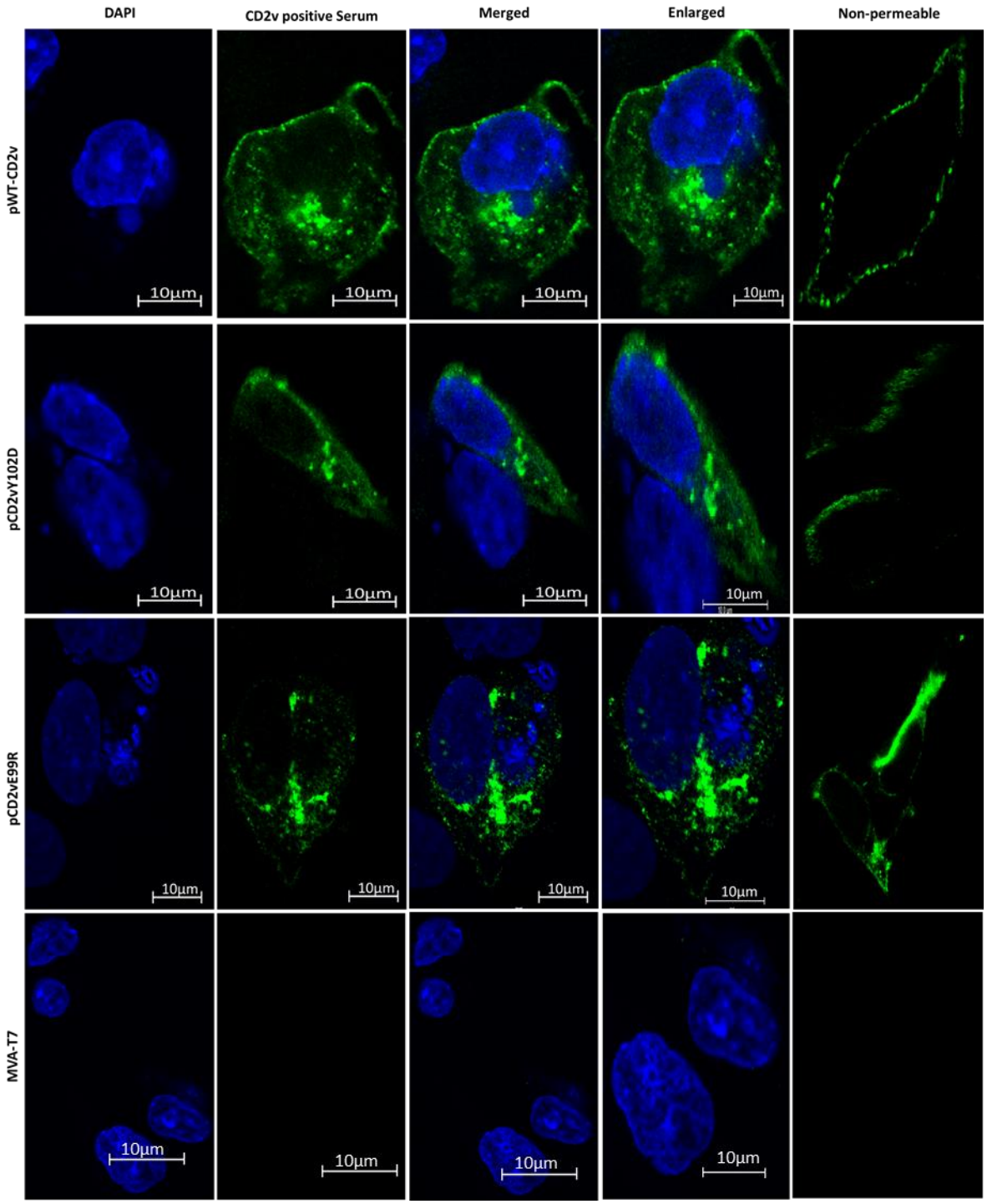

Figure 2.22: Vero cells infected with MVA-T7 and transfected with pWT-CD2v, pCD2vY102D and pCD2vE99R in two groups (permeabilized and non-permeabilized). The permeable cells were treated with 0.2% triton X-100, stained with serum from immunized pigs and probed with anti-pig 488 secondary antibody (shown in green). The permeable cells show expression of CD2v and mutants around the viral

factories as well as close to the cell surface, the non-permeable cells show the expression of CD2v and mutants on the cell surface. In permeable cells the nucleus was stained with DAPI (in blue).

To further investigate cell surface expression of pCD2vE99R and pCD2vY102D, immunofluorescence was performed using a cytoplasmic dye (Cellbrite fix membrane stain) in non-permeable cells (see chapter 5). Vero cells infected with MVA-T7 at MOI-1 were transfected with pCD2vE99R and pCD2vY102D (see section 5.3.2 & 5.3.3). The cells were incubated for 24 hours at 37°C and were fixed with 4% PFA, the cells were treated with Cellbrite fix stain for 5 minutes at -20°C. The cells were washed with PBS and stained with CD2v seropositive samples (primary antibodies) and subsequently labelled with anti-pig 488 (secondary antibodies).

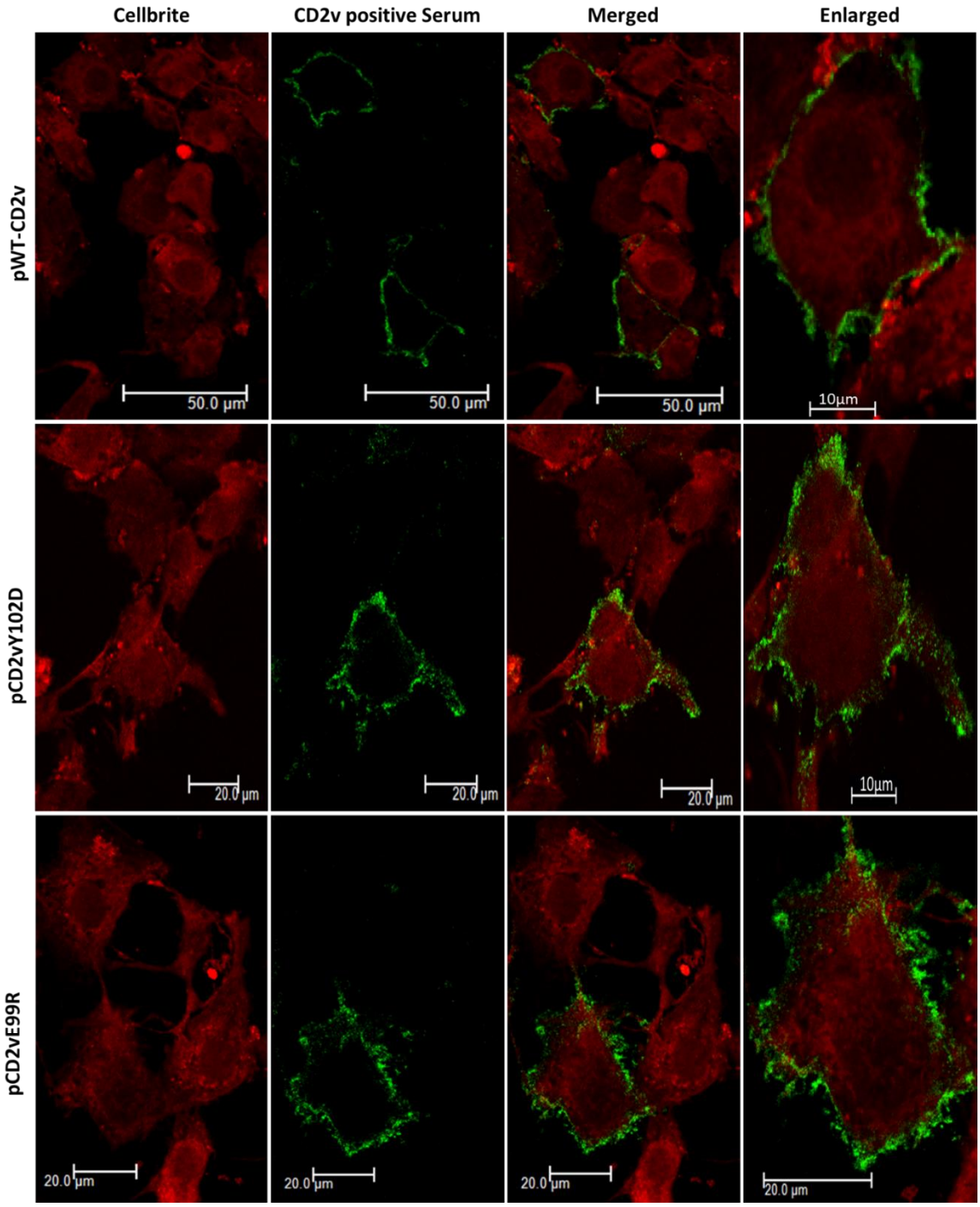

Figure 2.23: Vero cells infected with MVA-T7 at MOI-1 and transfected with pWT-CD2vHA, pCD2vY102D and pCD2vE99R. The cells were fixed with 4% PFA and without permeabilising the cells were stained with Cellbrite membrane fix (shown in red) and CD2v positive pig serum (primary antibody) probed with anti-pig 488 secondary antibody (shown in green). The image shows the cell surface expression of WT-CD2vHA, CD2vY102D and CD2vE99R.

The data clearly showed that pWT-CD2vHA and the mutants (pCD2vY102D and pCD2vE99R) were expressed on the cell surface in non-permeable cells (see figure 2.23). This provided evidence that the reduction in HAD phenotype is not due to the lack of expression on the surface. The amino acid residue at position 99 in CD2v is proposed to be a critical residue involved in binding of CD2v to RBC, the substitution from E to R at this position did not affect the expression at the cell surface but completely abrogate the HAD activity. Another residue at position 102 is also critical for CD2v function and mutation at this position from Y to D did not result in reduced expression or transport to the cell surface but reduced the HAD function.

The overall mutation analysis of CD2v Ig- domain 1 showed that the ligand-binding domain is possibly located at the GC loop of the β- sheets (see figure 2.1b & 2.11a). In total, 21 CD2v mutants were tested and 8 showed a reduced or non-HAD phenotype. However, out of these 8 CD2v mutants six contained multiple amino acid substitution and 2 mutants have single amino acid substitution (pCD2vE99R and pCD2vY102D) (see table 2.2, see figure 2.24 & 2.25). The model of CD2v Ig-domain generated by Dr. Simon Davies (University of Oxford) and Dr. Shinji Ikemizu (Katamotu University, Japan) predicted that the pCD2vY102D which resulted in partial HAD is in the hydrophobic core, the Y102 residue is buried in the structure and is more likely to have an effect on the structure rather than binding of CD2v with its ligand (see figure 2.24). However, the pCD2vE99R completely abrogates the binding of CD2v to its ligand and is predicted to be in the ligand-binding domain. The surface structure showed that the E99 residue is exposed and is in the lower region of the molecule. Therefore, E99R is an effective amino acid involved in the binding of CD2v to red blood cells (see figure 2.24). The mutant 2.2, which resulted in partial HAD has multiple charged amino acid residues substituted with alanine along with Asparagine residues that were predicted to

be glycosylated. The charged residues include the E99A substitution, as mentioned above the pCD2vE99R completely abrogated the binding of erythrocytes while mutant 2.2 induced much reduced HAD. This may be due to a less drastic substitution or may be due to the removal of potential glycosylated sites. However, this supports the idea that a drastic mutation is required to inhibit binding and that glycosylation may restrict the binding of ligands to the CD2v protein. Removal of glycosylation may enhance non-specific binding to the ligand, it also indicates that the glycosyl group may provide more stable interaction with the ligand.

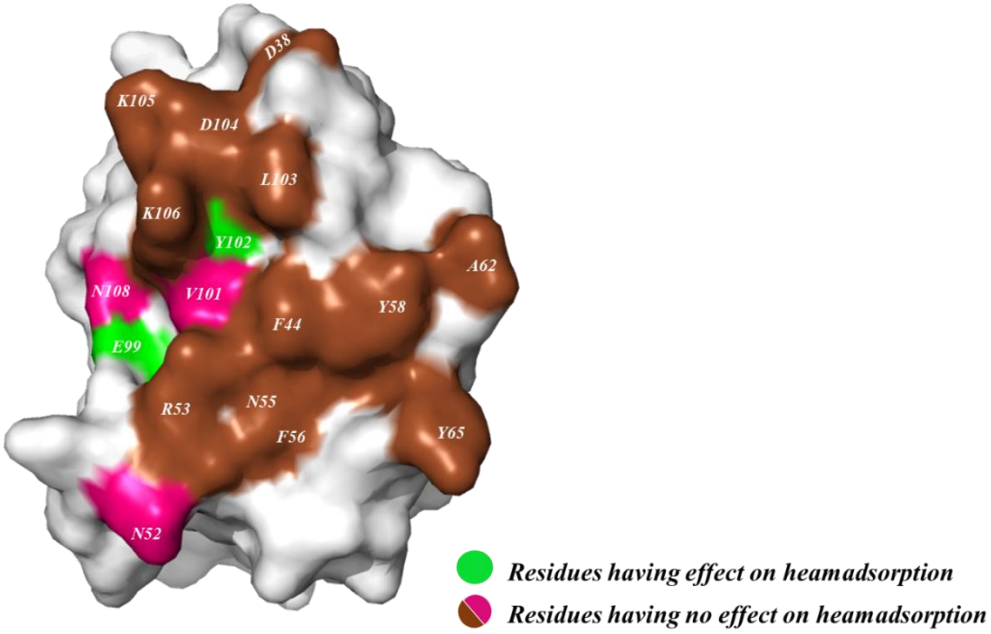

Figure 2.24: Predicted model of CD2v Ig-domain. The model shows the mutants tested to identify residues involve in HAD, the mutations introduced for constructing CD2v mutants are colored. The residues in pink and brown do not affect HAD while the residues shown in green effect HAD, this figure does not include mutants 2.2 which has multiple alanine substitutions.

Following the results from the mutational analysis of CD2v mutants, the predicted CD2v model of the Ig- domain was modified. The new predicted model showed that the F and G strands of the β-sheets are longer than those shown in the previous model

and therefore the D104, K105, and K106 are likely to be in the FG-loop of the β-sheets (see figure 2.1b & 2.25).

The batch 4 CD2v mutants (labelled in red) were designed based on the new model and the potential functional amino acid residues were determined. Since a single mutant was required for constructing a non-HAD recombinant virus, the work for generating the next candidates CD2v mutants and mapping of the ligand-binding domain was carried forward by Dr. Ana Reis and Dr. Vlad Petrovan (The Pirbright Institute).

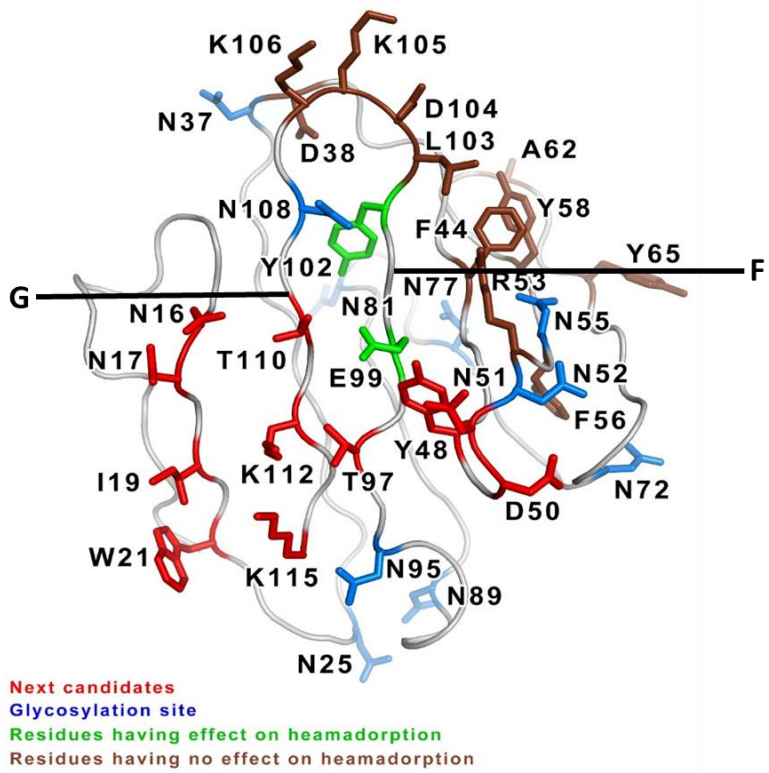

Figure 2.25: Modified predicted model of CD2v Ig-domain. The model was modified based on data from the mutational analysis showing a longer F and G loop. The residues affecting HAD are shown in green, residues tested but do not affect HAD are shown in brown. The potential glycosylation sites are shown in blue. The next proposed mutations are shown in red.

2.11 Discussion:

The mutational analysis of CD2v for the identification of functional amino acid residues showed that 3 mutant CD2v proteins resulted in reduced or non-HAD phenotype. One of the mutants which resulted in reduced HAD has a substitution from Y to D at position 102, this substitution is in the hydrophobic core and according to the predicted CD2v model this will have an effect on the folding and structure of protein rather than on the binding to its ligand. The CD2vY102D not only resulted in reduced HAD but a delay in HAD was also observed when compared with the WT-CD2vHA. The Y102 residue is predicted to be phosphorylated (^{98}YELVYLDKK^{106}) with highest score for a predicted phosphorylated residue (0.938) in the entire CD2v protein however the software couldn't predict the kinase involved in the phosphorylation (NetPhos 3.1, technical university of Denmark). Interestingly the predicted structure of CD2v Ig-domain showed that this residue is close to the E99 residue that completely abrogated HAD, suggesting that Y102 might be involved in interactions with other molecular targets which may be regulated by phosphorylation.

Another mutant that resulted in reduced HAD was CD2v2.2 (partial HAD) which has similar charged amino acid residues substituted as CD2v2.1 (non-HAD), apart from the mutation of 4 putative glycosylation sites in CD2v2.2 (N52A, N55A, N77A, N108A). Interestingly, both of these mutants have the E99 residue mutated, however in mutant CD2v2.2 two of the glycosylation sites (N77 and N108) that were mutated are located near the E99 residue. This may suggest that removal of glycosylation sites is possibly exposing the ligand binding site and hence the mutant CD2v2.2 resulted in reduced HAD phenotype. This was supported by functional analysis of mutant 3 which formed relatively large rosettes (based on surface area) and has two residues mutated at position 55 from N→R and at position 56 from F→L. The N55 residue was mutated in mutant

3 and an increase in HAD was indicated although further quantification is required to confirm this observation. The substitution resulted in the in disruption of N-linked glycosylation sites suggesting that mutation of glycosylation site may enhance HAD by exposing the residue critical for HAD function in the ligand binding site. It has been reported that CD2v encoded by different isolates contain varying number of predicted N-linked glycosylation sites (15 to 25 sites) and may possibly be the reason for the variation in HAD of different isolates (Kay-Jackson et al., 2004; Malogolovkin, Burmakina, Tulman, et al., 2015).

Interestingly the pig serum used to detect CD2v and mutants on the cell surface did not detect CD2v2.2. This suggests the epitope recognised by the pig sera might be disrupted, as the protein was transported to cell surface since it induced HAD. It also suggests that the antisera dosn't bind to the RBC attachment site.

All these glycosylation sites are located near the E99 residue and they may shield the ligand binding domain from the immune system. Other residues in this region may also be critical for interaction of CD2v with its ligand, the predicted functional residues in this region may include; T97, T110, K112 and K115 (see figure 2.25).

It was also observed that in mutant 2.4, 2.6 and 2.7 the amount of protein detected by Western blot was much less than in other mutant CD2v proteins or WT-CD2vHA protein, and the C-terminal 26 and additional 29 kDa fragments were not detected. This may be due to variation in transfection efficiency or other effects on expression for example, due to the expressed protein been misfolded and directed to the proteasome for degradation.

The Western blot data of the cells expressing WT-CD2vHA and mutant CD2v proteins detected an additional band at 29kDa in addition to the c-terminal 26 kDa band, this

could possibly be a phosphorylated form of the 26kDa C-terminal cytoplasmic domain. The C-terminal domain is predicted to be highly phosphorylated from residue S361 to T390, and potentially contains 8 phosphorylation sites, the residues predicted to be phosphorylated are highly conserved among ASFV isolates (see figure 2.26). The analysis was performed using the NetPhos 3.1 Server online tool (Department of Bio and Health Informatics, University of Denmark).

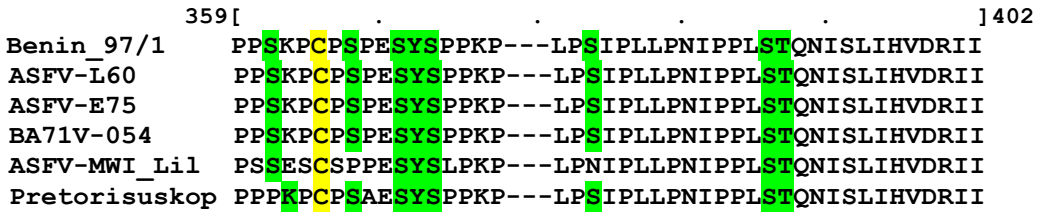

Figure 2.26. Multiple sequence alignment of the CD2v C-terminal domain of different ASFV isolates. The residues highlighted in green are predicted to be phosphorylated and the residue highlighted yellow shows the conserved cysteine residue.

These results showed that E99 residue has a role in binding of erythrocytes to CD2v. E99 is predicted to be on the surface of CD2v (see figure 2.24 and 2.25) and may interact directly with the ligand for CD2v. Mutation of the E residue to the oppositely charged R is predicted to disrupt binding to the ligand of CD2v on the surface of red blood cells. In contrast the hydrophobic Y102 residue is predicted to be buried in the structure (molecule) and the substitution to D may disrupt the folding and conformation of the ligand binding domain to prevent binding to red blood cells. The CD2v model showed that Y102 is involved in polar interactions with K106 and with I108 on the opposite loop. Substituting Y102 with D was predicted to impair the polar contact between Y102, K106 and I108. This could result in a shift in charges which may impair other polar contacts of this loop (see figure 2.27).

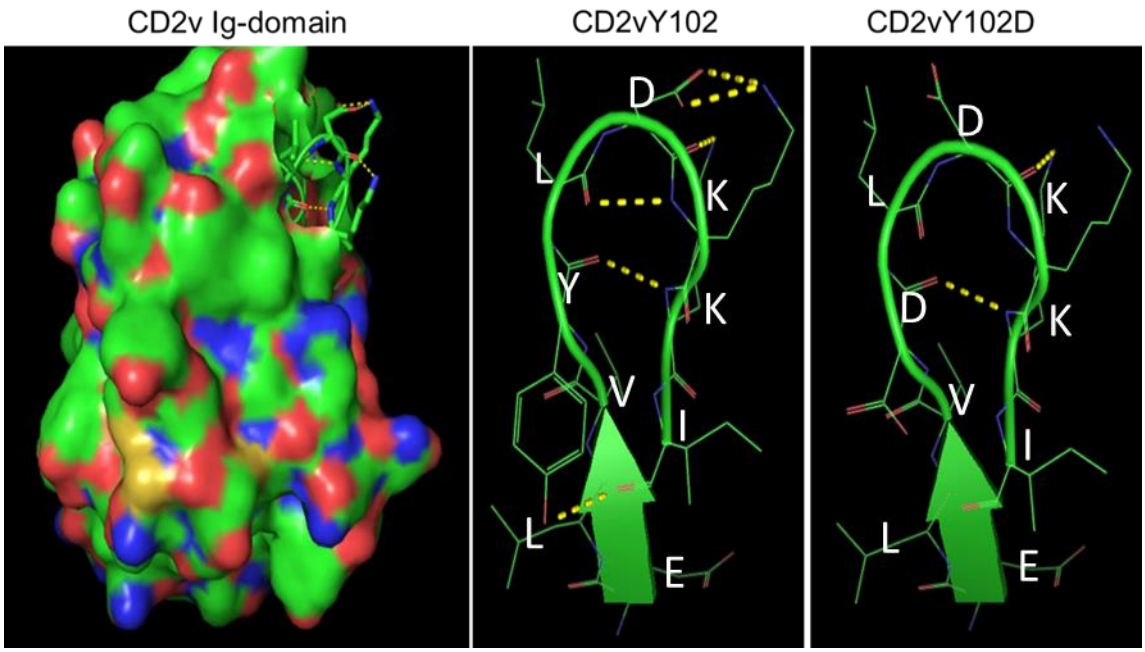

Figure 2.27: Predicted structure close to Y102 residue. The image on the left shows the predicted CD2v Ig- domain model showing the Y residue. The image in the middle shows the polar contacts between K106 and I108 residue with the Y residue in the WT-CD2v. The image on the right shows the effect of substitution from Y to D resulting in disruption of the polar contacts (hydrogen bonds- Shown in yellow dotted lines) between K106 and I108 residues.

The next steps were to investigate if the pCD2vE99R, mutant 2.2 (non-HAD) and the pCD2vY102D partial HAD retain the reduced or partial HAD phenotype in ASFV infected cells and to determine if there are any other viral factors that may contribute to the HAD. These mutants were tested in ASFV infected cells and the expression and functional analysis were determined by Western blot, immunofluorescence and HAD assay, the results are described in chapter 3.

Chapter 3- Expression and functional analysis of wild type CD2v and reduced HAD mutants in ASFV infected cells.

3.1 Introduction:

In the previous chapter, the HAD phenotype, localization and expression of WT-CD2vHA and mutant CD2v proteins, using a transient expression system, was described. The functional analysis by HAD assay identified two CD2v mutants (pCD2vY102D and pCD2vE99R) that resulted in reduced HAD or non-HAD phenotype that were chosen for further analysis. The expression analysis was carried out by immunofluorescence and Western blot. This showed that the mutant CD2v proteins were expressed at a similar size to the wild type CD2v and were localized in punctate areas close to the viral factories and on the inner side of the plasma membrane similar to the pWT-CD2vHA. The surface expression of the mutant CD2v proteins was detected in non-permeabilized transfected cells by using serum samples collected from previous ASFV immunization and challenge studies that contained antibodies that recognized CD2v. This analysis showed that the mutant CD2v proteins were transported and were expressed on the cell's surface (see chapter 2 for details). Since this work was performed in non ASFV infected cells it was important to also analyze the expression and function of mutant CD2v proteins (pCD2vE99R, pCD2vY102D, pCD2v2.2) in ASFV infected cells to determine if the mutant CD2v proteins retain the non- or reduced HAD phenotype and to investigate if other virus proteins may be involved in the HAD process. This was an important step before proceeding to generate recombinant ASFV expressing non-HAD mutant CD2v. To express wild type and mutant CD2v in ASFV infected cells involved cloning of the WT-CD2v gene under control its own viral promoter (VP). Previously it was reported that the promoter region of ASFV L60 strain is between (-1007 and +2) and in Malawi Lil 20/1 the promoter

region is within 350 bp upstream of the start codon (Portugal et al., 2017). However, when WT-CD2v was amplified from 120bp upstream of the start codon, cloned into pcDNA3 containing an HA tag and transfected into WSL cells confirmed that the protein is expressed in ASFV infected cells. Thus it was identified that in Benin 97/1 strain the CD2v promoter region is within -120bp upstream of the start codon. Since the natural target cells for ASFV replication, porcine macrophages, have a very low transfection efficiency, wild boar lung cells (WSL) were therefore tested for use in these ASFV infection and transfection experiments. These cells support replication of some ASFV strains (Keil et al., 2014).

3.2 Expression analysis of VP-WT-CD2vHA, VP-CD2vE99RHA and VP-CD2vY102DHA in ASFV infected WSL cells by Western blot:

WSL cells were infected with an ASFV Benin strain from which the EP402R/CD2v gene had been deleted (Rathakrishnan et al., 2020) and transfected with plasmids expressing VP-WT-CD2vHA or VP-CD2vE99RHA or VP-CD2vY102DHA. These genes had an HA tag fused at the 3' end of the gene to enable the detection of the expressed protein using anti-HA antibodies. The expression of the VP-CD2vE99RHA and VP-CD2vY102DHA was compared to VP-WT-CD2vHA by Western blot in extracts from ASFV infected and transfected cells. The aim was to confirm that VP-CD2vE99RHA and VP-CD2vY102DHA are expressed, processed by glycosylation and cleaved to produce similar sizes to the WT-CD2vHA in ASFV infected WSL cells.

The WT-CD2v gene along with its promoter (120bp upstream of the start codon) was amplified by PCR from Benin 97/1 genomic DNA and was cloned into pcDNA3 containing an HA tag that was fused to the 3' end of the CD2v gene to generate (VP-

WT-CD2vHA). The same plasmid construct (pVP-WT-CD2vHA) was modified and the WT-CD2v immunoglobulin (Ig) domain was replaced with Ig domain of the CD2v mutants as described in chapter 5 to generate pVP-CD2vE99RHA and pVP-CD2vY102DHA. The plasmid constructs were sequenced and amplified in bacterial cultures for transfection.

WSL cells grown in six well plates were infected with BeninΔCD2v at MOI 10. The cells were incubated for 2 hours at 37C° and were transfected with pVP-WT-CD2vHA, pVP-CD2vE99RHA, and pVP-CD2vY102DHA. The cells were lysed and a Western blot was performed on the extract according to the method descried in section 5.3.8.

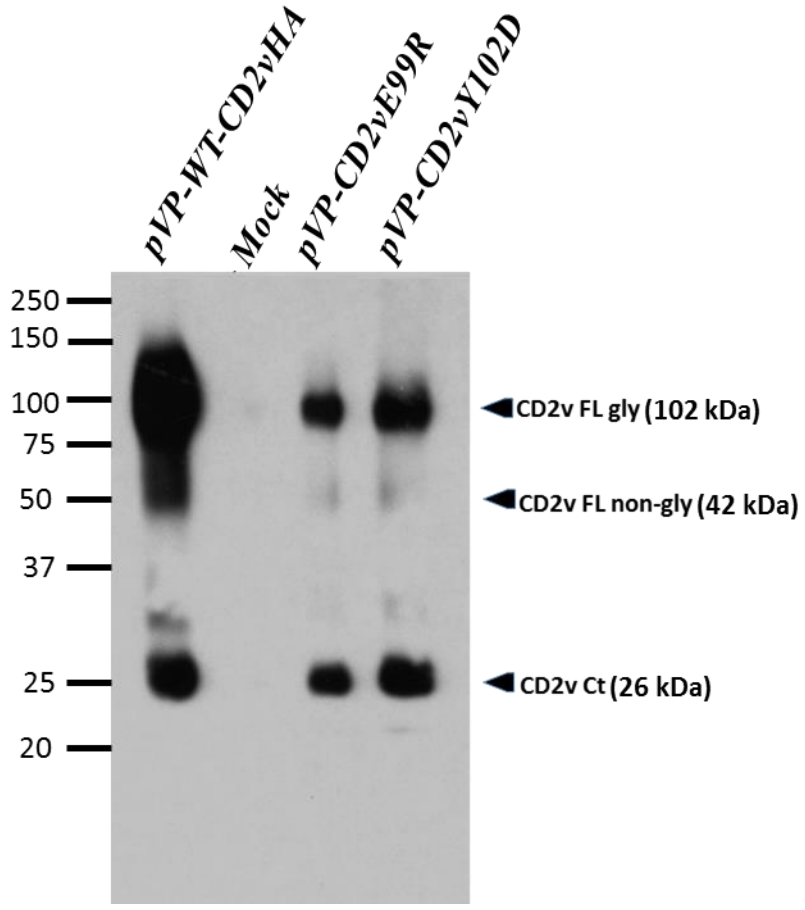

Figure 3.1: **WSL cells mock-infected or infected with BeninΔCD2v (MOI 10), transfected with plasmids expressing pVP-WT-CD2vHA, pVP-CD2vE99R, and**

pVP-CD2vY102D as indicated. The cell lysates were prepared and were separated by SDS-PAGE, probed with anti-HA primary antibody and anti-HA HRP secondary antibody. The image shows full length glycosylated CD2v (102 kDa), full length non-glycosylated CD2v (42 kDa) and the C terminal domain (26 kDa).

The results showed that mutant CD2v proteins (pVP-CD2vE99R and pVP-CD2vY102D) were expressed at the correct size (see figure 3.1), both mutants expressed the full-length glycosylated form of CD2v detected at 102 kDa. The full length non-glycosylated form of CD2v (42 kDa) was not detected in the mutant CD2v proteins and in the pVP-WT-CD2vHA, possibly the protein expression at lower levels in individual transfected cells may result in promoting the progression through the secretory pathway and hence reduced levels of the 42kDa non-glycosylated protein. It may be possible that the protein is expressed by the viral promoter at optimum level and thus the protein is efficiently progressed through the secretory pathway. Comparing with expression analysis of the mutant CD2v proteins in Vero cells also suggests that it may be due to difference in cells, the WSL cells may more efficiently transport the proteins. The non-glycosylated C-terminal domain was also detected in both mutants (26 kDa). This provide evidence that CD2v mutants were expressed and processed (cleaved) in correct sizes similar to the wild type CD2v. The amount of protein varied in cell lysates possibly due to difference in transfection efficiency although differences in protein expression or stability cannot be excluded.

3.3 Expression analysis of pVP-WT-CD2vHA, pVP-CD2vE99RHA and pVP-CD2vY102DHA in ASFV infected WSL cells by immunofluorescence:

The expression of pVP-CD2vE99RHA and pVP-CD2vY102DHA was analysed by immunofluorescence in ASFV infected cells in parallel with pVP-WT-CD2vHA. The

aim was to investigate if the pVP-CD2vE99RHA and pVP-CD2vY102DHA are expressed and, localised close to the ASFV viral factories similar to the pVP-WT-CD2vHA, described before for ASFV Malawi lil/20 and E75 strains (Goatley & Dixon, 2011; Perez-Nunez et al., 2015). WSL cells were infected with BeninΔCD2v at MOI 10 and were transfected with pVP-WT-CD2vHA, pVP-CD2vE99RHA and pVP-CD2vY102DHA. The cells were fixed with 4% PFA for 10 mins, the cover slips were transferred to another plate containing 4% PFA and were incubated for a further 10 mins. Cells were permeabilised with triton X-100 and stained with anti-HA (rat IgG) primary antibody and probed with alexaflour 568 (anti rat IgG) secondary antibody (see chapter 5 for details). A number of cells were observed (> 100 cells) expressing either the mutants or the pVP-WT-CD2vHA, both mutants were distributed in the cytoplasm and were predominantly co-localized close to the ASFV induced viral factories similar to the pVP-WT-CD2vHA in ASFV infected cells. The viral factories were detected with the DAPI stain (see figure 3.2).

This experiment was repeated twice in ASFV infected cells, a similar distribution was observed before in transient expression experiments where punctate staining of the CD2v protein was localized close to the MVA-T7 cytoplasmic viral factories (see chapter 2).

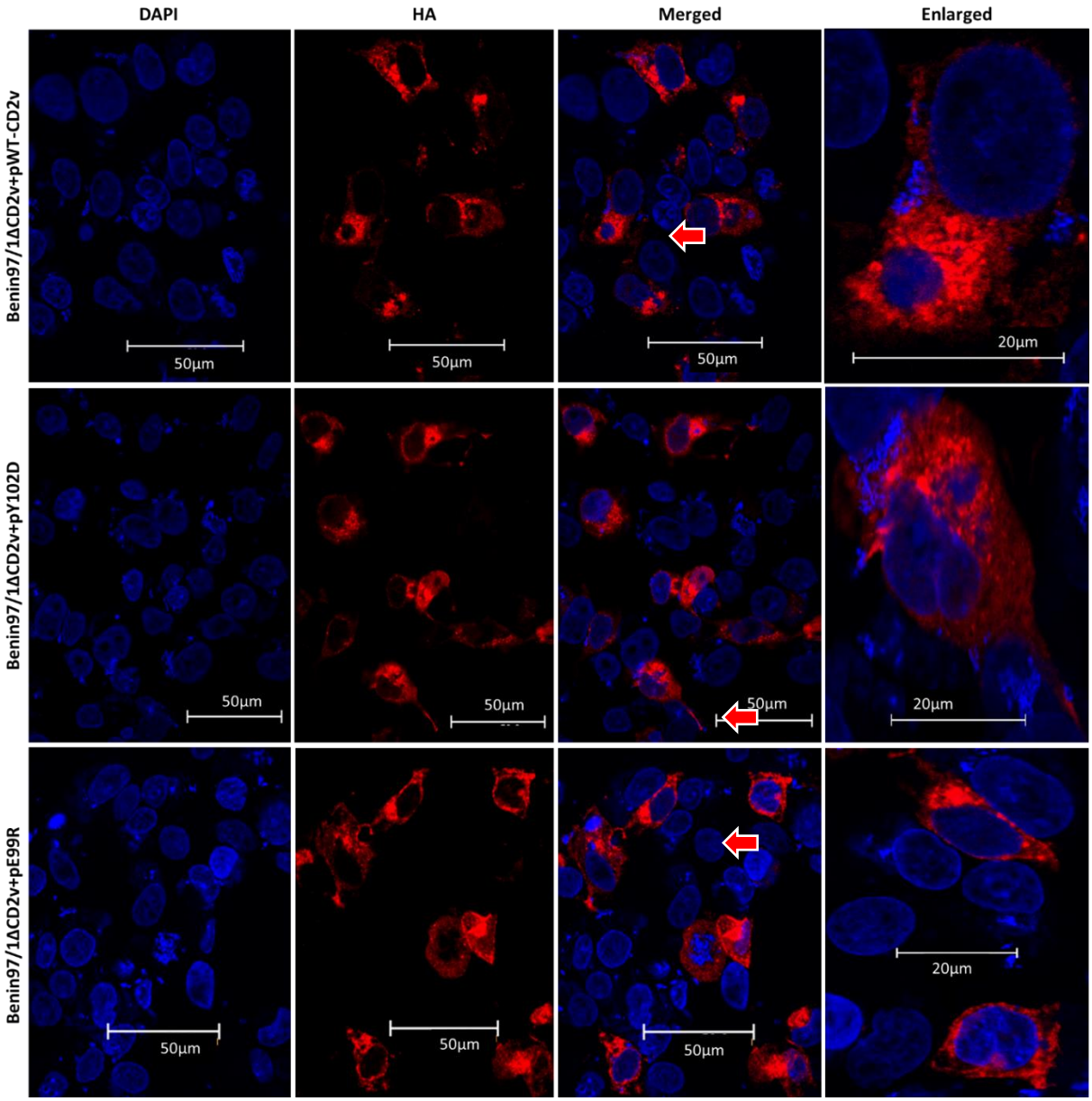

Figure 3.2: Wild boar lung cells (WSL) showing VP-WT-CD2v, VP-CD2vE99R and VP-CD2vY102D expression by confocal microscope. WSL cells were infected with Benin97/1ΔCD2v at MOI 10 and transfected with pVP-WT-CD2vHA, pVP-CD2vE99RHA and pVP-CD2vY102DHA. The cells were fixed and stained with anti-HA (rat) and probed with alexaflour 568 (shown in red), the nucleus and virus factory were stained with DAPI shown in blue.

3.4 Analysis of HAD induced by pVP-WT-CD2vHA, pVP-CD2vE99RHA and pVP-CD2vY102DHA in ASFV infected WSL cells;

The properties of CD2v mutants in ASFV infected cells were determined by HAD assay. This was performed to confirm that CD2v mutants (VP-CD2vE99RHA, VP-CD2vY102DHA) retain the reduced or lack of HAD phenotype in ASFV infected cells that was observed in cells infected with MVA-T7 (chapter 2). WSL cells were infected with Benin97/1ΔCD2v at an MOI 10 and were transfected with pVP-WT-CD2vHA, pVP-CD2vE99RHA and pVP-CD2vY102DHA, the VP-WT-CD2vHA was included as control (see chapter 5). To increase the transfection efficiency the cells were centrifuged at 600g for 45 mins at 26°C and were incubated for 18 hours at 37°C. A HAD assay was performed on cells infected with Benin97/1ΔCD2v and expressing pVP-WT-CD2vHA, pVP-CD2vE99RHA and pVP-CD2vY102DHA (described in section 5.3.5).The results showed that the pVP-CD2vY102DHA (partial HAD) and the pVP-CD2vE99RHA (non-HAD) mutant caused full HAD similar to that induced by WT-CD2v in ASFV infected cells (see figure 3.3). This contrasted with the results observed with cells not infected with ASFV described in chapter 2 in which these mutants did not induce HAD.

To investigate this unexpected result, two factors were taken into consideration, either a host or a viral factor is involved in enhancing HAD in ASFV infected WSL cells.

(A) Host/Cellular factor enhances transport or expression of CD2v mutants (pCD2vE99R, pCD2vY102D) to the cells surface:

To investigate if a swine host factor is involved in enhancing HAD, either by transporting or expressing CD2v in higher quantities on the cell's surface, WSL cells were infected with MVA-T7 at MOI-3 and incubated for 1 hour at 37°C, the cells were

transfected with pWT-CD2vHA, pCD2vE99RHA and pCD2vY102DHA (See chapter 2). A HAD assay was performed on cells expressing pVP-WT-CD2vHA, pVP-CD2vE99RHA and pVP-CD2vY102DHA infected with MVA-T7 (described in section 5.3.5). As expected the result showed that pCD2vY102DHA was again partially HAD (same as was observed in Vero cells) while the pCD2vE99RHA completely abrogated HAD and the pWT-CD2vHA control induced HAD, similar to the assay carried out in Vero cells (see figure 2.5). This indicated that a host factor is not involved in enhancing HAD in ASFV infected cells and a viral factor may possibly be involved.

B) A virus factor enhances cell surface expression or attachment of RBC to mutants CD2v (pVP-CD2vE99R, pVP-CD2vY102D):

The next step was to investigate if a viral factor is involved in enhancing the HAD phenotype of mutant CD2v E99R and Y102D. It was previously reported that the ASFV ORF EP153R encodes for a protein containing a C-type lectin domain and that expression of EP153R could enhance HAD caused by CD2v. A recombinant ASFV lacking EP153R gene showed a reduction in number of rosettes in infected macrophages and reduced numbers of RBC attached to the infected cells in vitro (Galindo et al., 2000). A role for EP153R/C-type lectin in inhibiting apoptosis and in down-regulation of the MHC-1 has also been described (Hurtado et al., 2011; Hurtado et al., 2004). A HAD assay was set up by infecting WSL cells with either OURT88/3 which has non-functional EP402R/CD2v and EP153R/C type lectin genes (Chapman et al., 2007) or with BeninΔCD2v (described in section 3.4) at an MOI 10. The cells were transfected with pVP-WT-CD2vHA, pVP-CD2vE99RHA and pVP-CD2vY102DHA (See chapter 5- section 5.3.5). The cells were treated according to the method described above in section 3.4. The results showed that cells infected with BeninΔCD2v and transfected with pVP-CD2vE99RHA (non-HAD) or pVP-

CD2vY102DHA (partial HAD) were HAD as observed with the cells transfected with pVP-WT-CD2vHA. In contrast, the cells infected with OURT88/3 or MVA-T7 and transfected with the same constructs either under the control of the CD2v promoter or T7 promoter resulted in partial HAD for the pVP-CD2vY102DHA mutant and no HAD for the pVP-CD2vE99RHA mutant. These results suggest that a virus factor, probably EP153R/C type lectin alone, is involved in enhancing HAD (see table 3.1 & figure 3.5).

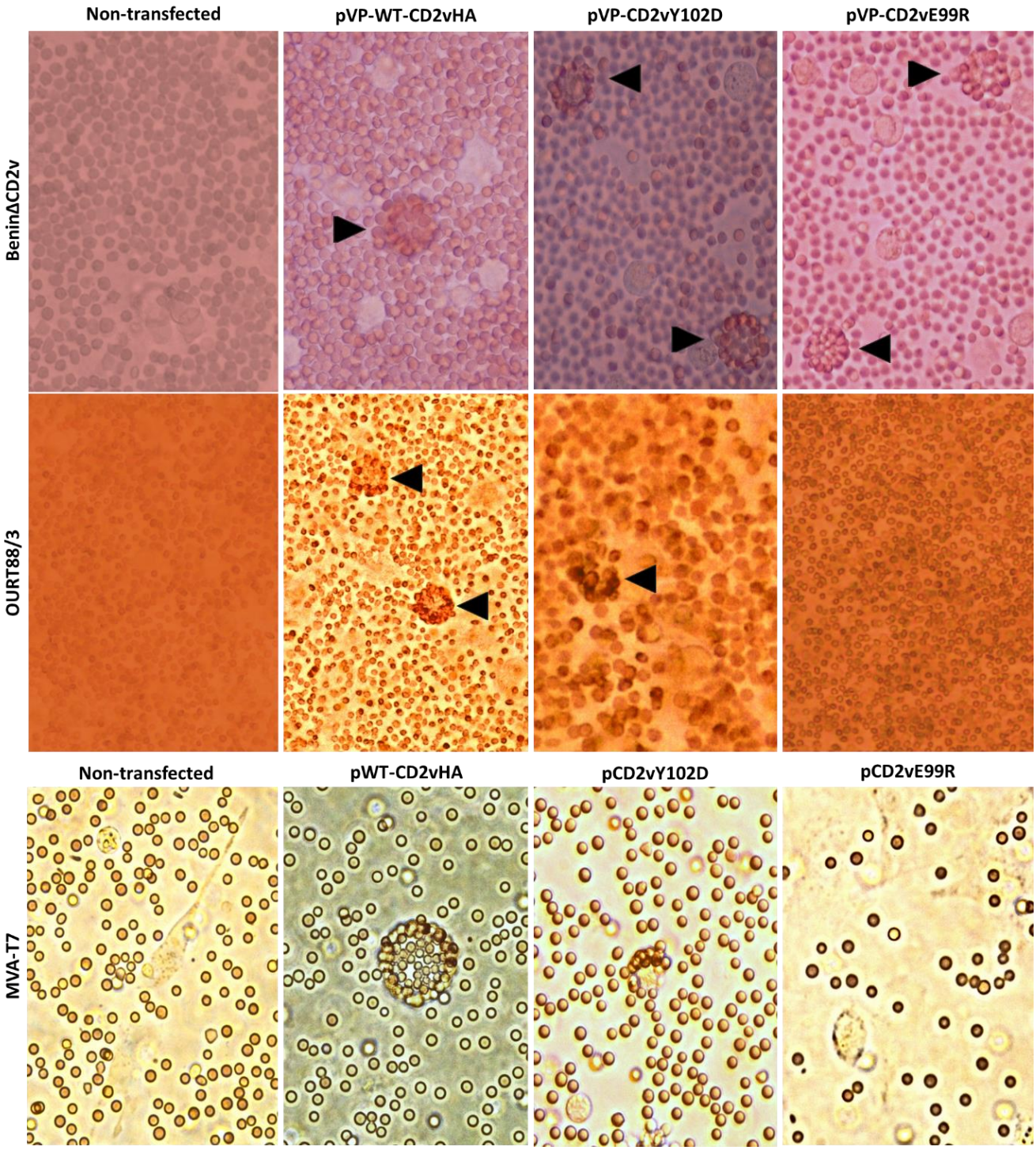

Figure 3.5: HAD assay showing the RBC attached to WSL cells infected with ASFV OURT88/3 or Benin97/1ΔCD2v and transfected with pVP-WT-CD2vHA or pVP-CD2vY102D or pVP-CD2vE99R. The cells were incubated for 18 hours post infection/transfection, heparinized whole pig blood was added to the cells and incubated again for 24 hours to observe rosette formation. The cells infected with

Benin97/1ΔCD2v and transfected with CD2v mutants were HAD similar to the wild type CD2v. In contrast, the mutant pVP-CD2vY102D showed a partial HAD and pVP-CD2vE99R showed no HAD in cells infected with OURT88/3. The cells infected with MVA-T7 and transfected with pCD2vY102D mutant showed partial HAD while in the cells transfected with pCD2vE99R no HAD was observed.

Table 3.1: A table showing HAD results from WSL cells infected with different strains of *ASFV* and MVA-T7.

Strain	**EP153R**	***EP402R***	**HAD_MutE99R**	**HAD_MutY102D**
OURT88/3	-	-	Non-HAD	Partial HAD
BeninΔCD2v	+	-	HAD	HAD
MVA-T7	-	-	Non-HAD	Partial HAD

(Strain) ASFV strain used for infections, (-) represent strains lacking a functional ORF, (+) represents strains containing a functional ORF.

3.5 Expression analysis of WT-EP153RV5 in MVA-T7 infected Vero cells by immunofluorescence:

To investigate the role of EP153R in HAD, a plasmid construct containing the wild type EP153R was cloned under T7 promoter in pcDNA3 was kindly provided by Dr. Anusyah Rathakrishnan (The Pirbright institute). The EP153R had a V5 tag fused at the C-terminal extracellular domain to enable the detection of the expressed protein using anit-V5 antibodies. The aim of this experiment was to detect if the EP153R co-localised with CD2v. The expression of EP153R was first validated by immunofluorescence. Vero cells were infected with MVA-T7 at MOI 1 and were

transfected with pEP153RV5. The cells were fixed and the cover slips were split into two groups; permeabilized and non-permeabilized to detect the expression of pEP153RV5 both on the cell surface and within the cells. For the non-permeabilized group, the cells were stained with anti-V5 (mouse IgG) primary antibody and probed with Alexaflour 594 (goat anti-mouse IgG) secondary antibody. For the permeabilized group, the cells were treated with triton X-100 and stained with anti-V5 (mouse IgG) primary antibody and probed with Alexaflour 594 (goat anti-mouse IgG) secondary antibody. More than 100 cells were observed in both groups expressing WT-EP153RV5, in permeabilized cells the protein was detected in a punctate pattern suggesting localisation in the secretory pathway while in non-permeabilized cells the protein was localised on the cell surface (see figure 3.6b). It was previously reported that EP153R is a type II transmembrane protein (Galindo et al., 2000) and hence the V5 tag was present at the extracellular C-terminus. The EP153R was clearly detected on the surface of the non-permeabilized cells using antibodies against the V5 tag (see figure 3.6a). This validated the expression and localisation of the pWT-EP153RV5. The proteomic analysis of ASFV virions indicated that CD2v is the only virus protein present on the extracellular virus (Alejo et al., 2018) and the virus probably acquires the protein when budding out from the cells. My results showed that EP153R is also expressed on the cell surface in transfected cells and thus may also be acquired by the virus during the budding process (see figure 3.6a). To further confirm the cell surface expression of EP153R, the serum that was used to detect pWT-CD2vHA on the cells surface in non-permeable Vero cells was used (see chapter 2) to detect pWT-EP153RV5 in permeabilized and non-permeabilized Vero cells. The cells were infected, transfected, and were stained with the same pig serum (from immunisation and challenge experiments as described in chapter 2) and probed with alexaflour 488

(goat anti-pig secondary antibodies) in permeabilized and non-permeabilized cells to detect pWT-EP153RV5 by immunofluorescence, as described above. Similar results were observed as for the detection of pWT-EP153RV5 using antibodies against the V5 tag. In permeabilized cells the EP153R protein was detected in a punctate staining pattern resembling localisation in the secretory pathway (see figure 3.6c), while in non-permeabilized cells WT-EP153RV5 was clearly detected on the cell surface using the serum from ASFV-infected pigs (see figure 3.6d). More than 100 cells in both groups of cells were observed stained with the serum. Both experiments (detection with V5 and detection with serum) were performed only once.

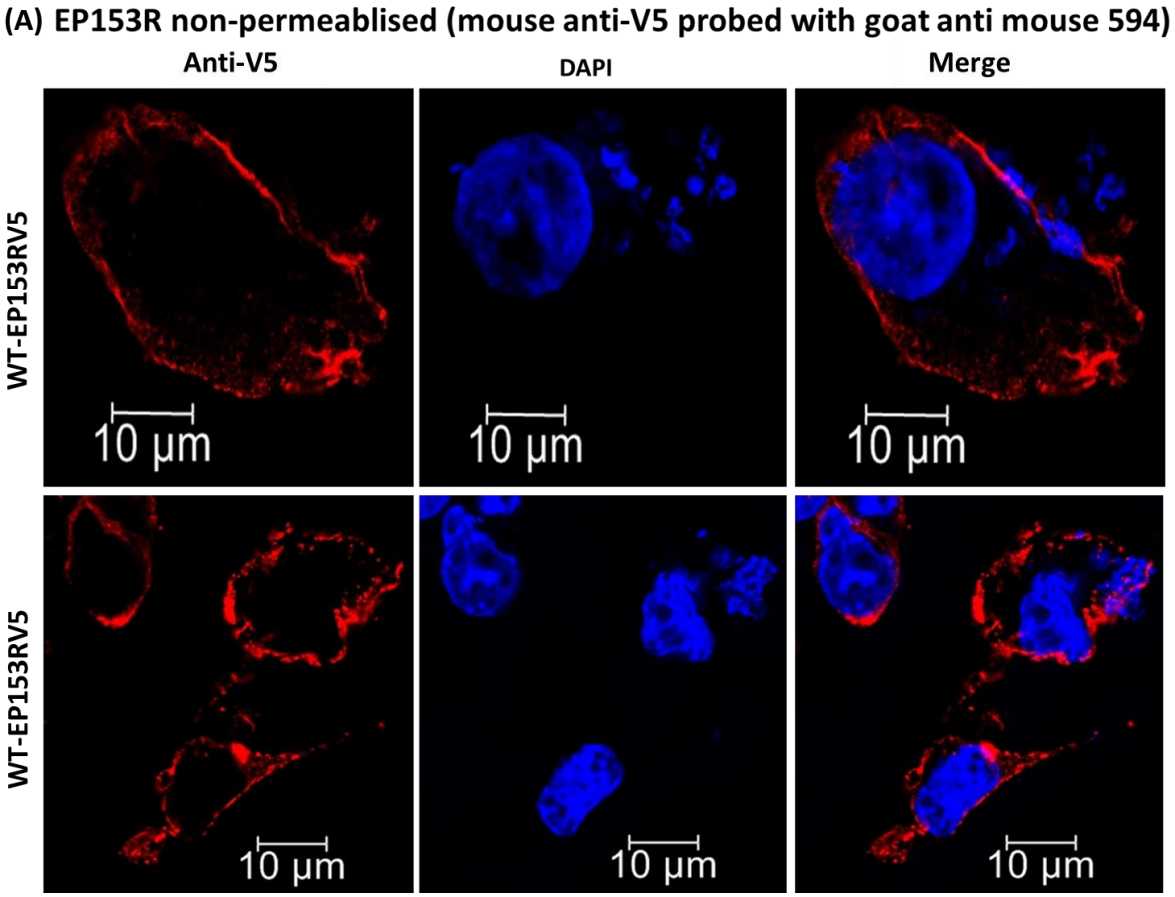

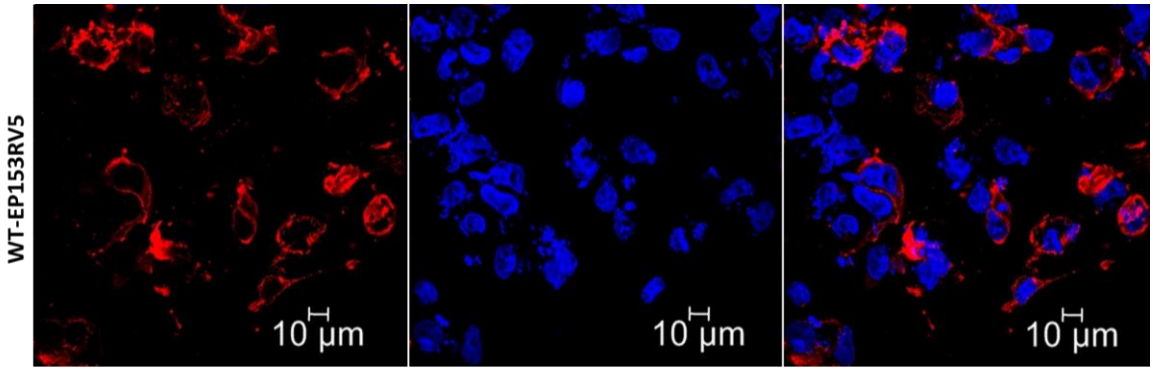

(B) EP153R permeable Vero cells (mouse anti-V5 probed with goat anti mouse 594)

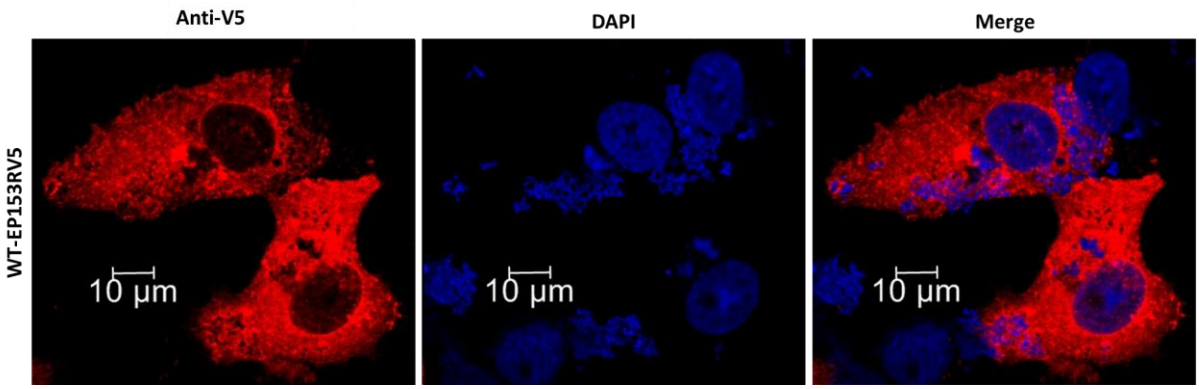

(C) EP153R permeable Vero cells (pig serum probed with goat anti pig 488)

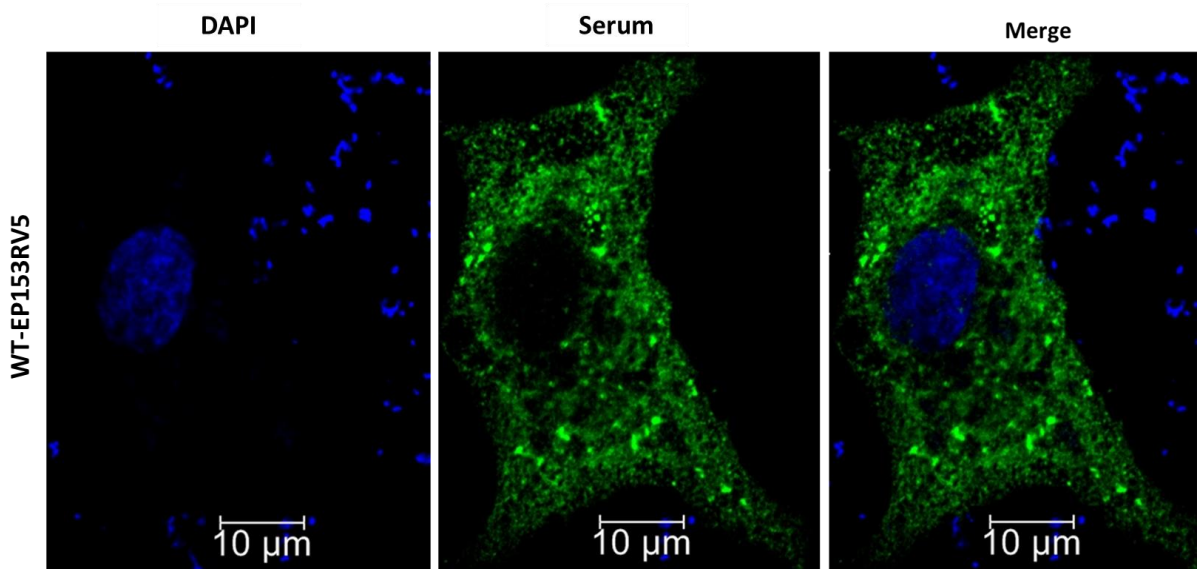

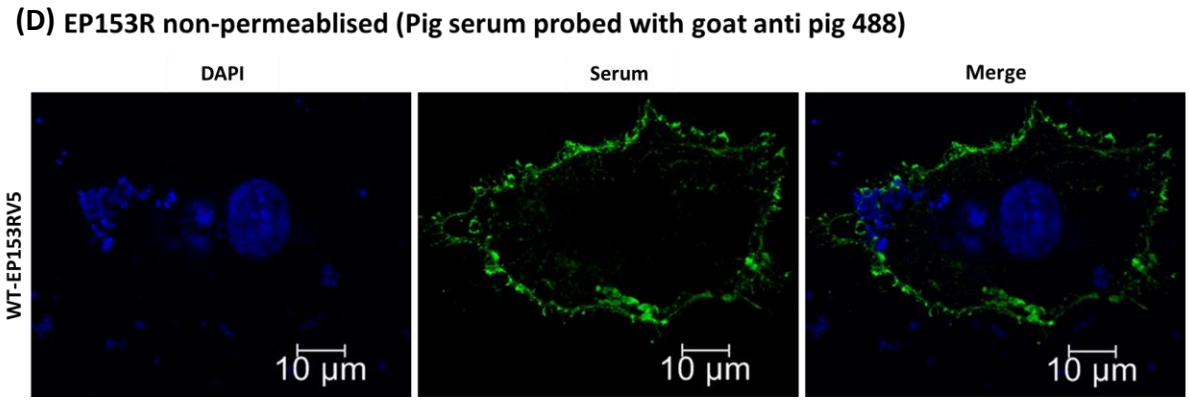

Figure 3.6: Expression analysis of EP153R: Vero cells infected with MVA-T7 and transfected with pWT-EP153RV5 **(A)** Non-permeable Vero cells stained with anti V5 (mouse IgG) and probed with goat anti mouse IgG (alexaflour 594) showing the localisation of pWT-EP153RV5 on the cell surface, the lower magnification image in the bottom panel indicates the transfection efficiency. **(B)** Permeable Vero cells stained with anti V5 (mouse IgG) and probed with goat anti mouse IgG (alexaflour 594) detected WT-EP153RV5 in a punctate pattern. **(C)** Permeable Vero cells stained with serum (from an ASFV pig immunisation and challenge experiment) and probed with goat anti pig 488, showing the WT-EP153RV5 in a punctate staining pattern. **(D)** Non-permeable cells stained with pig serum and probed with goat anti pig 488, showing the expression and localisation of WT-EP153RV5 on the cell surface.

3.6 Co-localisation analysis of pWT-CD2vHA and pWT-EP153RV5 in MVA-T7 infected Vero cells:

The functional analysis of CD2v mutants (pVP-CD2vE99R and pVP-CD2vY102D) indicated a role of EP153R/C-type in enhancing HAD (see section 3.4). To further investigate if CD2v and EP153R may interact their localisation in Vero cells expressing both proteins was investigated. Vero cells were infected with MVA-T7 at MOI 1 and were then co-transfected with pWT-EP153RV5 and pWT-CD2vHA (see section 5.3.2

& 5.3.3). The cells were fixed, permeabilized and were sequentially stained. The pWT-EP153RV5 was stained with primary antibody (mouse anti-V5) and probed with secondary antibody (goat anti mouse IgG dylight 594), this antibody do not cross-react with other immunoglobulins. The pWT-CD2vHA was stained with primary antibody (rat anti-HA) and probed with secondary antibody (donkey anti rat IgG 488) however this antibody has minimal cross reactivity with light chain of human and mouse immunoglobulins. The results showed that pWT-EP153RV5 and pWT-CD2vHA were co-localised and were detected close to the plasma membrane, punctate staining of the co-localised proteins was also detected close to the MVA-T7-induced viral factories (see figure 3.7). The results suggest that pWT-EP153RV5 and pWT-CD2vHA possibly interact, however further investigation is required to confirm the interaction, for instance; confirmation of interaction by proximity ligation assay (PLA).

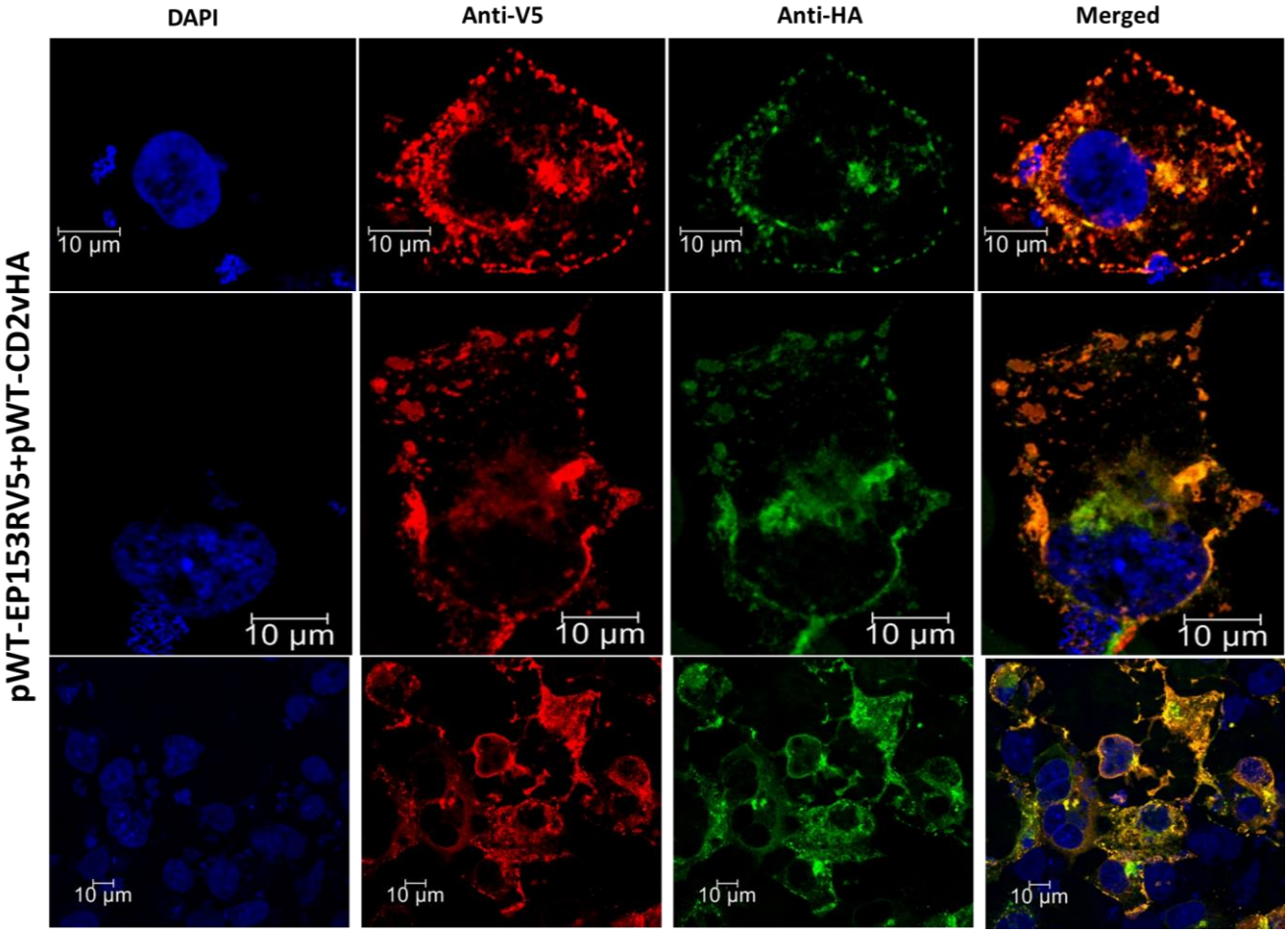

Figure 3.7; Co-localisation of pWT-EP153RV5 and pWT-CD2vHA. Vero cells infected with MVA-T7 and co-transfected with pWT-EP153RV5 and pWT-CD2vHA. The cells were permeabilized and sequentially stained, the pWT-EP153RV5 was stained with mouse anti-V5 and probed with goat anti mouse dylight 594. The pWT-CD2vHA was stained with rat anti-HA and probed with donkey anti rat 488. The results showed that the proteins co-localised, the nucleus and viral factories were stained with DAPI.

3.7 Expression of analysis of pVP-WT-EP153RV5 in ASFV infected WSL cells by immunofluorescence:

To analyse the expression of EP153R in ASFV infected cells, a plasmid construct containing the wild type EP153R under control of the ASFV viral promoter and with a V5 tag fused at the C-terminal extracellular domain of EP153R was ordered from Genscript. The V5 tag was used to enable the detection of the expressed protein using anit-V5 antibodies. The gene was cloned into pUC57 plasmid to generate (pVP-WT-EP153RV5). The plasmid construct was amplified in bacterial culture for transfections, this construct was designed and ordered by Dr. Ana Reis (The Pirbright Institute). The expression of pVP-WT-EP153R was first validated by immunofluorescence in ASFV infected WSL cells. WSL cells grown on coverslips were infected with the virulent BeninΔDP148R virus from which both the EP153R and CD2v genes were deleted (BeninΔDP148RΔEP153RΔCD2v was provided by Dr Anusyah Rathakrishnan-The Pirbright Institute) at MOI 2 and were transfected with pVP-WT-EP153R. The cells were fixed, permeabilized and stained with anti-V5 (rat IgG) primary antibody and probed with alexaflour 568 (goat anti rat IgG) secondary antibody (see chapter 5 for details). The recombinant virus contains a mNeongreen marker gene under the control of ASFV VP30 promoter, the expression of mNeongreen was used to determine the

infection efficiency (see section 3.11). The results showed that pVP-WT-EP153R was expressed and was detected in a punctate staining pattern in the cytoplasm similar to the pattern observed in MVA-T7 infected cells (see figure 3.8) (see section 3.5). More than 50 cells were observed expressing pVP-WT-EP153R, this experiment was performed once.

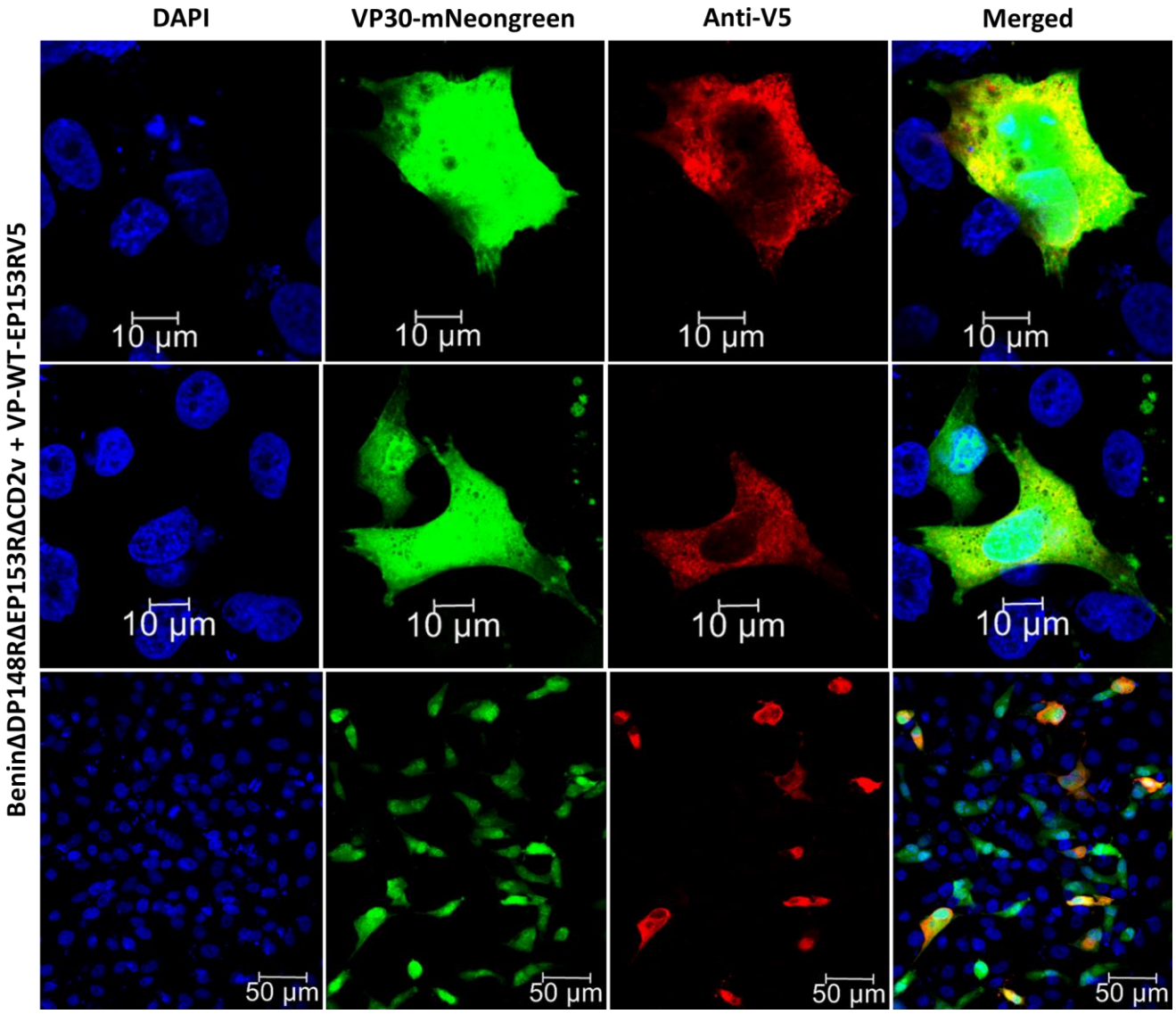

Figure 3.8: Expression validation of EP153R. The expression of pVP-WT-EP153RV5 was validated in WSL cells infected with BeninΔDP148RΔEP153RΔCD2v. The cells were stained with anti-V5 (rat IgG) and probed with alexaflour 568 (goat anti rat IgG). The images show the expression of pVP-

WT-EP153RV5 in permeable cells (red), the recombinant virus expresses the mNeongreen marker gene (green), the nucleus and the viral factories are stained with DAPI (blue). The bottom lower magnification panel indicates the transfection (red) efficiency and infection efficiency (green).

To further investigate if CD2v and EP153R co-localised in ASFV infected cells, WSL cells were infected with BeninΔDP148RΔEP153RΔCD2v at MOI 2 and were co-transfected with pWT-EP153RV5 and pWT-CD2vHA. The cells were fixed. permeabilized and were sequentially stained. The pVP-WT-EP153RV5 was stained with primary antibody (rat anti-V5) and probed with secondary antibody (goat anti rat IgG alexaflour 568), this antibody does not cross-react with other immunoglobulins and is specific to rat IgG. The pVP-WT-CD2vHA was stained with primary antibody (mouse anti-HA) and probed with secondary antibody alexaflour 633 (rabbit anti mouse IgG), this antibody does not cross react with other immunoglobulins and is specific to mouse IgG. Both secondary antibodies display red colour scheme (red and far red) upon excitation, however, the excitation peak and the emission peak are different. The excitation peak of alexaflour568 is 579 while the excitation peak of alexaflour633 is 631, both alexaflour were detected using the same channel but different laser wavelengths and the colour scheme for alexaflour 633 was changed to magenta from far red to enable the co-localisation detection. This was carried out as the recombinant virus expresses the mNeongreen marker gene (used for determining infected cells) and therefore the 488 channel could not be used. Interestingly, the results showed that both proteins (pWT-EP153RV5 and pWT-CD2vHA) were expressed and co-localised/co-occur in ASFV infected cells, a punctate staining pattern was observed for both proteins concentrated close to the ASFV induced viral factories (see figure 3.9). This experiment

was performed once and more than 30 cells were observed showing a similar co-localisation pattern.

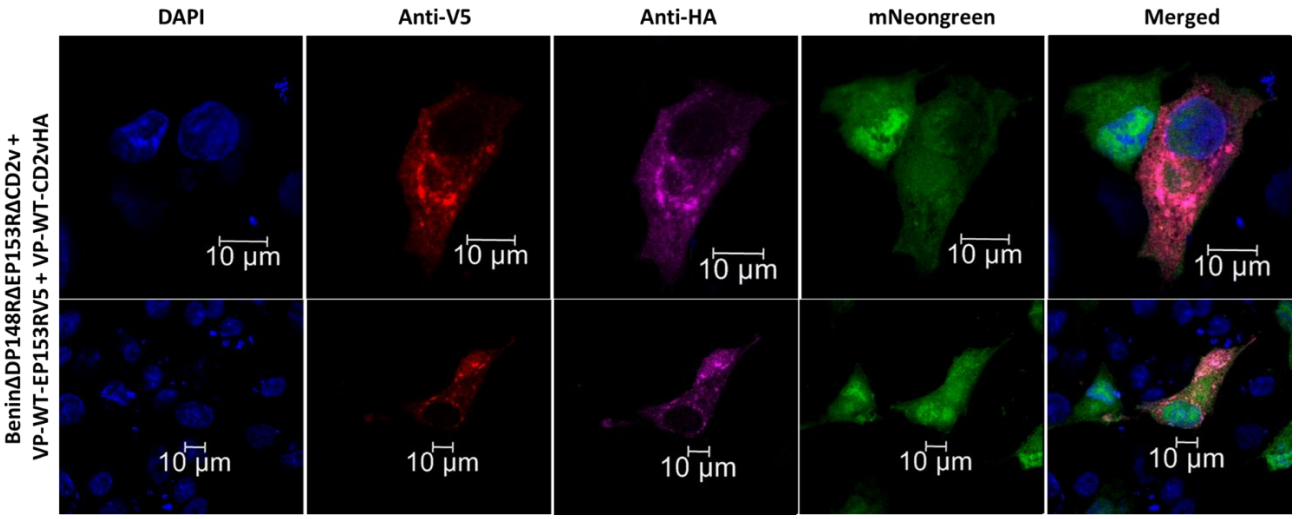

Figure 3.9: Co-localisation of CD2v and EP153R in ASFV infected cells. WSL cells were infected with BeninΔDP148RΔEP153RΔCD2v and co-transfected with pVP-WT-EP153RV5 and pVP-WT-CD2vHA. The VP-WT-EP153RV5 was stained with primary antibody (rat anti-V5) and probed with secondary antibody anti rat IgG alexaflour 568 (red). The VP-WT-CD2vHA was stained with primary antibody (mouse anti-HA) and probed with secondary antibody anti mouse IgG alexaflour 633 (blue-3rd panel). The recombinant virus expresses mNeongreen marker gene (shown in green), the nucleus and the viral factories are stained with DAPI (blue-1st panel). The merged image shows the co-localised pVP-WT-EP153RV5 and pVP-WT-CD2vHA and are shown in purple colour.

3.8 Detection of ASFV expressed proteins on the cell surface in non-permeable WSL cells by immunofluorescence:

The aim of this experiment was to investigate if ASFV expresses any other proteins on the cell surface except from CD2v and to determine the expression of pVP-WT-EP153R on the cells surface in ASFV infected cells. This was performed using the same

serum from ASFV-infected pigs that was used to detect pWT-CD2vHA on the cell surface in non-permeable Vero cells (see chapter 2). The serum was not previously tested using ASFV infected cells and was therefore screened to confirm if the serum can detect proteins on the cell surface in non-permeable cells infected with an ASFV deletion mutant from which both CD2v and EP153R genes were deleted. To perform this, WSL cells were infected with a recombinant virus BeninΔDP148RΔEP153RΔCD2v at MOI 2 and were incubated for 20 hours at 37°C. The recombinant virus BeninΔDP148RΔEP153RΔCD2v lacks CD2v (the only protein reported to be present on the surface of the extracellular enveloped ASFV virus particles) and EP153R/C-type lectin, the virus also contains a mNeongreen marker gene which was used to determine the infection efficiency (see section 3.11). The cells were fixed and stained with serum (from a previous ASFV pig infection experiment (Reis et al., 2017)) as primary antibody and probed with dylight 594 (goat anti-pig) secondary antibody. The results showed little or no detection of proteins on the cell surface, however, in 2 cells (out of 100 infected cells analysed) some staining was detected. This provides evidence that the serum does not detect any other proteins expressed on the cell surface in BeninΔDP148RΔEP153RΔCD2v infected WSL cells (see figure 3.10). In a further experiment, to determine if ASFV infected cells express EP153R on the cell surface, WSL cells were infected with recombinant virus BeninΔCD2v at MOI 2. The cells were stained for immunofluorescence using the method described above. The cell surface expression was detected in ASFV BeninΔCD2v infected cells but not in BeninΔDP148RΔEP153RΔCD2v infected cells, confirming the expression of EP153R on the cell surface in ASFV infected cells (see figure 3.11). This provides further evidence that EP153R as well as CD2v is expressed on the cell surface in ASFV infected cells. Interestingly, the experiment also suggested low levels or no expression

of additional ASFV proteins on the cell surface recognised by the serum from pigs immunised with BeninΔDP148R virus.

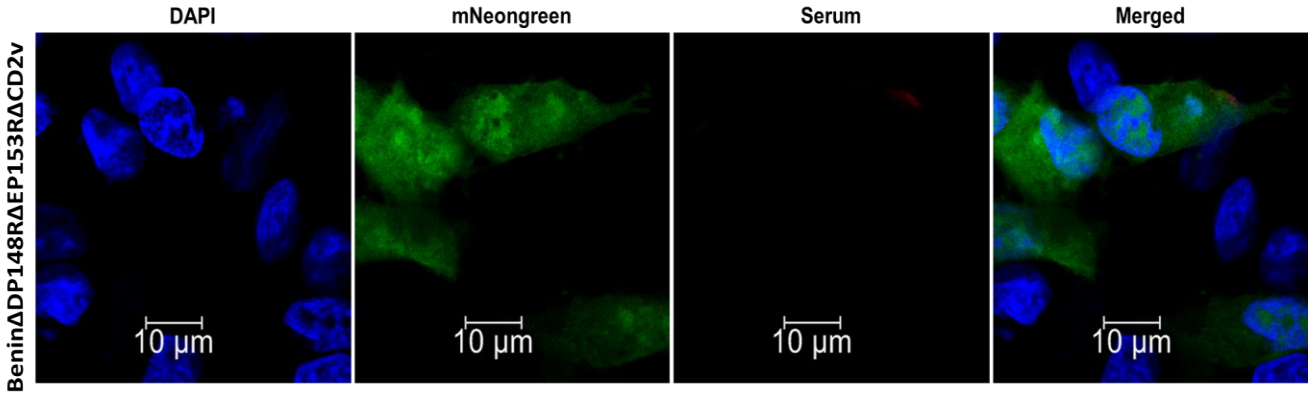

Figure 3.10: Detection of ASFV expressed cell surface proteins: WSL cells infected with BeninΔDP148RΔEP153RΔCD2v were stained with pig serum (which detected CD2v and EP153R in non-permeabilized cells), and probed with dylight 594 goat anti pig secondary antibody (shown in red). The virus expresses the mNeongreen marker gene (shown in green), the nucleus and the viral factories were stained with DAPI (shown in blue).

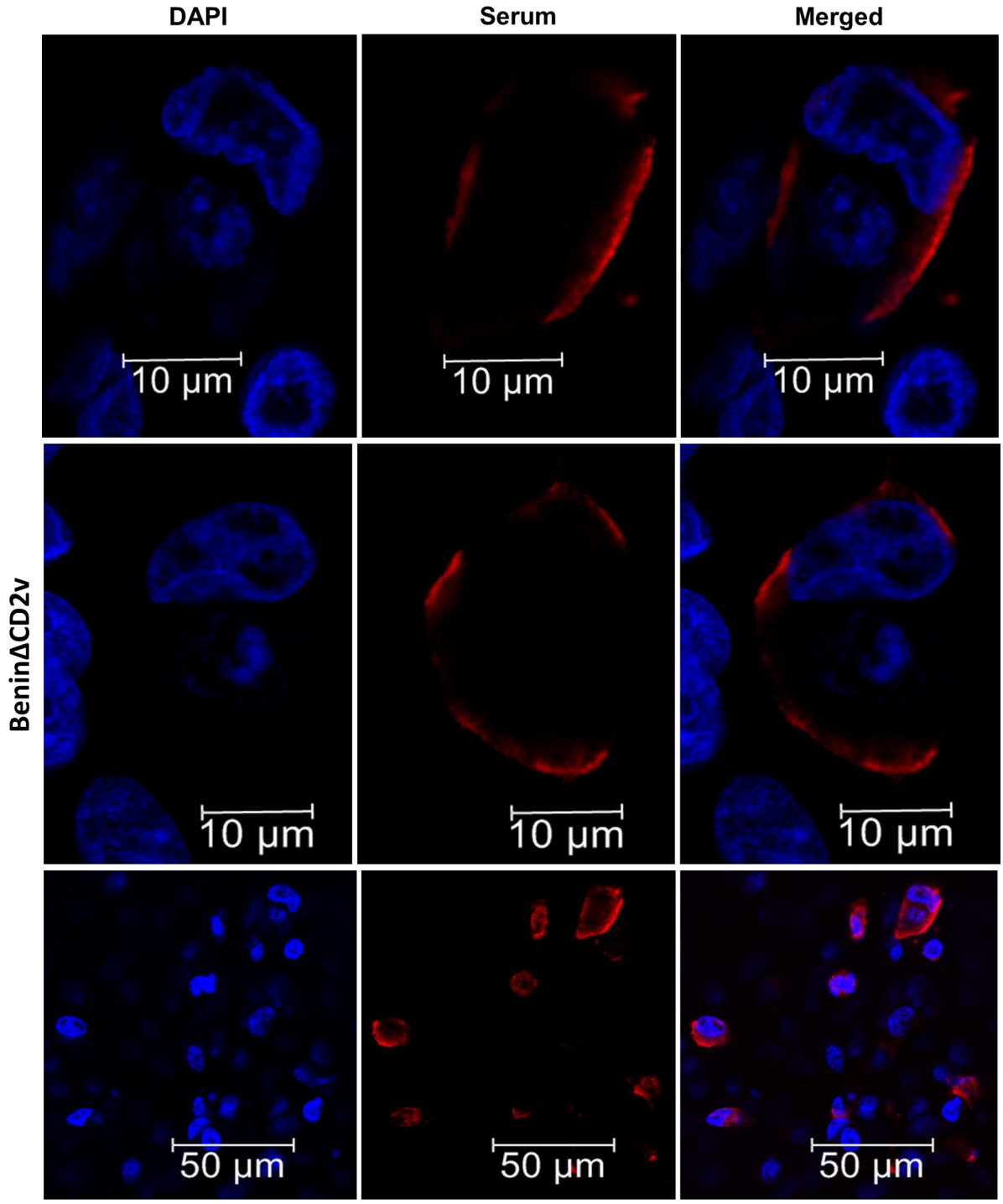

Figure 3.11: Detection of proteins recognised by sera from ASFV infected pigs on the surface of cells infected with BeninΔCD2v: WSL cells infected with BeninΔCD2v and were stained with pig serum (which detected CD2v on cells surface in non-permeabilized cell), and probed with dylight 594 goat anti pig secondary

antibody (shown in red). The nucleus and the viral factories were stained with DAPI (shown in blue).

3.9 Design of the plasmid construct for making BeninΔDP148RΔEP153R-CD2vE99R (Rec A);

Based on the analysis of HAD induced by the CD2v mutants pVP-CD2vY102D and pVP-CD2vE99R in ASFV infected cells and the role of EP153R in enhancing HAD that was indicated, it was decided to delete the EP153R gene and replace the wild type EP402R/CD2v gene with the E99R mutant CD2v. It was planned to use an already partially attenuated virus, Benin97/1ΔDP148R, as the backbone for the deletion. The BeninΔDP148R virus induces a transient fever and prolonged persistence of virus in blood after immunisation of pigs. Modification of this virus would mean that the effect of the CD2v modification on virus persistence could be studied. Since the EP153R and EP402R genes are adjacent on the virus genome the EP153R deletion and EP402R gene modification could be accomplished in one step. The plasmid construct was designed containing a left flanking region of the deletion and modification site (806bp), followed by a loxP site (34bp) upstream of the marker gene. A mNeonmarker gene (711 bp) under ASFV VP30 promoter (50 bp), CD2v promoter (120bp) upstream of with the mutant CD2vE99R gene (1206bp) and HA tag (27 bp), another loxP site (34bp) downstream of the HA tag followed by a right flanking region of the modification site (811 bp). The loxP sites were introduced to remove the entire cassette using Cre-recombinase, Cre-loxP is an efficient recombination system used for genetic manipulation, the Cre protein encoded by coliphage P1 promotes precise recombination of DNA in vitro at specific loxP sites (Sauer & Henderson, 1988).

The left flank starts 325 bp upstream of EP152R gene at genomic position 66244 bp and contains the EP152R gene along with 20 bp of the EP153R gene up to genome position 67050bp. The left flank is followed by a loxP site (at both ends of the marker gene) and a mNeongreen marker gene with or without the nuclear localization signal (NLS) under control of an ASFV P30 promoter. This marker gene will replace the EP153R in the recombinant virus. The EP402R/CD2v mutant E99R under control of its own viral promoter and with an HA tag tagged at the 3' end was designed to replace the wild type EP402R gene, this was followed by a loxP site. The recombination region (Region of Interest-ROI) is followed by a right flanking region which starts at position 68776bp in genome upstream of EP364R and covers the region up to genomic position 69581bp (see figure 3.12 & 3.13).

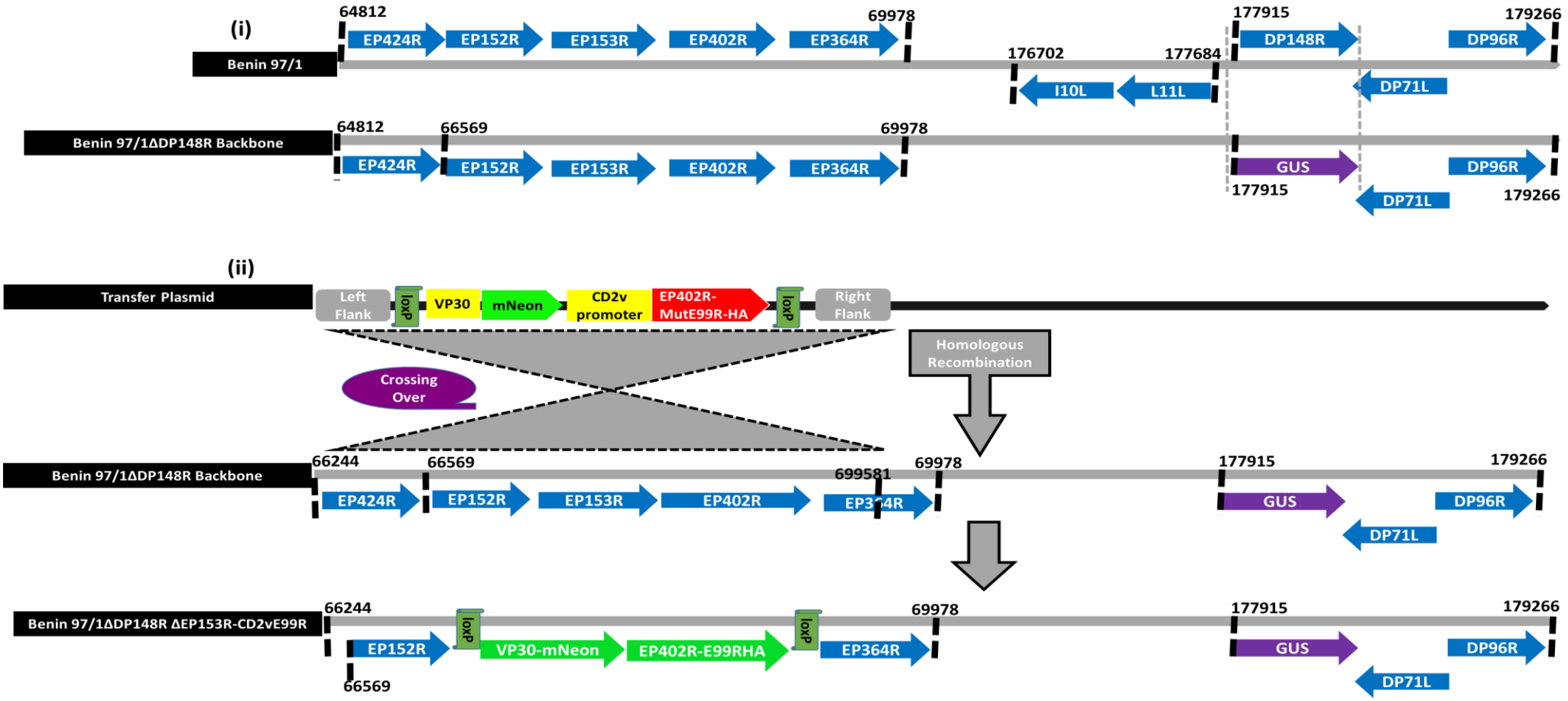

Figure 3.12: A schematic representation of generating BeninΔDP148RΔEP153R-CD2vMutE99R: The images shows the overall scheme of generating the recombinant virus **(i)** the images shows the wild type Benin 97/1 genome and the genes (exact scale), it also shows the BeninΔDP148R genome along with the gene that was deleted and replaced with the reporter gene. **(ii)** shows the recombination process and the viral backbone used to generate BeninΔDP148RΔEP153R-CD2vMutE99R (Rec A), it also shows the map of the transfer plasmid and the crossing over of the genes during recombination. The map at the end shows the newly generated recombinant virus.

The construct was ordered from Genscript cloned into pUC57 vector (See figure 3.7), subsequently the plasmid construct was amplified in bacterial cultures for transfections into porcine macrophages infected with BeninΔDP148RΔCD2v. I gave the plasmid construct to Dr. Ana Reis and Dr. Anusyah Rathakrishnan (The Pirbright institute) and they performed the experiments to generate a recombinant virus. The recombinant virus generated had 2 genes (DP148R and EP153R) deleted and one gene (EP40R/CD2v) replaced with the non-HAD mutant form of the gene (CD2vE99R). The EP402R is directly involved in the HAD mechanism while the EP153R augment the function of CD2v, hence the aim was to generate a non-HAD recombinant virus EP153R was therefore deleted.

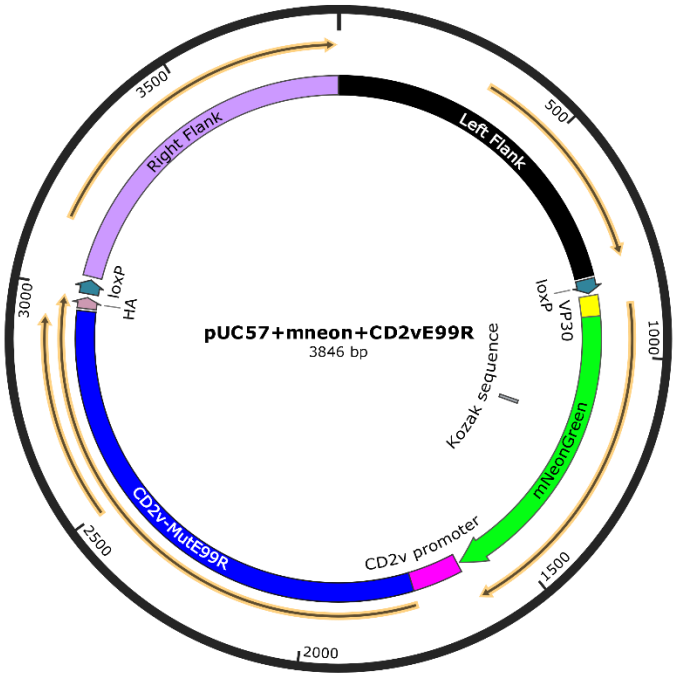

Figure 3.13: A map showing the transfer plasmid used for recombination into ASFV. The plasmid contains the regions flanking of the insertion site (left & right), the marker gene (mNeon) under control of ASFV VP30 promoter, and the CD2v mutant

E99R downstream from the CD2v promoter. This construct was used to generate the Rec A virus.

3.10 Design of the plasmid construct for making BeninΔDP148RΔEP153RΔCD2v (Rec B);

The functional and expression analysis of mutant CD2v E99R indicated the role of EP153R in HAD. To determine the effect of mutant CD2v E99R *in vivo* a recombinant virus with both EP153R and EP402R was deleted from an already attenuated ASFV BeninΔDP148R backbone (Rec A described in section 3.5). A second recombinant virus was designed recombinant B virus (BeninΔDP148RΔEP153RΔEP402R) to compare the effect of deleting the EP402R/CD2v gene with that of inserting the non-HAD CD2v mutant E99R instead of the wild type EP402R/CD2v gene. A plasmid construct was designed to delete the EP153R and EP402R/CD2v genes from the backbone virus BeninΔDP148R which contained the same left flanking region used to construct Rec A (see section 3.6) followed by loxP sites and the mNeon marker gene under the control of ASFV VP30 promoter. The right flanking region contained the identical sequences and regions as explained for generating the non-HAD CD2v mutant virus. The EP153R and EP402R genes in the BeninΔDP148R viral backbone were replaced by the selection cassette loxP, VP30 mNeon green, and loxP. In the ASFV genome, EP153R is located upstream of EP402R and downstream of EP152R at position 67030bp similarly the EP402R/CD2v is located upstream of EP364R at position 67567bp (See figure 3.14 & 3.15).

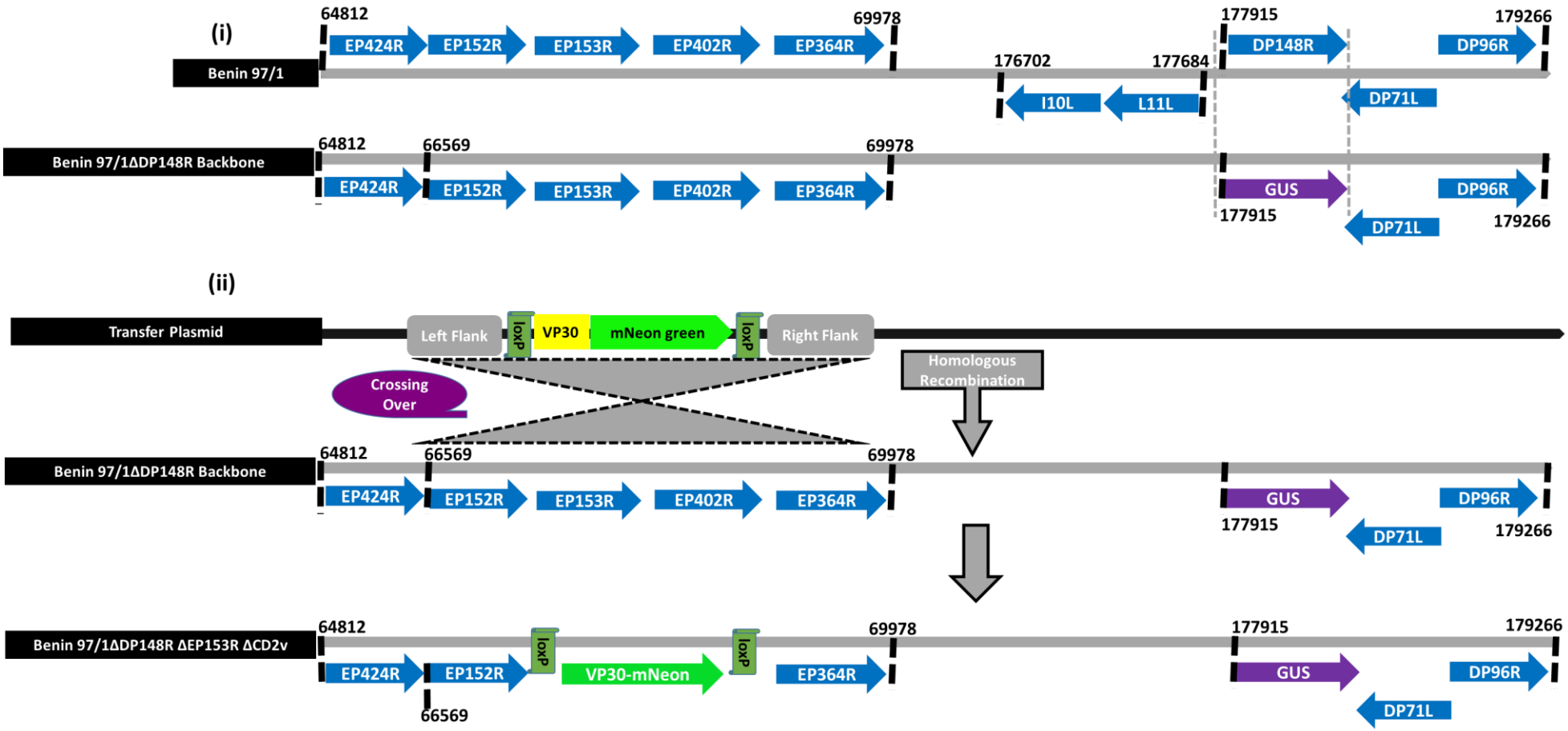

Figure 3.14; A schematic representation of generating BeninΔDP148RΔEP153RΔCD2v: The images shows the overall scheme of generating the recombinant virus **(i)** the images shows the wild type Benin 97/1 genome and the genes, BeninΔDP148R that was deleted and replaced with the reporter genes. **(ii)** Shows the recombination process and the viral backbone used to generate BeninΔDP148RΔEP153RΔCD2v (Rec B), it also shows the map of the transfer plasmid and the crossing over of the genes during recombination. The map at the bottom of the figure shows the newly generated recombinant virus.

The plasmid construct was ordered from Genscript and was delivered pre-cloned in pUC57 vector, the construct was amplified in bacterial culture for transfections. I handed over the plasmid constructs to Dr. Ana Reis & Dr. Anusyah Rathakrishnan (The Pirbright Institute) and they performed the experiments to generate the recombinant virus Rec B (BeninΔDP148RΔEP153RΔCD2v).

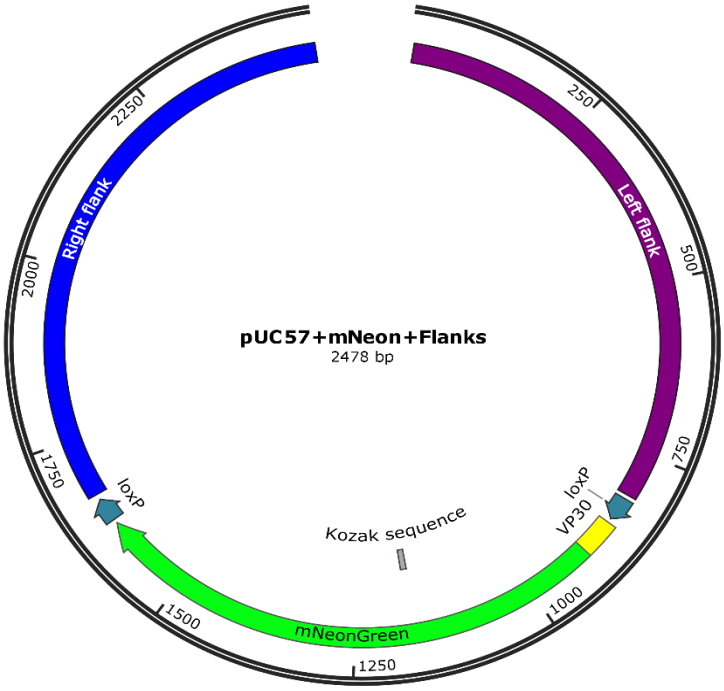

Figure 3.15: A transfer plasmid map showing the flanks (left & right), the marker gene (mNeon) under control of VP30 and the loxP sites. This construct was used to generate the Rec B virus.

3.11 Expression analysis of the plasmid construct (pUC57-VP30mNeon+VP-CD2vE99R) for BeninΔEP153RΔDP148R-CD2vE99R in ASFV infected WSL cells;

Expression analysis of VP30-mNeongreen and the pVP-CD2vE99R from the plasmid construct (pUC57-VP30mNeon+VP-CD2vE99R) used for generating the recombinant virus A (BeninΔDP148RΔEP153R-CD2vMutE99R) was determined by using

immunofluorescence. It was important to confirm that the marker gene (mNeon) and the mutant CD2vE99R are expressed before proceeding with making Rec A virus. WSL were infected with BeninΔDP148RΔCD2v at MOI 10 and were transfected with pUC57-VP30mNeon-VP-CD2vE99RHA plasmid construct. The cells were fixed, permeabilised and stained with anti-HA (rat IgG) primary antibody and probed with alexaflour 568 (goat anti rat IgG). The results showed that the marker gene (VP30-mNeon) and pVP-CD2vE99R were expressed. It was observed that pVP-CD2vE99R was expressed and was localised close to the plasma membrane and in the cytoplasm, no punctate were observed close to the ASFV induced viral factories. In contrast, transient expression of CD2vE99R in MVA-T7 infected Vero cells showed that CD2vE99R is mainly localised in cytoplasm and punctate were detected close to the MVA-T7 viral factories (see chapter 2). Since the cells were permeabilised and expression was detected using an antibody against a C-terminal tag it wasn't possible to conclude that the extracellular domain was exposed on the cell surface. However, the results suggest that CD2v is transported more efficiently to the cell surface in ASFV infected cells and the virus may possibly contain other factors that exploit the cellular transport machinery for efficient transport of cell surface proteins. (See figure 3.16). Since the cells were infected with ASFV and therefore other virus proteins could be expressed on the cell surface it wasn't possible to use pig sera from ASFV immunised pigs to confirm expression of CD2v on the cells surface in non-permeabilised cells.

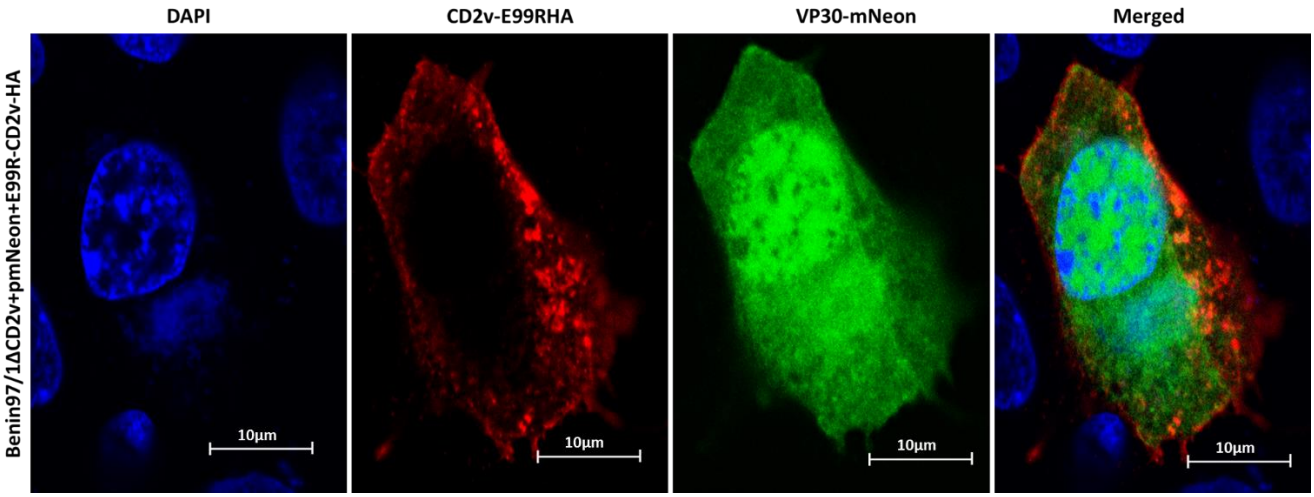

Figure 3.16: WSL cells infected with ASFV BeninΔCD2v (MOI 10) and transfected with pUC57-VP30mNeon-VP-CD2vE99RHA. The cells were stained with anti HA (rat IgG) primary antibodies and probed with alexaflour 568 goat anti-rat IgG (shown in red), the mNeon was expressed and is shown in green. The merged image is clearly showing that CD2v-E99R was expressed and transported to the cell surface.

3.12 Confirmation of a non-HAD phenotype induced by transfection of a plasmid construct for BeninΔDP148RΔEP153R-CD2vE99R (Rec A) in ASFV OURT88/3 infected cells:

Functional analysis of the CD2vE99R expressed from the plasmid construct (pUC57-VP30mNeon-CD2vE99RHA) used for making recombinant virus Rec A was performed by setting up a HAD assay. This was done to confirm that the mutant pVP-CD2vE99R is expressed but does not induce HAD prior to generating the recombinant virus Rec A. WSL cells were infected with ASFV OURT 88/3, which does not express functional CD2v or EP153R, at a MOI 3 and incubated for 2 hours at 37°C. The cells were transfected either with pUC57-VP30mNeon-CD2vE99RHA plasmid or pVP-WT-CD2v and were incubated again for 18 hours post infection/transfection. A HAD assay was performed on the cells expressing pUC57-VP30mNeon-CD2vE99RHA and pVP-

WT-CD2v, the results provided evidence that pVP-CD2vE99R mutant protein did not induce HAD in cells infected with ASFV that does not express functional CD2v and EP153R, as no rosettes were observed after another 18 hours of incubation at 37°C (see figure 3.17). In contrast, the cells transfected with VP-WT-CD2v induce HAD and more than 50 HAD cells were observed, this experiment was performed once.

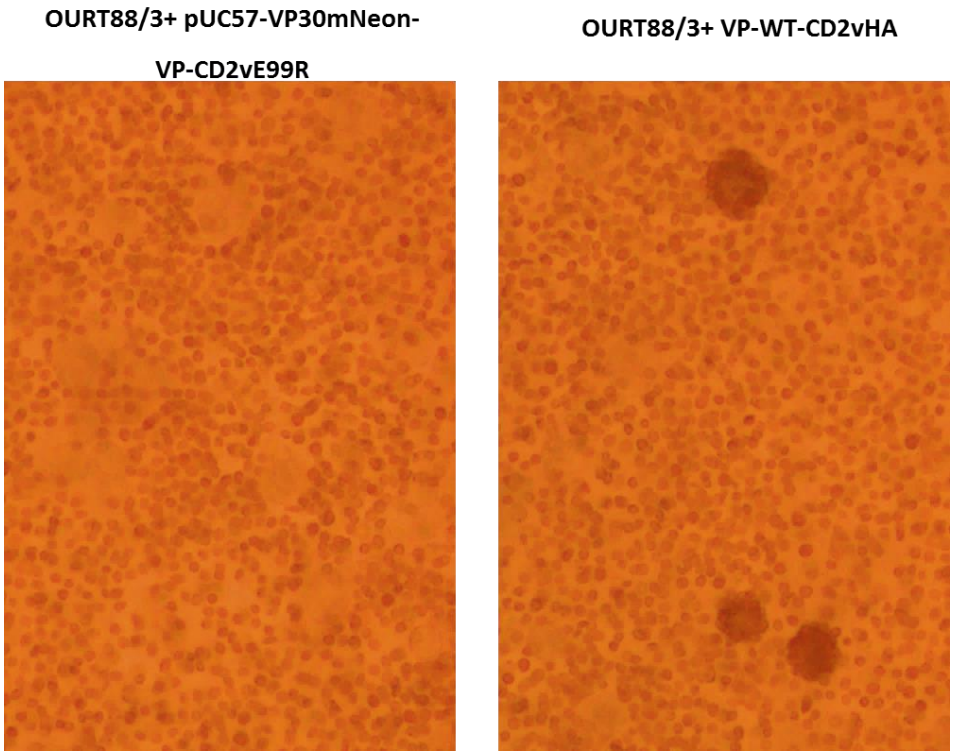

Figure 3.17: WSL cells infected with OURT88/3 at MOI-3 and transfected either with pUC57-VP30mNeon-CD2vE99RHA or VP-WT-CD2v. On the left the image is showing non-HAD phenotype of CD2vE99R and on the right the image is showing HAD phenotype of VP-WT-CD2v.

3.13 Analysis of expression of mNeongreen and VP-CD2vE99R in cells infected with recombinant ASFV BeninΔDP148RΔEP153R-CD2vE99R (Rec A) by immunofluorescence:

To analyse the expression of CD2v mutant E99R in primary porcine macrophages infected with the recombinant virus A, PBMs were grown on cover slips and were infected with recombinant virus A at MOI 1. The cells were incubated for 7 hours post infection at 37°C and were stained for immunofluorescence (see section 5.3.4). It was observed that cells infected with Rec A virus were expressing VP-CD2vE99R and P30-mNeon, the VP-CD2vE99R was mainly observed at the cell periphery rather than in the cytoplasm. A small amount of protein was observed to co-localise around the viral factories (see figure 3.18). More than 50 cells were observed showing the same expression and localisation of the VP-CD2vE99R, this experiment was performed once. Comparing these results with the previous immunofluorescence data where cells were infected with either ASFV or MVA-T7 and transfected with the plasmid VP-CD2vE99R (ASFV infected WSL) or with CD2vE99R (MVA-T7 infected Vero). In MVA-T7 infected and transfected cells the protein was mainly detected in the cytoplasm and less in the cell periphery, punctate staining of CD2vE99R was observed close to the viral factories (see chapter 2). This suggests that CD2vE99R is efficiently transported to the cell surface in macrophages, possibly due to the reduced expression of the protein from the viral genome compared to the expression in the transfected cells. Higher expression of the protein might result in delay in entering and progressing through the secretory system.

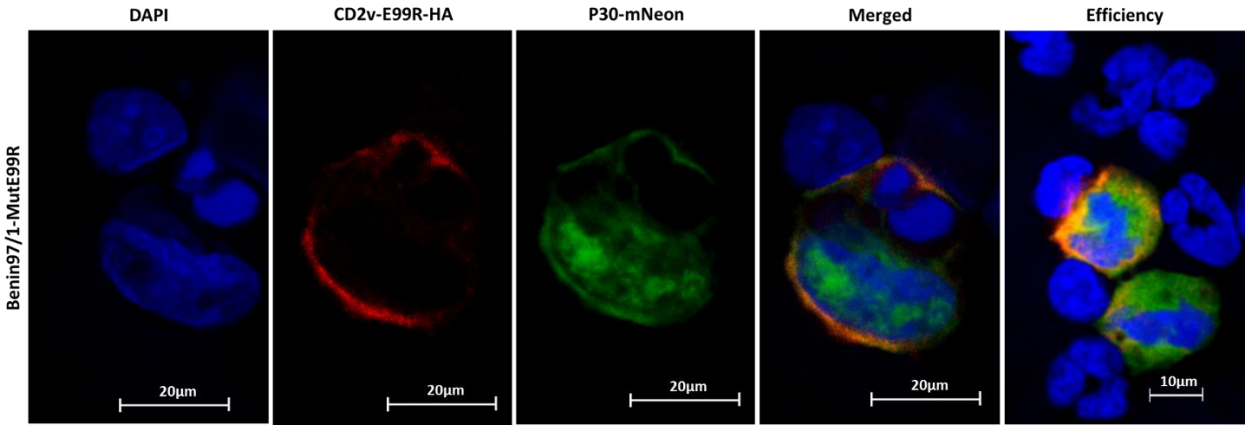

Figure 3.18: Porcine bone marrow cells infected with RecA virus at MOI 1, fixed and permeabilized. The cells were stained with anti -HA (anti rat) primary antibody, probed with Alexaflour 568 (goat anti-rat). The images shows the RecA virus is expressing CD2v-E99RHA (Red) and mNeon (green). The nucleus was stained with DAPI (blue). The merged image shows expression of CD2v-E99Rat the cell periphery.

3.14 Confirmation that HAD is not-induced in cells infected with Recombinant virus BeninΔDP148RΔEP153R- CD2vE99R (Rec A)*:*

A haemadsorption assay was set up to confirm that the recombinant virus containing CD2v-E99R is non-HAD. Porcine bone marrow (PBMs) cells containing 1% RBC were grown in a 6 well plate and were infected with either wild type Benin 97/1 or Benin ΔDP148RΔEP153R-CD2vE99R at MOI 1. The cells were incubated for 48 hours at 37°C to allow a greater proportion of cells to become infected and to induce rosette formation. It was observed that recombinant virus BeninΔDP148RΔEP153R-CD2vE99R did not induce HAD since no RBC were observed attached to the infected cells, although mNeon was expressed confirming that the cells were infected (see figure 3.19). In contrast, the wild type ASFV Benin 97/1 (which contains a wild type CD2v and EP153R) induced HAD (See figure 3.13). More than 100 HAD cells were observed in the control (Benin97/1), this experiment was performed once.

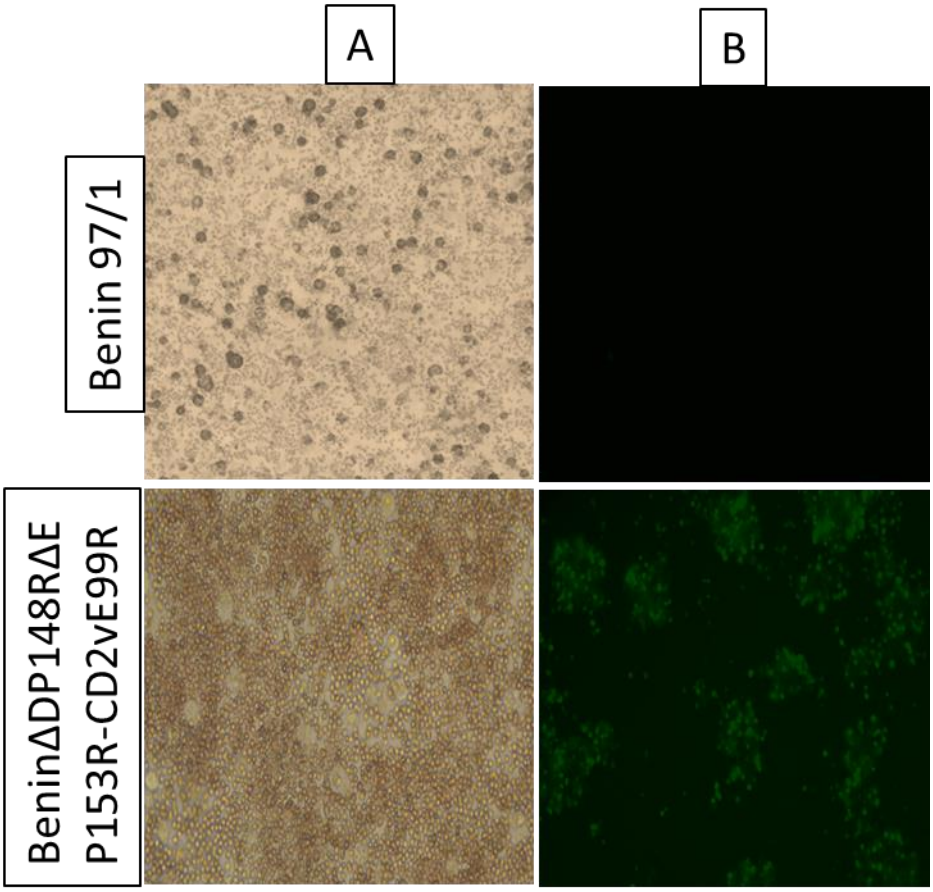

Figure 3.19: Porcine bone marrow cells infected with ASFV Benin97/1 or BeninΔDP148RΔEP153R-CD2vE99R Rec A at MOI 1. The cells were incubated for 48 hours post-infection and were analysed with a fluorescent microscope. In panel A, the top image shows HAD in cells infected with Benin97/1 and the bottom image shows non-HAD phenotype in cells infected with Rec A virus. In panel B, the top image shows cells infected with Benin97/1 and no expression of mNeon , the bottom image shows cells infected with RecA virus and expressing mNeon confirming they were infected.

The recombinant viruses generated (BeninΔDP148RΔEP153R-CD2vE99R and Benin 97/1ΔDP148RΔEP153RΔCD2v) were tested in an immunization and challenge experiment in pigs. The effect of the virus in inducing protection is described in chapter 4.

3.15 Discussion:

In this chapter, the expression and functional analysis of the reduced HAD and non - HAD mutant CD2v proteins in ASFV infected cells were described. The HAD assay in ASFV infected WSL cells showed that the cells expressing pVP-WT-CD2vHA were HAD, but the rosettes appeared were not as strong as were observed in the Vero cells transfected with T7-WT-CD2v. This suggest that either the ASFV/CD2v promoter is weak compared to the T7 promoter or the protein is transported efficiently to the cells surface in Vero cells than in WSL cells. However, the later mentioned is unlikely as the immunofluorescence data suggest that CD2v is transported efficiently in WSL cells. The immunofluorescence data also showed that CD2v is expressed in sufficient amount when expressed by the T7 promoter in Vero cells compared to the CD2v expressed by its own viral promoter in WSL cells.

The expression and functional analysis of the CD2v mutants (pVP-CD2vE99R and pVP-CD2vY102D) in ASFV infected cells suggested that EP153R gene enhanced HAD. This was indicated since the mutant versions of CD2v which reduced or abrogated HAD when expressed alone induced a HAD phenotype when tested in WSL cells infected with BeninΔCD2v. However, when these mutants were tested in WSL cells infected with OURT88/3 (with non-functional CD2v and EP153R genes (Chapman et al., 2007)) the mutants again showed reduced and non-HAD phenotype. Since expression of EP153R alone does not cause HAD (Galindo et al., 2000) this suggests that EP153R may either enhance the cell surface expression of CD2v or may augment the function of CD2v by interacting with sugars on RBC to anchor the cells, allowing even the mutant CD2v protein to bind RBC (see figure 3.20).

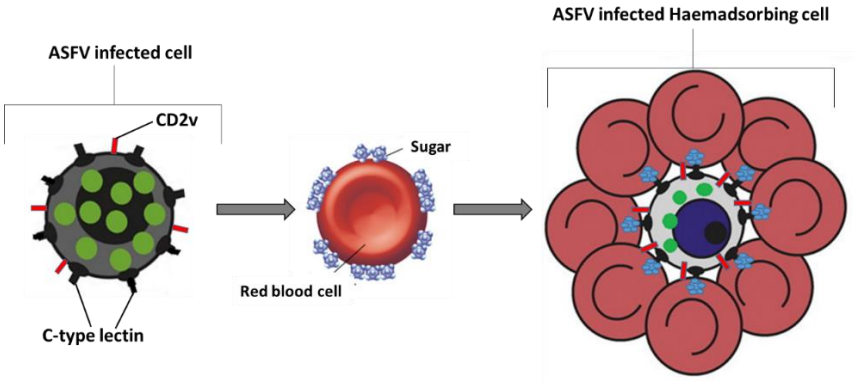

Figure 3.20: A schematic representation showing a possible role of EP153R/C-type in enhancing HAD. The image shows an ASFV infected cell expressing CD2v and C-type lectin on the surface, the interaction of C-type lectin with the long sugar molecules anchors the RBC and possibly enhance HAD.

The EP153R sequence contain a cell attachment (RGD) motif and a significant homology with the N-terminal region of CD44 molecules which is involved in cellular adhesion and T-cell activation (Hurtado et al., 2011; Hurtado et al., 2004). EP153R is also reported to modulate the expression of MHC-1 on the cells surface, it doesn't inhibit the synthesis process but is rather involved in regulating exocytosis (Hurtado et al., 2011). Since it has a role in regulating the cellular transport machinery, it is possible that EP153R enhance the surface expression of CD2v.

Analysis of CD2v and EP153R localisation in cells showed that both proteins are expressed on the cell surface. The CD2v protein was detected as the only virus protein on the external envelope of virus particles by proteomic analysis and in that study the EP153R protein was not detected in virus particles (Alejo et al., 2018). However, only small amounts of CD2v were detected in virions and it's possible that the EP153R protein was below the limit of detection. It would be interesting to determine if EP153R is incorporated in the external envelope along with CD2v. To achieve this a recombinant ASFV expressing the C-terminal epitope tagged EP153R gene could be

used. Preliminary evidence indicated that CD2v and EP153R co-localise in cells so may bind together to move to the surface although further evidence is needed to investigate this. In any case it is clear that CD2v protein can reach the cell surface in the absence of EP153R (chapter 3).

In line with these findings two recombinant ASFV (BeninΔDP148RΔEP153RΔCD2v and BeninΔDP148RΔEP153R-E99R) were constructed to determine the effect of CD2v, EP153R and CD2vE99R in vivo. The analysis and the results from in vivo studies are described in chapter 4.

Chapter 4- Determine the role of CD2v, EP153R in viremia, and persistence in pigs.

4.1 Introduction:

In the previous chapter, I described the expression analysis of VP-WT-CD2vE99R and, VP-WT-CD2vY102 in ASFV infected cells by Western blot, immunofluorescence, and HAD assay. It was shown that mutant CD2vE99R and CD2vY102D proteins were expressed in WSL cells, processed in the correct forms and sizes. However, the CD2vE99R (non-HAD) and CD2vY102D (reduced HAD) showed a positive HAD phenotype similar to the VP-WT-CD2vHA when transfected into WSL cells infected with ASFV CD2v deletion mutant (BeninΔCD2v). This suggested that either a host or a viral factor is involved in enhancing the HAD, previous literature suggested that a C-type lectin protein encoded by ASFV gene EP153R may enhance HAD although EP153R did not alone induce HAD (Galindo et al., 2000). Serum antibodies against both CD2v and EP153R were shown to mediate haemadsorption inhibition (HAI) and to be involved in serotype-specific protective immunity, representing good targets for ASFV serotype classification (Malogolovkin, Burmakina, Tulman, et al., 2015). The mutant CD2vE99R and CD2vY102D proteins showed no HAD or reduced HAD phenotype when transfected into WSL cells infected with OURT88/3 strain, which has non-functional EP402R and EP153R (Chapman et al., 2007). This indicated that EP153R is indeed involved in enhancing HAD. Previous data has shown that EP153R has a role in inhibiting apoptosis mediated by the p53 pathway and reduction of surface expression of swine leukocyte antigen I (SLAI) (Hurtado et al., 2011; Hurtado et al., 2004).

In this chapter a pilot pig immunization and challenge experiment was performed to analyse the role of CD2v in virus persistence. Pigs were immunized with the recombinant virus BeninΔDP148RΔCD2v (the recombinant virus was constructed and provided by Dr. Ana Reis, the Pirbright Institute) BeninΔDP148RΔEP153RΔCD2v, and BeninΔDP148RΔEP153R-CD2vE99R (provided by Dr Anusyah Rathakrishnan the Pirbright Institute) and challenged with a lethal dose of the parental Benin 97/1 virus. Deletion of the DP148R gene attenuates the Benin 97/1 virus although moderate clinical signs and viremia are observed and the viremia persists over a period up to 60 days for virus genome and 30 days for infectious virus (Reis et al., 2017). The aim was to establish the role of the CD2v protein in virus persistence in blood and induction of clinical signs.

This chapter is divided into three parts to enhance the clarity; the results from experiment 1 are described in part 1, and the results from experiment 2 are described in part 2. The 3rd part explains the comparative analysis from both experiments.

PART-1 (EXPERIMENT-1)

4.2 Design of animal immunisation and challenge experiment with recombinant BeninΔDP148RΔCD2v Virus (experiment 1):

A pilot animal immunization and challenge experiment was carried out in the SAPO4 high containment animal housing facility at The Pirbright Institute. In this experiment, 4 Large White Landrace pigs (15-20kg) were immunized with 1ml of recombinant virus BeninΔDP148RΔCD2v (Group C) by the intramuscular route (IM) at 10^3 $TCID_{50.}$ The pigs were boosted on day 20 post-immunization with 1ml of the same recombinant virus by the IM route at 10^4 $TCID_{50}$. Naïve control pigs (Group F) and immunized pigs

were challenged on day 42 by the IM route with a single dose of virulent Benin97/1 isolate at 10^4 HAD_{50}. Pigs reaching the moderate severity humane endpoint were euthanized by an overdose of barbiturates, the surviving pigs were euthanized on day 62 post-immunization by culling the pigs with an overdose of barbiturates. Necropsies were performed on the pigs to identify ASFV related pathological signs (see figure 4.1).

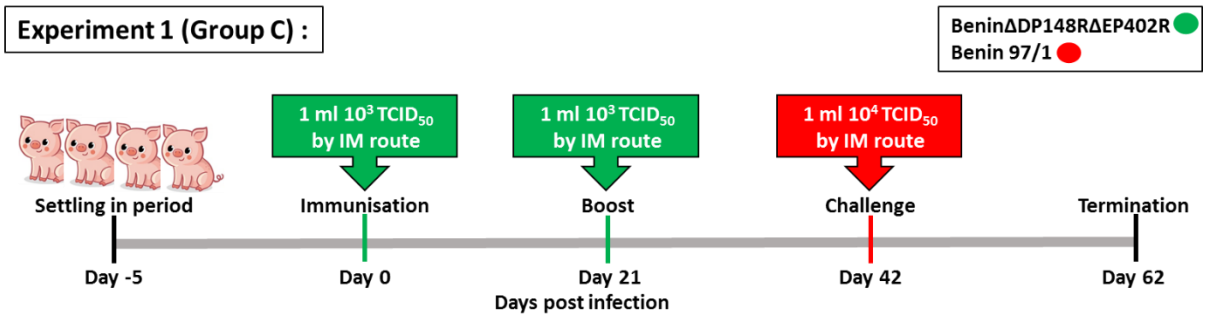

Figure 4.1: Chronological representation of animal experiments 1. The recombinant viruses used for primary immunization and boost are shown in green, the virus used for the challenge is shown in red. The days are shown as day post-infection, referring to the first inoculation of the virus, the route of infection and dosage used are shown for each event (immunization, boost, and challenge).

4.3 Clinical signs post-immunization and challenge (experiment 1):

The pigs in the pilot experiment were monitored daily throughout the study by the animal isolation staff (The Pirbright Institute). Rectal temperatures along with other clinical signs were recorded in the clinical score sheet for ASFV (see appendix 2). Animals reaching the moderate severity endpoint defined in the relevant home Office License were euthanized.

In this experiment, pig C3 developed fever above 40.5 °C with no other clinical signs on day 5 post-immunization for 1 day while pig C2 developed fever above 41°C for 2 days (day 6 and 8) post-immunization (see figure 4.2A and 4.2B). Pig C1 developed

fever above 41°C for 1 day (day 8), pig C4 had a fever above 40.5°C for 2 days (day 7 and 8) and was euthanized on day 9 due to non-ASFV specific clinical observation. No fever above 40.5°C was recorded in the 3 remaining pigs from day 9 post-immunization until termination of the experiment, however, mild anorexia was observed in all pigs on day 11 and 12 post-immunization. Naïve non-immunized control pigs (Group F) developed a high fever and other clinical signs of acute ASF, including loss of appetite and lethargy, on day 3 post-challenge and were euthanized on day 4, all of the remaining pigs in group C survived the lethal challenge with ASFV Benin 97/1 virulent strain (see figure 4.2C).

(A)

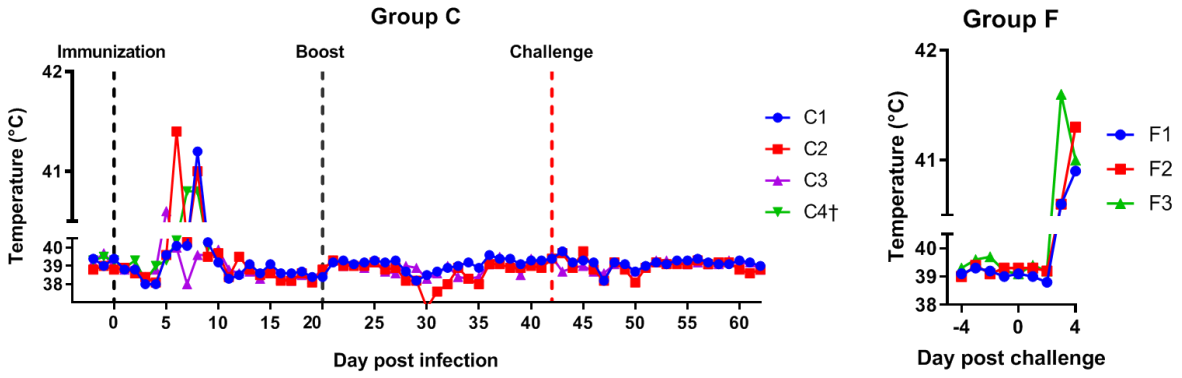

(B)

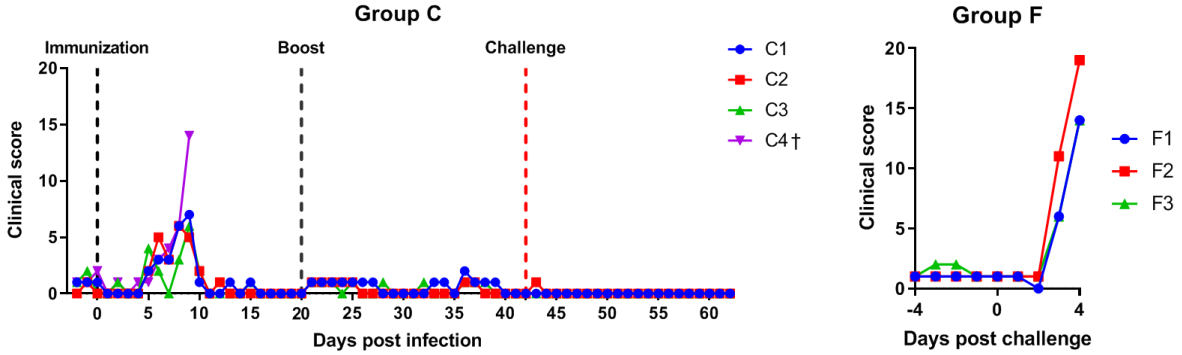

(C)

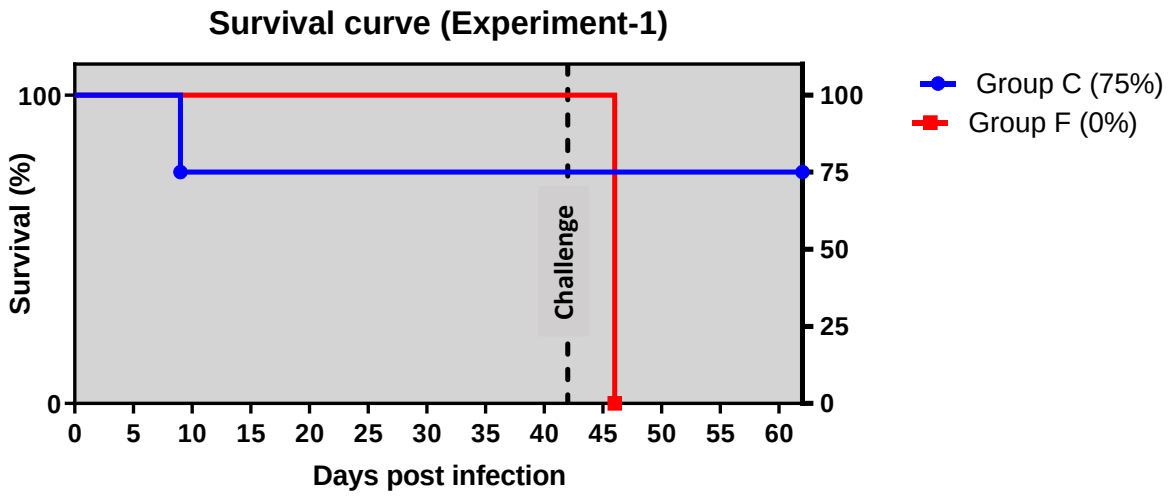

Figure 4.2: Rectal temperatures, Clinical signs, and survival of pigs in Group C (Experiment 1): (A) Rectal temperatures of pigs: Daily temperature record of pigs immunized with BeninΔDP148RΔCD2v (Group C) and challenged with Benin 97/1. The days for naïve non-immunized pigs are shown as days post-challenge (Group F). The temperature is shown in degree Celsius with a threshold of 40.5°C for scoring towards the moderate severity humane endpoint, the euthanized pig is represented by (†) symbol. The dotted lines show the event and the coloured line represents the individual pig in each group. **(B) Clinical scores of pigs:** Clinical scores post-immunization and challenge of pigs is shown in Group C and Group F. These scores include temperature and other signs such as lethargy and loss of appetite **(C) Survival curve of pigs:** The survival percentage of pigs immunized with BeninΔDP148RΔCD2v (blue line) and challenged with Benin 97/1. The days are given as days post-infection referring to primary inoculation, the naïve pigs (Group F) are represented by a red line. The dotted line shows the day pigs were inoculated with Benin 97/1. One pig immunised with BeninΔDP148RΔCD2v was culled due to a non-ASFV related clinical sign.

4.4 Pathological and macroscopic evaluation at Necropsies (experiment 1):

The pathological observation and macroscopic scoring of all pigs were performed at post-mortem according to the score sheets for ASFV (see appendix 2). The post-mortems and pathological evaluations were carried out by Dr. Linda Dixon, Dr. Ana Reis, Dr. Anusyah Rathakrishnan (The Pirbright Institute), and Dr. Pedro Sanchez-Cordon (Animal and Plant Health Agency). The pigs in Group C showed few macroscopic lesions except for the slight enlargement of lymph nodes. This does not include pig C4 which was euthanized at day 9 post-immunization due to welfare reasons before the challenge. Naïve control pigs (Group F) showed gross lesions characteristic of acute ASF, including haemorrhage in some lymph nodes, enlarged spleens and enlarged/haemorrhagic tonsils, pericardial effusion, and ascites (see figure 4.3).

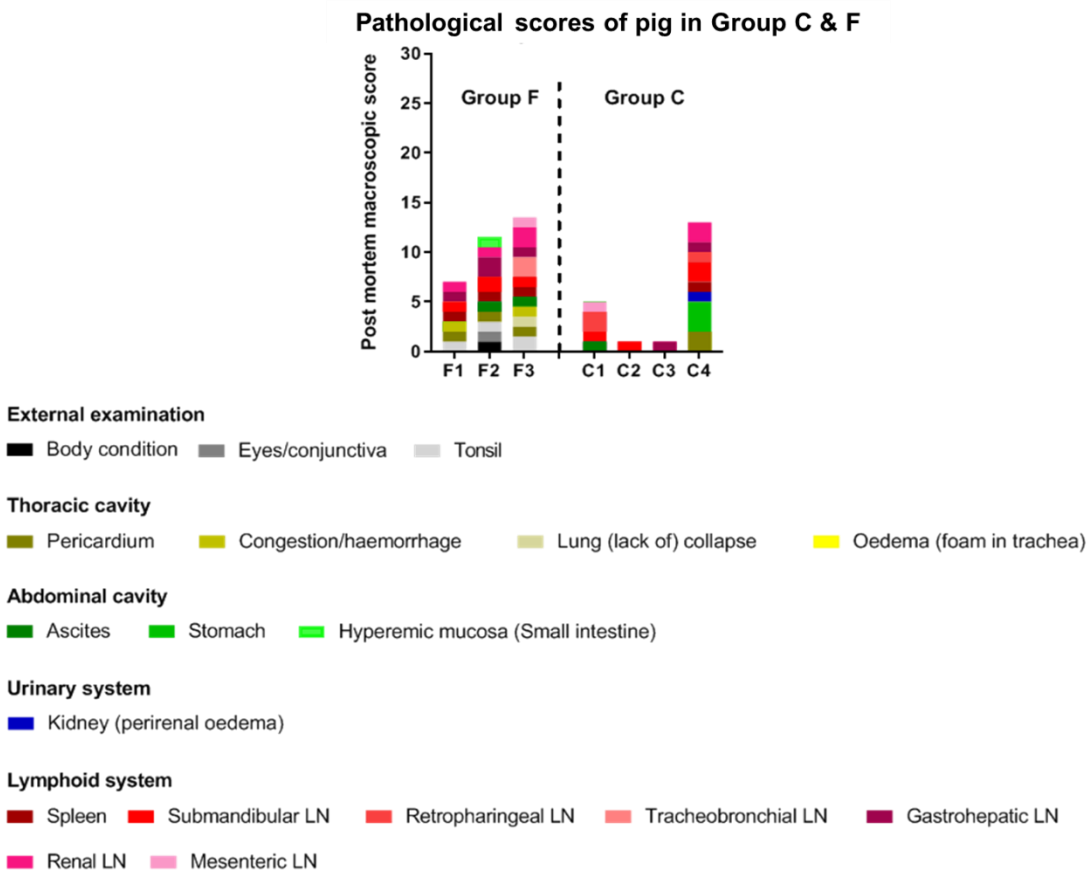

Figure 4.3: Pathological scores of pig in Group C & F (experiment 1): The figure shows pathological scores of individual pigs at post-mortems in experiment 1 and 2. The scores are represented by a coloured bar and correspond either to an organ, tissue, or lesions.

4.5 Detection of genome copies in whole blood by qPCR in pigs immunised with BeninΔDP148RΔCD2v (Group C) post-immunization (experiment- 1):

The previous experiment carried out at The Pirbright Institute showed that the deletion of the DP148R gene from the genome of the virulent Benin97/1 genotype I isolate attenuated the virus in pigs and induced high levels of protection against lethal challenge with the parental virus. In pigs immunized with BeninΔDP148R, virus genome copies were detected in blood at day's 3-4 post-immunization and the viremia peak was detected at 5-7 days post-immunization coinciding with the onset of clinical signs. The BeninΔDP148R virus genome persisted in blood for an extended period (over 60 days) and the infectious virus persisted in blood for up to day 30 (Reis et al., 2017).

To investigate the role of CD2v in virus persistence in blood, the recombinant virus with CD2v deletion (BeninΔDP148RΔCD2v) was constructed from the parental BeninΔDP148R genome. The recombinant virus was tested in pigs (Group C) by immunization and challenge experiment, to identify the role of CD2v in the extended persistence of the virus in the blood. The blood samples were collected at different times post-immunization and challenge. I extracted genomic DNA and a quantitative PCR (qPCR) was performed to detect virus genome copies. A delay in viremia was observed and no virus genome copies were detected at day 3 post-immunization. A peak of viremia was observed on day 7 post-immunisation in all pigs and the virus

genome detected was between $10^{2.9}$ to 10^{6} genome copies per ml with the lowest in pig C3. The levels of virus genome copies gradually declined after day 7 in all pigs and were detectable until day 14 post-immunization at a level between 10^{3} to $10^{3.5}$ genome copies per ml. Data for pig C4 is shown until it was euthanized at day 9 post-challenge due to welfare reasons. No further viremia was detected throughout the experiment after day 14 post-immunization in the immunized pigs (See figure 4.4). In contrast, high levels of virus genome copies were detected in naïve non-immunized pigs at day 3 post-challenge (up to 10^{8} copies per ml) and these pigs were euthanized on day 4 post-challenge. These results showed that deletion of CD2v from the attenuated BeninΔDP148R dramatically reduced the persistence of virus genome in blood. The BeninΔDP148RΔCD2v virus genome persisted in the blood for 11 days while the parental virus BeninΔDP148R persisted in blood for up to 60 days (Reis et al., 2017).

A short delay in viremia and onset of clinical signs were also observed in BeninΔDP148RΔCD2 compared to the parental BeninΔDP148R (Reis et al., 2017), the onset of clinical signs were delayed by 1 day. The genome copies detected post-immunisation remained similar in pigs from both experiment (BeninΔDP148R and BeninΔDP148RΔCD2), however, the duration of virus genome persistence in blood was significantly reduced (from 60 days to 11 days). This suggest that CD2v may not be directly involved in the induction viremia but is involved in virus genome persistence in blood.

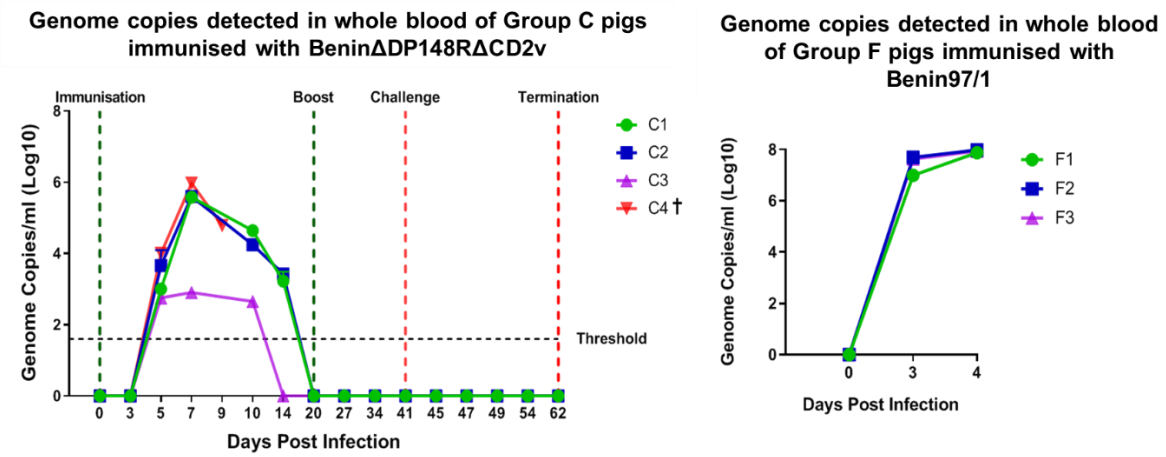

Figure: 4.4: Genome copy numbers in blood (Group C): Virus genome copies per ml detected in the blood of pigs immunized with BeninΔDP148RΔCD2v and challenged with virulent Benin 97/1. The green dotted line shows the day of primary immunization and boost, the red dotted line shows the days of challenge and termination. Each coloured line represents individual pigs and the euthanized pig is represented by (†) symbol.

4.6 Detection of genome copies in different blood fractions by qPCR in pigs immunised with BeninΔDP148RΔCD2v (Group C) post-immunization (experiment- 1):

To investigate the distribution of virus in blood fractions, the blood samples were collected at different times post-immunisation from pigs infected with Benin 97/1 (Group F) and BeninΔDP148RΔCD2v (Group C). The blood samples were fractioned into plasma, erythrocytes, and PBMC by performing density gradients using Histopaque®-1077 (see section 5.4.1 & 5.4.2 for details). A qPCR was performed to measure viral genome load in fractioned blood by extracting genomic DNA. The virus genome copies were detected in RBC, plasma, and PBMC at day 5 in all pigs (Group C BeninΔDP148RΔCD2v) ranging between $10^{2.6}$ to 10^{4} genome copies/ml. In the

erythrocyte (RBC) fraction, genome copies were detected in all pigs except C3. In the pigs C1, C2, C4, virus genome was detected from day 5 reaching a peak in RBC fraction at day 7 post-immunization at which time approximately 10^5 genome copies/ml were detected. Virus genome then declined but was detectable in pig C1 until day 14 (see figure 4.5A). In the control pig group (Group F, Benin97/1), 10^8 genome copies/ml were detected in the RBC fractions at days 3 and 4 post-infection (see figure 4.5A).

Similarly, in PBMC fraction the viremia peak was observed at day 7 post-immunization in all pigs except pig C3, the viremia peak in pig C3 was observed at day 5 post-immunization and this pig had the lowest amount of genome copies (10^2 genome copies/10^6 cells). In the remaining pigs the amount of genome copies detected in PBMC were variable and ranged between ($10^{3.2}$-10^4 genome copies/10^6 cells) (see figure 4.5B). In samples from the control pigs (Goup F- Benin97/1) the level of genome copies detected in PBMCs were $10^{5.5}$ copies/10^6 cells (see figure 4.5C).

The highest amount of genome copies was detected in plasma fraction in all pigs, the peak was detected at day 7 and the genome copies were detected between 10^{5}-10^7 genome copies/ml (see figure 4.5C). The lowest amount was detected in pig C3 while the highest amount of genome copies was detected in pig C4. In the control pigs (Group F-Benin97/1) the amount of genome copies detected varied between $10^{7.5}$ to $10^{8.2}$ genome copies/ml (see figure 4.5C). These results show that the highest level of virus genome copies was present in the plasma fraction, which gradually declined and was cleared at day 20 post-immunisation. Previous studies have reported that more than 90% of the virus is associated with RBC fraction (Wardley & Wilkinson, 1977), the Extracellular ASFV particles are known to bind to the surface of red blood cells, and this is mediated by the CD2v protein (Rodriguez et al., 1993b). Since the CD2v is deleted, the extracellular ASFV particles are not bound to the RBC and therefore a

higher level of genome copies was detected in plasma fraction. In contrast, the control pigs which were challenged with Benin97/1, the highest level of genome copies were detected in RBC fraction.

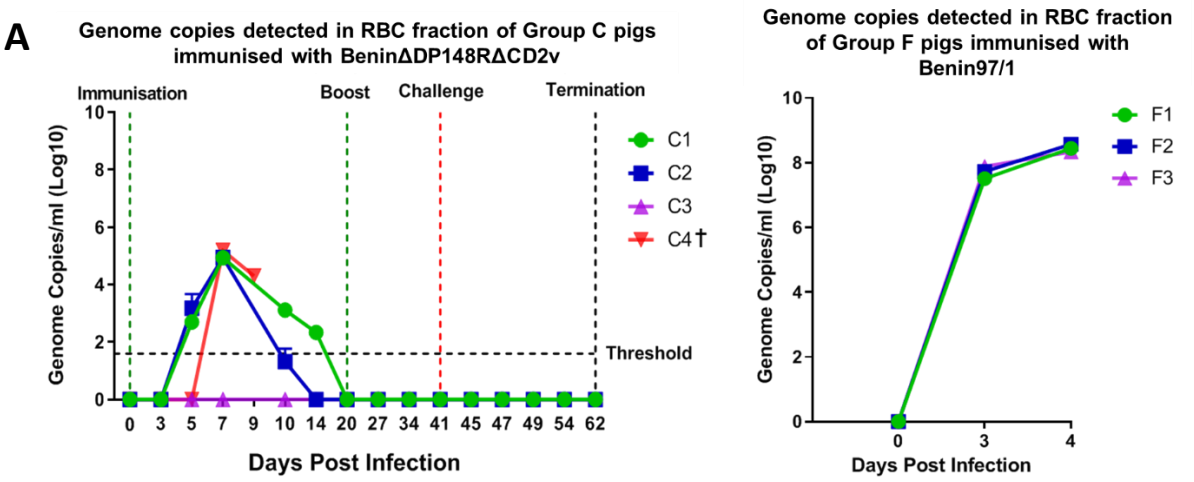

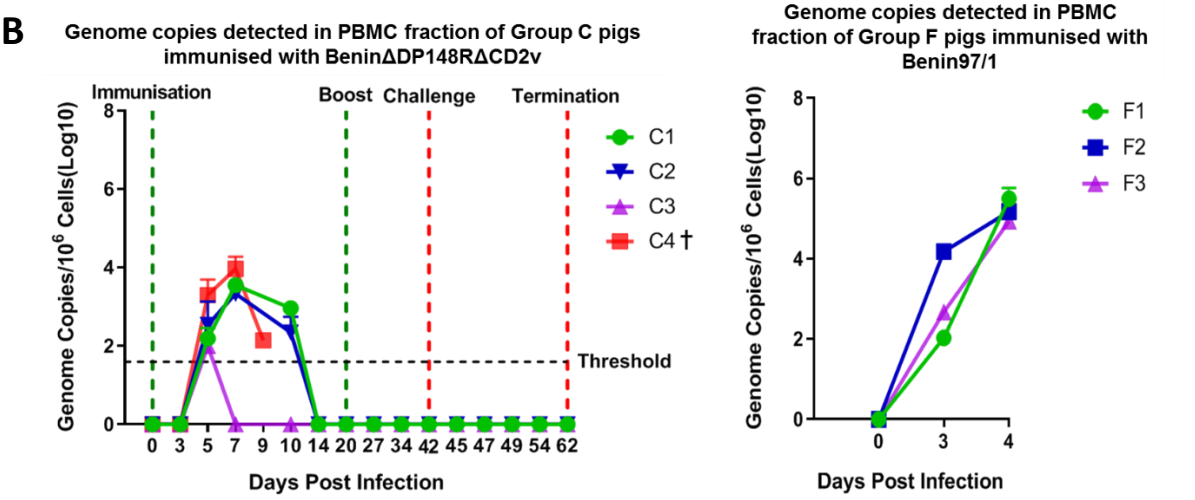

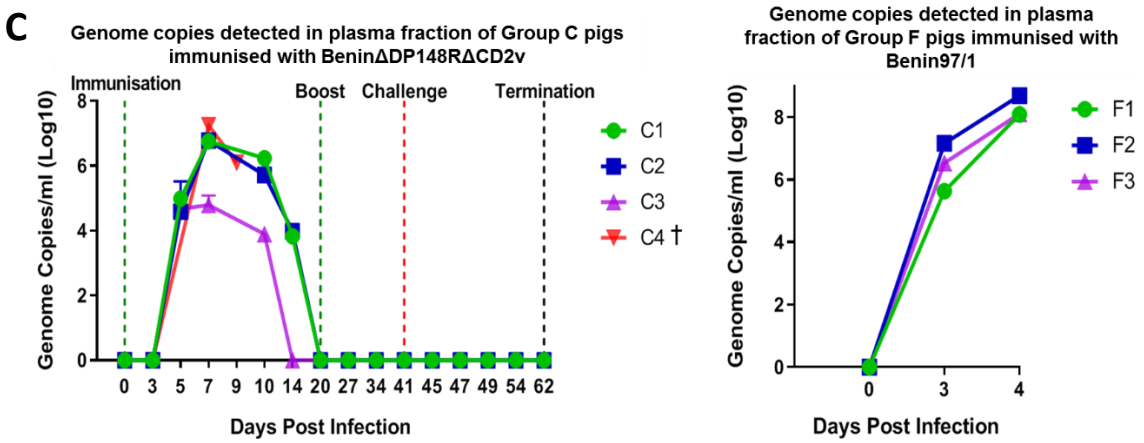

Figure 4.5 Genome copy numbers in different blood fractions (Group C):

A, B, C virus genome copies detected in plasma, erythrocytes, and PBMC of pigs immunized with BeninΔDP148RΔCD2v (Group C) and challenge with virulent Benin 97/1. The green dotted line shows primary immunization and boost, the red dotted line shows challenge and termination. Each coloured line represents individual pig and the euthanized pig is represented by (†) symbol.

4.7 Detection of antibody responses by ELISA in pigs immunised with BeninΔDP148RΔCD2v (Group C) in experiment 1:

The antibody levels against ASFV p72 capsid protein were determined by using a commercial blocking ELISA kit. The ELISA was performed by Dr. Ana Reis (The Pirbright Institute), the antibody response was detected in pigs immunized with BeninΔDP148RΔCD2v (Group C) at 10 days post-immunization except from pig C3. The antibody response was detected in all remaining pigs after the boost, however, in pig C1 the antibody level dropped after boost for a short period. All pigs showed a high antibody response by day 35 and the level remained constant until termination of the experiment (See figure 4.6).

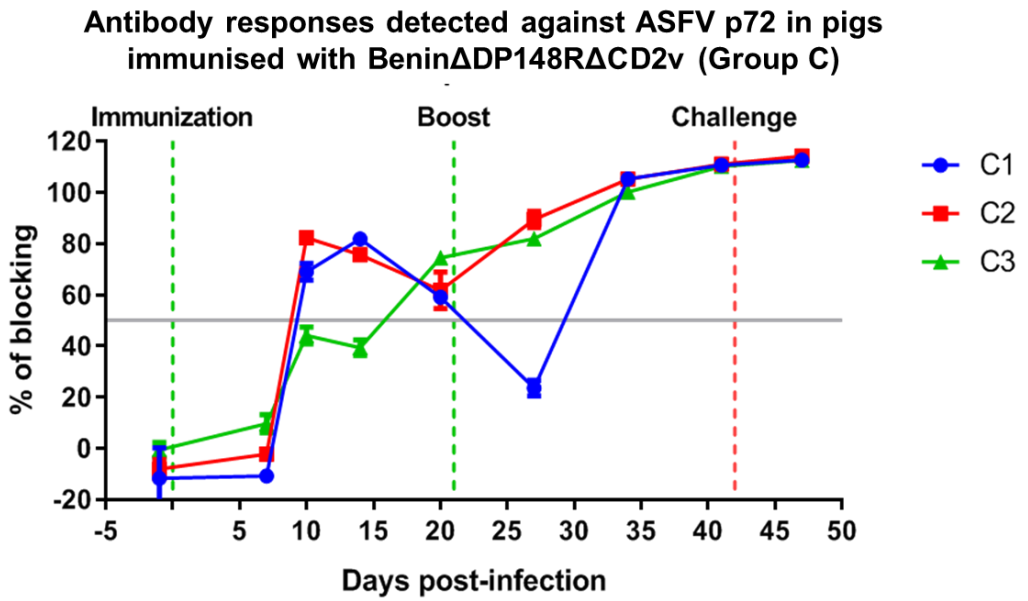

Figure 4.6: Antibody responses in Group C (BeninΔDP148RΔCD2v) pigs against ASFV P72 (Experiment 1): The antibody levels in serum from immunized pigs from experiments 1 were measured using a commercial blocking ELISA and shown as the percentage of blocking with sera from immunised pigs. Each coloured line represents individual pig and the vertical dotted green line shows immunization and boost. The red dotted line shows challenge and the horizontal grey line shows 50 percent blocking. The days are shown as days post-infection and corresponds to the primary immunization.

4.8 Detection of IFN responses by ELIspot in pigs immunised with BeninΔDP148RΔCD2v (Group C) in experiment 1:

ASFV specific T cells responses from immunized pigs were measured by an IFN-γ ELIspot assay, this was performed by Dr. Ana Reis and Dr. Anusyah Rathakrishnan (The Pirbright Institute). The PBMC were isolated from blood at different time points post-immunization and the number of IFN-γ secreting cells was measured by using mouse anti-swine IFNγ capture antibody and biotinylated mouse anti-swine IFNγ

detection antibody. The cells were stimulated with ASFV either Benin or Georgia (10^5 infectious units per well) and with phytohaemagglutinin (PHA) as control. High numbers of IFNγ producing cells were detected in pigs from Group C (1200-1600 spots/10^6 cells) before boost following stimulation with Benin 97/1. The numbers gradually declined after boost until challenge and the number of spots detected was between 550-1250 spots/10^6 cells (see figure 4.7). Since all pigs survived the challenge, this suggests that IFN-γ secreting cells are possibly involved in inducing protection against ASFV in pigs infected with Benin97/1.

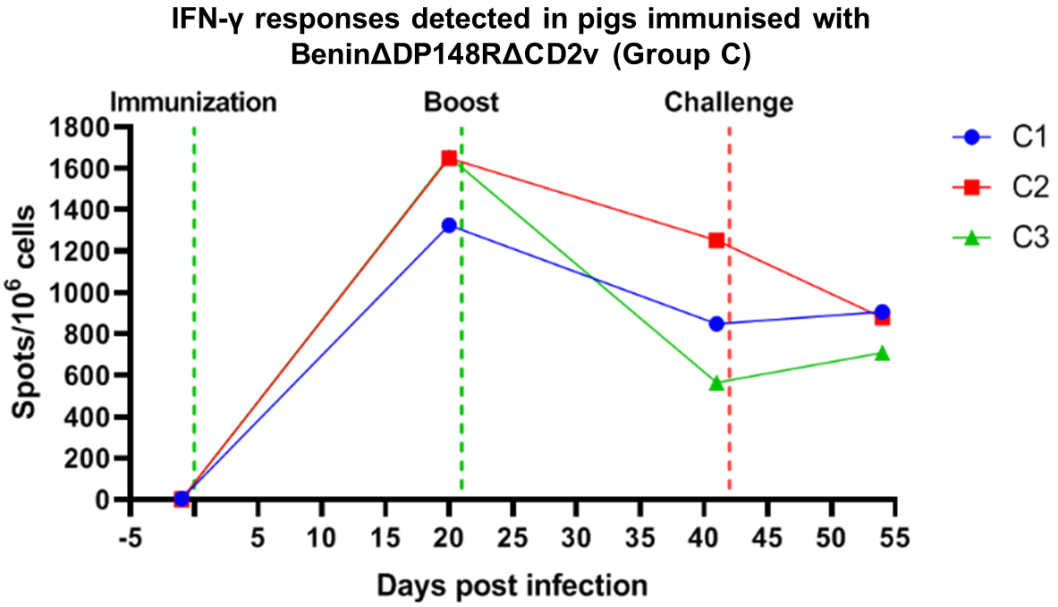

Figure 4.7: IFN-γ responses in Group C pigs: (experiment 1): The number of IFN-γ secreting cells were measured by ELIspot assays and were presented as spots per 10^6 cells. Each coloured symbol indicates individual pigs and the euthanized pigs are represented by (†) symbol. The vertical dotted green line shows immunization and boost and the red line shows challenge, the days are shown as days post-infection and correspond to the primary immunization.

PART-2 (EXPERIMENT-2)

4.9 Design of animal immunisation and challenge experiment with attenuated BeninΔDP148RΔEP153RΔCD2v, and BeninΔDP148RΔEP153R-CD2vE99R Virus (experiment 2):

In this experiment, two groups of pigs (8 pigs in Group A and 6 pigs in Group B) were immunized by the IM route with 1ml of recombinant BeninΔDP148RΔEP153RΔCD2v (Group A) and BeninΔDP148RΔEP153R-CD2vE99R (Group B) at 10^4 $TCID_{50}$. The pigs in both groups were boosted on day 21 with the same viruses by the IM route at 10^4 $TCID_{50}$, the pigs in Group A were boosted again on day 28 post-immunization with the same virus and route at 10^6 $TCID_{50}$. This was because analysis of immune response indicated this group of pigs had a low antibody and cellular response to ASFV. Naïve control pigs (Group E) and immunized pigs in both groups were challenged on day 45 post-immunization by the IM route with 1ml of virulent Benin 97/1 at 10^3 HAD_{50}. Pigs reaching the moderate severity humane endpoint were euthanized by an overdose of barbiturates, the experiment was terminated on day 65 post-immunization, and post-mortems were performed for evaluation of pathological signs (see figure 4.8).

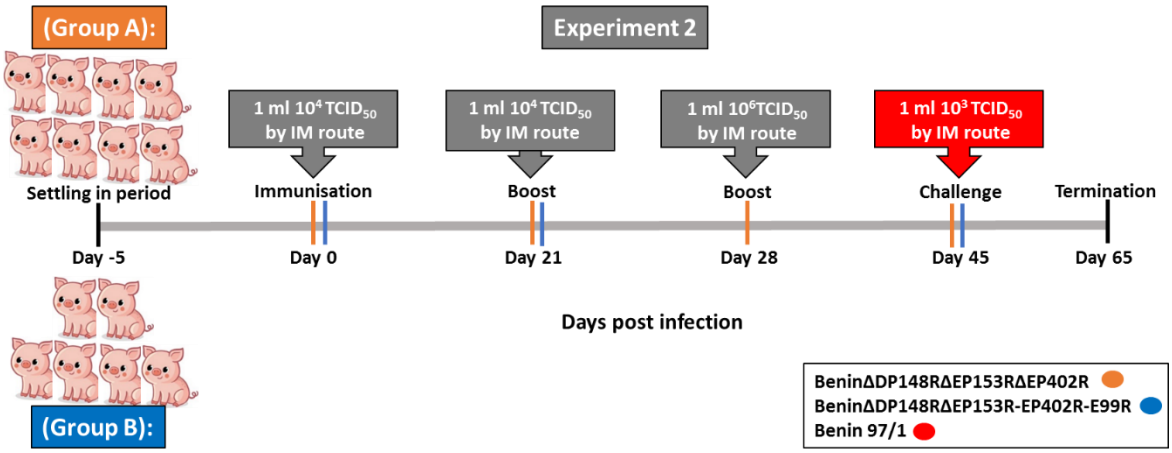

Figure 4.8; Chronological representation of animal experiments 2; The recombinant viruses used for primary immunization and boost are shown in green, the virus used for the challenge is shown in red. The days are shown as day post-infection, referring to the first inoculation of the virus, the route of infection and dosage used are shown for each event (immunization, boost, and challenge).

4.10 Clinical signs post-immunization and challenge (experiment 2):

The pigs in this experiment were monitored daily throughout the study by the animal isolation staff (The Pirbright Institute). Rectal temperatures along with other clinical signs were recorded in the clinical score sheet for ASFV. Animals reaching the moderate severity endpoint defined in the relevant home Office License were euthanized.

The pigs in Group A (BeninΔDP148RΔEP153ΔCD2v) did not develop fever or any other clinical signs before the challenge. In contrast, 3 pigs in Group B (BeninΔDP148RΔEP153-CD2vE99R) developed fever on day 5 post-immunisation. Pig B1 and B2 had a fever of 41.1°C for 1 day while pig B4 had a fever of 40.9 for 1 day, no other clinical signs were observed in Group A and B pigs' post-immunization. However, all pigs in both groups developed fever above 41°C with mild clinical signs on day 4 post-challenge, except pig B2, which did not show fever or any other clinical signs (see figure 4.9A and 4.9B). The clinical signs of pig A3, A4 (in group A), and B4 in group B reached the moderate severity humane endpoint and these pigs were euthanized on day 5 post-challenge. Naïve control pigs (Group E) developed high fever and clinical signs of ASF post-challenge and were euthanized on day 6 (see figure 4.9A and 4.9B). The remaining pigs in both groups survived the challenge with ASFV Benin 97/1 virulent strain**.** No fever or clinical signs were observed in the remaining pigs in

group A (A1, A2, A5, A6, A7 and A8) from day 6 post-challenge, and in group B (B1, B2, B3, B5, B6) from day 5 post-challenge (See figure 4.9C).

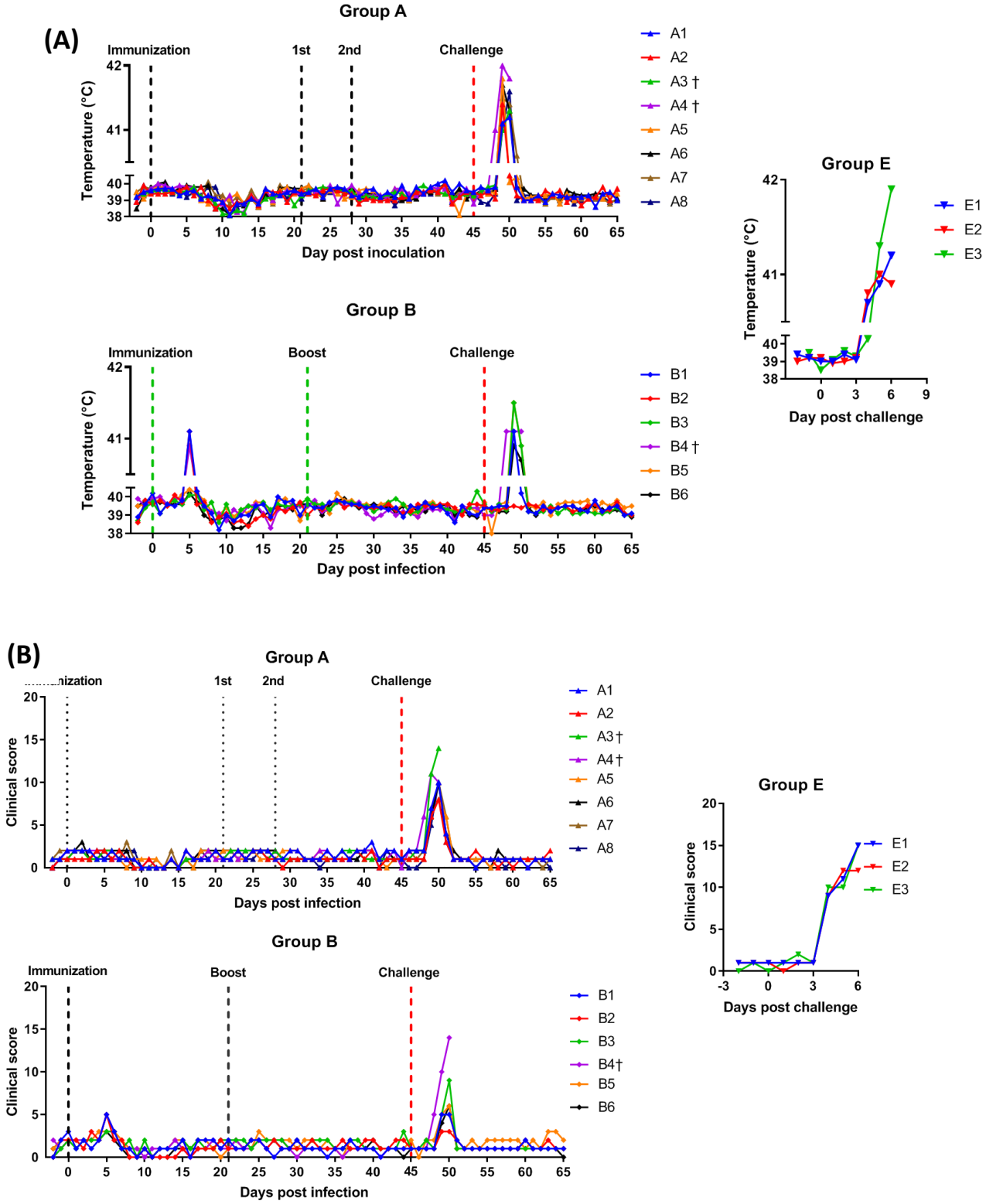

(C)

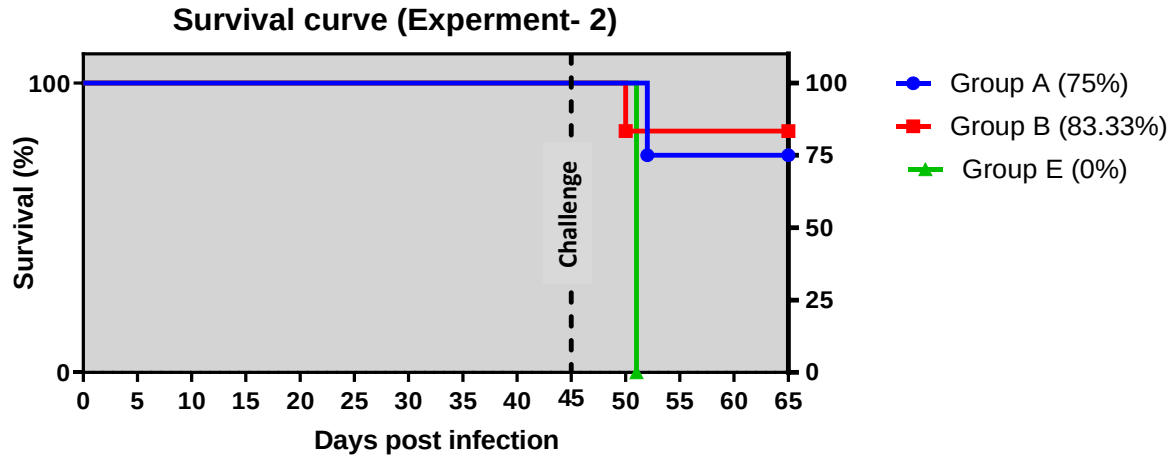

Figure 4.9: Rectal temperatures, clinical signs, and survival of pigs (Experiment 2): (A) Rectal temperatures of pigs; daily temperature record of pigs immunized with either BeninΔDP148RΔEP153RΔCD2v (Group A) or BeninΔDP148RΔEP153R-CD2vE99R (Group B) and challenged with Benin 97/1. The days are shown as post-infection referring to primary inoculation of pigs, and days post-challenge for control non-immunized pigs (Group E). The temperatures are shown in degree Celsius with a threshold of 40.5 C for scoring towards the humane endpoint, the euthanized pigs are represented by (†) symbol. The dotted lines show the event and the coloured line represents the individual pig in each group. **(B) Clinical scores of pigs:** The daily observation and clinical scoring of pigs infected with either BeninΔDP148RΔEP153RΔCD2v (Group A) or BeninΔDP148RΔEP153RCD2vE99R (Group B) and challenged with Benin 97/1. The days are given as days post-infection referring to the primary inoculation of pigs and days post-challenge for non-immunized control pigs (Group E). The dotted line shows day of inoculations and the coloured lines represents individual pigs. **(C) Survival curve of pigs:** The survival percentage of pigs immunized with either BeninΔDP148RΔEP153RΔCD2v (blue line) or BeninΔDP148RΔEP153RCD2vE99R (red line) and challenged with Benin 97/1. The

days are given as days post-infection referring to primary inoculation, the naïve pigs (Group E) are represented by a green line. The dotted line shows the day pigs were inoculated with Benin 97/ 1.

4.11 Pathological and macroscopic evaluation at Necropsies (experiment 2):

The pathological observation and macroscopic scoring of all pigs (Group A, B and E) in experiment 2 were performed at post-mortem according to the score sheets for ASFV (see appendix 2). The post-mortems and pathological evaluations were carried out by Dr. Linda Dixon, Dr. Ana Reis, Dr. Anusyah Rathakrishnan (The Pirbright Institute), and Dr. Pedro Sanchez-Cordon (Animal and Plant Health Agency). The pathological observation of pigs in Group A displayed higher macroscopic lesions than in the pigs in Group C from the previous experiment. Two pigs (A3, A4) displayed high macroscopic lesions and were euthanized at day 5 post-challenge, pig A1, A7 and A8 had enlarged submandibular lymph node (LN), pig A7 displayed splenomegaly and pig A8 had enlarged Renal LN. No pathological signs were observed in the remaining pigs (see figure 4.10). In Group B, pigs showed reduced pathological signs compared to Group A with submandibular lymph node mildly affected. No other macroscopic lesion or ASF related signs were observed in any pig except pig B5 which had ascites and hydropericardium (See figure 4.10). This analysis did not include pig B4 which was euthanized at day 5 post-immunization. Naïve control pigs (Group E) developed high macroscopic lesions related to acute ASF, with various enlarged lymph nodes, hydropericardium, lack of lung collapse, edema (foam in the trachea), and ascites. Pig E1 also displayed congestion and hyperaemic mucosa (small intestine). The pathological scores of control pigs in group E was higher than the naïve control pigs in Group F (experiment 1), this is due to the pigs been euthanized at different time points post infection. The naïve control pigs in group E were euthanized on day 6 while the

control pig in group F were euthanized on day 4. Moreover, the pigs in group E were challenged by the IM route at 10^3 $TCID_{50}$ while the control pigs in group F were challenged by the IM route at 10^4 $TCID_{50}$.

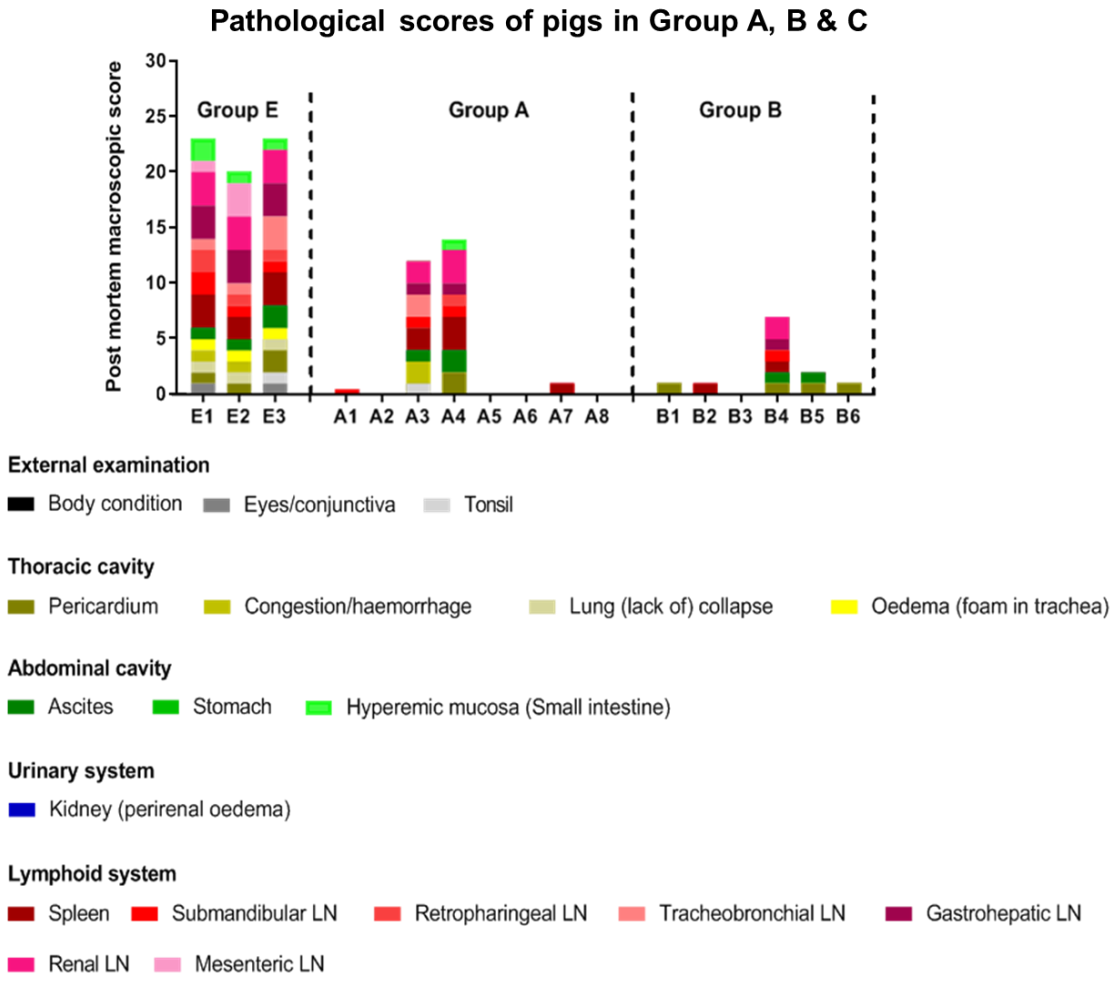

Figure 4.10: Pathological scores of pig in experiment 2: The figure shows pathological scores of individual pigs at post-mortems in experiment 2. The scores are represented by a coloured bar and correspond either to an organ, tissue, or lesions. The dotted line separates the groups.

4.12 Virus genome detected in blood from pigs immunised with BeninΔDP148RΔEP153RΔCD2v (Group A) or BeninΔDP148RΔEP153RCD2vE99R (Group B) Experiment 2.

4.12.1 BeninΔDP148RΔEP153RΔCD2v (Group A):

In the second experiment, an additional gene, EP153R, was deleted from the genome of BeninΔDP148RΔCD2v (tested in a previous animal experiment, described above). The *in vitro* experiments showed that EP153R augments the HAD of mutant CD2vE99R (described in chapter 3). A recombinant virus BeninΔDP148RΔEP153RΔCD2v was constructed and was tested in immunization and challenge experiments in pigs (Group A). Blood samples were collected at different times post-immunization and challenge and a qPCR was performed to detect viral genome load in blood. No virus genome was detected before the challenge; however, genome copies were detected at day 3 post-challenge. A peak of the viral genome copies was observed on day 7 post-challenge in all pigs and the virus genome detected was between 10^2 to 10^6 genome copies per ml with the lowest in pig A5. In pigs A3 and A4 high levels of genome copies (approximately 10^6 genome copies per ml) were observed which coincided with clinical signs, these pigs were euthanized after reaching the moderate severity humane endpoint at day 7 post-challenge. In pigs A1, A2, A6 and A7 the level of virus genome copies varied and was detected between 10^2 to $10^{5.5}$ copies per ml of blood. The genome copy number gradually declined after the viremia peak until the end of the experiment and was undetectable in 2 pigs (A5, A8) at day 17 post-challenge. In the remaining pigs, the virus genome levels dropped to $10^{1.9}$ to $10^{2.6}$ genome copies per ml by day 17 post-challenge except for pig A7 in which levels remained at $10^{4.5}$ genome copies per ml until the end of the experiment (see figure 4.11). These results provide evidence that the deletion of EP153R along with EP402R further

attenuated the virus the parental virus BeninΔDP148R, since no virus genome or clinical signs were detected before the challenge. The further attenuation of BeninΔDP148R dramatically reduced the level of protection in pigs as the protection was dropped from 100% (observed with BeninΔDP148R), (Reis et al., 2017) to 75%. In the previous experiment (described above) where pigs were infected with BeninΔDP148RΔCD2v the virus persisted in blood for 11 days, however, pigs infected with BeninΔDP148RΔEP153RΔCD2v showed no viremia and hence no virus persistence, suggesting a possible role of EP153R in development and persistence of viremia. This supports the *in vitro* results from chapter 3 where it was observed that EP153R enhances the HAD phenotype of the non-HAD CD2v mutant E99R suggesting that EP153R and CD2v act co-operatively.

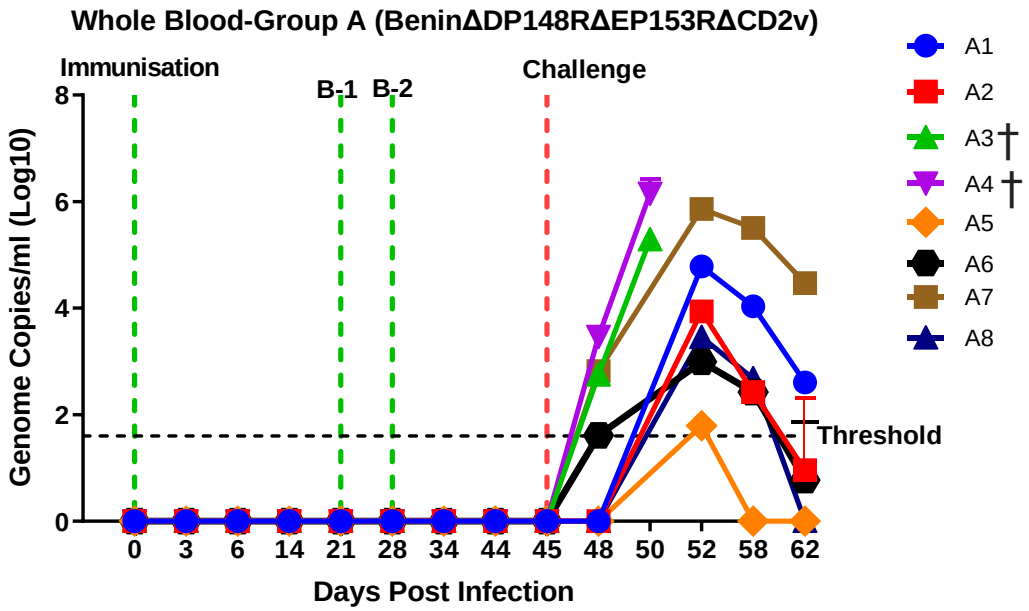

Figure: 4.11: Genome copy numbers in blood (Group A): Virus genome copies detected in the blood of pigs immunized with BeninΔDP148RΔEP153RΔCD2v (Group A) and challenged with virulent Benin 97/1. The green dotted line shows the day of primary immunization and boost (B1 and B2 refer to 1st and 2nd boost), the red dotted

line shows the challenge day. Each coloured line represents individual pigs and the euthanized pigs are represented by (†) symbol.

4.12.2 BeninΔDP148RΔEP153RCD2vE99R (Group B):

To determine the effect of CD2vE99R mutant (non-HAD) in pigs, another recombinant virus was constructed with EP153R deleted and the wild type CD2v replaced with CD2vE99R from the genome of already attenuated BeninΔDP148R. The recombinant virus (BeninΔDP148RΔEP153R-CD2vE99R) was generated (described in chapter 3) and tested in immunization and challenge experiments in six pigs (Experiment 2, Group B). The blood samples were collected at different time points post-immunization until termination of the experiment and the levels of virus genome copies were detected by qPCR. Low level of virus genome were detected in 3 pigs (B1, B5, and B6) at day 6 post-immunization, the virus genome was detected at 10^2 to$10^{3.8}$ copies/ml in these pigs and this declined by day 7 or 8 and was not detectable by day 14 post-immunization. No virus genome was detected in the remaining pigs before the challenge. However, moderate levels of virus genome were detected in the blood of pigs B1, B3, B5, B6, after challenge which gradually declined by termination. In pig B2 no genome copies were detected. In pig B4 at day 5 post-challenge a high level of virus genome was detected at $10^{7.3}$ copies per ml and the pig was euthanized as it reached the moderate severity humane endpoint. In the other pigs, the peak of viremia was detected at day 7 post-challenge and the virus genome detected varied between the pigs from $10^{5.7}$ to $10^{3.8}$ copies per ml. The genome copies declined significantly in three pigs (B1, B3, B6) by day 20 post-challenge and the virus genome detected varied between 10^3 to $10^{2.3}$ copies per ml. In pig B5, the genome copies declined gradually compared to other pigs and the virus genome was detected at $10^{4.8}$ copies per ml by termination (see figure 4.11).

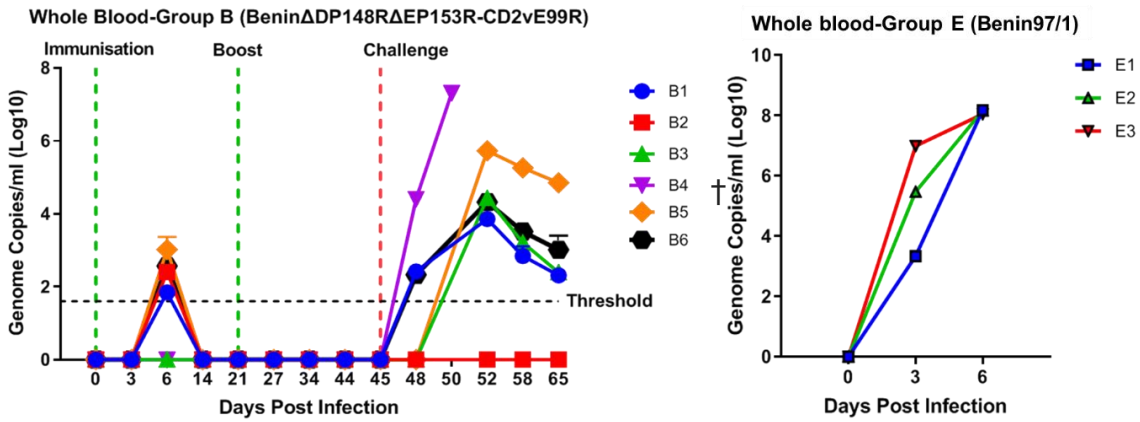

Figure: 4.11: Genome copy numbers in blood (Group B): Virus genome copies per ml detected in the blood of pigs immunized with BeninΔDP148RΔEP153R-CD2vE99R (Group B) and challenged with virulent Benin 97/1. Naïve control pigs (Group E) were challenged with Benin97/1. The green dotted line shows the day of primary immunization and boost, the red dotted line shows challenge and termination. Each coloured line represents an individual pig, the euthanized pig is represented by (†) symbol and the genome copies are shown as log10 copies per ml.

These results provide evidence that CD2v is involved in enhancing virus persistence for an extended period and has a role in induction of early viremia in pigs. Hence, the deletion of this gene from the attenuated BeninΔDP148R genome significantly reduced virus persistence and caused a delay in viremia which coincided with the clinical signs. While replacing the CD2v with a non-HAD mutant (E99R) and deleting the EP153R further reduce virus genome persistence in blood and delay the induction of viremia.

4.13 Detection of infectious virus in pigs immunised with BeninΔDP148RΔEP153R-CD2vE99R (Group B) recombinant virus:

Titration was performed on Group B (BeninΔDP148RΔEP153R-CD2vE99R) samples to detect the infectious virus at different time points in blood (see Figure 4.12). The

infectious virus after immunization was calculated based on the expression of mNeon marker gene by the recombinant virus and after challenge calculated as HAD_{50}/ml.

The blood collected at different times post-immunisation was inoculated on PBMs, the cells were incubated at 37°C for 72 hours to allow the virus in the blood to infect a higher proportion of PBMs. The levels of infectious virus after immunisation and challenge was calculated. No infectious virus was detected before the challenge in any of the pigs, however, varied amount of infectious virus was detected in pigs after challenge. The highest amount of virus was detected in pig B4 (10^7 HAD_{50}/ml) which was euthanized at day 5 post-challenge. In pig B5 a moderate amount of infectious virus was detected (10^5 HAD_{50}/ml) which gradually declined by termination at which time it was detected at $10^{2.5}$ HAD_{50}/ml. These pigs B4 and B5 had the lowest numbers of ASFV stimulated IFNγ producing cells and antibody responses (see figure 4.15). In the remaining pigs, infectious virus was detected at day 7 post-challenge ($10^{2.5}$ to 10^4 HAD_{50}/ml) which gradually declined, and no virus was detected by termination (see figure 4.12). This suggest that the level of infectious virus clear rapidly compared to the number of genome copies.

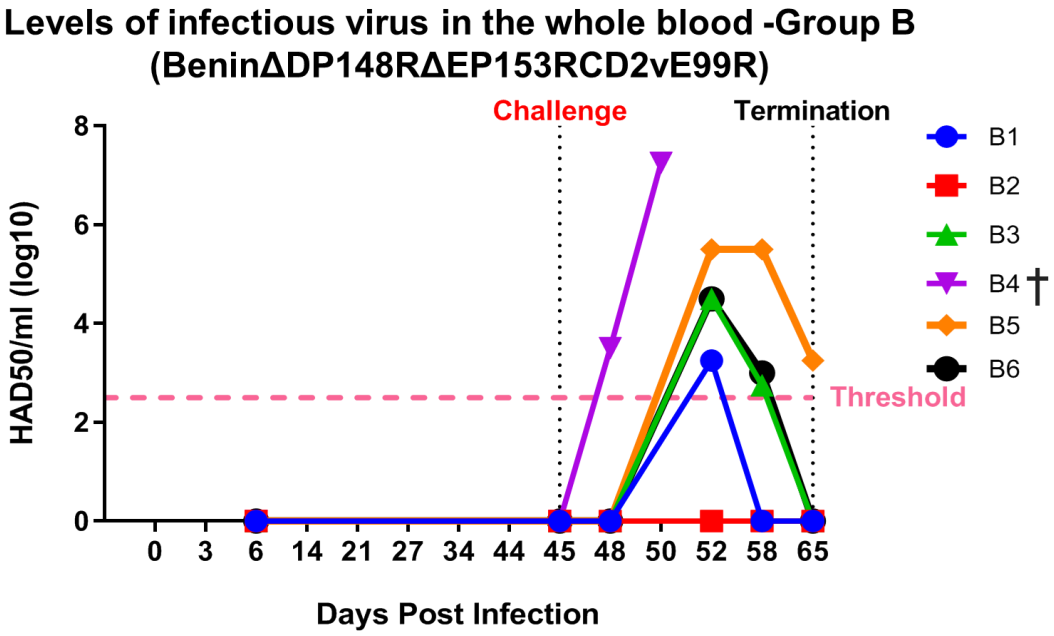

Figure 4.12: Levels of infectious virus in the blood (Group B): Infectious virus in blood were detected by titration and was calculated as log10 of HAD_{50}/ml. The days are shown as days post-infection and refer to the primary immunization, each coloured line represents an individual pig. The vertical dotted line shows the challenge with ASFV virulent isolate Benin 97/1 and termination of the experiment while the horizontal dotted line shows the threshold of the method used. The euthanized pig is represented by (†) symbol.

4.14 Detection of genome copies in different blood fractions by qPCR in pigs immunised with BeninΔDP148RΔEP153RΔCD2v (Group A) or BeninΔDP148RΔEP153R-CD2vE99R (Group B) (experiment- 2):

To investigate the distribution of virus in blood fractions, the blood samples were collected at different times post-immunisation from pigs infected with Benin 97/1 (Group E) BeninΔDP148RΔEP153RΔCD2v (Group A) and BeninΔDP148R-ΔEP153RCD2vE99R (Group B). The blood samples were fractioned into plasma,

erythrocytes, and PBMC by performing density gradients using Histopaque®-1077 (see section 5.4.1 & 5.4.2 for details). A qPCR was performed to measure viral genome load in fractioned blood by extracting genomic DNA. No genome copies were detected in the blood fractions from Group A (BeninΔDP148RΔEP153RΔCD2v) pigs (data not shown).

In Group B (BeninΔDP148RΔEP153R-CD2vE99R) genome copies in pigs were detected at a lower level compared to pigs the in-Group C (BeninΔDP148RΔCD2v). Virus genome was detected in only 2 pigs (B5 and B6) at day 6 post-immunisation in all fractions. The amount of virus genome detected in the RBC, plasma and PBMC fraction of pig B5 and B6 ranged between 10^2-10^3 genome copies/ml (for PBMC fraction genome copies/10^6 cells). The remaining pigs in Group B did not had any detectable viral genome copies in any of the blood fractions (see figure 4.13A, 4.13B, 4.13C). Previous studies has reported that ASFV genome can persist in PBMC for up to 500 days and the data from Experiment 1 (Group C- BeninΔDP148RΔCD2v) showed that the virus genome copies in PBMC fraction coincided with genome copies. However, deletion of EP153R (Group A and B) has shown a reduction in virus genome copies in PBMC fraction and suggesting a possible role of EP153R in virus genome persistence in PBMC fraction.

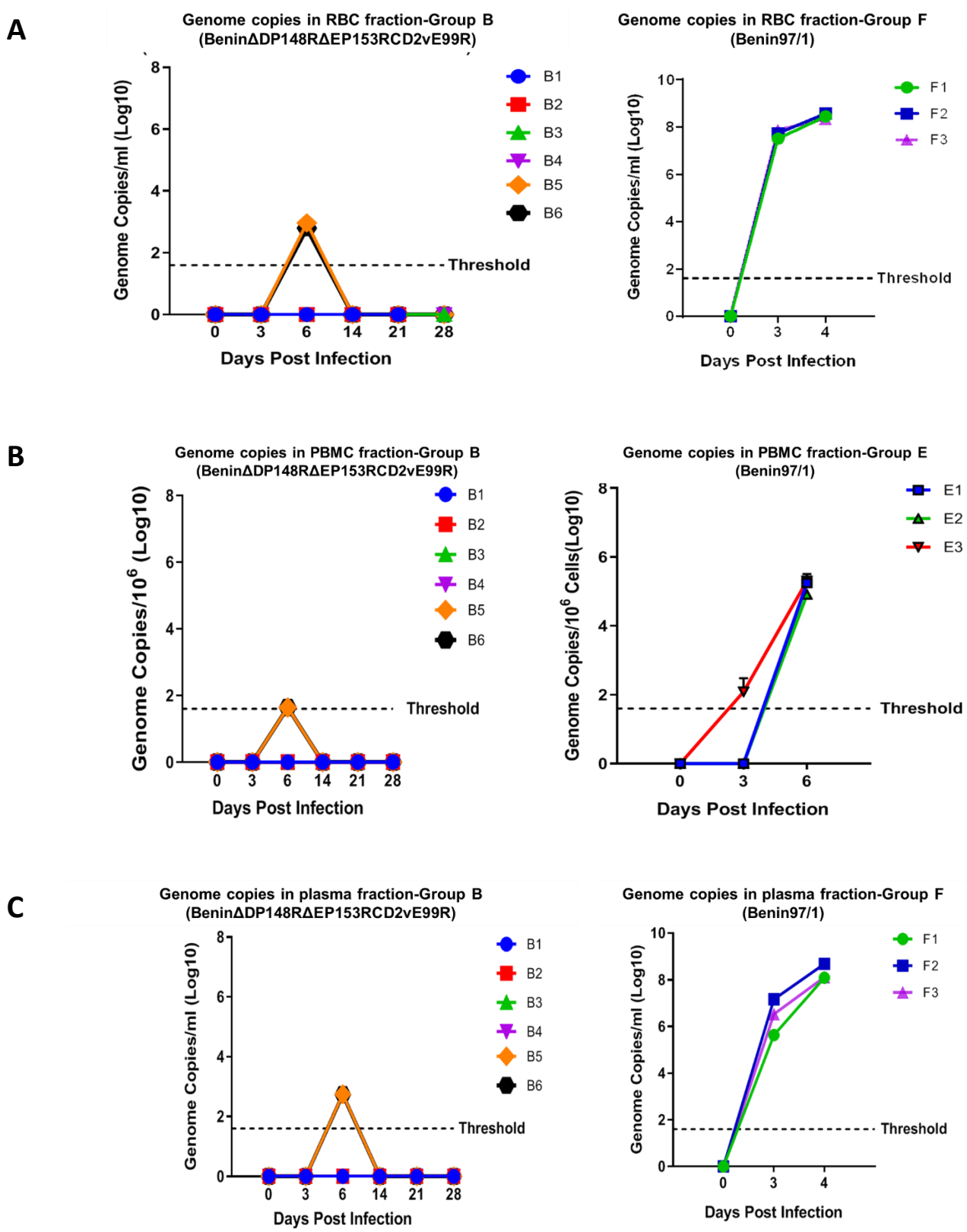

Figure 4.13: Genome copies number in different blood fraction (Group B): (A, B, C) virus genome copies detected in plasma, erythrocytes, and PBMC of pigs

immunized with BeninΔDP148RΔEP153R-CD2vE99R and in control pigs challenged with virulent Benin 97/1.

In the second experiment, a low level of virus genome was detected in the whole blood, plasma, erythrocytes, and PBMC from pigs in Group B (BeninΔDP148RΔEP153R-CD2vE99R) at day 6 post-immunization (viremia peak). The highest level of virus genome was present in the whole blood and plasma fraction while a low level of virus genome was detected in PBMC and RBC fraction. In contrast, naïve control pigs infected with the Benin97/1 virulent isolate had the highest levels of virus associated with RBC. No virus genome was detected before the challenge in all pigs from Group A (BeninΔDP148RΔEP153RΔCD2v) (see figure 4.13).

4.15 Detection of antibody responses by ELISA in pigs immunised with BeninΔDP148RΔEP153RΔCD2v (Group A) or BeninΔDP148RΔEP153RCD2vE99R (Group B) in experiment 2.

The antibody levels against ASFV p72 capsid protein were determined by using a commercial blocking ELISA kit. In the second experiment, I performed an ELISA with Dr. Vlad Petrovan (The Pirbright Institute) to determine the antibody levels against ASFV p72 in Group A and B. Pigs in Group B showed similar antibody responses to the pigs immunised with BeninΔDP148RΔCD2v (Group C) in experiment 1, high levels of antibodies were detected in all pigs at 14 days post-immunization except pig B1 and B3. The levels were increased in all pigs at 21 days post-immunization and remained high, similar levels of antibodies were detected in all pigs before challenge (see figure 4.14B). In contrast, very low levels of antibodies were detected in Group A pigs before boost, however, a sudden increase in antibody levels was observed in Group A pigs after the first boost. The levels were increased in all pigs except A4 before the

second boost, the antibody response was increased after the second boost (day 34) in all pigs and remained at high levels until challenge (see figure 4.14A).

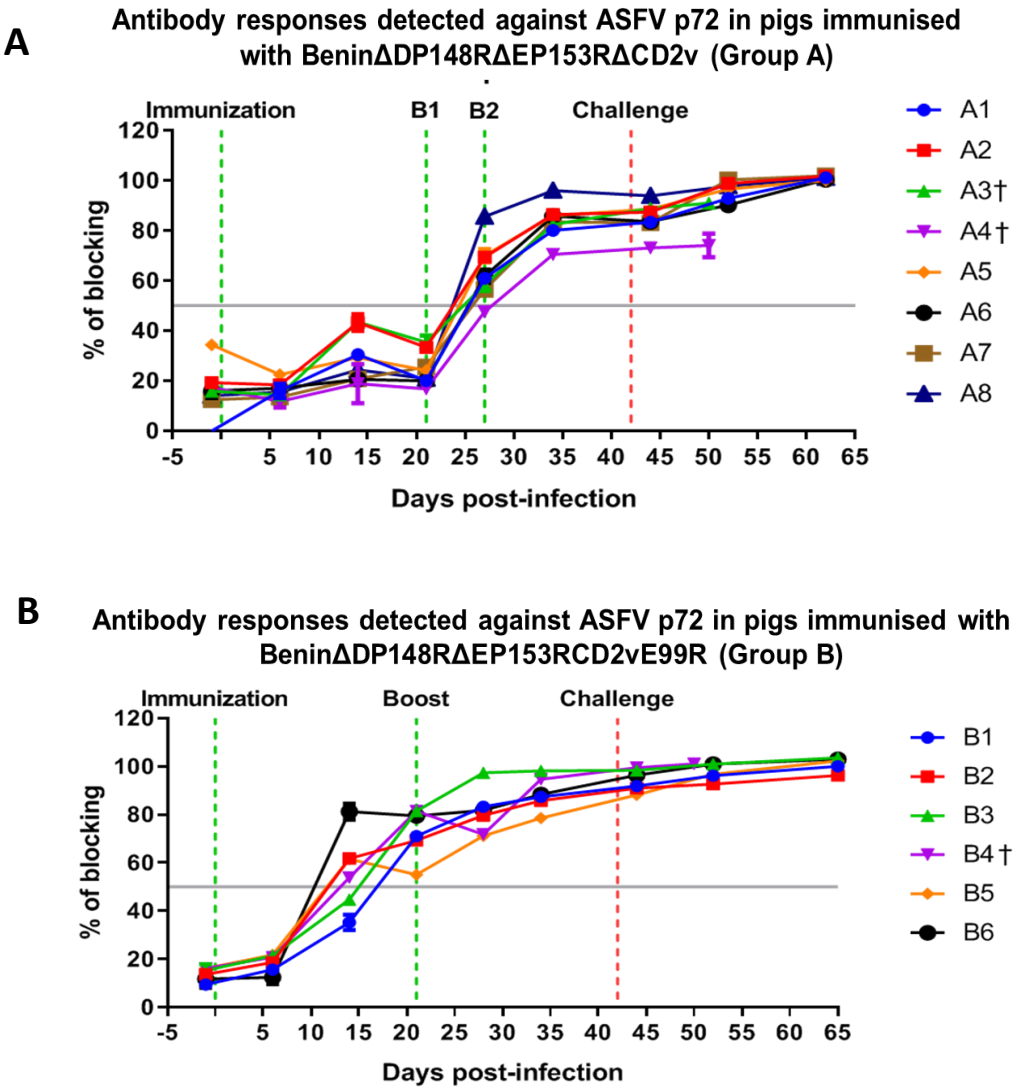

Figure 4.14: Antibody responses in pigs against ASFV P72 (Experiment 2); Group A (BeninΔDP148RΔEP153RΔCD2v), Group B (BeninΔDP148RΔEP153R-CD2vE99R. The antibody levels in serum from immunized pigs from experiments 1 and 2) were measured using a commercial blocking ELISA and shown as the percentage of blocking with sera from immunised pigs. Each coloured line represents indicates individual pigs and the euthanized pigs are represented by (†) symbol. The vertical dotted green line shows immunization and boost and the red line shows challenge, the

horizontal grey line shows 50 percent blocking. The days are shown as days post-infection and corresponds to the primary immunization.

4.16 Detection of IFN responses by ELIspot in pigs immunised with BeninΔDP148RΔEP153RΔCD2v (Group A) or BeninΔDP148RΔEP153RCD2vE99R (Group B) in experiment 2.

ASFV specific T cells responses from immunized pigs were measured by an IFN-γ ELIspot assay, this was performed by Dr. Ana Reis and Dr. Anusyah Rathakrishnan (The Pirbright Institute). The PBMC were isolated from blood at different time points post-immunization and the number of IFN-γ secreting cells was measured by using mouse anti-swine IFNγ capture antibody and biotinylated mouse anti-swine IFNγ detection antibody. The cells were stimulated with ASFV either Benin or Georgia (10^5 infectious units per well) and with phytohaemagglutinin (PHA) as control. Low number of IFN-γ secreting cells were detected in Group A before boost following stimulation with Benin 97/1, the numbers gradually increased after first and second boost until challenge (380-550 spots/10^6 cells)(see figure 4.15). In contrast, high numbers of IFN-γ secreting cells were detected in Group B (200-900 spots/10^6 cells) before boost, the lowest number was detected in pigs B4 and B5. The highest number was detected in pig B2 and B6, the levels were slightly decreased after boost until challenge in all pigs except B2 where a constant increase in IFN-γ secreting cells were observed until challenge. The number of cells before the challenge was slightly lower than the cells detected at boost and the levels were between 120-1150 spots/10^6 cells, the lowest was in pigs B4 and B5 (120-150 spots/10^6 cells). Pig B4 was euthanized at day 5 post-immunization while in pig B5 high levels of virus genome copies and infectious virus were detected after challenge which slowly declined by the termination of the

experiment (see figure 4.15). This suggests that IFN-γ secreting cells are possibly involved in inducing protection against ASFV in pigs.

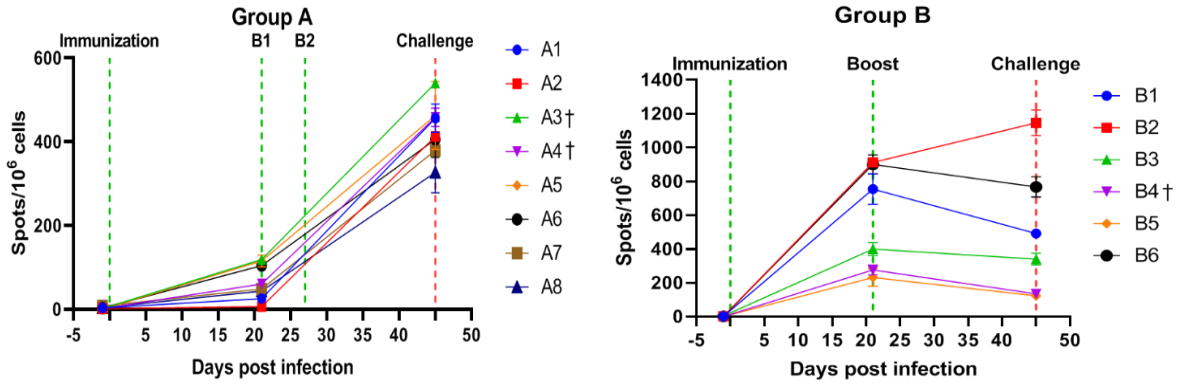

Figure 4.15: IFN-γ responses in pigs (experiment 2): (Groups A & B) The number of IFN-γ secreting cells were measured by ELIspot assays and were presented as spots per 10^6 cells. Each coloured symbol indicates individual pigs and the euthanized pigs are represented by (†) symbol. The vertical dotted green line shows immunization and boost and the red line shows challenge, the days are shown as days post-infection and correspond to the primary immunization.

PART- 3 (COMPARITIVE ANALYSIS)

4.17 Comparative analysis of genome copies numbers in blood from pigs in experiment 1 & 2:

4.17.1 Genome copies number comparison post-immunisation:

To investigate the role of CD2v, EP153R, and CD2vE99R in virus genome persistence in blood, the variation of genome copy number in whole blood from pigs in Group F (Benin97/1) or Group C (BeninΔDP148RΔCD2v) or Group A (BeninΔDP148RΔEP153RΔCD2v) or Group B (BeninΔDP148RΔEP153R-CD2vE99R) was analysed. The mean values of virus genome copies number detected in blood fractions at the viremia peak (post-immunisation) in each Group (A, B, C, and F) were calculated, and the variation was determined by 2-way ANOVA following Tukey's multiple comparison tests. A significant difference was observed in genome copies number in blood from pigs infected with different viral strains (P values = 0.0001 to 0.0190). The number of genome copies detected in blood was significantly different when these groups were compared except from the comparison between; (1) Benin and BeninΔDP148R, (2) BeninΔDP148R and BeninΔDP148RΔCD2v, and (3) BeninΔDP148RΔEP153RΔCD2v and BeninΔDP148-RΔEP153R-CD2vE99R, which was statistically insignificant (see figure 4.16a). In the comparison between BeninΔDP148RΔEP153RΔCD2v (Group A) and BeninΔDP148RΔEP153R-CD2vE99R (Group B), the difference in genome copy number was insignificant (P=0.058), which is slightly above the threshold of P-value for 95% confidence level (see figure 4.16A).

This suggests that the BeninΔDP148RΔEP153RCD2vE99R has a role in induction of viremia levels when compared to infections with BeninΔDP148RΔEP153RΔCD2v

virus (which did not induce viremia in any infected pigs), However, the BeninΔDP148RΔEP153RCD2vE99R elicited a higher antibody and T cell response and hence a better protection was observed compared to BeninΔDP148RΔEP153RΔCD2v. Viremia was detected in 4 out of 6 pigs immunised with BeninΔDP148RΔEP153R-CD2vE99R while no viremia was detected in pigs immunised with BeninΔDP148RΔEP153RΔCD2v (Group A). this also indicated the viremia post-immunisation may coincide with protection in recovered animals.

Genome copies number comparison at viremia peak post-immunisation

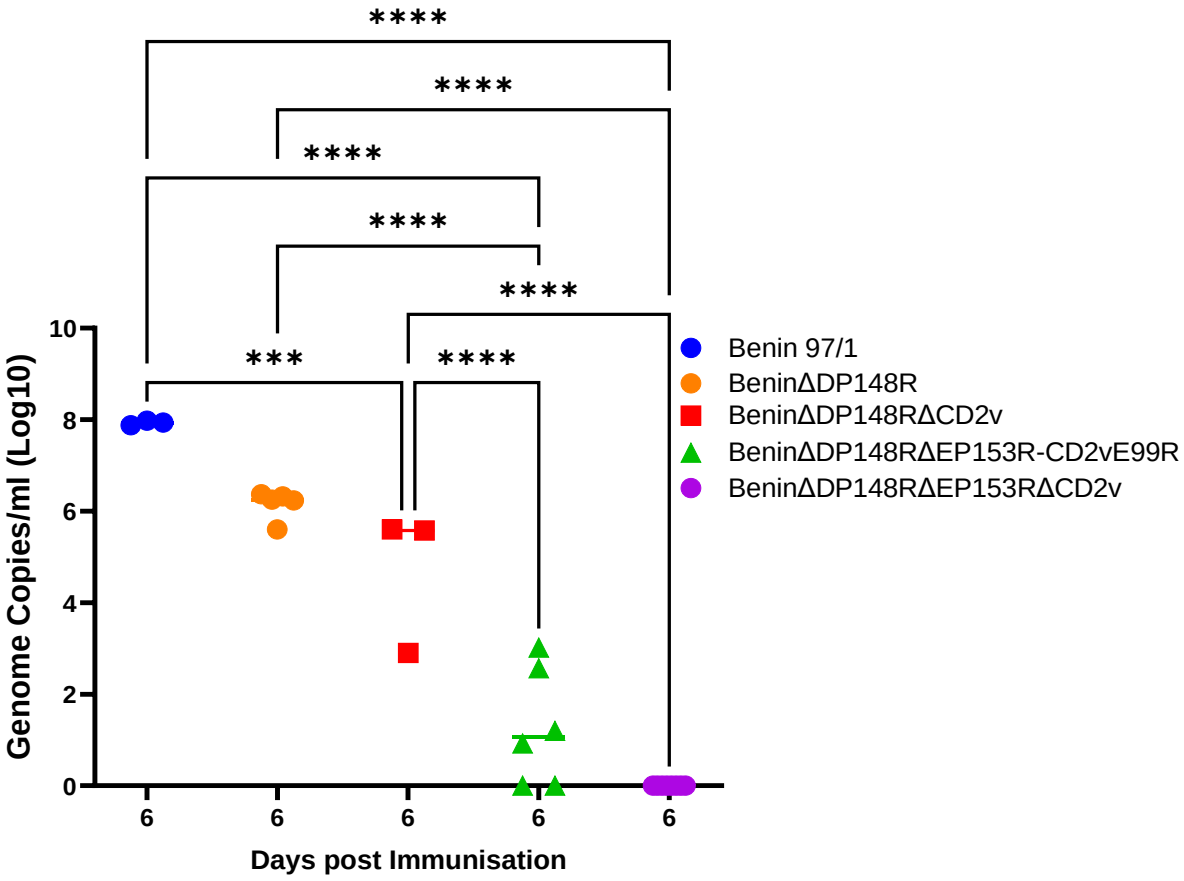

Figure 4.16a: Genome copies comparison Experiment 1 & 2: Virus genome copies pigs from the current and the previous experiment (BeninΔDP148R (Reis et al., 2017) at viremia peak post-immunization were compared to determine the statistical significance of any differences observed between following immunization with the

recombinant viruses. The genome copies are represented as genome copies/ml, days post-infection refers to the primary infection/immunization. The statistical significance is represented by (*) symbols, the p-values less than 0.001 are represented by (***), the p-values less than 0.01 are represented by (**) and the p-values less than 0.05 are represented by (*).

4.17.2 Genome copies number comparison post- challenge:

As the clinical signs are often correlated with viremia, comparison of the genome copies number at viremia peak (post-challenge) in pigs immunised with different viruses can give an indication of the level of protection. The genome copies number in blood at viremia peak (post-challenge) was compared for BeninΔDP148RΔCD2v BeninΔDP148RΔEP153RΔCD2v and BeninΔDP148RΔEP153R-CD2vE99R (Figure 4.16 b). The variation was determined by 1-way ANOVA following multiple comparison of the mean value of each group.

No significant difference was observed in genome copies number in blood at viremia peak post-challenge between BeninΔDP148RΔEP153RΔCD2v and BeninΔDP148RΔEP153R-CD2vE99R. However, a significant difference in genome copies number at viremia peak (post-immunisation) was observed in Group C when compared to Group A and B. No viremia was detected (post challenge) in Group C pigs (see figure 4.16b). This confirmed that BeninΔDP148RΔCD2v induced the strongest protection since no viremia was observed post-challenge. Viremia peaks between pigs surviving after challenge following immunisation with BeninΔDP148RΔEP153RΔCD2v and BeninΔDP148RΔEP153R-CD2vE99R were very similar and no statistically significant difference was detected. However, survival rates in this experiment differed since 4/6 survived after immunisation with

BeninΔDP148RΔEP153RDCD2v and 5/6 after BeninΔDP148RΔEP153R-CD2vE99R immunisation. Further experiments are required to confirm if this difference in survival rates is significant.

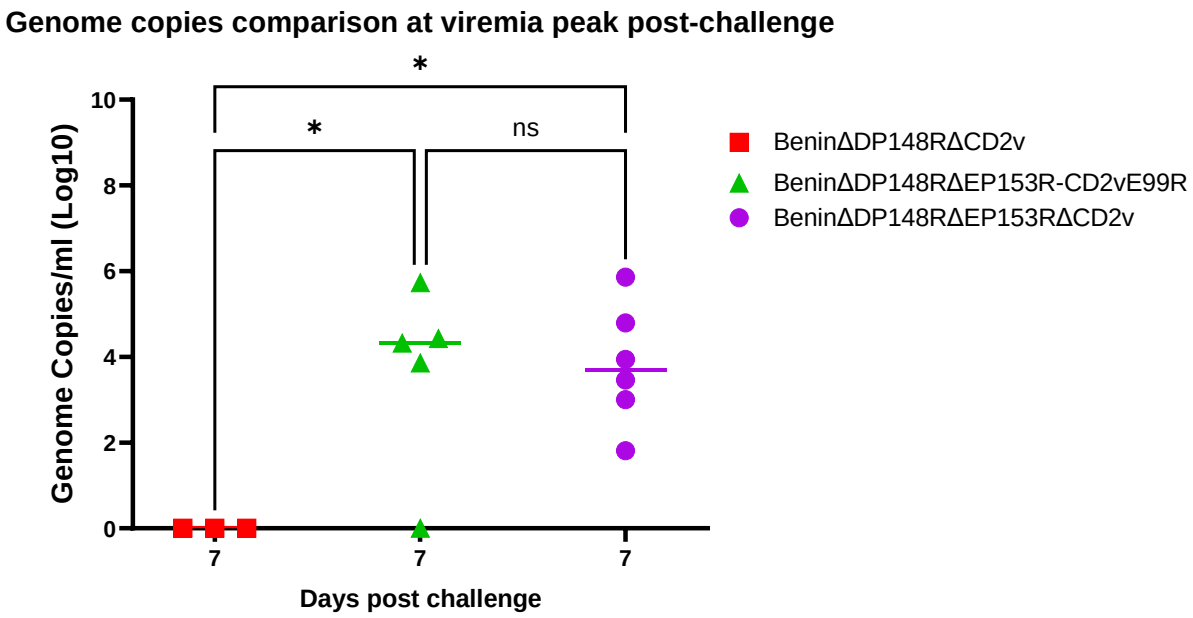

Figure 4.16b: Genome copies comparison Experiment 1 & 2: Virus genome copies of pigs from the current experiment at viremia peak post-challenge was compared to determine the statistical significance of the impact of vaccination with recombinant viruses on virus replication post-challenge. The genome copies are represented as genome copies/ml, days post-challenge at the viremia peak.

4.18 Comparative analysis of recombinant viruses based on genome copy number in different blood fractions:

To investigate the role of CD2v, EP153R, and CD2vE99R in virus distribution in blood, the variation of genome copy number in different blood fractions from pigs in Group F (Benin97/1) or Group C (BeninΔDP148RΔCD2v) or Group A (BeninΔDP148RΔEP153RΔCD2v) or Group B (BeninΔDP148REP153R-CD2vE99R) was analysed. The mean values of virus genome copy number detected in blood

fractions at the viremia peak in each Group (A, B, C, and F) were calculated and the variation was determined by 2-way ANOVA following Tukey's multiple comparison tests. A significant difference was observed in genome copies number in blood fractions from pigs infected with different viral strains (P values = 0.0001 to 0.0190). The number of genome copies detected in blood fractions was significantly different in these groups when compared, except from the comparison between BeninΔDP148RΔEP153R-ΔCD2v and BeninΔDP148RΔEP153R-CD2vE99R which was statistically insignificant.

A significant reduction in the level of genome copies number was detected in Group A (BeninΔDP148RΔEP153RΔCD2v) when compared with Group C (BeninΔDP148RΔCD2v) in all blood fractions. This suggests that either the deletion of EP153R further attenuates the virus by reducing its replication or the EP153R is involved in inducing viremia. The comparison of genome copies in blood fractions from pigs in Group B (BeninΔDP148RΔEP153R-CD2vE99) and Group C (BeninΔDP148RΔCD2v) indicates that the presence of CD2vE99R may induces a lower level of viremia in some pigs. However, when the viremia was compared between the groups immunised with BeninΔDP148RΔEP153R-CD2vE99 (Group B) and BeninΔDP148RΔCD2v (Group C), a significant reduction in viremia was detected (see figure 4.17a and 4.17b).

In Group C (BeninΔDP148RΔCD2v), the highest level of virus genome was detected in the plasma fraction and the lowest level was detected in RBC fraction. In contrast, in control pigs, high levels of virus genome were detected in RBC fraction possibly due to the virus bound to RBC (see figure 4.17a and 4.17b).

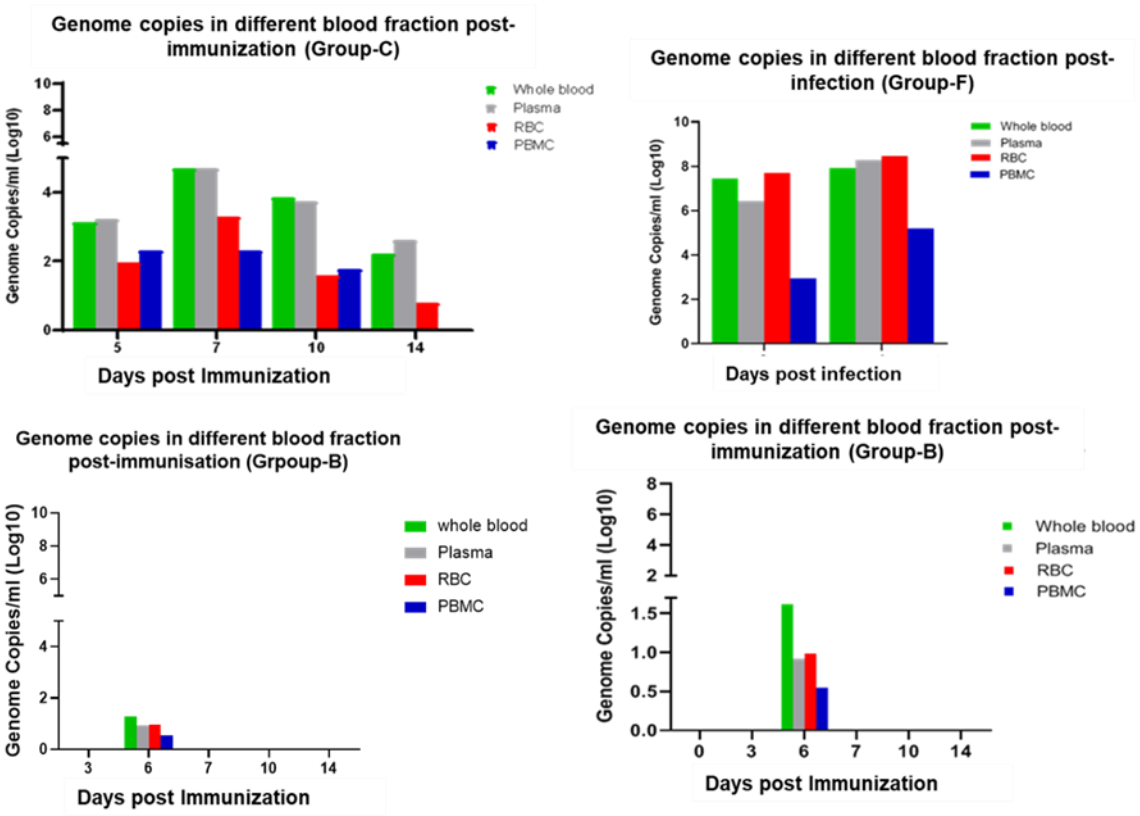

Figure: 4.17a: Genome copy number in blood fractions: Virus genome copies detected in blood fractions of pigs after in infection with either BeninΔDP148RΔCD2v (Group C experiment 1) or BeninΔDP148RΔEP153R-CD2vE99R (Group B experiment 2) and or with virulent Benin 97/1 (Group F). The mean values of virus genome in each fraction from 3 pigs were plotted, each colour represents blood fractions. The values were calculated as genome copies/ml except for PBMC where genome copies were detected as genome copies/10^6 cells.

The deletion of DP148R and CD2v showed a significant reduction in genome copy numbers compared to Benin 97/1, the deletion of both CD2v and EP153R showed a further reduction in viremia compared to BeninΔDP148RΔCD2v. This indicates that both CD2v and EP153R may have a combined effect on induction of viremia. As described in chapter 3, the proteins appear to co-operate to induce HAD which appears linked to levels and persistence of viremia. Finally, the deletion of EP153R and

replacement of WT-CD2v with mutant CD2vE99R balanced the induction of viremia, and no significant difference in virus genome copies was observed in blood fractions however a significant increase in whole blood was detected when compared to immunisation with the triple deletion (BeninΔDP148RΔEP153RΔCD2v) recombinant virus.

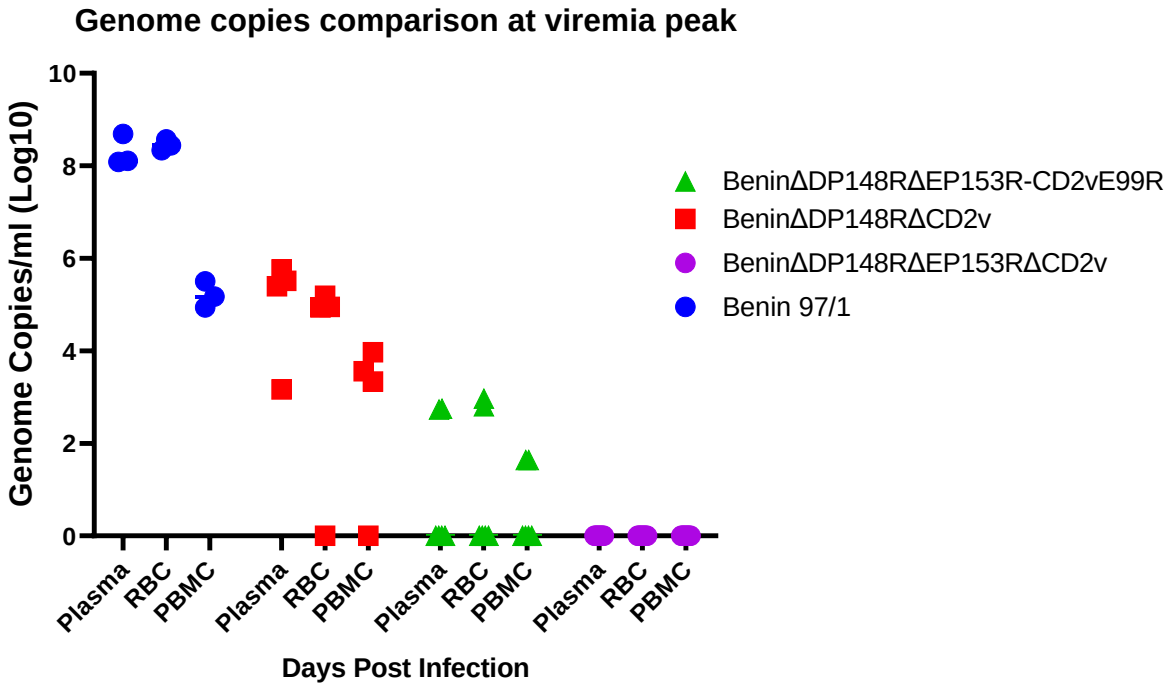

Figure 4.17b: Comparison of infections with different recombinant gene-deleted and wild type viruses based on genome copies in different fractions (Experiments 1 & 2); Virus genome copies in blood fractions at viremia peak in infected pigs were compared from infections with 4 different viruses, each symbol represents an individual pig and the colour corresponds to the virus used to infect the pigs. Genome copies were calculated at log10 copies per ml except from PBMC fraction where the genome copies were calculated log 10 genome copies per 10^6 cells.

4.19 Comparative analysis of antibody responses by ELISA in pigs immunised with BeninΔDP148RΔCD2v (Group C) in experiment 1 or BeninΔDP148RΔEP153RΔCD2v (Group A) or BeninΔDP148RΔEP153RCD2vE99R (Group B) in experiment 2.

The comparison of antibody responses between Group A and Group C showed significant difference at day 20/21 and day 34 before challenge (P= 0.0192, P= 0.0185) and at day 41/44 post challenge (P=0.0073), no difference in antibody levels were observed at other time points. Similarly, a significant difference was observed in antibody levels of Group A and Group B pigs before challenge at day 20 and day 27 (P=0.0005 & P=0.0426), no difference in antibody levels were observed between these two groups at other time point until termination (see figure 4.18). This indicates that induction of antibody response was correlated with the induction of viremia, the deletion of EP153R possibly further attenuated the virus and hence no viremia was detected, and antibody responses were only detected after the boost. However, in pigs infected with the BeninΔDP148RΔEP153RCD2vE99R virus in Group B the mutant non-HAD CD2vE99R protein is expressed. This leads to induction of low viremia in some pigs. The non-HAD virus phenotype may also result in better exposure of virus particles to the host humoral immune response and thus the induction of an early antibody response. Further research is needed to confirm this hypothesis.

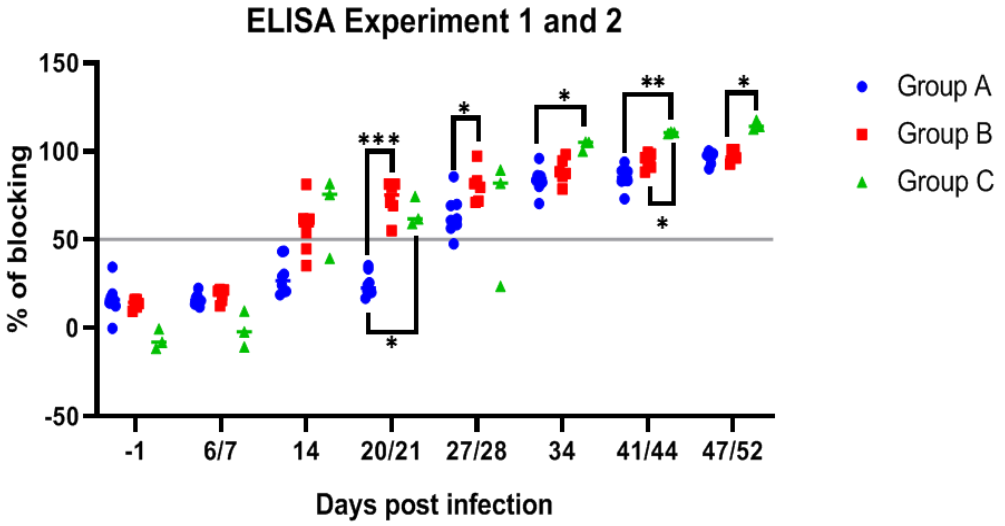

Figure 4.18: Antibody responses in pigs against ASFV P72 (Experiment 1 & 2); Group A (BeninΔDP148RΔEP153RΔCD2v), Group B (BeninΔDP148RΔEP153R-CD2vE99R, Group C (BeninΔDP148RΔCD2v) The figure shows a group comparison of the antibody responses, each coloured symbol refers to each group, and the days are shown as days post-infection referring to primary immunization. The statistical significance is represented by (*) symbols, the p-values less than 0.001 are represented by (***), the p-values less than 0.01 are represented by (**) and the p-values less than 0.05 are represented by (*).

4.20 Comparative analysis of IFN responses by ELIspot in pigs immunised with BeninΔDP148RΔCD2v (Group C) in experiment 1 or with BeninΔDP148RΔEP153RΔCD2v (Group A) or BeninΔDP148RΔEP153RCD2vE99R (Group B) in experiment 2.

The comparison of T-cell IFN-γ responses in Group A and B, (experiment 2) and Group C (experiment 1) was performed to determine the variation in T cells mediated responses. T-cell IFN-γ responses were shown to be a correlate of protection in immunised and challenge pigs, it was important to determine that the variation in

induction of T-cell IFN-γ responses in the current study (experiment 1 and 2) are statistically significant. The variation was determined by performing 2-way ANOVA following Tukey's multiple comparison tests. A significant difference was observed between all groups before boost. Group C had the highest number of IFN-γ producing cells followed by group B and group A which had a low number IFN-γ producing cells. The number of T-cell IFN-γ response correlates with protection, as 3/4 animals survived the lethal challenge in Group C (1 pig died of non ASF related condition). While in group B 5/6 pigs survived the lethal challenge and in group A 6/8 pigs survived the lethal challenge. This indicates that the levels of T-cell IFN-γ response correlates with protection.

After boost, a significantly higher levels of IFN-γ secreting cells were detected in group C (induced good protection) when compared to the other 2 groups. The variation in levels of IFN-γ secreting cells between Group A and B was also statistically significant after boost, however, no significant difference was observed in levels of IFN-γ secreting cells between Group A and Group B before challenge (see figure 4.19). This comparison suggests that early T-cell IFN-γ responses doesn't necessarily means that the animals will be protected and that the T-cell IFN-γ responses at the time challenge is associated in induction of protection. This indicate a role for T-cell IFN-γ responses during early phase of ASFV infection.

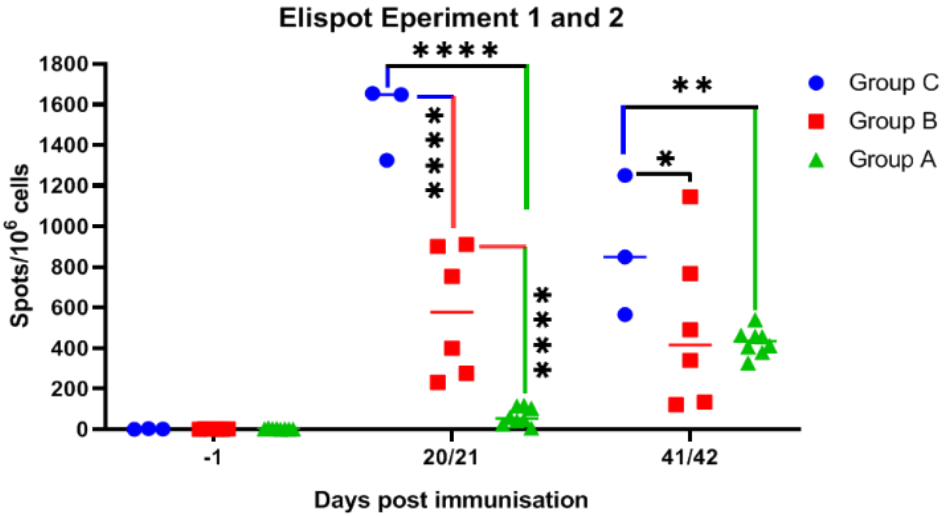

Figure 4.19: IFN-γ responses in pigs (experiment 1 & 2): (Groups A, B, C) The figure shows the group comparison of the IFN-γ responses, each coloured symbol refers to pigs in different groups group, and the days are shown as days post-infection referring to primary immunization. The statistical significance is represented by (*) symbols, the p-values less than 0.0001 are represented by (****), the p-values less than 0.001 are represented by (***), the p-values less than 0.01 are represented by (**) and the p-values less than 0.05 are represented by (*).

4.21 Discussion:

In this chapter the role of CD2v, C-type lectin and mutant CD2vE99R (non-HAD) protein in virus persistence and dissemination was investigated in pigs. This was performed by analysing samples from two separate animal experiments and by using 3 recombinant ASFV with different molecular targets removed. The recombinant ASFV expressing non-HAD CD2vE99R protein was constructed with additional deletion of the EP153R from the genome of previously attenuated BeninΔDP148R. This additional deletion was based on the *in vitro* analysis from the mutant CD2v protein which showed that EP153R augments CD2v HAD function (described in chapter 4). In addition, to determine the effect of the expression of the mutant CD2vE99R protein another ASFV recombinant virus was constructed with EP402R/CD2v, EP153R and DP148R genes deleted. The viruses were constructed by transfecting transfer plasmid into WSL cells infected with a parental virus BeninΔDP148R (described in chapter 4). The viruses were purified by using FACS single cell sorter following a published method (Rathakrishnan et al., 2020). These recombinant viruses were tested in pigs by performing immunization and challenge experiments to further investigate the role of CD2v and C-type lectin in virus persistence and dissemination in pigs.

In experiment 1, the pigs were infected with BeninΔDP148RΔCD2v and were challenged with the ASFV Benin 97/1 (virulent strain). The aim was to identify if the CD2v protein is involved in virus persistence in pigs. The previously attenuated BeninΔDP148R induced 100% in pigs but the virus persisted in blood for an extended period (up to 60 days) (Reis et al., 2017). The data from the recent experiment (BeninΔDP148RΔCD2v) was compared with the previously published data on BeninΔDP148R, it was observed that the virus persistence in blood was significantly reduced (from 60 days to 11 days) after the deletion of CD2v from BeninΔDP148R

genome. This indicated that CD2v is involved in virus persistence in pigs. As described above and in detail in chapter 4, the in vitro results suggested that ASFV EP153R/C-type lectin augment the function of CD2v protein. To investigate if EP153R also has role in virus persistence (either directly in attachment with RBC or by enhancing the cell surface expression of CD2v), the EP153R gene and CD2v were deleted from the BeninΔDP148R genome in parallel. The newly generated recombinant ASFV BeninΔDP148RΔEP153RΔCD2v (Rathakrishnan et al., 2020) was tested in pigs (experiment 2).

In experiment 2, the effect of deleting EP153R was determined by experimental infection of pigs. The samples from pigs immunised with BeninΔDP148RΔEP153RΔCD2v (Group A) were analysed by qPCR and the data was compared with previous experiments where BeninΔDP148RΔCD2v was tested in pigs (Group C). It was observed that in pigs immunised with BeninΔDP148RΔCD2v a peak of viremia was observed at day 7 post-immunization in all pigs and the levels of virus genome copies detected in blood varied between ($10^{2.9}$ to 10^{6} copies/ml) (see figure 5.5). In contrast, no viremia was detected in pigs immunised with BeninΔDP148RΔEP153RΔCD2v (Group A). This suggests that deletion of EP153R further attenuated the virus, since there was no viremia it was difficult to conclude if EP153R is also involved in virus persistence in pigs. The onset of clinical signs coincided with viremia, in pigs immunised with BeninΔDP148RΔCD2v mild clinical signs were observed in pigs (from day 5 to day 10 post-immunisation) while in pigs immunised with BeninΔDP148RΔEP153RΔCD2v no clinical signs were observed post-immunization supporting the idea that EP153R has a role in virus attenuation.

In the second experiment, where pigs were immunized with BeninΔDP148RΔEP153RΔEP402R (Group A) no virus genome was detected in the

blood before the challenge and no clinical signs were observed. However, in pigs immunized with BeninΔDP148RΔEP153R-CD2vE99R (Group B), a peak of viremia was observed in three pigs on day 6 and the level of virus genome detected in blood was significantly lower (10^2 to$10^{3.8}$ copies/ml) than in pigs from Group C (BeninΔDP148RΔCD2v) where the amount of genome copies at viremia peak post immunization was 10^6 copies /ml. Thus the deletion of EP153R and modification to CD2vE99R to abrogate HAD, had the effect of reducing levels of viremia compared to the deletion of CD2v gene alone (BeninΔDP148RΔCD2v) but increased viremia in some pigs compared to pigs immunised with BeninΔDP148RΔEP153RΔCD2v.

Overall, when all recombinant viruses were compared to investigate its effect on virus persistence, viremia, onset and duration of clinical signs the following observations and conclusions were drawn.

Onset and duration of clinical signs in pigs:

It was observed that deletion of CD2v from BeninΔDP148R genome delayed the onset of clinical signs by 2 days in pigs (Group C). However the duration of clinical signs increased by 1 day in pigs immunised with BeninΔDP148RΔCD2v compared to BeninΔDP148R.

In pigs immunised with BeninΔDP148RΔEP153RΔCD2v, no clinical signs were observed before challenge possibly due to the further attenuation of the virus. However in pigs immunised with BeninΔDP148RΔEP153R-CDE99R the onset of clinical signs was delayed by 2 days similar to the BeninΔDP148RΔCD2v but the duration of clinical signs were reduced to 1 day (in BeninΔDP148RΔCD2v clinical signs were observed for 5 days). This may either be due to the deletion of EP153R which attenuated the virus or due to the non-HAD CD2vE99R expression on the surface of infected cells and

virions. This may have resulted in a higher antibody response to CD2v and possibly other virion proteins due to better exposure to the host immune system. Antibody responses to the p72/B646L capsid protein were measured using a blocking ELISA which reached the saturation level after the boost. To measure an effect on antibody levels against CD2v a different more quantitative test would have to be established perhaps based on a recombinant protein or fixed cell ELISA using cells expressing CD2v. Another possibility is that EP153R and CD2v co-operate and therefore the presence of EP153R in BeninΔDP148RΔCD2v may have increased the duration of clinical signs. Since previous results showed that levels of viremia correlate with clinical signs the reduction in virus persistence and dissemination have an effect to the onset and duration of clinical signs. Each of the gene-modified viruses tested replicated to similar high titres as the parental virulent virus in primary bone marrow cells. Thus differences observed in immunised pigs were unlikely to be caused by a difference in replication in cells.

Virus persistence, dissemination and viremia:

In experiment 1, the virus persistence in pigs immunised with BeninΔDP148RΔCD2v (Group C) was reduced to 11 days from 60 days when compared to the parental BeninΔDP148R. This clearly showed the role of CD2v in virus persistence but surprisingly the viremia peak in both Groups was similar (at 7 days post-immunisation). This indicates that the virus is disseminated from sites of primary replication at the same rate in both Groups, suggesting that other viral factors may be involved in virus dissemination.

In experiment 2, pigs immunized with BeninΔDP148RΔEP153RΔCD2v did not develop viremia and therefore it was not possible to conclude its effect on virus

persistence. This possibly indicates that virus disseminated at a slow pace and therefore that viremia was not induced, suggesting a role for EP153R in virus dissemination. The C-type lectins are reported to be involved in the interaction with glycans on the cells surface and may facilitate the attachment of the viruses to different cells.

On the other hand, in pigs immunised with BeninΔDP148RΔEP153R-CD2vE99R the virus persistence was reduced to 2 days post-immunisation compared to the BeninΔDP148RΔCD2v in which virus persisted for 11 days post immunisation. This possibly indicates that the deletion of EP153R reduced virus dissemination which in turn resulted in reduced viremia and in a shorter persistence of the virus.

In summary the results suggest that deletion of CD2v reduced virus persistence and delayed the onset of clinical signs but had little effect on induction of viremia or virus dissemination. The deletion of both EP153R and CD2v attenuated the virus and resulted in no clinical signs, no viremia was induced possibly due to reduced virus dissemination and due to reduced virus attachment to the cells. However the virus clearly replicated in tissues since a cellular and antibody response was induced following immunisation and boost. Deletion of EP153R and insertion of mutant CD2vE99R in BeninΔDP148R genome resulted in reduced viremia compared to BeninΔDP148RΔCD2v, since mild clinical signs of reduced duration were observed and virus persistence was reduced. The insertion of mutant CD2v E99R and the deletion of EP153R increased the viremia compared to BeninΔDP148RΔEP153RΔCD2v, but reduced virus persistence and dissemination when compared to other recombinant viruses (BeninΔDP148R, BeninΔDP148RΔCD2v,).

Table 5.1: The overall summary of the effect of recombinant viruses in pigs. The viremia is shown as genome copies/ml (log10). The data of Benin97/1 shown is from (Group E-Experiment AR000962).

Virus used	Days to clinical signs post-immunisation	Duration of clinical signs post immunisation	Viremia post-immunisation	Duration of virus persistence post immunisation	Viremia post-challenge
Benin 97/1	Day 3	3 days (terminated on day 6)	N/A	N/A	10^8 genome copies/ml
BeninΔDP148R (Reis et al., 2017)	Day 3	4 days (up to day 7)	10^5-$10^{6.3}$	60 days *	10^5-$10^{6.3}$ genome copies/ml
BeninΔDP148RΔ CD2v	Day 5	5 days (up to day 10)	$10^{2.9}$ to 10^6	11 days	None
BeninΔDP148RΔ EP153RΔCD2v	None	None	None	None	10^2 to 10^6 genome copies/ml
BeninΔDP148RΔ EP153R-CD2vE99R	Day 5	1 day	10^2 to$10^{3.8}$	2 days	$10^{3.8}$- $10^{5.7}$ genome copies/ml

* The virus genome detected after challenge in pigs immunised with BeninΔDP148R was assumed to be persisting immunising virus since no clinical signs were observed.

Chapter 5- Materials and Methods

5.1 Bioinformatics Methods:

5.1.1 Primer designing:

Primers for the amplification of WT-CD2v and the CD2v mutants were designed using a bioinformatics tool (Vector NTI), each primer had a unique restriction enzyme site at the terminus for convenient cloning and sub-cloning. All primers were kept at -20°C as 400nm/µl stocks, a list of primers along with the restriction enzyme sites, function and the product generated are shown in Appendix 1.

The primers for site-directed mutagenesis with desired substitutions were designed using the Agilent QuickChange primer design program, according to the guidelines from the manufacturer. This is available online at (www.agilent.com/genomics/qcpd).

5.1.2 Multiple sequence alignments:

The multiple sequence alignment was performed online using ClustalW bioinformatics tool (EMBL-EBI, Wellcome Genome Campus, Hinxton, Cambridgeshire, UK). The CD2v protein sequences were obtained from the National Centre for Bioinformatics Information (NCBI) and the Viral Bioinformatics Resource Centre (VBRC). The protein sequences of human, rat, and pig CD2 was obtained from NCBI, the alignment of CD2v and CD2 was performed and the results were analysed using MView (EMBL-EBI, Wellcome Genome Campus, Hinxton, Cambridgeshire). The amino acid residues corresponding to those that were shown to be responsible for rosetting of red blood cells to human CD2 were selected for mutation in ASFV encoded CD2v (see results chapter 2 for details).

The Sanger sequencing data was analysed by using the Vector NTI software. The contigs were assembled and were aligned with the consensus sequence to identify any mutation in the cloned fragments.

5.1.3 Maps for CD2v mutants in pcDNA3:

The maps for each CD2v mutant were constructed using Vector NTI software. The Benin 97/1 encoded WT-CD2v sequence was obtained from NCBI and the pcDNA3 sequence was obtained from Addgene UK. The WT-CD2v sequence without a translation stop codon was inserted into pcDNA3 in the multiple cloning site (MCS) between *Bam*HI and *Hind*III restriction enzyme sites. An HA-tag sequence (5' TAT CCA TAT GAT GTT CCA GAT TAT GCT 3') was inserted downstream of the *Hind*lll restriction enzyme site. The stop codon was inserted downstream of the HA-tag and upstream of the *Xba*l restriction enzyme site. The CD2v open reading frame was translated using Expasy translate tool. This construct was then modified with planned substitution/mutations in the immunoglobulin domain. Each mutant map was constructed and was translated using Expasy translate online tool to determine if any of the constructs resulted in a frame stop codon and to confirm the expression of a full length CD2vHA.

5.1.4 Protein modelling tool:

The predicted model for CD2v Ig-domain was generated by PyMOL protein modelling tool (The PyMOL Molecular Graphics System, Version 1.2r3pre, Schrödinger, LLC).

The mutant CD2v was analysed using Pymol to predict the effect of the substitution on the structure of CD2v.

The predicted ribbon model for CD2v Ig-domain was generated using the RaptorX online protein modelling tool. The sequence of the Ig-domain was submitted online on the RaptorX website (http://raptorx.uchicago.edu/) and the model was generated.

5.2 DNA Methods:

5.2.1 Polymerase chain reaction:

The PCR was performed using AccuPrime™ Pfx DNA Polymerase (Thermofisher Scientific, UK). A 25µl reaction was set up according to AccuPrime™ Pfx DNA polymerase protocol available online; https://assets.fishersci.com/TFS-Assets/LSG/manuals/accuprimepfx_man.pdf .

5.2.2 Gel Electrophoresis:

Gel electrophoresis was performed using 1% agarose gel (Sigma, UK). 5µl of 10mg/ml ethidium bromide (Sigma, UK) was added to the melted agarose. The agarose was cast in the gel tray and was left to solidify. 1µl of 10X purple loading dye (NEB, UK) was added to each sample before loading the samples onto the gel. 1 KB NEB quick ladder (NEB, UK) was used as a marker (in some gels the 100bp, 1 KB plus, 2-log DNA ladder from NEB, UK was used).

5.2.3 Cloning:

The WT-CD2v fragment and mutant CD2v were cloned into TOPO II blunt-end cloning vector from Invitrogen (UK). TOPO II is a linearized vector with blunt ends and is convenient for cloning of blunt-ended PCR products. A 10µl ligation reaction was prepared following the manufacturer's protocol, the PCR products were ligated into the cloning site in the vector. The kit also contains M13, T7 and SP6 priming sites for convenient sequencing of the inserts. The CD2v mutants were cloned and modified in

TOPO II and were sub-cloned into a mammalian expression vector system pcDNA3 (Addgene UK). The pcDNA3 vector containing the Malawi Lil 20/1 CD2v gene upstream of an HA-tag and a stop codon was provided by Lynnette Goatley (The Pirbright Institute). This insert was removed by digestion with *Hind*III and *Bam*HI restriction enzymes and was replaced with Benin 97/1 CD2v to generate WT-CD2vHA and the mutant CD2vHA.

5.2.4 Strategy for constructing mutant versions of the CD2v gene:

The WT-CD2v sequence from Benin 97/1 was analysed for restriction enzyme sites using Vector NTI software. A ~393 bp restriction enzyme fragment was identified in the EP402R/CD2v gene containing both immunoglobulin domains and the sites planned to be mutated. A single *Scal* site was present upstream of the immunoglobulin domain and single *Mfel* site downstream of the immunoglobulin domain. The sequence of this fragment from the Benin WT-CD2v gene and the planned substitution in Ig domains were designed by vector NTI and were synthesized by GeneArt with the same restriction enzyme sites at the termini (*Scal* and *Mfel*). These sequences with the desired mutations were planned to be replaced in the sequences of the WT-CD2v immunoglobulin domain cloned in pcDNA3 and to contain an HA-tag fused in frame at the C-terminus (see figure 2.5). In the first batch of mutants, 7 mutant versions of CD2v were constructed (see figure 2.4).

The Vector NTI software was used to design the plasmid constructs (WT-CD2v and CD2v mutants). The Benin 97/1 WT-CD2v sequence was obtained from NCBI and the pcDNA3 vector sequence was obtained from Addgene website. The assembled sequences were analysed to confirm that premature stop codons or frameshift mutations had not been introduced. The strategy for cloning of the gene is shown in figure 5.1.

The WT-CD2v without the stop codon was amplified by PCR from Benin 97/1 genomic DNA (see appendix 1 for primer sequences) provided by Lynnette Goatley (The Pirbright Institute). The amplified WT-CD2v was cloned into pcDNA3 under control of a T7 promoter and containing a C-terminal HA-tag, fused in frame, followed by a stop codon to generate pWT-CD2vHA. The pcDNA3 expression vector was also provided by Lynnette Goatley (The Pirbright Institute). As described in the above section, the CD2v mutant fragments (Ig-domain) from GeneArt were digested with restriction enzymes to replace the wild type Ig-domain in pWT-CD2vHA with the mutant Ig domain. All mutants were successfully cloned except from mutant 7 which didn't work after several attempts, the cloned mutants were transformed into bacterial *E.coli* (DH5α) cells and were grown in midi preps, the mutant plasmid DNA was isolated and was sequenced by Sanger sequencing using T7 forward and reverse primers (see appendix 1 for primer sequences).

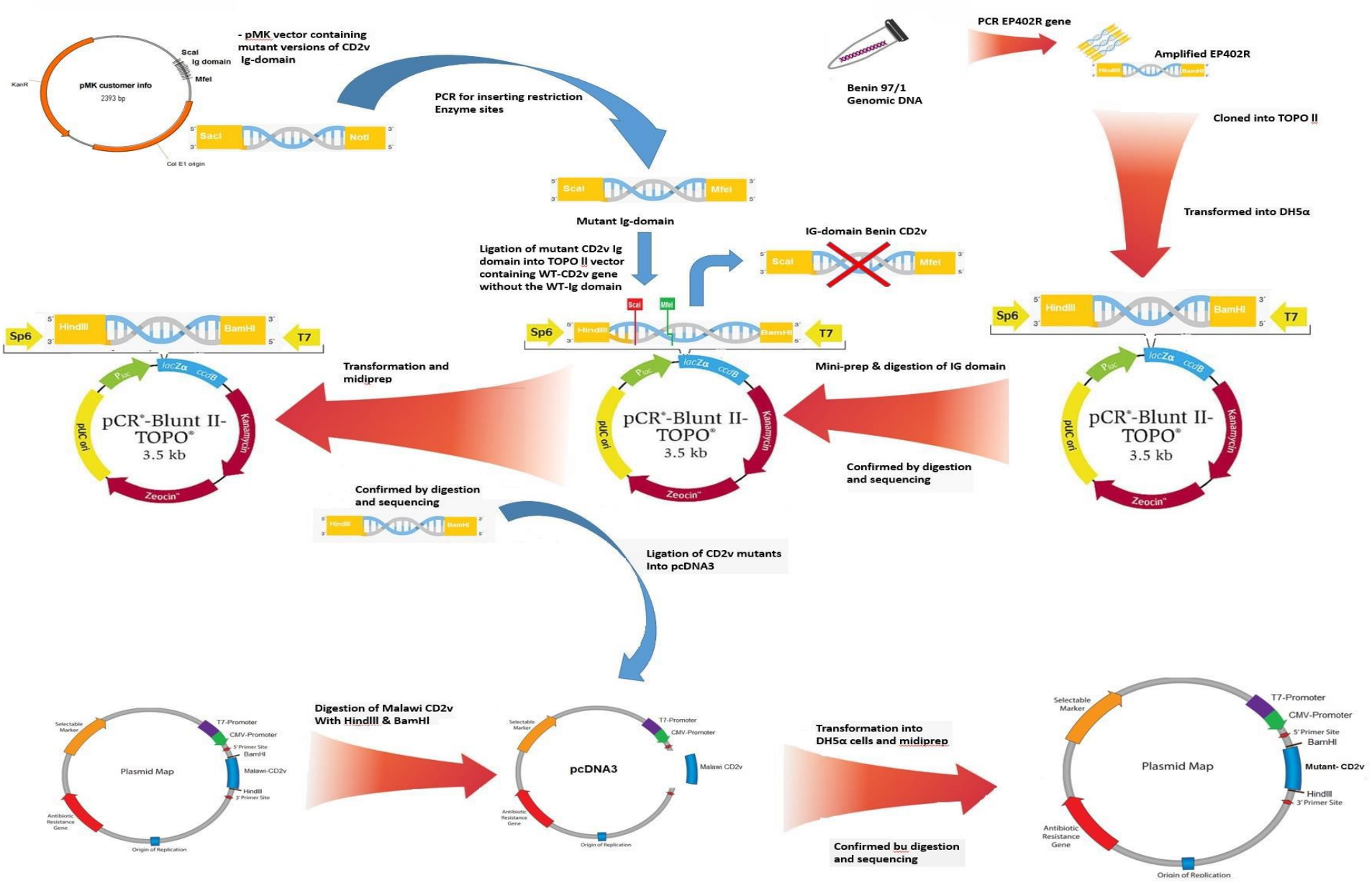

Figure 5.1 ; a schematic diagram representing cloning strategy and the different steps involved in constructing CD2v mutants

5.2.5 Sequencing PCR:

A sequencing PCR was performed by using BigDye™ Terminator v3.1 Cycle Sequencing Kit (Applied Biosystems, Thermofisher scientific, UK). This involves two main steps; preparation of sequencing reaction and ethanol precipitation of the PCR product. 10µl reactions were set up (See table 5.1) and were placed in a conventional thermal cycler using the following program (See table 5.2).

Table 5.1: Composition of reaction mixes for Sanger Sequencing

Reaction component	1 reaction
5x Sequencing Buffer	2.0 µl
BigDye® Terminator v3.1	0.5 µl
Primer (at 1.6pmol)	3.0 µl
Template (5-20ng for 500-1000bp)	1.0 µl
RNase free water	3.5 µl
Total Volume	10.0 µl

Table 5.2: Thermal cycler programme for Sanger sequencing:

96 °C	1min	1 CYCLE
96 °C 50 °C 60 °C	10 sec 5 sec 4 min	25 CYCLES
10 °C	hold	

A 5µl of 125mM EDTA (Thermofisher scientific, UK) and 60µl of 100 % ethanol was added to each PCR tube. The tubes were vortexed gently and were incubated in the dark for 15 minutes at room temperature. This allowed the product to precipitate, after incubation the samples were spun at 13000 rpm for 30 minutes and the supernatant was removed. 60µl of 70% ethanol was added to the precipitated samples and they were vortexed, the samples were again centrifuged at 13000rpm for 30 minutes and the

supernatant was removed. The samples were then dried in dark for 15 minutes at room temperature and 20µl of Hi-Di Formamide was added to each sample before loading.

5.2.6 Plasmid DNA isolation:

The plasmid DNA was isolated using either the Qiagen Plasmid Mini prep Kit, Qiagen Plasmid Midi Kit or the Qiagen Plasmid Maxi prep Kit (Qiagen, UK) according to the standard protocol available online from Qiagen. https://www.qiagen.com/gb/resources/resourcedetail?id=c164c4ce-3d6a-4d18-91c4-f5763b6d4283&lang=en

5.2.7 Ligation:

The ligation reaction was carried out by using either T4 DNA ligase (Promega, UK) or LigaFast-TM rapid ligation (Promega, UK) following the manufacturer's protocol.

Available online from https://www.promega.co.uk/resources/protocols/product-information-sheets/g/ligafast-rapid-dna-ligation-system-protocol/

5.2.8 Cloning:

The WT-CD2v fragment and mutant CD2v were cloned into TOPO II blunt-end cloning vector from Invitrogen (UK). TOPO II is a linearized vector with blunt ends and is convenient for cloning of blunt-ended PCR products. A 10µl ligation reaction was prepared following the manufacturer's protocol, the PCR products were ligated into the cloning site in the vector. The kit also contains M13, T7 and SP6 priming sites for convenient sequencing of the inserts. The CD2v mutants were cloned and modified in TOPO II and were sub-cloned into a mammalian expression vector system pcDNA3 (Addgene UK). The pcDNA3 vector containing the Malawi Lil 20/1 CD2v gene upstream of an HA-tag and a stop codon was provided by Lynnette Goatley (The

Pirbright Institute). This insert was removed by digestion with *Hind*III and *Bam*HI restriction enzymes and was replaced with Benin 97/1 CD2v to generate WT-CD2vHA and the mutant CD2vHA.

5.2.9 Transformation of *E. coli*:

An aliquot of 50µl chemically competent *E.coli* DH5α cells were thawed on ice and 2µl ligation mix was added to each vial of competent cells. The samples were then incubated on ice for 30 minutes and were flicked after every 15 minutes to evenly distribute the cells and the plasmid DNA. The cells were heat-shocked for 1 minute at 42^{o}C and were immediately transferred to ice and were incubated for 5 minutes. A volume of 500µl of Super Optimal broth with Catabolite repression (SOC) media (ThermoFisher scientific, UK) was added to each transformation vial and they were incubated in the shaking incubator for 1 hour at 37^{o}C. The samples were inoculated on agar plates with Lysogeny broth (LB-agar plates) containing either 100µg/ml ampicillin (Sigma, UK) or 50µg/ml kanamycin (Sigma, UK) (see table 5.7 & 5.8 for recipe) depending on the antibiotic resistance gene of the plasmid vector.

Table 5.7: Recipe for preparing ampicillin stock solution (1000X).

Ingredient	Quantity
Ampicillin (Sigma, UK)	1 gram
Water	5ml
Ethanol	5ml

Table 5.8: Recipe for preparing kanamycin stock solution (50mg/ml).

Ingredient	Quantity

Kanamycin (Sigma, UK)	50mg/ml
Water	10 ml

5.2.10 Chemically competent cells:

Chemically competent *E.coli* DH5α cells were made from a previous stock. A 50µl frozen aliquot of chemically competent cells were thawed and were grown in 10 ml lysogeny broth (LB) overnight at 37ºC in a shaking incubator. 200ml of LB was added to the pre-grown inoculum and the cultures were incubated at 37ºC in a shaking incubator until the OD600 of the culture reached 0.4-0.6. The cells were then centrifuged in 50ml falcon tubes at 4000 rpm for 10 minutes, the supernatant was discarded and the pelleted cells were suspended in 35ml of RF1 (see table 5.3) and were incubated on ice for 5 mins. The cell suspension was again centrifuged at 4000 rpm for 10 mins and the supernatant was discarded, the pellet was suspended in 10 ml of RF2 (see table 5.4) and was incubated on ice for 60 minutes. 200µl of cells were aliquoted in sterile pre-chilled Eppendorf tubes and were quick-frozen in liquid nitrogen and were stored at -80°C.

Table 5.3: Chemicals used in RF1 (PH 5.8) reaction mix for making competent cells using rubidium chloride.

RbCl	100mM	1.3g/100ml
MnCl2	50mM	1g/100ml
KAc	30mM	300mg/100ml
CaCl2	10mM	150mg/100ml
Glycerol	15% (v/v)	

Table 5.4: Chemicals used in RF2 (PH 6.8) reaction mix for making competent cells using rubidium chloride.

MOPS	10mM	210mg/10ml
RbCl	10mM	120mg/10ml
CaCl2	75mM	1.1g/10ml
Glycerol	15% v/v	

5.2.11 Site directed mutagenesis:

Site-directed mutagenesis was performed using the Agilent QuikChange lightning kit (Agilent technologies, LDA, UK Ltd) and following the manufacturer's protocol available online from https://www.agilent.com/cs/library/usermanuals/Public/200523.pdf .

The 3rd batch of mutants were constructed individually (one by one) by performing SDM and using pWT-CD2vHA (cloned in pcDNA3, described elsewhere) as a template. The SDM-PCR products were transformed into bacterial *E.coli* (DH5α) cells and were grown in midi preps, the mutant plasmid DNA was isolated and was sequenced by Sanger sequencing using T7 forward and reverse primers (see appendix 1 for primer sequences).

5.3 Cell culture and protein methods:

5.3.1 Primary and secondary cells:

Adherent Vero cells were used for *in vitro* expression of WT-CD2v and mutant CD2v by MVA-T7. The Vero cells were obtained from CSU (central services unit) at Pirbright Institute in a 175cm^2 flask at passage 49. The cells were grown in GibcoTM DMEM

media supplemented with 1% GibcoTM Penicillin/Streptomycin (10,000 IU/ug/ml) (Life technologies, UK) and 10% LSP fetal bovine serum (FBS) (Life sciences group Ltd, UK).

The WSL-R cells were used for *in vitro* expression of WT-CD2v and mutant CD2v in ASFV-infected cells. The cells were originally from FLI (Keil et al., 2014) and provided by Dr. Raquel Portugal (The Pirbright Institute) at passage 18 and were grown in ZB28 medium ; GibcoTM Ham's F12 Nutrient Mix medium, 50% GibcoTM IMDM supplemented with 1% GibcoTM Penicillin/Streptomycin (10,000 IU/ug/ml), 1% GibcoTM L-Glutamine 200 mM (100x) (Life technologies, UK), 10% LSP fetal bovine serum (FBS) (Life sciences group Ltd, UK).

Porcine bone marrow (PBMs) cells were used for propagation of ASFV stocks and titrations. The PBM cells were isolated from crushed bones of piglets, the fragmented bones were added to a 1 litre conical flask containing 500ml PBS, 1% GibcoTM Penicillin/Streptomycin (10,000 IU/µg/ml) (Life technologies, UK) and 1% LSP fetal bovine serum (FBS) (Life sciences group Ltd, UK). This suspension was then incubated at 37°C in a shaking incubator for 90 mins, the bone fragments were separated from the suspension by a muslin filter. The cells suspension was then centrifuged at 350G for 10 mins, the supernatant was discarded and the pelleted cells were suspended in PBS. The cells were again centrifuged at 350G for 10 mins, the supernatant was discarded and the pelleted cells were suspended in Earle's Balanced Salt Solution (Sigma, UK) supplemented with 1% GibcoTM Penicillin/Streptomycin (10,000 IU/ug/ml) (Life technologies, UK) and 10% porcine serum (Life technologies, UK).

Purified PBMs were used for performing immunofluorescence and Western blots in ASFV infected cells. PBM cells obtained as described above were purified by

performing density gradients using Histopaque®-1077 (Sigma-Aldrich Co. LLC, UK). The cells were grown in RPMI-1640 medium (Sigma, UK) supplemented with 1% GibcoTM Penicillin/Streptomycin (10,000 IU/ug/ml) (Life technologies, UK), 10% LSP fetal bovine serum (FBS) (Life sciences group Ltd, UK) and 100 ng/mL of recombinant porcine macrophage colony-stimulating factor (CSF1) (Roslin Technologies, Midlothian, UK).

5.3.2 Transfection of adherent cell cultures using TransIT-LT1:

The transfections were performed using the TransIT®-LT1 DNA Transfection Reagent (Mirus Bio LLC, US), as per the manufacturer's guidelines. The protocol is available online at https://www.bioscience.co.uk/userfiles/pdf/TransIT%20LT1%20Protocol.pdf

5.3.3 Infection of adherent cell cultures with MVA-T7:

MVA-T7 (Sutter et al., 1995) was grown in chicken embryo fibroblasts (CEF) and was used to infect Vero cells (to drive the expression of CD2v cloned under T7 promoter) for approximately 1-2 hours before transfection with CD2v expression plasmids. The titre of the MVA-T7 used was 2.7 X 10^7 pfu/ml, the virus was diluted in DMEM medium and was added to the Vero cells at an MOI 1.

5.3.4 Immunofluorescence labelling of cells grown on coverslips:

The cells were passaged at seeding density of $0.15x10^5$ cell/ml on coverslips in 24 well plates and were incubated at 37ºC overnight. The cells were then infected with MVA-T7 (see section 2.3.4) and were subsequently transfected (see 2.3.3) with pcDNA3 containing WT- CD2v and mutant CD2v. The cells were incubated at 37ºC overnight. The cells were washed twice with 1ml of Ca/Mg free PBS and 1 ml of 4% paraformaldehyde in PBS (Santa Cruz biotechnology, Texas, US) was added to fix the cells on coverslips. The cells were incubated for 10 minutes at room temperature and

were washed 3 times with 1ml of Ca/Mg free PBS. The cells (only for staining permeabilised cells and not for non-permeabilised cells) were treated for 5 mins with 1 ml of 0.2% Triton X- 100 (Sigma, UK) made up in Ca/Mg free PBS and was followed by washing the cells 3 times with 1ml of Ca/Mg free PBS. A blocking buffer, 0.5% bovine serum albumin BSA (Sigma, UK) in Ca/Mg free PBS, was added to the cells and they were incubated for 5 minutes at room temperature. The primary antibody was diluted in blocking buffer (1:1000) and 200µl was added to the cells followed by incubation at room temperature for 30 minutes. The cells were then washed 3 times with blocking buffer. The secondary antibody was diluted in blocking buffer at 1:500 and 200µl was added to the cells. The cells were incubated for 30 minutes at room temperature and washed twice with blocking buffer and with Ca/Mg free PBS. A drop of Vectashield (containing DAPI) (Vector Laboratories, UK) mounting medium was applied on the slide and the cover slip was dipped into de-ionised water and placed on the mounting medium. The coverslips were sealed with nail varnish and were stored at 4^{o}C.

The following antibodies were used for immunofluorescence:

***Primary antibodies;** rat α-HA high affinity (Sigma, UK, cat# 11867423001), mouse α-V5 (Thermo scientific, UK), Rabbit α-Flag (Sigma UK,), rat α-V5 (Novus, UK), mouse α-HA (Thermo scientific, UK), Serum from immunisation and challenge experiments in pigs (Reis et al., 2016; Reis et al., 2017), (All primary antibodies were used at dilution of 1:1000 and the serum was used at 1:500 dilution).

***Secondary antibodies;** goat α- pig Dylight594 (Abcam, UK, cat# ab102132), rabbit α-mouse 633 (Thermo fisher scientific, UK, Catalog # A-21063), donkey α- rabbit 488

or 568, goat α- rat 488 or 568 (Abcam, UK, cat# ab150157 and ab175476), (all secondary antibodies were used at a dilution of 1:500)

Cellular organelles; Nucleus (DAPI at dilution 1:10,000) (Sigma, UK), Cytoplasm (Cellbrite fix, Biotium).

5.3.5 Haemadsorption Assay:

Vero cells were grown in a supplemented DMEM media (see section 1) in a 6 well plate. The cells were seeded at a density of (1 X 10^5/ml) and grown at 37°C until they reached a confluency of 70-80%. The cells were infected with MVA-T7 at an MOI 1 prior to the transfection for 1 hour and were then transfected with WT-CD2vHA and its mutants (see transfection of adherent cells). The cells were incubated at 37°C for 24 hrs and were washed twice with PBS. The cells were detached by using GibcoTM Trypsin-EDTA (0.25%) phenol red (Thermo fisher scientific, UK), an equal volume of supplemented DMEM was added to the cells. To induce HAD, 50µl of porcine red blood cells, diluted in PBS, was added to each well and the cells were incubated again for 16 hours at 37°C. All plates were analysed on a Leica microscope attached to a (Leica MC120 HD) 2.5 Megapixel HD Microscope Camera.

5.3.6 Viruses stocks (Growth and harvest):

All procedures using live ASFV were carried out in SAPO4 licensed laboratories at the Pirbright Institute according to the procedures approved by the Health Safety and Biosafety Department and Health and Safety Executive of the UK Government. The virus stocks were grown in PBM cells in a T175 cm flask (50ml of cell suspension at a concentration of 1.5×10^7cells/ml), 500µl of the virus inoculum was added to the RPMI-1640 media in the flask. The flask was gently rocked and the flask cap was replaced with a filter cap, the flask was transferred into a secondary container and was incubated

at 37°C until a cytopathic effect (CPE) was observed in 90-100% cells (usually 4-5 days). Two sets of falcon tubes were labelled (one for the supernatant and one for the pellet) with name, virus strain, and date, SAPO4 infectivity status and the culture from the flask was transferred to falcon tubes using a pipette. The tubes were centrifuged at 1200 RPM for 15 minutes, the supernatants were transferred to a fresh falcon tube and were stored at 4°C. The tubes containing the pellet were transferred and stored at –80°C, the tubes were frozen and thawed 3 times, 5 ml RPMI-1640 was added to the tubes and centrifuged again at 1200 rpm for 10 minutes. The pellets were discarded and the supernatants were transferred to the supernatant obtained in the previous step.

Virus used were; Benin 97/1 (Chapman et al., 2007), OURT88/3 (Boinas et al., 2004), BeninΔCD2v (Reis et al., unpublished), BeninΔDP148RΔEP153RΔCD2v (Rathakrishnan et al., 2020), BeninΔDP148RΔEP153R-CD2vHA (Rathakrishnan et al..,unpublished) , BeninΔDP148RΔEP153R-CD2vE99R (Rathakrishnan et al..,unpublished).

5.3.7 Titrations (HAD50/ml and TCID50/ml);

The harvested viruses were titrated on PBM cells (100µl cell suspension at a concentration of 1.5×10^7 cell/ml) grown in 96 well plates containing the supplemented RPMI-1640 medium (see section 5.3.1). The media was changed before adding the viruses to the cells, the virus stocks were serially diluted in 96 deep wells plates by adding 50µl of the virus stock into 450ul RPMI-1640 media in first well (which is 1: 10) and making up to 8 1 in 10 dilutions. After the virus was diluted in the deep well plates, 100µl was transferred to the PBMs containing 100µl media in quadruplicate wells to determine the HAD_{50}/ml (Reed & Muench., 1938, (Leon et al., 2013). The

plates were sealed with a plastic sealer and were incubated at 37°C for 3 days or until HAD or CPE is observed.

Fixing and labelling virus for titration by immunofluorescence;

The viruses were titrated by staining infected cells with antibodies against an ASFV protein and detecting bound antibodies by immunofluorescence to determine $TCID_{50}$/ml. PBM cells, grown in a 96 well plate, were infected with ASFV, the plates were sealed and were incubated at 37°C for 3 days or until HAD or CPE was observed. The media was discarded and the plates including the lids were submerged into 4% PFA for 1 hour. The plates were then washed 3 times with PBS and were transferred to non-virus handling lab for staining in a secondary container. The cells were washed again with PBS and 100µl 0.2% triton x-100 made up in PBS was added to each well and the plates were incubated for 5 minutes at room temperature. The cells were washed 3 times with PBSa, primary antibody 4H3 against ASFV protein P72 was diluted in PBS at 1:1000 and 100ul was added to each well. The plates were incubated at room temperature for 45 minutes and were washed 3 times with PBS. The secondary antibody mouse α-pig 488 was diluted in PBS at 1:500 and 100µl was added to each well and cells were incubated for 1 hour in the dark. The plates were washed 3 times with PBSa and were left to dry. The plates were again washed with PBS and were analysed by indirect immunofluorescence microscope. The titres were calculated using Spearman and Karber equation (Wulff et al., 2012).

5.3.8 Western blot:

The infected or transfected cells were washed with cold PBS and lysed in 400-500µl of RIPA buffer (Sigma, UK) .The cells lysate was centrifuged at 13000 rpm to remove nuclear debris and the supernatant was diluted in electrophoresis sample Buffer (2X)

(Santa Cruz Biotechnology, Inc). The lysates were heated for three to five minutes at ninety to ninety-five degrees centigrade in a heat block. The lysates were loaded onto a sodium dodecyl sulfate-polyacrylamide gel electrophoresis SDS/PAGE gel with a 12% resolving gel (see table 5.5, 5.6 for resolving and stacking gel recipe). The glass cassette was placed in the gel tank containing Tris-glycine-SDS (TGS) (Bio-rad, UK) running buffer and the samples were run at 100-150 volts until the running dye has reached the bottom of the gel. The gel was carefully removed from the glass plates, the filter paper and the Polyvinylidene difluoride (PVDF) membrane (Amersham™ Hybond®, sigma UK) was cut smaller than the cassette. The membrane was soaked in 100 % methanol for 5-10 seconds, the membrane and the gel were sandwiched between the filters in a cassette and were placed in blotting apparatus. The cassette was submerged in transfer buffer (20% methanol in TGS) and was run at 100 volts for 1 hour. The membrane was blocked overnight with 5% milk powder (Marvel, premier food, UK) (w/v) in PBS at 4°C and with 0.2% PBS Tween ® 20 (Sigma, UK). The membrane was incubated with primary rat anti-HA (Sigma, UK) antibody and secondary goat anti-Rat IgG, HRP (Life technologies Ltd) antibodies at room temperature for 1 hour. The membranes were washed with PBS containing 0.2% Tween 20, and then the bound antibodies were detected using Immobilon Western Chemiluminescent HRP Substrate (Sigma, UK) followed by exposure to X-ray films.

Table 5.5: Recipe for making 40ml of 12% resolving gel.

Ingredients	**volume**
40% acrylamide (Sigma, UK)	12.0ml
1.5M Tris-HCl pH 8.8	8.0ml
water	19.2ml

10% SDS (Sodium dodecyl sulfate)- (10 grams SDS dissolved in 100ml water)	400 µl
10% APS (Ammonium persulphate solution) (1g Ammonium persulphate in 10ml distilled water)	400 µl
Temed (Sigma, UK)	20-200 µl

Table 5.6: Recipe for making 20ml of stacking gel.

Ingredients	**Volume**
40% acrylamide (Sigma, UK)	1.95ml
0.5M Tris-HCl pH 6.8	5.0ml
water	12.65ml
10% SDS (Sigma, UK)	200 µl
10% APS (Sigma, UK)	4200 µl
Temed (Sigma, UK)	10-100µl

5.4 Animal experiments methods:

All procedures performed on samples from animal experiments were carried out in SAPO4 licensed laboratories at the Pirbright Institute according to the procedures approved by the Health Safety and Biosafety Department and Health and Safety Executive of the UK Government.

5.4.1 Plasma collection from blood samples:

The blood samples from animal were collected in BD Vacutainer™ PPT™ tubes and were transferred to the BSL-2 lab in a sealed container. The samples tubes were taken

out from the container inside MBSC (class II) and wiped with FAM (1:200). The sample tubes were place in centrifuge containers and were centrifuge at 1500 RPM for 10 minutes. The containers were opened inside the MBSC and take 1ml of plasma and transfer it to the screw cap tubes and were stored at -80ºC.

5.4.2 Buffy coat and RBC collection from blood samples:

The blood samples from animal were collected in BD Vacutainer™ PPT™ tubes and were transferred to the BSL-2 lab in a sealed container. The samples tubes were taken out from the container inside MBSC (class II) and wiped with FAM (1:200). The falcon tubes (50ml) were labelled (3 tubes for each sample), Histopaque®-1077 (sigma, UK) was warm up at room temperature and 10 ml was added to a 50 ml falcon tube. The tubes were shaked to mix the plasma, the blood was then added to a fresh falcon tube and was diluted in DPBS (Dulbecco's phosphate-buffered saline) (Sigma, UK) to make up 35ml suspension. The diluted blood was gently added to the tubes containing Histopaque®-1077 (sigma, UK), dispensing the blood slowly on top of the Histopaque®-1077 (sigma, UK). DPBS was added to the vacutainer to wash off the remaining cells and was added to the Histopaque®-1077 (sigma, UK). The falcon tubes were wiped with the FAM (1:200) and were placed in the centrifuge containers and were centrifuged at 1000g for 30 min with no brake on. Gently collect the buffy coat and add it to a fresh falcon tube containing PBS to suspend the cells, add PBS to the suspended cells and make it up to 45ml. The tubes were wiped with FAM and were placed in centrifuge containers, the tubes were centrifuged at 400g for 10 min with brakes on.

At this point the supernatant was discarded from the tubes containing the Histopaque®-1077 (sigma, UK) and 1 ml RBC pellet was transferred to a screw cap tube and stored at -80°C.

After centrifugation, the PBS was discarded by decanting the tubes and the buffy coat cells were re-suspended in RBC lysis buffer (Biolegend, BioLegend Way, San Diego, CA, USA) for 5 minutes. PBS was added to the tubes and were centrifuged again at 400g for 10 mins, the supernatant was discarded and the cells were re-suspended in PBS and were centrifuged again at 400g for 10 mins. The supernatant was discarded and the cells were re-suspended in 1ml PBS. The cells were counted using haemocytometer and required volume was added to a screw cap tube and store at -80°C.

***Counting the cells:** The cells were diluted by adding 10µl of cell to 90 µl PBS, and transferring 10µl of the diluted cells to another tube containing 90 µl trypan blue. The cells were then added onto the haemocytometer and were counted using a light microscope. The cells were then transferred to screw cap tube and were stored at -80°C.

5.2.3 Genome extraction:

The ASFV genome was extracted from whole blood, erythrocytes, plasma and the PBMC using the MagVet™ Universal Isolation Kit (Thermo Fisher Scientific, Waltham, MA, USA), according to the manufacturers protocol. The genomic DNA was isolated from the lysed samples by using high-throughput KingFisher™ Flex Extraction System, KingFisher with 96 PCR head (Thermo Fisher Scientific, Waltham, MA, USA).

5.2.4 Real time qPCR:

The quantification of ASFV genome was performed by using Brilliant III Ultra-Fast QPCR Master Mix kit and with the QPCR machine Mx3005P (Agilent technologies,

LDA, UK Ltd), according to the published protocol for detection of ASFV (King et al., 2003).

List of Buffers

Buffer Used	Recipe
TAE (Tris-acetate buffer)	EDTA disodium salt 50 mM (MW=372.24 g/mol), Tris 2 M (MW=121.14 g/mol),acetic acid 1 M (60.05)
10X TGS (Tris-glycine-SDS) (Biorad)	25 mM Tris, 192 mM glycine, 0.1% SDS, pH 8.3
Transfer buffer per 1000ml	10X TGS (100ml), Methanol (200 ml), ddH2O (700ml).
2X sample buffer (santa cruz biotechnology)	Glycerol, TCEP-HCl, DTT, SDS, MES, EDTA, Triton X-100 and bromophenol blue.
Ligation buffer (Promega, UK)	10mM Tris-HCl (pH 7.4 at 25°C), 50mM KCl, 1mM DTT, 0.1mM EDTA and 50% glycerol.
PBS	NaCl (mw: 58.4 g/mol) 8 g (concentration 0.137 M), KCl (mw: 74.551 g/mol) 200 mg (concentration 0.0027 M), Na2HPO4 (mw: 141.96 g/mol) 1.44 g (concentration 0.01 M), KH2PO4 (mw: 136.086 g/mol) 245 mg (concentration 0.0018 M).
0.2 % Triton X- 100 (Sigma, UK)	PBS (500ml), Triton (1ml)

CutSmart buffer (NEB, UK)- used for digestion	50 mM Potassium Acetate, 20 mM Tris-acetate, 10 mM Magnesium Acetate, 100 µg/ml BSA.
Blocking buffer	BSA 2.5g (Bovine Serum Albumin) (Sigma, UK), PBS (500ml).

APPENDIX 1;

S.No	Oligo Name	Sequence	Function
1.	EP402R Left flank fwd	GCGC**AAGCTT**CCTATTTTTGAATTTCATGTTGTGATGG	For amplifying left flank of CD2v, region upstream of the CD2v gene
2.	EP402R Left flank REV	GCGC**GAATTC**CTATTATTATCATTTTATACACATATATG	
3.	EP402R Right flank fwd	GCGC**GAATT**CCATGTATTTATTAAATACCACG	For amplifying right flank of CD2v, region upstream of the CD2v gene
4.	EP402R Right flank Rev	GCGCC**TCGAGC**TTCATCCGTGGGGGTGAGGGAGG	
5.	Benin EP402R(CMV)FWD	GCGC**ggatcc**CATATATGTGTATAAAATGATAATAATAG	For amplifying CD2v gene along with HA tag and stop codon, without the viral promoter.
6.	Benin EP402R(CMV+ VP)REV	**GCGGCCGC**AGCGTAATCTGGAACATCGTATGGGTACGCGAATTCAATAATTCTATCTACATGAATAAGCG	
7.	Benin EP402R(VP)FWD	GCGC**ggatcc**GTAGACAATTAAATGGTACACTTGC	For amplifying CD2v gene along with HA tag and stop codon, the viral promoter.
8.	Benin EP402R(CMV+ VP)REV	**GCGGCCGC**AGCGTAATCTGGAACATCGTATGGGTACGCGAATTCAATAATTCTATCTACATGAATAAGCG	
9.	Benin EP402R FWD	GTAGACAATTAAATGGTACACTTGC	For amplifying CD2v gene without viral

10	Benin EP402R Rev	CACATGATGTTCTCGATGATCCGCCAC	promoter, HA tag, and stop codon.
11	CD2v_Ig domain_ FWD	CGGAGTACTCTAAACCAAAC	For inserting ScaI and MfeI restriction enzyme sites to the mutant Ig domain fragments.
12	CD2v_Ig domain_ Rev	CGGATATCTCCATTAGTATC	
13	Ig domain (REV) MfeI	GCCCAATTGTATTGTTAATAATTAAAT	
14	T7 forward	TAATACGACTCACTATAGGG	Used for sequencing
15	BGH reverse	TAGAAGGCACAGTCGAGG	Used for sequencing

APPENDIX 2 (Clinical score sheets- Courtesy by the Pirbright Institute)

ITEM	Score	Description/Lesion
External examination		
Body condition	0-4	0: Normal → 4: Cachectic
Eyes/conjunctiva	0-3	1: Slight hyperaemia 2: Hyperaemia, swelling of eyelids and clear ocular discharge 3: Congested ocular mucosa with haemorrhages, inflamed eyelids and intense cloudy ocular discharge (gummed up eyes)
Nostrils	0-3	1: Moderate nasal discharge 2: Intense mucosal nasal discharge 3: Foam material in nostrils 3: Nasal haemorrhages (epistaxis)/blood traces around nostrils
Tonsils	0-3	2: Erythema in tonsils 3: Necrotic areas in tonsils
Oral cavity	0-3	3: Necrotic areas in tongue 3: Foamy material in mouth
Skin	0-6	1: Areas with skin erythema (ears, flanks, abdomen)

		1: Cyanotic areas (tip of the ears or tail, distal limbs, chest and abdomen) 3: Generalized reddening of the skin with haemorrhages all over body 4: Varioliform skin eruptions 4: Abscess 5: Necrotic areas on skin/chronic skin ulcers 6: Necrotic areas/chronic skin ulcers all over the body
Subcutis	0-3	2: Areas with subcutaneous oedema, haemorrhages and haematomas 3: Generalized subcutaneous oedema, haemorrhages and haematomas all over the body
Musculoskeletal system		
Skeletal muscle	0-3	2: Areas with oedema/haemorrhages within the fascial planes 3: Generalized oedema/haemorrhages within the fascial planes all over the body
Joints	0-4	3: Moderate joint swelling due to serofibrinous periarthritis/arthritis [1] 4: Severe joint swelling with difficulty walking due to purulent periarthritis/arthritis[1]
Thoracic cavity		
Exudates	0-3	1: Moderate hydrothorax (with reddish fluid) 2: Severe hydrothorax (with deep red fluid) 3: Haemothorax
Pericardium	0-3	1: Moderate hydropericardium (with reddish fluid) 2: Severe hydropericardium (with reddish fluid) 3: Hemopericardium 3: Fibrinous pericarditis
Heart	0-3	1: Petechial haemorrhages on epicardium 2: Variable presence of petechial haemorrhages/ecchymoses on epicardium, myocardium and endocardium 3: Haemorrhagic heart with extensive coalescent haemorrh (ecchymoses) on epicardium, myocardium and endocardium
Lung (lack of) collapse	0-3	1: Mild lack of collapse with no rib's impressions 2: Moderate lack of collapse with mild or scarce ribs impressions 3: Moderate to severe lack of collapse with apparent ribs impressions
Congestion/haemorrhage	0-3	1: Mild congestion or active hyperaemia, diffuse or patchy distributed in parenchyma. No haemorrhages 2: Variable degree of congest. or active hyperaemia. Multifocal to coalescent randomly distributed petechiae and purpurae

		3: Variable degree of congest/hyper. Multifocal to coalescent random and interlobul. distributed haemorrh (ecchymoses)
Oedema (foam in trachea)	0-3	1: Scarce or no presence of foamy material in trachea/bronchus (alveolar oedema) and minimal (interstitial oedema) 2: Mild to moderate presence of foamy material in trachea/bronchus and moderate distension of interlobular walls 3: Marked presence of foamy material in trachea/brochus and intense distension of interlobular walls
Consolidation of pulmonar parenchyma	0-4	1: Minimal to mild cranio-ventral (uni/bilateral) consolidation (bronchopneumonia) 2: Moderate cranio-ventral (uni/bilateral) consolidation (bronchopneumonia) 3: Marked-extended cranio-ventral (uni/bilateral) consolidation bronchopneum. (with red and grey hepatization of lobules) 4: Necrotic pneumonia 4: Purulent lesions
Pleura	0-3	3: Fibrinous pleuritis/pleural adhesions
Abdominal cavity		
Ascites	0-4	1: Slight 2: Moderate 3: Intense 4: Hemoabdomen
Stomach	0-4	1: Petechiae on serosa surface 2: Petechiae/ecchymoses on serosa surface 3: Petechiae/ecchymoses on serosa & haemorrhages on mucosa surface 4: Necrotic areas/ulcers
Duodenum	0-4	1: Petechiae on serosa surface 2: Petechiae/ecchymoses on serosa surface 4: Petechiae/ecchymoses on serosa & haemorrhages on mucosa surface 4: Necrotic areas/ulcers
Jejunum	0-4	
Ileum	0-4	
Ileoceal valve	0-4	
Cecum	0-4	
Colon	0-4	
Rectum	0-4	
Gastrointestinal content	0-4	1: Absence of gastric content 2: Scarce mucous-liquid content 3: Presence of digested blood content (black) 4: Presence of fresh hemorrhagic content (red)
Liver	0-3	1: Mild multifocal parenchymatous colour changes with slight hepatomegaly 2: Hepatomegaly, moderate congestion and presence multifocal punctiform redness areas/haemorrhages

		3: Hepatomegaly, intense congestion and presence of coalescent punctiform redness areas/ haemorrhages
Gallbladder	0-4	1: Mild to moderate oedema affecting gallbladder wall/cystic duct 2: Oedema affecting gallbladder wall/cystic duct with haemorrhages on serosa/submucosa surface 3: Intense oedema affecting gallbladder wall/cystic duct with severe haemorrhages on ser/subm surface and blood clots 4: Necrotic areas/ulcers
Urinary system		
Kidney	0-1	1: Perirrenal oedema
Parenchymal kidney hemmorhages (cortico-medular)	0-3	1: Mild multifocal cortical and medullar petechiae with multifocal vascular angiectasia 2: Moderate multifocal cortical (petechiae) and medullar (purpurae) haemorrhages with moderate pelvic dilation 3: Marked diffuse cor-med haemo. with diffuse general renal darkness, marked pelvic dilation and extens. subcapsul haemo
Parenchymal kidney hemmorhages (medulo-cortical)	0-3	1: Minimal to mild multifocal cortical and medullar petechiae 2: Moderate multifocal cortical and medullar haemorrhages (petechiae) with preponderance of cortical affectation 3: Marked multif. cor-med petechiae with preponder. of cortical affectation with/without multif. moderate pelvic purpurae
Urinary Bladder	0-3	1: Mild multifocal petechiae on mucosa surface without/with mild colour changes in urinary bladder wall 2: Multifocal petechiae and ecchymoses on mucosa, submucosa and serosa with oedema in urinary bladder wall 3: Coalescent haemo. on muc. Subm. and ser. with intense oedem. in urin. bladd. wall and presence of clots on muc. surface
Lymphoid system		
Spleen	0-4	1: Mild hyperemic splenomegaly (minimal to mild bleeding after sectioning) 2: Moderate/partial hyperemic splenomegaly (moderate bleeding after sectioning) 3: Intense hyperemic splenomegaly (marked bleeding after sectioning) 3: Focal necrosis/infarcts 4: Hyperplasic splenomegaly (no bleeding after sectioning)/cicatrization of partial hyperemic splenomegaly
Submandibular LN	0-3	

Retropharingeal LN	0-3	1: Increased size and edematous with moderate colour changes 2: Increased size, edematous and haemorrhagic 3: Increased size, edematous and completely haemorrhagic similar to a blood clot 4: Hyperplasia without haemorrhagic changes/with occasional peripheral haemorrhages
Tracheobronchial LN	0-3	
Gastrohepatic LN	0-3	
Renal LN	0-3	
Mesenteric LN	0-3	
Thymus	0-2	1: Moderate colour changes with occasional petechiae 2: Petechiae and ecchymoses
Endochrine system		
Thyroid gland	0-1	1: Increased size/haemorrhages
Adrenal gland	0-1	
Pancreas	0-1	
Nervous system		
Brain	0-4	1: Hyperemic meninges/oedema 2: Hyperemia with occasional petechiae 3: Severe vascular changes with petechiae and ecchymoses 4: Meningitis (meninges appear thickened with loss of transparency)
Cerebellum	0-4	
Medulla oblongata	0-4	

Appendix-3 (3rd batch of mutants):

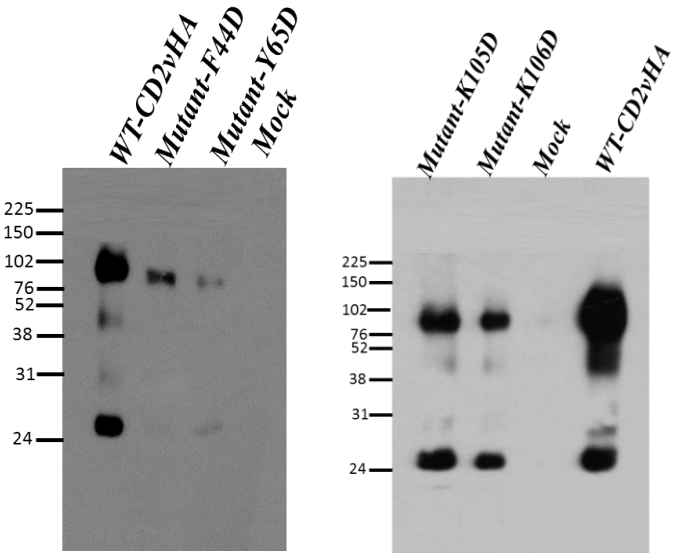

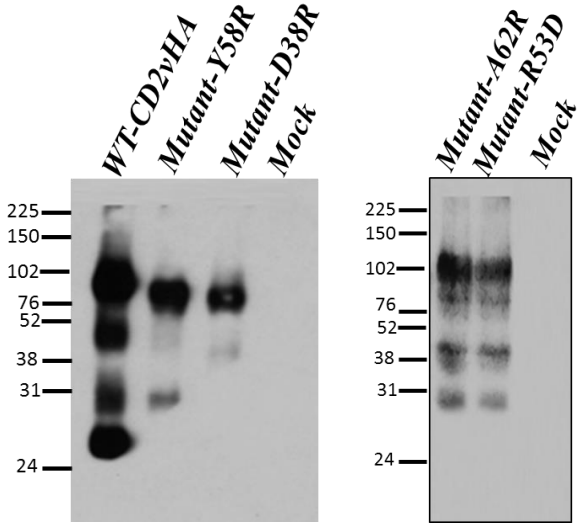
WT-CD2vHA
Mutant-Y58R
Mutant-D38R
Mock
Mutant-A62R
Mutant-R53D
Mock
225
150
102
76
52
38
31
24
225
150
102
76
52
38
31
24

6.0 Summary:

The aim of this project was to investigate the molecular mechanisms involved in the binding of red blood cells to ASFV infected cells. This knowledge was used to determine the role of HAD in ASFV persistence in blood and induction of clinical signs in pigs infected with gene-deleted or gene-modified ASFV.

To achieve this the first objective was to determine the key functional residues in CD2v that are involved in the attachment of red blood to the ASFV infected cells and to extracellular virions. This was performed by introducing single or multiple amino acid substitutions in the extracellular immunoglobulin domain-1 of CD2v. The information about the possible functional amino acid residues was obtained from various sources; the previously published data on human CD2, from an online predicted model, and from a model generated by the collaborators (Dr. Simon Davies & Dr. Shinji Ikemizu).

The expression of mutant CD2v proteins were analysed by Western blot and confocal microscope and the effect of the mutations on attachment of RBC was determined by a HAD assay. The expression analysis of mutant CD2v showed that the mutants were expressed, processed by glycosylation, cleaved in to correct forms and sizes, and localised similar to the WT-CD2v although some may have been expressed at a lower level than others. In total 21 mutant CD2v proteins were designed/tested. Two mutants with single amino acid substitutions and several with multiple amino acid substitutions when expressed alone in mammalian cells induced reduced or no binding of red blood cells. The mutant CD2vY102D and the mutant CD2v2.2 (N52A, R53A, N55A, N77A, E99A, D104A, K105A, K106A, and N108A) showed a reduced HAD while the mutant CD2vE99R completely abrogated the attachment of RBC. The mutant CD2vE99R, CD2vY102D were detected on the cell surface in non permeabilized cells using pig

serum from ASFV infected pigs to confirm that they are transported to the cell's surface. The identification of the functional residues gave an indication of the possible ligand binding domain of the CD2v. These findings provide the first indication for the location of the CD2v RBC ligand binding domain and could be extended to map in finer detail the ligand binding domain, it could be also used to identify the functional amino acid residues in CD2v encoded by other isolates.

The mutant CD2vE99R and CD2vY102D were then tested in ASFV infected cells to determine if the mutants retain the reduced or non-HAD phenotype and also to investigate if the virus encodes other molecular mechanism involved in the HAD. The expression analysis of mutant CD2vE99R and CD2vY102D showed that the mutants are expressed, processed, cleaved in to correct forms and sizes, and localised similar to the WT-CD2v. Interestingly, when mutant CD2vE99R and CD2vY102D were analysed by HAD in cells infected with ASFV from which the CD2v gene was deleted (BeninΔCD2v) it was observed that the mutant CD2v proteins CD2vE99R and CD2vY102D induced HAD similar to the wild type CD2v. The investigation led to another novel finding that ASFV encoded C-type lectin/EP153R gene is also involved in HAD as the mutant CD2vE99R and CDvY102D were non-HAD when tested by expression in cells infected with ASFV isolate OURT88/3 which has non-functional interrupted EP153R and CD2v genes. The role of the EP153R in HAD was further investigated. It was confirmed that EP153R does not induce HAD when expressed alone in cells. The expression analysis of an epitope tagged EP153R showed that it is expressed on the cell surface both in transfected and ASFV-infected cells. These findings open other avenues to investigate, apart from the role of EP153R in augmenting HAD, such as the role of EP153R in attachment to other cells and the

potential role in immune evasion or pathogenesis. It was also observed that CD2v and EP153R co-localise on the cell surface in transfected cells.

To investigate the role of CD2v in virus persistence in pigs, a recombinant virus lacking CD2v (BeninΔDP148RΔCD2v) was constructed (by Dr Anusyah Rathakrishnan, The Pirbright Institute) and used in an immunisation and challenge experiment in pigs. The virus persistence in pigs was significantly reduced (from 60 days to 11) and the onset of clinical signs post immunisation was delayed by 1 day compared to the parental attenuated ASFV (BeninΔDP148R). This virus (BeninΔDP148RΔCD2v) provided 100% protection to the pigs following challenge and the significant reduction in the virus persistence clearly demonstrated the role of CD2v in virus persistence in blood for extended periods. Since the *in vitro* analysis of mutant CD2v proteins (CDvE99R and CD2vY102D) showed that EP153R is involved in enhancing HAD, another recombinant virus (BeninΔDP148RΔEP153RΔCD2v) was constructed (by Dr Anusyah Rathakrishnan, The Pirbright Institute) with both CD2v and EP153R deleted.

The recombinant virus (BeninΔDP148RΔEP153RΔCD2v) was used in immunization and challenge experiment to determine the role of EP153R in pigs. Surprisingly, no viremia or clinical signs were observed in pigs post-immunisation and the virus provided 75% protection to the pigs following challenge. Since there was no viremia post-immunization it was difficult to conclude if EP153R is involved in virus persistence but overall results clearly showed that deletion of EP153R further attenuated the virus. To balance the level of virus attenuation, a recombinant virus (BeninΔDP148RΔEP153R-CD2vE99R) was generated, this was made from the parental BeninΔDP148R virus in a single step to delete EP153R and replace the wild type CD2v with CD2vE99R.

The recombinant virus (BeninΔDP148RΔEP153R-CD2vE99R) was used in an immunization and challenge experiment to determine the effect of CD2vE99R in pigs. Interestingly, the virus persistence in blood in pigs post immunization was reduced to 2 days, the onset and duration of clinical signs was decreased (1 day) and the viremia was also reduced by approximately 3 logs. This demonstrated that deletion of EP153R and the insertion of mutant CD2vE99R balanced the level of virus attenuation, and hence resulted in a reduced virus persistence, mild clinical signs for a reduced duration, a decrease in viremia and provided an overall protection of 83.3%. This recombinant virus has an increased safety profile compared to the parental vaccine candidate (BeninΔDP148R) and satisfy the pre-requisites set for an efficacious vaccine against ASFV.

The questions that remained unanswered and would be interesting to investigate include;

What other residues are present in the ligand binding domain?

The analysis of mutant CD2v proteins and the prediction from the CD2v Ig-domain indicated that the E99 residue is possibly in the ligand binding domain, which is located in the F loop of the β- sheets. Previous studies showed that the ligand binding domain of human CD2 is present in the GFCC' loops of the β- sheets. In mutant CD2v proteins the G and F loops were mostly targeted, in total six different amino acid residue (E99, Y102, L103, D104, K105, K106) were substituted individually in this region and 2 mutants (E99, Y102) showed either a partial or complete inhibition of the binding with its ligand (see figure 3.17). These residues are located in lower half of the F loop while all other residues analysed by mutation are present in the top half of the F loop. This suggests that the ligand binding domain is possibly at the bottom of the molecule and

therefore the residues in the lower half of GF loop may possibly be in the ligand binding domain. The predicted functional residues in this region may include; T97, T110, K112 and K115. Ultimately high-level expression of the extracellular domain of CD2v and crystallisation to obtain a detailed structure would reveal at atomic resolution the structure of this region. Similar methods could be used as those used to obtain the structure of CD2v.

What is the ligand for CD2v? And is the ligand expressed on other cells?

The ligand for human CD2 is CD58 and CD59 and is widely distributed on different cells including antigen presenting cells. Similarly, the ligand for rat CD2 is CD48 and is widely distributed however the ligand for CD2v is not known. To determine if CD58 is also a ligand for CD2v different approaches could be used. (i) by blocking CD58 with an anti-CD58 antibody on erythrocytes and analysis by HAD assay (ii) by a yeast two hybrid system to determine if the CD2v interacts with CD58 (iii) by co-immunoprecipitation. It is possible that CD2v binds to other ligands. These could be identified using different approaches for example by expression of a cDNA library cloned from RBC and screening for binding of a recombinant CD2v extracellular domain. Identifying the ligand would also indicate if it may be expressed on other cells and hence extend the possible roles of CD2v in virus pathogenesis or immune evasion.

Is CD2v also involved in virus entry?

CD2v is a highly glycosylated glycoprotein with predicted 19 putative glycosylation sites, of which 18 are located in the extracellular N-terminal domain. When the mature virus particles egress from the cells they acquire the outer envelope which contains CD2v and a high numbers of glycans. The binding of glycans (present on CD2v and on extracellular virus) with lectins on APC may induce phagocytosis, as reported in other

vertebrates suggesting its role in virus entry. Although no difference was observed in replication of virus lacking CD2v this may be due to the fact that ASFV uses multiple mechanisms to enter the cells.

What other possible roles does C-type lectin may have? And how is it involved in HAD?

The *in vitro* analysis of EP153R expression in ASFV-infected cells has indicated its role in HAD, EP153R encodes for a C-type lectin which may bind to glycans expressed on other cells. The erythrocytes contain a large number of sugars on its membrane and these play an important role in the physiology of the RBC. The sialic acid is one of the glycans that are found on the membrane of the erythrocytes, the C-type lectin may possibly binds with the glycans on RBC and enhance HAD by increasing the interaction between ASFV infected cells and RBC. Although EP153R has not as yet been detected on the surface of extracellular virions further investigation should be carried out. To do this a recombinant virus expressing an epitope-tagged EP153R gene could be used to enable the presence of EP153R in virions and on the surface of infected cells to be followed.

Another possibility is that C-type lectin may enhance the cell surface expression of CD2v. C-type lectin has been shown to modulate the expression of MHC-1 on the cell surface by impairing the exocytosis process and is therefore possible that it may regulate the cellular trafficking and enhance the cell surface expression of CD2v. The preliminary data showed that C-type lectin and CD2v co-localise in transfected cells, this suggests that either both proteins interact or the proteins are in the secretory pathway at the same time in transfected cells. The interaction between CD2v and the

C-type lectin could be determined by using the proximity ligation assay or co-immuno precipitation.

The EP153R sequence contain a cell attachment (RGD) motif and shares a significant homology with the N-terminal region of CD44 molecules which is involved in cellular adhesion and T-cell activation. I detected C-type lectin on the cell surface in non-permeable ASFV infected cells. When the mature virus particle egresses from the cells they acquire the outer envelope which contains CD2v and possibly EP153R. Since C-type lectin can bind to glycans and also contain the RGD attachment motif, it may also be involved in the attachment of virus to other cells.

Investigation of safety issues relating to vaccine development:

The results indicate that the BeninΔDP148RΔEP153RCD2vE99R is a possible candidate for further development as a vaccine, its further development would depend on further testing of safety and efficacy. These include testing safety and efficacy at different doses and after repeat and overdoses. Other key question include: do immunised pigs shed enough virus to infect other pigs either before or after challenge? To control outbreaks a vaccine should inhibit spread of the challenge virus to non-immune animals.

The infection of ASFV initiates in the pigs via oral-nasal route, by the tick bite and by scratches. The infected pigs can shed the virus and is detectable in faeces, urine, oral and nasal fluids discharges, the virus can also be detected in air samples however this was associated with detection of virus in faeces. The infectious dose of ASFV via the oral and nasal route is estimated to be 10 HAD50 which means even a small amount of infective material could lead to transmission. It was shown that faecal samples may contain up to $10^{4.8}$ TCID50/g and urine samples contain $10^{2.94}$ TCID50/ml infectious

virus and therefore the excretion of ASFV in the faeces and urine of infected pigs may be an important route of transmission of ASFV in pigs that are housed together (Davies et al., 2017).

All this data is based on either highly or moderately ASFV isolates, the virus shedding and transmission largely vary among different isolates. Transmission using a low virulence non-HAD ASFV strain showed that Non-HAD viruses could be transmitted by contact but with a lower efficiency (42-50 %) compared with HAD virulent ASFV strain (100%) (Boinas et al., 2004). Another study where a recombinant virus ASFV-G-Δ9GL was analysed, the infected pigs developed low to medium viremia however the virus was not detected in the nasal cavities. Pigs infected ASFV-G-ΔI177L also developed low viremia but showed no virus shedding (Borca et al., 2020) .

In the current study the viremia in pigs immunised with BeninΔDP148RΔEP153R-CD2vE99R was detected at lower levels (between 10^2 to $10^{3.8}$ genome copies/ml) at viremia peak. It is therefore unlikely that the pigs will shed enough virus to infect other pigs, however, the infectious virus at viremia post challenge was detected at ($10^{2.5}$ to 10^5 HAD_{50}/ml) which gradually declined and no virus was detected by termination in 4/5 pigs. It is possible that the pigs may shed virus during the viremia peak post challenge, however it requires further investigation to determine the safety parameters of the vaccine candidate.

Is the cost effective production of the vaccine candidate possible?

MLAV are the most promising vaccine candidates against ASFV however there are challenges associated with the safe and cost effective production of these candidates. One major challenge is the requirement of high biocontainment facility for the production of the attenuated virus, other challenges include the availability of a suitable

cell line for the production. The vaccine could be produced in porcine bone marrow cell in high titres, however, it's unlikely to be used in production of the virus due to variation among different batches of cells and due to the high cost associated with it. This issue could be overcome by the adaptation of some ASFV isolates to grow in different stable cell lines, such as Vero cells, which have been routinely used for biological studies, production, and purification of the adapted virus. However, the adaptation of ASF viruses has always resulted in genomic changes. Different cell lines of porcine monocyte origin have been developed which support the growth of ASFV including: ZMAC, WSL, and IPAM WT. In addition, the COS-cell line has shown to be highly efficient to support the replication of ASF viruses with little adaptation. The MLAV BA71ΔCD2 produced in COS cells was an effective vaccine able to confer homologous and heterologous protection. The use of these cell lines for production of the virus can significantly reduce the cost and satisfy the pre-requisite of the efficacious vaccine by the regulatory authorities. However, further evaluation studies are required to determine a suitable cell line that has a minimal or no effect on the candidate vaccine genome during production.

What would be the ideal vaccine against ASF?

- The ideal MLAV must have the following requisites before reaching the market;
- The vaccine should provide sterile immunity which would improve the safety by reducing the risk of transmission in the contact animal on the farms.
- The vaccine candidate shown demonstrate to be efficacious as well as safe for using in the field.
- The vaccinated pigs should be differentiated from non-vaccinated or naturally infected pigs.

- The vaccine should ideally be produced in stable cell lines, to comply with GMP according to the policies of regulatory agencies.
- Ideally the vaccine should provide heterologous protection against different viruses and genotypes.
- The identification of DIVA targets to differentiate between vaccinated and non-vaccinated animals is required in case of MLAV, which is likely to be the first vaccine available in the market against ASFV.

What are the major challenges in the development of viable and effective vaccine against ASF?

The main challenge in the development of vaccine is the complexity of ASFV and the lack of knowledge in understanding the mechanisms involved in the protection and the identification of antigens involved in inducing protection. Although a subunit vaccine would be the first choice but the lack of efficacy compared to MLAV is a major problem. On the other hand, MLAV have higher efficacy but have other disadvantages (safety, production, official registration, commercialization), however the MLAV will be the first technology to reach the market, while subunit vaccines will need much further research to become a successful commercial reality.

References :

Abrams, C. C., Goatley, L., Fishbourne, E., Chapman, D., Cooke, L., Oura, C. A., Netherton, C. L., Takamatsu, H. H., & Dixon, L. K. (2013). Deletion of virulence associated genes from attenuated African swine fever virus isolate OUR T88/3 decreases its ability to protect against challenge with virulent virus. *Virology*, *443*(1), 99-105. https://doi.org/10.1016/j.virol.2013.04.028

Achenbach, J. E., Gallardo. C, Pelegrın, E. N., Arroyo, B. R., Negi, T. D., Arias, M., Jenberie, S., Mulisa, D. D., Gizaw, D., Gelaye, E., Chibssa, T. R., Belaye, A., Loitsch, A., Forsa, M., Yami, M., Diallo, A., Soler, A., Lamien, C. E., & Vizcaino, M. S. (2016). Identification of a New Genotype of African Swine Fever Virus in Domestic Pigs from Ethiopia. *Transboundary and Emerging Diseases*, *64*, 1393–1404. https://doi.org/doi:10.1111/tbed.12511

Alejo, A., Andres, G., & Salas, J. (2003). African Swine Fever Virus Proteinase Is Essential for Core Maturation and Infectivity. *Journal of General Virology*, *77*(10), 5571–5577. https://doi.org/DOI: 10.1128/JVI.77.10.5571–5577

Alejo, A., Matamoros, T., Guerra, M., & Andres, G. (2018). A Proteomic Atlas of the African Swine Fever Virus Particle. *Journal of Virology*, *92*(23). https://doi.org/ARTN e01293-18

10.1128/JVI.01293-18

Alonso, C., Galindo, I., Cuesta-Geijo, M. A., Cabezas, M., Hernaez, B., & Munoz-Moreno, R. (2013). African swine fever virus-cell interactions: from virus entry to cell survival. *Virus Res*, *173*(1), 42-57. https://doi.org/10.1016/j.virusres.2012.12.006

Alonso, C., Miskin, J., Hernaez, B., Fernandez-Zapatero, P., Soto, L., Canto, C., Rodriguez-Crespo, I., Dixon, L., & Escribano, J. M. (2001). African swine fever virus protein p54 interacts with the microtubular motor complex through direct binding to light-chain dynein. *Journal of Virology*, *75*(20), 9819-9827. https://doi.org/Doi 10.1128/Jvi.75.20.9819-9827.2001

Andres, G. (2017). African Swine Fever Virus Gets Undressed: New Insights on the Entry Pathway. *J Virol*, *91*(4), 1-5. https://doi.org/10.1128/JVI.01906-16

Andres, G., Charro, D., Matamoros, T., Dillard, R. S., & Abrescia, N. G. A. (2020). The cryo-EM structure of African swine fever virus unravels a unique architecture comprising two icosahedral protein capsids and two lipoprotein membranes. *Journal of Biological Chemistry*, *295*(1), 1-12. https://doi.org/10.1074/jbc.AC119.011196

Andres, G., Escudero, R. G., Mateo, C. S., & Vinuela, E. (1998). African Swine Fever Virus Is Enveloped by a Two-Membraned Collapsed Cisterna Derived from the Endoplasmic Reticulum. *Journal of Virology*, *72*(11), 8988–9001.

Andres, G., Escudero, R. G., Vinuela, E., Salas, M. L., & Rodriguez, J. M. (2001). African Swine Fever Virus Structural Protein pE120R Is Essential for Virus Transport from Assembly Sites to Plasma Membrane but Not for Infectivity. *Journal of Virology*, *75*(15), 6758–6768. https://doi.org/DOI: 10.1128/JVI.75.15.6758–6768.2001

Argilaguet, J. M., Perez-Martin, E., Gallardo, C., Salguero, F. J., Borrego, B., Lacasta, A., Accensi, F., Diaz, I., Nofrarias, M., Pujols, J., Blanco, E., Perez-Filgueira, M., Escribano, J. M., & Rodriguez, F. (2011). Enhancing DNA immunization by targeting ASFV antigens to SLA-II bearing cells. *Vaccine*, *29*(33), 5379-5385. https://doi.org/10.1016/j.vaccine.2011.05.084

Argilaguet, J. M., Perez-Martin, E., Nofrarias, M., Gallardo, C., Accensi, F., Lacasta, A., Mora, M., Ballester, M., Galindo-Cardiel, I., Lopez-Soria, S., Escribano, J. M., Reche, P. A., & Rodriguez, F. (2012). DNA Vaccination Partially Protects against African Swine Fever Virus Lethal Challenge in the Absence of Antibodies. *PLoS One*, *7*(9). https://doi.org/ARTN e40942

10.1371/journal.pone.0040942

Arias, M., de la Torre, A., Dixon, L., Gallardo, C., Jori, F., Laddomada, A., Martins, C., Parkhouse, R. M., Revilla, Y., Rodriguez, F., & Sanchez-Vizcaino, J. M. (2017). Approaches and Perspectives for

Development of African Swine Fever Virus Vaccines. *Vaccines*, *5*(4), Article 35. https://doi.org/10.3390/vaccines5040035

Arulanandam, A. R. N., Kister, A., Mcgregor, M. J., Wyss, D. F., Wagner, G., & Reinherz, E. L. (1994). Interaction between Human Cd2 and Cd58 Involves the Major Beta-Sheet Surface of Each of Their Respective Adhesion Domains. *Journal of Experimental Medicine*, *180*(5), 1861-1871. https://doi.org/DOI 10.1084/jem.180.5.1861

Barasona, J. A., Gallardo, C., Cadenas-Fernandez, E., Jurado, C., Rivera, B., Rodriguez-Bertos, A., Arias, M., & Sanchez-Vizcaino, J. M. (2019). First Oral Vaccination of Eurasian Wild Boar Against African Swine Fever Virus Genotype II. *Frontiers in Veterinary Science*, *6*. https://doi.org/ARTN 137

10.3389/fvets.2019.00137

Boinas, F. S., Hutchings, G. H., Dixon, L. K., & Wilkinson, P. J. (2004). Characterization of pathogenic and non-pathogenic African swine fever virus isolates from Ornithodoros erraticus inhabiting pig premises in Portugal. *J Gen Virol*, *85*(Pt 8), 2177-2187. https://doi.org/10.1099/vir.0.80058-0

Borca, M. V., Carrillo, C., Zsak, L., Laegreid, W. W., Kutish, G. F., Neilan, J. G., Burrage, T. G., & Rock, D. L. (1998). Deletion of a CD2-like gene, 8-DR, from African swine fever virus affects viral infection in domestic swine. *Journal of Virology*, *72*(4), 2881-2889. <Go to ISI>://000072586900036

Borca, M. V., Kutish, G. F., Afonso, C. L., Irusta, P., Carrillo, C., Brun, A., Sussman, M., & Rock, D. L. (1994). An African swine fever virus gene with similarity to the T-Lymphocyte surface antigen CD2 mediates hemadsorption. *Virology*, *199*, 463-468.

Borca, M. V., Ramirez-Medina, E., Silva, E., Vuono, E., Rai, A., Pruitt, S., Holinka, L. G., Velazquez-Salinas, L., Zhu, J., & Gladue, D. P. (2020). Development of a Highly Effective African Swine Fever Virus Vaccine by Deletion of the I177L Gene Results in Sterile Immunity against the Current Epidemic Eurasia Strain. *Journal of Virology*, *94*(7). https://doi.org/ARTN e02017-19

10.1128/JVI.02017-19

Cackett, G., Matelska, D., Sykora, M., Portugal, R., Malecki, M., Bahler, J., Dixon, L., & Werner, F. (2020). The African Swine Fever Virus Transcriptome. *Journal of Virology*, *94*(9). https://doi.org/ARTN e00119-20

10.1128/JVI.00119-20

Carrascosa, A. L., Sastre, I., & Vinuela, E. (1991). African Swine Fever Virus Attachment Protein. *Journal of Virology*, *65*(5), 2283-2289. <Go to ISI>://A1991FG77700016

Carrascosa, J. L., Carazo, J. M., Carrascosa, A. L., Garcia, N., Santisteban, A., & Vinuela, E. (1984). General Morphology and Capsid Fine-Structure of African Swine Fever Virus-Particles. *Virology*, *132*(1), 160-172. <Go to ISI>://A1984SB96500015

Carrillo, C., Borca, M. V., Afonso, C. L., Onisk, D. V., & Rock, D. L. (1994). Long-term persistent infection of swine monocytes/macrophages with African swine fever virus. *J Virol*, *68*(1), 580-583. https://doi.org/10.1128/JVI.68.1.580-583.1994

Chapman, D. A., Tcherepanov, V., Upton, C., & Dixon, L. K. (2007). Comparison of the genome sequences of non-pathogenic and pathogenic African swine fever virus isolates. *J Gen Virol*, *89*(Pt 2), 397-408. https://doi.org/10.1099/vir.0.83343-0

Chenais, E., Depner, K., Guberti, V., Dietze, K., Viltrop, A., & Stahl, K. (2019). Epidemiological considerations on African swine fever in Europe 2014-2018. *Porcine Health Manag*, *5*, 6. https://doi.org/10.1186/s40813-018-0109-2

Chenais, E., & Fischer, K. (2018). Increasing the Local Relevance of Epidemiological Research: Situated Knowledge of Cattle Disease Among Basongora Pastoralists in Uganda. *Frontiers in Veterinary Science*, *5*. https://doi.org/ARTN 119

10.3389/fvets.2018.00119

Chenais, E., Stahl, K., Guberti, V., & Depner, K. (2018). Identification of Wild Boar-Habitat Epidemiologic Cycle in African Swine Fever Epizootic. *Emerging Infectious Diseases*, *24*(4), 810-812. https://doi.org/10.3201/eid2404.172127

Cobbold, C., & Wileman, T. (1998). The Major Structural Protein of African Swine Fever Virus,

p73, Is Packaged into Large Structures, Indicative of Viral

Capsid or Matrix Precursors, on the Endoplasmic Reticulum. *Journal of Virology*, *72*(6), 5215-5223.

Coelho, J., Ferreira, F., Martins, C., & Leitao, A. (2016). Functional characterization and inhibition of the type II DNA topoisomerase coded by African swine fever virus. *Virology*, *493*, 209-216. https://doi.org/10.1016/j.virol.2016.03.023

Costard, S., Mur, L., Lubroth, J., Sanchez-Vizcaino, J. M., & Pfeiffer, D. U. (2013). Epidemiology of African swine fever virus. *Virus Res*, *173*(1), 191-197. https://doi.org/10.1016/j.virusres.2012.10.030

Costard, S., Wieland, B., de Glanville, W., Jori, F., Rowlands, R., Vosloo, W., Roger, F., Pfeiffer, D. U., & Dixon, L. K. (2009). African swine fever: how can global spread be prevented? *Philos Trans R Soc Lond B Biol Sci*, *364*(1530), 2683-2696. https://doi.org/10.1098/rstb.2009.0098

Das, S. C., Baron, M. D., Skinner, M. A., & Barrett, T. (2000). Improved technique for transient expression and negative strand virus rescue using fowlpox T7 recombinant virus in mammalian cells. *Journal of Virological Methods*, *89*(1-2), 119-127. https://doi.org/Doi 10.1016/S0166-0934(00)00210-X

Davies, K., Goatley, L. C., Guinat, C., Netherton, C. L., Gubbins, S., Dixon, L. K., & Reis, A. L. (2017). Survival of African Swine Fever Virus in Excretions from Pigs Experimentally Infected with the Georgia 2007/1 Isolate. *Transbound Emerg Dis*, *64*(2), 425-431. https://doi.org/10.1111/tbed.12381

Davis, S. J., Davies, E. A., Tucknott, M. G., Jones, E. Y., & van der Merwe, P. A. (1998). The role of charged residues mediating low affinity protein–protein recognition at the cell surface by CD2. *Proceedings of the National Academy of Sciences of the United States of America*, *95*(10), 5490-5494. https://doi.org/https://doi.org/10.1073/pnas.95.10.5490

De Silva, F. S., Lewis, W., Berglund, P., Koonin, E. V., & Moss, B. (2007). Poxvirus DNA primase. *Proceedings of the National Academy of Sciences of the United States of America*, *104*(47), 18724-18729. https://doi.org/10.1073/pnas.0709276104

del Moral, M. G., Ortuno, E., Fernandez-Zapatero, P., Alonso, F., Alonso, C., Ezquerra, A., & Dominguez, J. (1999). African swine fever virus infection induces tumor necrosis factor alpha production: Implications in pathogenesis. *Journal of Virology*, *73*(3), 2173-2180. <Go to ISI>://000078603800050

Dixon, L. K., Chapman, D. A., Netherton, C. L., & Upton, C. (2013). African swine fever virus replication and genomics. *Virus Res*, *173*(1), 3-14. https://doi.org/10.1016/j.virusres.2012.10.020

Dixon, L. K., Stahl, K., Jori, F., Vial, L., & Pfeiffer, D. U. (2020). African Swine Fever Epidemiology and Control. *Annual Review of Animal Biosciences, Vol 8, 2020*, *8*, 221-246. https://doi.org/10.1146/annurev-animal-021419-083741

Driscoll, P. C., Cyster, J. G., Campbell, I. D., & Williams, A. F. (1991). Structure of Domain-1 of Rat Lymphocyte-T Cd2 Antigen. *Nature*, *353*(6346), 762-765. <Go to ISI>://A1991GL69600071

Epifano, C., Locker, J. K., Salas, M. L., Rodriguez, J. M., & Salas, J. (2006). The African Swine Fever Virus Nonstructural Protein pB602L Is Required for Formation of the Icosahedral Capsid of the Virus Particle. *Journal of Virology*, *80*(24), 12260–12270. https://doi.org/doi:10.1128/JVI.01323-06

Freitas, F. B., Frouco, G., Martins, C., & Ferreira, F. (2019). The QP509L and Q706L superfamily II RNA helicases of African swine fever virus are required for viral replication, having non-redundant activities. *Emerging Microbes & Infections*, *8*(1), 291-302. https://doi.org/10.1080/22221751.2019.1578624

Frouco, G., Freitas, F. B., Coelho, J., Leitao, A., Martins, C., & Ferreira, F. (2017). DNA-Binding Properties of African Swine Fever Virus pA104R, a Histone-Like Protein Involved in Viral Replication and Transcription. *Journal of Virology*, *91*(12). https://doi.org/ARTN e02498-16

UNSP e02498-16

10.1128/JVI.02498-16

Galindo, I., Almazan, F., Bustos, M. J., Vinuela, E., & Carrascosa, A. L. (2000). African swine fever virus EP153R open reading frame encodes a glycoprotein involved in the hemadsorption of infected cells. *Virology*, *266*(2), 340-351. https://doi.org/10.1006/viro.1999.0080

Galindo, I., & Alonso, C. (2017). African Swine Fever Virus: A Review. *Viruses-Basel*, *9*(5). https://doi.org/ARTN 103

10.3390/v9050103

Garcia-Escudero, R., Andres, G., Almazan, F., & Vinuela, E. (1998). Inducible gene expression from African swine fever virus recombinants: Analysis of the major capsid protein p72. *Journal of Virology*, *72*(4), 3185-3195. <Go to ISI>://000072586900073

Gaudreault, N. N., & Richt, J. A. (2019). Subunit Vaccine Approaches for African Swine Fever Virus. *Vaccines*, *7*(2). https://doi.org/ARTN 56

10.3390/vaccines7020056

Ge, S. Q., Li, J. M., Fan, X. X., Liu, F. X., Li, L., Wang, Q. H., Ren, W. J., Bao, J. Y., Liu, C. J., Wang, H., Liu, Y. T., Zhang, Y. Q., Xu, T. G., Wu, X. D., & Wang, Z. L. (2018). Molecular Characterization of African Swine Fever Virus, China, 2018. *Emerging Infectious Diseases*, *24*(11), 2131-2133. https://doi.org/10.3201/eid2411.181274

Goatley, L. C., & Dixon, L. K. (2011). Processing and localization of the african swine fever virus CD2v transmembrane protein. *J Virol*, *85*(7), 3294-3305. https://doi.org/10.1128/JVI.01994-10

Goatley, L. C., Reis, A. L., Portugal, R., Goldswain, H., Shimmon, G. L., Hargreaves, Z., Ho, C. S., Montoya, M., Sanchez-Cordon, P. J., Taylor, G., Dixon, L. K., & Netherton, C. L. (2020). A Pool of Eight Virally Vectored African Swine Fever Antigens Protect Pigs against Fatal Disease. *Vaccines*, *8*(2). https://doi.org/ARTN 234

10.3390/vaccines8020234

Gogin, A., Gerasimov, V., Malogolovkin, A., & Kolbasov, D. (2013). African swine fever in the North Caucasus region and the Russian Federation in years 2007-2012. *Virus Res*, *173*(1), 198-203. https://doi.org/10.1016/j.virusres.2012.12.007

Gomez-Puertas, P., RODRI´GUEZ, F., Oviedo, J. M., A, B., Alonso, C., & Escribano, J. M. (1998). The African Swine Fever Virus Proteins p54 and p30 Are Involved in Two Distinct Steps of

Virus Attachment and Both Contribute to the Antibody-Mediated Protective Immune Response. *Virology*, *243*, 461-471, Article VY989068.

Gomez-Puertas, P., Rodriguez, F., Oviedo, J. M., Brun, A., Alonso, C., & Escribano, J. M. (1998). The African swine fever virus proteins p54 and p30 are involved in two distinct steps of virus attachment and both contribute to the antibody-mediated protective immune response. *Virology*, *243*(2), 461-471. <Go to ISI>://000073371100020

Gomez-Villamandos, J. C., Bautista, M. J., Sanchez-Cordon, P. J., & Carrasco, L. (2013). Pathology of African swine fever: the role of monocyte-macrophage. *Virus Res*, *173*(1), 140-149. https://doi.org/10.1016/j.virusres.2013.01.017

Gomez-Villamandos, J. C., Carrasco, L., Bautista, M. J., Sierra, M. A., Quezada, M., Hervas, J., De Lara, F. C. M., Ruiz-Villamor, E., Salguero, F. J., Sonchez-Cordon, P. J., Romanini, S., Nunez, A., Mekonen, T., Mendez, A., & Jover, A. (2003). African swine fever and classical swine fever: a review of the pathogenesis. *Deutsche Tierarztliche Wochenschrift*, *110*(4), 165-169. <Go to ISI>://WOS:000183294200009

Gonzalez, A., Talavera, A., Almendral, J. M., & Vinuela, E. (1986). Hairpin Loop Structure of African Swine Fever Virus-DNA. *Nucleic Acids Research*, *14*(17), 6835-6844. <Go to ISI>://A1986E041300004

Granja, A. G., Nogal, M. L., Hurtado, C., Salas, J., Salas, M. L., Carrascosa, A. L., & Revilla, Y. (2004). Modulation of p53 cellular function and cell death by African swine fever virus. *Journal of Virology*, *78*(13), 7165-7174. <Go to ISI>://000222153800049

Greig, A. (1972). Pathogenesis of African swine fever in pigs naturally exposed to the disease. *J Comp Pathol*, *82*(1), 73-79. https://doi.org/10.1016/0021-9975(72)90028-x

Guinat, C., Gogin, A., Blome, S., Keil, G., Pollin, R., Pfeiffer, D. U., & Dixon, L. (2016). Transmission routes of African swine fever virus to domestic pigs: current knowledge and future research directions. *Veterinary Record*, *178*, 262-267. https://doi.org/doi: 10.1136/vr.103593

Hammond-Kosack, M. C., Kilpatrick, M. W., & Docherty, K. (1992). Analysis of DNA structure in the human insulin gene-linked polymorphic region in vivo. *J Mol Endocrinol*, *9*(3), 221-225. https://doi.org/10.1677/jme.0.0090221

Hernaez, B., Guerra, M., Salas, M. L., & Andres, G. (2016). African Swine Fever Virus Undergoes Outer Envelope Disruption, Capsid Disassembly and Inner Envelope Fusion before Core Release from Multivesicular Endosomes. *PLoS Pathog*, *12*(4), e1005595. https://doi.org/10.1371/journal.ppat.1005595

Hubner, A., Petersen, B., Keil, G. M., Niemann, H., Mettenleiter, T. C., & Fuchs, W. (2018). Efficient inhibition of African swine fever virus replication by CRISPR/Cas9 targeting of the viral p30 gene (CP204L). *Sci Rep*, *8*(1), 1449. https://doi.org/10.1038/s41598-018-19626-1

Hurtado, C., Bustos, M. J., Granja, A. G., de Leon, P., Sabina, P., Lopez-Vinas, E., Gomez-Puertas, P., Revilla, Y., & Carrascosa, A. L. (2011). The African swine fever virus lectin EP153R modulates the surface membrane expression of MHC class I antigens. *Archives of Virology*, *156*(2), 219-234. https://doi.org/10.1007/s00705-010-0846-2

Hurtado, C., Granja, A. G., Bustos, M. J., Nogal, M. L., de Buitrago, G. G., de Yebenes, V. G., Salas, M. L., Revilla, Y., & Carrascosa, A. L. (2004). The C-type lectin homologue gene (EP153R) of African swine fever virus inhibits apoptosis both in virus infection and in heterologous expression. *Virology*, *326*(1), 160-170. https://doi.org/10.1016/j.virol.2004.05.019

Ikemizu, S., Sparks, L. M., Merwe, P. A. V., Harlos, K., Stuart, D. I., Jones, E. Y., & Davis, S. J. (1999). Crystal structure of the CD2-binding domain of CD58 (lymphocyte function-associated antigen 3). *Biochemistry*, *96*, 4289-4294.

Iyer, L. M., Aravind, L., & Koonin, E. V. (2001). Common Origin of Four Diverse Families of Large Eukaryotic DNA Viruses. *Journal of General Virology*, *75*(23), 11720–11734.

Iyer, L. M., Balaji, S., Koonin, E. V., & Aravind, L. (2006). Evolutionary genomics of nucleo-cytoplasmic large DNA viruses. *Virus Res*, *117*(1), 156-184. https://doi.org/10.1016/j.virusres.2006.01.009

Javier, M., Rodriguez., Rafael, J., Yaznez., Almazan, F., Vinuela, E., & Rodriguez, J. F. (1993). African Swine Fever Virus Encodes a CD2 Homolog Responsible for the Adhesion of Erythrocytes to Infected Cells. *Journal of Virology*, *67*(9), 5312-5320.

Jia, N., Ou, Y. W., Pejsak, Z., Zhang, Y. G., & Zhang, J. (2017). Roles of African swine fever virus structural proteins in viral infection. *Journal of Veterinary Research*, *61*(2), 135-143. https://doi.org/10.1515/jvetres-2017-0017

Jones, E. Y., Davis, S. J., Williams, A. F., Harlos, K., & Stuart, D. I. (1992). Crystal-Structure at 2.8-Angstrom Resolution of a Soluble Form of the Cell-Adhesion Molecule Cd2. *Nature*, *360*(6401), 232-239. https://doi.org/DOI 10.1038/360232a0

Jori, F., Vial, L., Penrith, M. L., Perez-Sanchez, R., Etter, E., Albina, E., Michaud, V., & Roger, F. (2013). Review of the sylvatic cycle of African swine fever in sub-Saharan Africa and the Indian ocean. *Virus Res*, *173*(1), 212-227. https://doi.org/10.1016/j.virusres.2012.10.005

Jouvenet, N., Monaghan, P., Way, M., & Wileman, T. (2004). Transport of African swine fever virus from assembly sites to the plasma membrane is dependent on microtubules and conventional kinesin. *J Virol*, *78*(15), 7990-8001. https://doi.org/10.1128/JVI.78.15.7990-8001.2004

Kay-Jackson, P. C., Goatley, L. C., Cox, L., Miskin, J. E., Parkhouse, R. M., Wienands, J., & Dixon, L. K. (2004). The CD2v protein of African swine fever virus interacts with the actin-binding adaptor protein SH3P7. *J Gen Virol*, *85*(Pt 1), 119-130. https://doi.org/10.1099/vir.0.19435-0

Keil, G. M., Giesow, K., & Portugal, R. (2014). A novel bromodeoxyuridine-resistant wild boar lung cell line facilitates generation of African swine fever virus recombinants. *Archives of Virology*, *159*(9), 2421-2428. https://doi.org/10.1007/s00705-014-2095-2

Kerr, M. C., & Teasdale, R. D. (2009). Defining macropinocytosis. *Traffic*, *10*(4), 364-371. https://doi.org/10.1111/j.1600-0854.2009.00878.x

King, K., Chapman, D., Argilaguet, J. M., Fishbourne, E., Hutet, E., Cariolet, R., Hutchings, G., Oura, C. A., Netherton, C. L., Moffat, K., Taylor, G., Le Potier, M. F., Dixon, L. K., & Takamatsu, H. H. (2011). Protection of European domestic pigs from virulent African isolates of African swine fever virus by experimental immunisation. *Vaccine*, *29*(28), 4593-4600. https://doi.org/10.1016/j.vaccine.2011.04.052

Leitao, A., Cartaxeiro, C., Coelho, R., Cruz, B., Parkhouse, R. M. E., Portugal, F. C., Vigario, J. D., & Martins, C. L. V. (2001). The non-haemadsorbing African swine fever virus isolate ASFV/NH/P68 provides a model for defining the protective anti-virus immune response. *Journal of General Virology*, *82*, 513-523.

Leon, P. D., Bustos, M. J., & Carrascosa, A. L. (2013). Laboratory methods to study African swine fever virus. *virus research*, *173*, 168– 179.

Lithgow, P., Takamatsu, H., Werling, D., Dixon, L., & Chapman, D. (2014). Correlation of cell surface marker expression with African swine fever virus infection. *Vet Microbiol*, *168*(2-4), 413-419. https://doi.org/10.1016/j.vetmic.2013.12.001

Liu, S., Luo, Y. Z., Wang, Y. J., Li, S. H., Zhao, Z. N., Bi, Y. H., Sun, J. Q., Peng, R. C., Song, H., Zhu, D. J., Sun, Y., Li, S., Zhang, L., Wang, W., Sun, Y. P., Qi, J. X., Yan, J. H., Shi, Y., Zhang, X. Z., Wang, P. Y., Qiu, H. J., & Gao, G. F. (2019). Cryo-EM Structure of the African Swine Fever Virus. *Cell Host & Microbe*, *26*(6), 836-+. https://doi.org/10.1016/j.chom.2019.11.004

Malogolovkin, A., Burmakina, G., Titov, I., Sereda, A., Gogin, A., Baryshnikova, E., & Kolbasov, D. (2015). Comparative analysis of African swine fever virus genotypes and serogroups. *Emerg Infect Dis*, *21*(2), 312-315. https://doi.org/10.3201/eid2102.140649

Malogolovkin, A., Burmakina, G., Tulman, E. R., Delhon, G., Diel, D. G., Salnikov, N., Kutish, G. F., Kolbasov, D., & Rock, D. L. (2015). African swine fever virus CD2v and C-type lectin gene loci mediate serological specificity. *J Gen Virol*, *96*(Pt 4), 866-873. https://doi.org/10.1099/jgv.0.000024

McKercher, P. D., Hess, W. R., & Hamdy, F. (1978). Residual viruses in pork products. *Appl Environ Microbiol*, *35*(1), 142-145. https://doi.org/10.1128/AEM.35.1.142-145.1978

McMahon, H. T., & Boucrot, E. (2011). Molecular mechanism and physiological functions of clathrin-mediated endocytosis. *Nat Rev Mol Cell Biol*, *12*(8), 517-533. https://doi.org/10.1038/nrm3151

Monteagudo, P. L., Lacasta, A., Lopez, E., Bosch, L., Collado, J., Pina-Pedrero, S., Correa-Fiz, F., Accensi, F., Navas, M. J., Vidal, E., Bustos, M. J., Rodriguez, J. M., Gallei, A., Nikolin, V., Salas, M. L., & Rodriguez, F. (2017). BA71DeltaCD2: a New Recombinant Live Attenuated African Swine Fever Virus with Cross-Protective Capabilities. *J Virol*, *91*(21). https://doi.org/10.1128/JVI.01058-17

Montgomery, R. E. (1921). On a form of swine fever occuring in british east africa (Kenya colony). *The journal of comparative pathology and therapeutics*, *34*(3).

Moss, B. (2013). Poxvirus DNA replication. *Cold Spring Harb Perspect Biol*, *5*(9). https://doi.org/10.1101/cshperspect.a010199

Murcia, P., Donachie, W., & Palmarini, M. (2009). Viral Pathogens of Domestic Animals and Their Impact on Biology, Medicine and Agriculture. *Encyclopedia of Microbiology*, *3*, 805–819.

Neilan, J. G., Zsak, L., Lu, Z., Burrage, T. G., Kutish, G. F., & Rock, D. L. (2004). Neutralizing antibodies to African swine fever virus proteins p30, p54, and p72 are not sufficient for antibody-mediated protection. *Virology*, *319*(2), 337-342. <Go to ISI>://000220014400017

Oliveros, M., Yanez, R. J., Salas, M. L., Salas, J., Vinuela, E., & Blanco, L. (1997). Characterization of an African swine fever virus 20-kDa DNA polymerase involved in DNA repair. *Journal of Biological Chemistry*, *272*(49), 30899-30910. https://doi.org/10.1074/jbc.272.49.30899

Oura, C. A., Powell, P. P., & Parkhouse, R. M. (1998). African swine fever: a disease characterized by apoptosis. *J Gen Virol*, *79 (Pt 6)*, 1427-1438. https://doi.org/10.1099/0022-1317-79-6-1427

Oura, C. A. L., Denyer, M. S., Takamatsu, H., & Parkhouse, R. M. E. (2005). In vivo depletion of CD8+ T lymphocytes abrogates protective immunity to African swine fever virus. *J Gen Virol*, *86*(Pt 9), 2445-2450. https://doi.org/10.1099/vir.0.81038-0

Perez-Nunez, D., Garcia-Urdiales, E., Martinez-Bonet, M., Nogal, M. L., Barroso, S., Revilla, Y., & Madrid, R. (2015). CD2v Interacts with Adaptor Protein AP-1 during African Swine Fever Infection. *PLoS One*, *10*(4), e0123714. https://doi.org/10.1371/journal.pone.0123714

Perez-Nunez, D., Sunwoo, S. Y., Sanchez, E. G., Haley, N., Garcia-Belmonte, R., Nogal, M., Morozov, I., Madden, D., Gaudreault, N. N., Mur, L., Shivanna, V., Richt, J. A., & Revilla, Y. (2019). Evaluation of a viral DNA-protein immunization strategy against African swine fever in domestic pigs. *Veterinary Immunology and Immunopathology*, *208*, 34-43. https://doi.org/10.1016/j.vetimm.2018.11.018

Peterson, A., & Seed, B. (1987). Monoclonal antibody and ligand binding sites of the T cell erythrocytes receptor *Letter to Nature*, *329*, 842-846.

Popescu, L., Gaudreault, N. N., Whitworth, K. M., Murgia, M. V., Nietfeld, J. C., Mileham, A., Samuel, M., Wells, K. D., Prather, R. S., & Rowland, R. R. R. (2017). Genetically edited pigs lacking CD163 show no resistance following infection with the African swine fever virus isolate, Georgia 2007/1. *Virology*, *501*, 102-106. https://doi.org/10.1016/j.virol.2016.11.012

Portugal, R. S., Bauer, A., & Keil, G. M. (2017). Selection of differently temporally regulated African swine fever virus promoters with variable expression activities and their application for transient and recombinant virus mediated gene expression. *Virology*, *508*, 70-80. https://doi.org/10.1016/j.virol.2017.05.007

Quembo, C. J., Jori, F., Vosloo, W., & Heath, L. (2018). Genetic characterization of African swine fever virus isolates from soft ticks at the wildlife/domestic interface in Mozambique and identification of a novel genotype. *Transboundary and Emerging Diseases*, *65*(2), 420-431. https://doi.org/10.1111/tbed.12700

Rathakrishnan, A., Moffat, K., Reis, A. L., & Dixon, L. K. (2020). Production of Recombinant African Swine Fever Viruses: Speeding Up the Process. *Viruses*, *12*(6). https://doi.org/10.3390/v12060615

Reis, A. L., Abrams, C. C., Goatley, L. C., Netherton, C., Chapman, D. G., Sanchez-Cordon, P., & Dixon, L. K. (2016). Deletion of African swine fever virus interferon inhibitors from the genome of a virulent isolate reduces virulence in domestic pigs and induces a protective response. *Vaccine*, *34*(39), 4698-4705. https://doi.org/10.1016/j.vaccine.2016.08.011

Reis, A. L., Goatley, L. C., Jabbar, T., Sanchez-Cordon, P. J., Netherton, C. L., Chapman, D. A. G., & Dixon, L. K. (2017). Deletion of the African Swine Fever Virus Gene DP148R Does Not Reduce Virus Replication in Culture but Reduces Virus Virulence in Pigs and Induces High Levels of Protection against Challenge. *Journal of Virology*, *91*(24). https://doi.org/ https://doi.org/10.1128/JVI.01428-17.

Rodriguez, J. M., & Salas, M. L. (2013). African swine fever virus transcription. *Virus Res*, *173*(1), 15-28. https://doi.org/10.1016/j.virusres.2012.09.014

Rodriguez, J. M., Yanez, R. J., Almazan, F., Vinuela, E., & Rodriguez, J. F. (1993a). African Swine Fever Virus Encodes a Cd2 Homolog Responsible for the Adhesion of Erythrocytes to Infected-Cells. *Journal of Virology*, *67*(9), 5312-5320. <Go to ISI>://A1993LR77700026

Rodriguez, J. M., Yanez, R. J., Almazan, F., Vinuela, E., & Rodriguez, J. F. (1993b). African swine fever virus encodes a CD2 homolog responsible for the adhesion of erythrocytes to infected cells. *J Virol*, *67*(9), 5312-5320. https://doi.org/10.1128/JVI.67.9.5312-5320.1993

Rowlands, R. J., Michaud, V., Heath, L., Hutchings, G., Oura, C., Vosloo, W., Dwarka, R., Onashvili, T., Albina, E., & Dixon, L. K. (2008). African swine fever virus isolate, Georgia, 2007. *Emerg Infect Dis*, *14*(12), 1870-1874. https://doi.org/10.3201/eid1412.080591

Ruiz-Gonzalvo, F., Rodriguez, F., & Escribano, J. M. (1996). Functional and Immunological Properties of the Baculovirus-Expressed Hemagglutinin of African Swine Fever Virus. *Virology*, *218*, 285-289.

Salas, J., Salas, M. L., & Vinuela, E. (1988). Effect of Inhibitors of the Host-Cell Rna Polymerase-Ii on African Swine Fever Virus Multiplication. *Virology*, *164*(1), 280-283. <Go to ISI>://A1988N143100034

Salas, M. L., & Andres, G. (2013). African swine fever virus morphogenesis. *Virus Res*, *173*(1), 29-41. https://doi.org/10.1016/j.virusres.2012.09.016

Salas, M. L., Kuznar, J., & Vinuela, E. (1981). Polyadenylation, methylation, and capping of the RNA synthesized in vitro by African swine fever virus. *Virology*, *113*(2), 484-491. https://doi.org/10.1016/0042-6822(81)90176-8

Salas, M. L., Rey-Campos, J., Almendral, J. M., Talavera, A., & Vinuela, E. (1986). Transcription and translation maps of African swine fever virus. *Virology*, *152*(1), 228-240. http://www.ncbi.nlm.nih.gov/pubmed/3716203

Salguero, F. J. (2020). Comparative Pathology and Pathogenesis of African Swine Fever Infection in Swine. *Frontiers in Veterinary Science*, *7*. https://doi.org/ARTN 282

10.3389/fvets.2020.00282

Salguero, F. J., Sanchez-Cordon, P. J., Nunez, A., de Marco, M. F., & Gomez-Villamandos, J. C. (2005). Proinflammatory cytokines induce lymphocyte apoptosis in acute African swine fever infection. *Journal of Comparative Pathology*, *132*(4), 289-302. <Go to ISI>://000229527000005

Sanchez-Cordon, P. J., Montoya, M., Reis, A. L., & Dixon, L. K. (2018). African swine fever: A re-emerging viral disease threatening the global pig industry. *Vet J*, *233*, 41-48. https://doi.org/10.1016/j.tvjl.2017.12.025

Sanchez-Torres, C., Gomez-Puertas, P., Gomez-del-Moral, M., Alonso, F., Escribano, J. M., Ezquerra, A., & Dominguez, J. (2003). Expression of porcine CD163 on monocytes/macrophages correlates with permissiveness to African swine fever infection. *Archives of Virology*, *148*(12), 2307-2323. https://doi.org/10.1007/s00705-003-0188-4

Sanchez-Vizcaino, J. M., Mur, L., Gomez-Villamandos, J. C., & Carrasco, L. (2015). An Update on the Epidemiology and Pathology of African Swine Fever. *Journal of Comparative Pathology*, *152*(1), 9-21. https://doi.org/10.1016/j.jcpa.2014.09.003

Sanchez-Vizcaino, J. M., Mur, L., & Martinez-Lopez, B. (2013). African swine fever (ASF): five years around Europe. *Vet Microbiol*, *165*(1-2), 45-50. https://doi.org/10.1016/j.vetmic.2012.11.030

Sanchez, E. G., Quintas, A., Nogal, M., Castello, A., & Revilla, Y. (2013). African swine fever virus controls the host transcription and cellular machinery of protein synthesis. *Virus Res*, *173*(1), 58-75. https://doi.org/10.1016/j.virusres.2012.10.025

Sanchez, E. G., Riera, E., Nogal, M., Gallardo, C., Fernandez, P., Bello-Morales, R., Lopez-Guerrero, J. A., Chitko-McKown, C. G., Richt, J. A., & Revilla, Y. (2017). Phenotyping and susceptibility of established porcine cells lines to African Swine Fever Virus infection and viral production. *Scientific Reports*, *7*. https://doi.org/ARTN 10369

10.1038/s41598-017-09948-x

Sauer, B., & Henderson, N. (1988). Site-Specific DNA Recombination in Mammalian-Cells by the Cre Recombinase of Bacteriophage-P1. *Proceedings of the National Academy of Sciences of the United States of America*, *85*(14), 5166-5170. https://doi.org/DOI 10.1073/pnas.85.14.5166

Smith, A. E., & Helenius, A. (2004). How Viruses Enter Animal Cells. *Cellular Invasions*, *304*(5668), 237-242. https://doi.org/DOI: 10.1126/science.1094823

Somoza, C., Driscoll, p. C., Cyster, J. G., & Williams, A. F. (1993). Mutational Analysis of the CD2/CD58 Interaction: The Binding Site for CD58 Lies on One Face of the First Domain of Human CD2. *J. Exp. Med.*, *178*.

Sun, Z. Y. J., Dotsch, V., Kim, M., Li, J., Reinherz, E. L., & Wagner, G. (1999). Functional glycan-free adhesion domain of human cell surface receptor CD58: design, production and NMR studies. *Embo Journal*, *18*(11), 2941-2949. https://doi.org/DOI 10.1093/emboj/18.11.2941

Sutter, G., Ohlmann, M., & Erfle, V. (1995). Non-replicating vaccinia vector efficiently expresses bacteriophage T7 RNA polymerase. *FEBS Lett*, *371*(1), 9-12. https://doi.org/10.1016/0014-5793(95)00843-x

Takamatsu, H., Denyer, M. S., Oura, C., Childerstone, A., Andersen, J. K., pullen, L., & Parkhouse, R. M. (1999). African swine fever virus: a B cell-mitogenic virus in vivo and in vitro. *Journal of General Virology*, *80*, 1453–1461.

Tulman, E. R., Delhon, G. A., Ku, B. K., & Rock, D. L. (2009). African swine fever virus. *Current Topics Microbiol Immunology*, *328*, 43-87.

van der Merwe, P. A., McNamee, P. N., Davies, E. A., Barclay, A. N., & Davis, S. J. (1995). Topology of the CD2–CD48 cell-adhesion molecule complex: implications for antigen recognition by T cells. *Current Biology*, *5*(1), 74-84. https://doi.org/https://doi.org/10.1016/S0960-9822(95)00019-4

Wang, H. P., Wang, X., Ke, Z. J., Comer, A. L., Xu, M., Frank, J. A., Zhang, Z., Shi, X. L., & Luo, J. (2015). Tunicamycin-induced unfolded protein response in the developing mouse brain. *Toxicology and Applied Pharmacology*, *283*(3), 157-167. https://doi.org/10.1016/j.taap.2014.12.019

Wang, J. H., Smolyar, A., Tan, K., Liu, J. H., Kim, M., Sun, Z. J., Wagner, G., & Reinherz, E. L. (1999). Structure of a Heterophilic Adhesion Complex between the Human CD2 and CD58 (LFA-3) Counterreceptors. *Cell*, *97*, 791–803.

Wardley, R. C., & Wilkinson, P. J. (1977). The association of African swine fever virus with blood components of infected pigs. *Arch Virol*, *55*(4), 327-334. https://doi.org/10.1007/BF01315054

Weller, S. K., & Coen, D. M. (2012). Herpes Simplex Viruses: Mechanisms of DNA Replication. *Cold Spring Harbor Perspectives in Biology*, *4*(9). https://doi.org/ARTN a013011

10.1101/cshperspect.a013011

Wulff, N. H., Tzatzaris, M., & Young, P. J. (2012). Monte Carlo simulation of the Spearman-Kaerber TCID50. *J Clin Bioinforma*, *2*(1), 5. https://doi.org/10.1186/2043-9113-2-5

Zhu, J. J., Ramanathan, P., Bishop, E. A., O'Donnell, V., Gladue, D. P., & Borca, M. V. (2019). Mechanisms of African swine fever virus pathogenesis and immune evasion inferred from gene expression changes in infected swine macrophages. *PLoS One*, *14*(11). https://doi.org/ARTN e0223955

10.1371/journal.pone.0223955

Zsak, L., Onisk, D. V., Afonso, C. L., & Rock, D. L. (1993). Virulent African Swine Fever Virus Isolates Are Neutralized by Swine Immune Serum and by Monoclonal-Antibodies Recognizing a 72-Kda Viral Protein. *Virology*, *196*(2), 596-602. <Go to ISI>://A1993LY07100022